Journal of Oncology

Diagnostic, Prognostic, and Predictive Biomarkers in Breast Cancer

Lead Guest Editor: Chia-Jung Li
Guest Editors: Hui-Ming Chen and Ji-Ching Lai

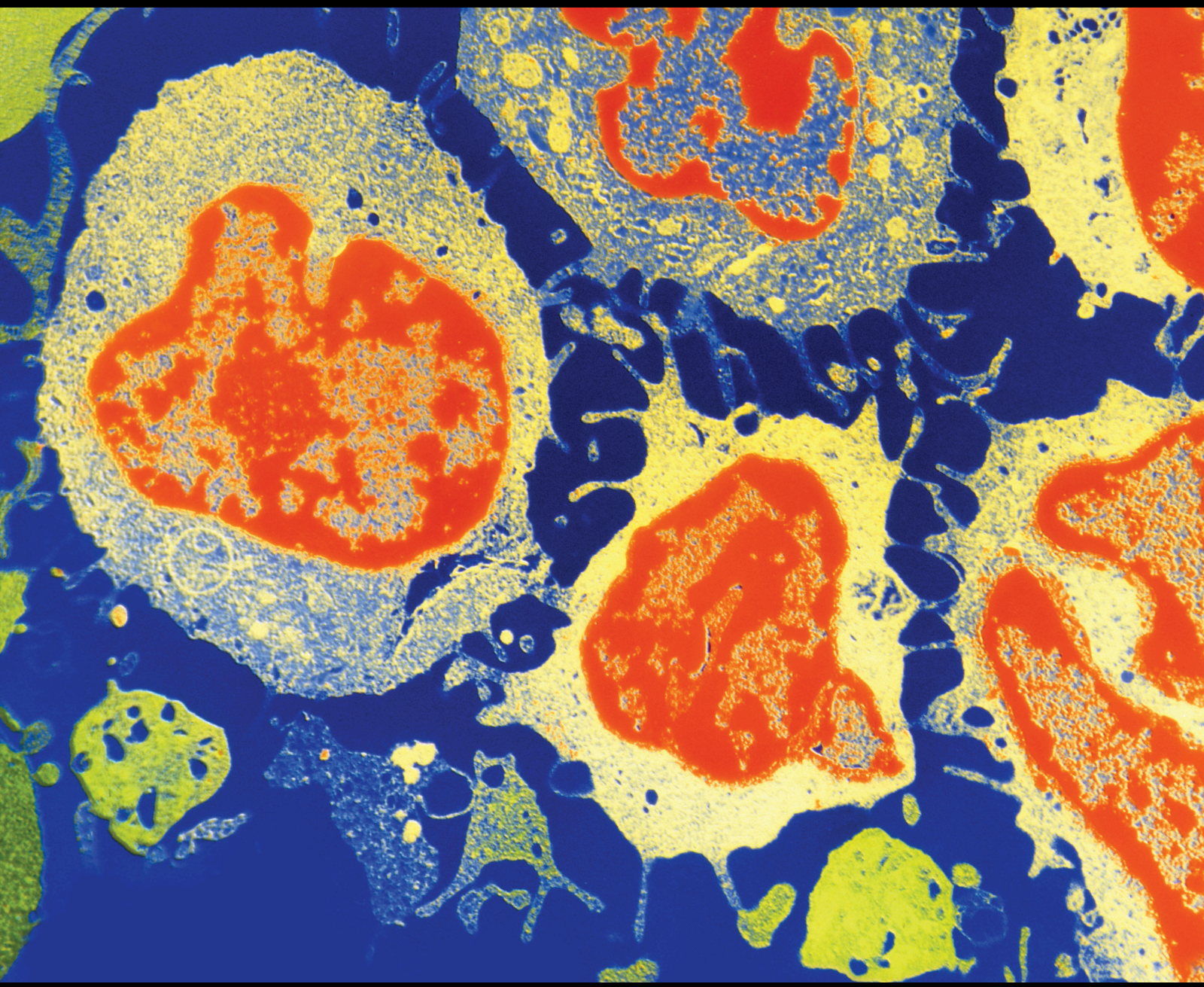

Diagnostic, Prognostic, and Predictive Biomarkers in Breast Cancer

Journal of Oncology

Diagnostic, Prognostic, and Predictive Biomarkers in Breast Cancer

Lead Guest Editor: Chia-Jung Li
Guest Editors: Hui-Ming Chen and Ji-Ching Lai

Contents

Diagnostic, Prognostic, and Predictive Biomarkers in Breast Cancer
Chia-Jung Li, Hui-Ming Chen, and Ji-Ching Lai
Editorial (2 pages), Article ID 1835691, Volume 2020 (2020)

Attenuated Total Reflection-Fourier Transform Infrared (ATR-FTIR) Spectroscopy Analysis of Saliva for Breast Cancer Diagnosis
Izabella C. C. Ferreira, Emília M. G. Aguiar, Alinne T. F. Silva, Letícia L. D. Santos, Léia Cardoso-Sousa, Thaise G. Araújo, Donizeti W. Santos, Luiz R. Goulart, Robinson Sabino-Silva, and Yara C. P. Maia
Research Article (11 pages), Article ID 4343590, Volume 2020 (2020)

Exploring the Role of Breast Density on Cancer Prognosis among Women Attending Population-Based Screening Programmes
Laia Domingo, Maria Sala, Javier Louro, Marisa Baré, Teresa Barata, Joana Ferrer, Maria Carmen Carmona-Garcia, Mercè Comas, Xavier Castells, and CAMISS Study Group
Research Article (8 pages), Article ID 1781762, Volume 2019 (2019)

CD133 in Breast Cancer Cells: More than a Stem Cell Marker
Federica Brugnoli, Silvia Grassilli, Yasamin Al-Qassab, Silvano Capitani, and Valeria Bertagnolo
Review Article (8 pages), Article ID 7512632, Volume 2019 (2019)

N-Acetyltransferase 1 Knockout Elevates Acetyl Coenzyme A Levels and Reduces Anchorage-Independent Growth in Human Breast Cancer Cell Lines
Marcus W. Stepp, Raúl A. Salazar-González, Kyung U. Hong, Mark A. Doll, and David W. Hein
Research Article (11 pages), Article ID 3860426, Volume 2019 (2019)

Dovitinib Triggers Apoptosis and Autophagic Cell Death by Targeting SHP-1/p-STAT3 Signaling in Human Breast Cancers
Yi-Han Chiu, Yi-Yen Lee, Kuo-Chin Huang, Cheng-Chi Liu, and Chen-Si Lin
Research Article (14 pages), Article ID 2024648, Volume 2019 (2019)

Pregnancy Hypertension and a Commonly Inherited IGF1R Variant (rs2016347) Reduce Breast Cancer Risk by Enhancing Mammary Gland Involution
Mark J. Powell, Suzanne M. Dufault, Jill E. Henry, Anna C. Allison, Renata Cora, and Christopher C. Benz
Research Article (8 pages), Article ID 6018432, Volume 2019 (2019)

Association of ESR1 Mutations and Visceral Metastasis in Patients with Estrogen Receptor-Positive Advanced Breast Cancer from Brazil
Tomás Reinert, Guilherme Portela Coelho, Jovana Mandelli, Edinéia Zimermann, Facundo Zaffaroni, José Bines, Carlos Henrique Barrios, and Marcia Silveira Graudenz
Research Article (5 pages), Article ID 1947215, Volume 2019 (2019)

Identification of Cell-Free Circulating MicroRNAs for the Detection of Early Breast Cancer and Molecular Subtyping
Karen C. B. Souza, Adriane F. Evangelista, Letícia F. Leal, Cristiano P. Souza, René A. Vieira, Rhafaela L. Causin, A. C. Neuber, Daniele P. Pessoa, Geraldo A. S. Passos, Rui M. V. Reis, and Marcia M. C. Marques
Research Article (11 pages), Article ID 8393769, Volume 2019 (2019)

Role of Four ABC Transporter Genes in Pharmacogenetic Susceptibility to Breast Cancer in Jordanian Patients
Laith N. AL-Eitan, Doaa M. Rababa'h, Mansour A. Alghamdi, and Rame H. Khasawneh
Research Article (8 pages), Article ID 6425708, Volume 2019 (2019)

Notch Signaling Activation as a Hallmark for Triple-Negative Breast Cancer Subtype
M. V. Giuli, E. Giuliani, I. Screpanti, D. Bellavia, and S. Checquolo
Review Article (15 pages), Article ID 8707053, Volume 2019 (2019)

A Review of the Hereditary Component of Triple Negative Breast Cancer: High- and Moderate-Penetrance Breast Cancer Genes, Low-Penetrance Loci, and the Role of Nontraditional Genetic Elements
Darrell L. Ellsworth, Clesson E. Turner, and Rachel E. Ellsworth
Review Article (10 pages), Article ID 4382606, Volume 2019 (2019)

A Novel Role for Cathepsin S as a Potential Biomarker in Triple Negative Breast Cancer
Richard D. A. Wilkinson, Roberta E. Burden, Sara H. McDowell, Darragh G. McArt, Stephen McQuaid, Victoria Bingham, Rich Williams, Órla T. Cox, Rosemary O'Connor, Nuala McCabe, Richard D. Kennedy, Niamh E. Buckley, and Christopher J. Scott
Research Article (12 pages), Article ID 3980273, Volume 2019 (2019)

Overexpression of Kynurenine 3-Monooxygenase Correlates with Cancer Malignancy and Predicts Poor Prognosis in Canine Mammary Gland Tumors
Yi-Han Chiu, Han-Jung Lei, Kuo-Chin Huang, Yi-Lin Chiang, and Chen-Si Lin
Research Article (10 pages), Article ID 6201764, Volume 2019 (2019)

Human Mitotic Centromere-Associated Kinesin Is Targeted by MicroRNA 485-5p/181c and Prognosticates Poor Survivability of Breast Cancer
Huajun Lu, Chaoqun Wang, Lijun Xue, Qi Zhang, Frank Luh, Jianghai Wang, Tiffany G. Lin, Yun Yen, and Xiyong Liu
Research Article (13 pages), Article ID 2316237, Volume 2019 (2019)

Hindawi
Journal of Oncology
Volume 2020, Article ID 1835691, 2 pages
https://doi.org/10.1155/2020/1835691

Editorial

Diagnostic, Prognostic, and Predictive Biomarkers in Breast Cancer

Chia-Jung Li,[1,2] **Hui-Ming Chen**,[3] **and Ji-Ching Lai**[4]

[1]*Department of Obstetrics and Gynecology, Kaohsiung Veterans General Hospital, Kaohsiung, Taiwan*
[2]*Institute of BioPharmaceutical Sciences, National Sun Yat-Sen University, Kaohsiung, Taiwan*
[3]*Houston Methodist Research Institute, Houston, TX, USA*
[4]*Department of Medical Research and Development, Chang Bing Show Chwan Memorial Hospital, Changhua, Taiwan*

Correspondence should be addressed to Ji-Ching Lai; jichinglai@gmail.com

Received 17 February 2020; Accepted 17 February 2020; Published 9 March 2020

Breast cancer is the most frequently diagnosed cancer type and the second leading cause of cancer-related deaths among women worldwide. The causes of breast cancer are not yet fully known, although a number of risk factors have been identified. Tumor biomarker is a term used to describe potential markers of cancer development and progression. As we explore these biomarkers further, we must try to understand the underlying mechanisms of tumor development, as we move along the path to discovery of novel therapies that will increase our ability to offer personalized patient care in the future. With the migration of advanced high throughput technologies, such as Next Generation Sequencing from clinical practice, biomarker research and discovery are poised to explode once again. Translation of novel biomarkers into clinical practice and diagnostic laboratories is coupled with regulatory and administrative requirements that must be met, while collaboration between research institutions, industry, and the private sector drives further advancements in the field of breast cancer biomarker discovery and application.

The aim of this special issue is to provide new findings regarding molecular pathways and biomarkers that could improve the diagnosis and the prognostic classification of breast cancers, their application in the clinical setting, and their potential utility in personalized patient therapy. The total of submissions is 50. After single-blind peer review by at least two reviewers, 14 papers were finally accepted to be published. The accepted rate is 28%. The average number of authors for each accepted paper is 7. The affiliated institutes of the authors are from Brazil, China, Italy, Iraq, Jordan, Portugal, Spain, Saudi Arabia, Taiwan, the UK, and the USA. These accepted papers can be organized in different groups. The focus of the first group of articles is on prognosis and therapy in breast cancer. The findings of the paper titled "Exploring the Role of Breast Density on Cancer Prognosis among Women Attending Population-Based Screening Programmes" by Domingo et al. reveal that increased breast density was associated with worse survival outcomes among women participating in breast cancer screening. The paper titled "Attenuated Total Reflection-Fourier Transform Infrared (ATR-FTIR) Spectroscopy Analysis of Saliva for Breast Cancer Diagnosis" by Ferreira et al. showed ATR-FTIR spectroscopy can be used in saliva samples to discriminate breast cancer patients from benign patients and healthy subjects. The paper titled "Dovitinib Triggers Apoptosis and Autophagic Cell Death by Targeting SHP-1/p-STAT3 Signaling in Human Breast Cancers" by Chiu et al. has provided the evidence for anticancer effect of dovitinib to suggest it as a potential target for breast cancer therapy. The focus of the second group of articles is on biomarkers in breast cancer. The paper titled "A Novel Role for Cathepsin S as a Potential Biomarker in Triple Negative Breast Cancer" by Wilkinson et al. investigated the expression profile of Cathepsin S in breast cancer patients. The paper titled "Identification of Cell-Free Circulating MicroRNAs for the Detection of Early Breast Cancer and Molecular Subtyping" by Souza et al. identified the molecular signature miRNA as noninvasive biomarkers in patients with breast cancer. The

paper titled "CD133 in Breast Cancer Cells: More Than a Stem Cell Marker" by Brugnoli et al. reviewed the value of CD133 as prognostic factor of malignant progression of breast cancer. The other four papers titled "*N*-Acetyltransferase 1 Knockout Elevates Acetyl Coenzyme A Levels and Reduces Anchorage-Independent Growth in Human Breast Cancer Cell Lines" by Stepp et al., "Overexpression of Kynurenine 3-Monooxygenase Correlates with Cancer Malignancy and Predicts Poor Prognosis in Canine Mammary Gland Tumors" by Chiu et al., "Notch Signaling Activation as a Hallmark for Triple Negative Breast Cancer Subtype" by Giuli et al., and "Human Mitotic Centromere-Associated Kinesin is Targeted by MicroRNA 485-5p/181c and Prognosticates Poor Survivability of Breast Cancer" by Lu et al. contributed different biomarkers of breast cancer which may help to assess prognosis or predictive indicators. The focus of the third group of articles is on genetic mutations in breast cancer. The paper titled "Association of ESR1 Mutations and Visceral Metastasis in Patients with Estrogen Receptor-Positive Advanced Breast Cancer from Brazil" by Reinert et al. observed an association of ESR1 mutations with metastasis. The paper titled "Role of Four ABC Transporter Genes in Pharmacogenetic Susceptibility to Breast Cancer in Jordanian Patients" by AL-Eitan et al. proposed the ABCB1 mutation associated with breast cancer in Jordanian Arabs. The paper titled "A Review of the Hereditary Component of Triple Negative Breast Cancer: High- and Moderate-Penetrance Breast Cancer Genes, Low-Penetrance Loci and the Role of Nontraditional Genetic Elements" by Ellsworth et al. described genes and genetic elements, which have been associated with increased risk of triple negative breast cancer. The paper titled "Pregnancy Hypertension and a Commonly Inherited IGF1R Variant (rs2016347) Reduce Breast Cancer Risk by Enhancing Mammary Gland Involution" by Powell et al. observed that statistically significant decrease in terminal duct lobular unit counts signifies increased breast epithelial involution in women with prior hypertension who inherited the TT genotype of IGF1R SNP (rs2016347).

In summary, the research papers cover a wide range of applications including potential diagnostics, predictions, and treatment. Furthermore, this special issue also includes regional genetic mutation, breast density on cancer prognosis, small RNA as a biomarker, surface marker of cancer stem cells, potential marker of cancer metastasis, and spectroscopy predicting the rate of cancer. This may be helpful in assessing prognostic or predictive indicators, as well as developing new therapies and new insights aimed at improving breast cancer.

Conflicts of Interest

The authors declare that they have no conflicts of interest.

Chia-Jung Li
Hui-Ming Chen
Ji-Ching Lai

Hindawi
Journal of Oncology
Volume 2020, Article ID 4343590, 11 pages
https://doi.org/10.1155/2020/4343590

Research Article

Attenuated Total Reflection-Fourier Transform Infrared (ATR-FTIR) Spectroscopy Analysis of Saliva for Breast Cancer Diagnosis

Izabella C. C. Ferreira,[1] **Emília M. G. Aguiar**,[2] **Alinne T. F. Silva**,[1] **Letícia L. D. Santos**,[1] **Léia Cardoso-Sousa**,[2] **Thaise G. Araújo**,[1] **Donizeti W. Santos**,[3] **Luiz R. Goulart**,[1] **Robinson Sabino-Silva**,[2] **and Yara C. P. Maia**[1,4]

[1]*Laboratory of Nanobiotechnology, Institute of Biotechnology, Federal University of Uberlandia, Uberlandia 38405-302, Brazil*
[2]*Department of Physiology, Institute of Biomedical Sciences, Federal University of Uberlandia, Uberlandia 38405-302, Brazil*
[3]*Obstetric Division, University Hospital, Federal University of Uberlandia, Uberlandia 38405-320, Brazil*
[4]*School of Medicine, Federal University of Uberlandia, Uberlandia 38405-320, Brazil*

Correspondence should be addressed to Izabella C. C. Ferreira; izabellacostaferreira@gmail.com, Robinson Sabino-Silva; robinsonsabino@gmail.com, and Yara C. P. Maia; yara.maia@ufu.br

Received 26 April 2019; Accepted 28 July 2019; Published 10 February 2020

Guest Editor: Chia-Jung Li

Saliva biomarkers using reagent-free biophotonic technology have not been investigated as a strategy for early detection of breast cancer (BC). The attenuated total reflection-Fourier transform infrared (ATR-FTIR) spectroscopy has been proposed as a promising tool for disease diagnosis. However, its utilization in cancer is still incipient, and currently saliva has not been used for BC screening. We have applied ATR-FTIR onto saliva from patients with breast cancer, benign breast disease, and healthy matched controls to investigate its potential use in BC diagnosis. Several salivary vibrational modes have been identified in original and second-derivative spectra. The absorbance levels at wavenumber 1041 cm^{-1} were significantly higher ($p < 0.05$) in saliva of breast cancer patients compared with those of benign patients, and the ROC curve analysis of this peak showed a reasonable accuracy to discriminate breast cancer from benign and control patients. The 1433–1302.9 cm^{-1} band area was significantly higher ($p < 0.05$) in saliva of breast cancer patients than in control and benign patients. This salivary ATR-FTIR spectral area was prevalidated as a potential diagnostic biomarker of BC. This spectral biomarker was able to discriminate human BC from controls with sensitivity and specificity of 90% and 80%, respectively. Besides, it was able to differentiate BC from benign disease with sensitivity and specificity of 90% and 70%, respectively. Briefly, for the first time, saliva analysis by ATR-FTIR spectroscopy has demonstrated the potential use of salivary spectral biomarkers (1041 cm^{-1} and 1433–1302.9 cm^{-1}) as a novel alternative for noninvasive BC diagnosis, which could be used for screening purposes.

1. Introduction

Breast cancer is a complex and heterogeneous disease caused by several factors, and its dissemination involves a succession of clinical and pathological stages beginning with carcinoma in situ, progressing to invasive lesion and culminating in metastatic disease [1, 2]. According to the World Cancer Report 2014 from the World Health Organization (WHO), breast cancer was the type with the highest incidence and highest mortality in the female population worldwide (1.7 million) in both developing and developed countries [3]. Early diagnosis and proper treatment are the main advantages of breast cancer screening tests. Basically, breast cancer diagnostic comprises four conventional techniques: histopathology, mammography, ultrasonography, and magnetic resonance imaging (MRI). However, in general these techniques have critical limitations related to efficacy and production of false positive or false negative results [4, 5].

Therefore, the increasing worldwide incidence of breast cancer and the absence of sufficient reliable, cost-effective, and high-throughput methods for detection requires a search for other diagnostic tools. The attenuated total reflection-Fourier transform infrared (ATR-FTIR) spectroscopy is a fast, nondestructive, noninvasive, label- and reagent-free, inexpensive, sensitive, and highly reproducible physicochemical tool for characterization of biological molecules in fluids. FTIR requires only a small amount of sample for analysis with easy and quick preparation if necessary, and it allows automated and repetitive analyses, leading to nonsubjective evaluation of the sample [4, 6, 7]. Furthermore, ATR, the experimental configuration for FTIR spectra acquisition utilized in this study, presents high signal-to-noise ratio (SNR), does not present unwanted spectral contributions, and enables a sample to be analyzed without further preparation simply by placing it in direct contact with a crystal with a refractive index higher than the sample [8–11].

FTIR can effectively provide information concerning the structure and chemical composition of biological samples at the molecular level and then the characterization of proteins, lipids, nucleic acids, and carbohydrates. FTIR is also sensitive to detect changes in molecular compositions according to diseased state, providing fingerprints of biological samples, like tissues, cells, and biological fluids. The generation and progression of malignancy at the molecular level in cells occur before morphological alterations in cancer. FTIR spectroscopy is capable to show changes in carcinogenesis-related vibrational modes to several human cancers [8, 12–14]. Specifically for breast cancer, FTIR spectroscopy has been used for many purposes [15–24], mainly for detection [4, 25–28]. Most FTIR spectroscopy studies in breast cancer used normal breast tissue and breast tumors [4, 29–31], breast cell lines [11, 32, 33], and blood of breast cancer patients [25, 27]. To our knowledge, there are no studies using ATR-FTIR spectroscopy for breast cancer diagnosis using saliva as the biological sample.

Saliva is a complex and dynamic biological fluid composed of 98% water and 2% of other important compounds, such as electrolytes, mucus, enzymes, proteins/peptides, nucleic acids, and hormones. Most of the organic compounds of saliva are produced in the salivary glands; however, some molecules originated from a diseased process may be transported from the blood to acinar cells via transcellular or paracellular fluxes into the acinar lumen [34–36]. Then, salivary biomarkers can be exploited for the early diagnosis of some systemic diseases [36–39]. Among the advantages, saliva may reflect several physiological states of the body; is simple, fast and safe to collect; is convenient to store; is noninvasive and, compared to blood, is painless to the patient, and requires less handling during diagnostic proceeding [38, 40, 41].

Here, we tested the hypothesis that specific salivary vibrational modes can be used to discriminate patients with breast cancer from benign patients and matched healthy controls, which may prove that salivary spectral biomarkers are suitable in diagnosing breast cancer. In this manner, the aim of the present study was to establish specific salivary vibrational modes, analyzed by ATR-FTIR spectroscopy, to detect breast cancer fingerprints that are suitable for diagnosis.

2. Materials and Methods

2.1. Ethical Aspects and Study Subjects. The study was conducted at the Clinics' Hospital of the Federal University of Uberlandia (HC-UFU, Uberlandia, Minas Gerais, Brazil) under the approval of the UFU Research Ethics Committee (protocol number 064/2008) and based on the standards of the Declaration of Helsinki. All research were performed in accordance with the relevant guidelines and regulations. Written informed consent was obtained from all the participants of this study including controls and patients. The subjects were randomly selected from the population before performing routine breast cancer screening and/or surgery. Exclusion criteria were age below 18 years, primary tumor site other than the breast, and physical and/or mental inability to respond to the tools necessary for data collection. The study group included 30 subjects: 10 with confirmed breast cancer by clinical, histological, and pathologic examination; 10 with some benign breast disease, like fibroadenomas, atypical ductal hyperplasia, papilloma, or others; and 10 without pathological findings, the control group. In this study was used the tumor-node-metastasis (TNM) cancer classification, which is according to the American Joint Committee on Cancer (AJCC) and the International Union for Cancer Control (UICC). This classification evaluates the extent of the primary tumor (T), regional lymph nodes (N), and distant metastases (M) and provides staging based on T, N, and M [42].

2.2. Sample Collection and Preparation. For each participant, saliva samples were collected before surgery in Salivette® tubes (Sarstedt, Germany), consisting of a neutral cotton swab and a conical tube. The patient chewed the swab for three minutes, which was then returned to the tube that was covered with a lid. Then, the saliva from the swab was recovered by centrifugation for 2 minutes at 1000 $\times g$ and stored at -20°C. Then, the saliva samples (200 μL) were lyophilized overnight. This freeze-drying of the samples removes the strong water infrared light absorption from spectra which may mask the signal from the sample and may reduce the intensity of the compounds under investigation [25, 43].

2.3. ATR-FTIR Spectroscopy. The spectra were measured in the 4000 to 400 cm^{-1} wavenumber region using a FTIR spectrometer VERTEX 70/70v (Bruker Corporation, Germany) coupled with Platinum Diamond ATR, which consists of a diamond disc as an internal reflection element. The lyophilized sample was placed on the ATR crystal, and then the spectrum was recorded. The spectrum of air was used as a background before each sample analysis. Background and sample spectra were taken in a room with a temperature around 21–23°C, at a spectral resolution of 4 cm^{-1}, and to each measurement 32 scans were performed.

2.4. Spectral Data Preprocessing. The original FTIR spectra were normalized, and the baseline was corrected using OPUS software. This software was also used to calculate absorbance of area under spectral regions that correspond to specific saliva components, applying parameters already described [43]. Second differentiation spectra from the original were carried out using the Savitzky–Golay method in Origin 9.1 software in order to accentuate the bands, resolve overlapped bands, and increase the accuracy of analysis by revealing the genuine biochemical characteristics [25, 44]. In the smoothing pretreatment, the parameters of the Savitzky–Golay filter such as the polynomial order and points of window were chosen in order to find the relatively optimum smoothing effect. The parameters were set as 2 for polynomial order and 20 for points of window examined. The second derivative gives negative peaks (valleys) instead of bands from the original absorption spectrum. Therefore, the analyzed wavenumbers in the second derivative are the height of valleys.

2.5. Statistical Analysis. After the spectral preprocessing, the original and derivative values were used on the statistical analysis. First, values of absorbance at specific wavenumbers and spectral regions were submitted to the normality test. According to the results, parametric tests for variables with normal distribution or nonparametric tests for variables without normal distribution were performed. The specific tests applied are indicated on the legend of the figures. A confidence interval (CI) of 0.95 and an alpha level of 0.05 were assumed, so a P value less than 0.05 was considered statistically significant. All the tests utilized were two-tailed. Statistical analyses were carried out using GraphPad Prism versions 5.00 and 7.03 (GraphPad Software, USA).

3. Results

3.1. Patient's Characterization. Demography characteristics of the subjects are demonstrated in Table 1. The breast cancer, benign breast disease, and control patients consisted of 10 women, each one with a mean age ± standard deviation (SD) of 53.3 ± 11.2, 41.5 ± 4.2, and 43.2 ± 16.0 years, respectively. The smoking and alcoholism patterns were similar ($P > 0.05$) in breast cancer, benign breast disease, and control patients. History of smoking had a frequency of 30% in breast cancer, 40% in benign, and 30% in control. Family history of breast cancer was reported only in cancer patients (40%). The clinical, hormonal, diagnostic, and therapy characteristics of patients with breast cancer are summarized in Table 2.

3.2. FTIR Analysis of Saliva Spectra between Breast Cancer, Benign, and Control Patients. The averages of the infrared original spectrum of whole saliva of breast cancer, benign, and control patients are represented in Figure 1 with a superposition of several salivary components as proteins, nucleic acids, lipids, and carbohydrates. The protein content is mainly attributed to wavenumbers at 1636 cm^{-1} and 1549 cm^{-1} that corresponds to amide I and amide II, respectively. CH_3 asymmetric bending and ν_s (COO^-) are related with wavenumbers 1447 cm^{-1} and 1404 cm^{-1}, respectively. The wavenumbers 1350 cm^{-1} and 1244 cm^{-1} indicate amide III. The 1045 cm^{-1} and 995 cm^{-1} bands indicate ν_s (PO_2^-) and C-O ribose/C-C, respectively. A resume of the assignments of main vibrational modes and their respective salivary component is shown in Table 3.

Table 1: Demography characteristics of breast cancer, benign breast disease, and control patients.

Characteristics	Breast cancer $n = 10$	Benign $n = 10$	Control $n = 10$
Age (years)			
Range	42.0–75.0	33.0–49.0	22.0–63.0
Average ± SD	53.3 ± 11.2	41.5 ± 4.2	43.2 ± 16.0
History of smoking (%)	30	40	30
Family history of breast cancer (%)	40	0	0

The second-derivative infrared spectra of whole saliva of breast cancer, benign, and control patients were analyzed in detail to identify specific spectral components. The averages of the second-derivative infrared spectra of saliva for each group of patients are presented in Figure 2. The major wavenumbers detected in whole saliva were found at ~2964, 2929, 2875, 2659, 2358, 2322, and 2285 (3000 cm^{-1}—2200 cm^{-1} region, Figure 2(a)), 2059, 1635, 1544, 1450, 1404, and 1313 (2200 cm^{-1}—1300 cm^{-1} region, Figure 2(b)), and 1242, 1159, 1120, 1041, 987, 877, and 613 cm^{-1} (1300 cm^{-1}—600 cm^{-1} region, Figure 2(c)). The vibrational modes and related molecular sources of these wavenumbers are presented in Table 4.

3.3. Prevalidation as Diagnostic Potential by ROC Curve and Pearson Correlation. Considering that sensitivity and specificity are basic characteristics to determine the accuracy of a diagnostic test, ROC analysis were used to ascertain the potential diagnosis of each vibrational modes of the original and second-derivative spectrum. A resume of statistical analysis (mean ± SD; t-test; ROC curve P value, sensitivity, and specificity) of all FTIR vibrational modes of the second-derivative spectra (described in Figure 2) are presented as supplementary material in Table S1. Here, we show our results with more potential diagnosis between all bands analyzed, peak 1041 cm^{-1}, and region between 1433 cm^{-1} and 1302.9 cm^{-1}. The comparison of the 1041 cm^{-1} salivary vibrational mode in the second derivative of breast cancer, benign, and control patients is presented in Figure 3. This salivary vibrational mode was increased ($P < 0.05$) in breast cancer than in benign patients. However, this vibrational mode was similar ($P > 0.05$) in breast cancer patients and matched controls. Specifically, the vibrational mode showed higher absorption in breast cancer than in benign patients ($P = 0.039$), and no matched significant difference compared with the controls ($P = 0.094$). As expected, the 1041 cm^{-1} salivary vibrational mode was similar ($P = 0.740$) in control and benign patients (Figure 3(a)). Since the 1041 cm^{-1} salivary vibrational mode can be used to discriminate breast cancer and benign patients, we evaluated the ROC curve and calculated the area under the curve

Table 2: Clinical, hormonal, diagnostic, and therapy characteristics of breast cancer patients.

Variable	Patients ($n = 10$)	
	N	%
Histological subtype		
Invasive ductal carcinoma	6	60
In situ ductal carcinoma	3	30
Mucinous carcinoma	1	10
Histological grade		
G2	5	50
G3	2	20
NR	3	30
Primary tumor		
ptx	1	10
pTis	3	30
pT1	4	40
pT2	2	20
Regional lymph nodes		
pNX	2	20
pN0	5	50
pN1	1	10
pN2	1	10
NR	1	10
Distant metastases		
pM0	7	70
NR	3	30
TNM staging		
0	2	20
I	1	10
II	2	20
NR	5	50
Status ER		
Positive	8	80
NR	2	20
Status PR		
Positive	8	80
NR	2	20
Status HER2		
Positive	2	20
Negative	6	60
NR	2	20
p53		
Positive	8	80
NR	2	20
Ki67		
≤14%	5	50
>14%	3	30
NR	2	20
Molecular phenotype		
Luminal A	4	40
Luminal B	4	40
NR	2	20
Therapy		
Surgery (S)	1	10
S + radiotherapy (RT)	1	10
S + RT + hormone therapy (HT)	3	30
S + RT + HT + chemotherapy (CT)	5	50

G1, grade 1; G2, grade 2; G3, grade 3; NR, not reported; ER, estrogen receptor; PR, progesterone receptor; HER2, human epidermal growth factor receptor 2; p53, tumor protein p53; ki67, antigen ki67.

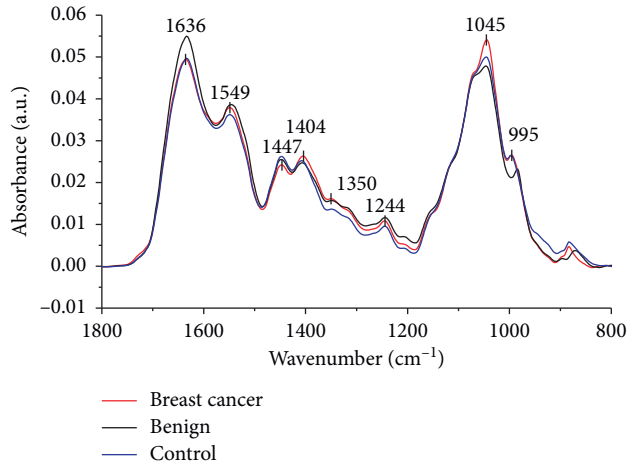

Figure 1: FTIR spectra for breast cancer, benign breast disease, and control saliva. Average original spectra with the absorbance bands of the major functional groups in biomolecules indicated between wavenumbers 1800 cm^{-1} and 800 cm^{-1} for breast cancer (red line), benign breast disease (black line), and control saliva (blue line).

Table 3: Assignments of main wavenumbers indicated in the average original saliva ATR-FTIR spectra of Figure 1 and assignments based on different references [45–48].

Peak (cm^{-1})	Proposed vibrational mode	Molecular source
1636	Amide I [ν (C=O), ν (C–N), δ (N–H)]	Protein
1549	Amide II [ν (N–H), ν (C–N)]	Protein
1447	CH_3 asymmetric bending [δ_{as} (CH_3)]	Protein (methyl groups)
1404	COO^- symmetric stretching [ν_s (COO^-)]	Lipid (fatty acids)/Protein (amino acids)
1350 1244	Amide III [ν (C–N)]	Protein
1045	C-O stretching, C-O bending of the C-OH groups [ν (C-O), δ (C-O)]	Carbohydrates (glycogen glucose, fructose)
995	C-O ribose/C-C; RNA uracil ring stretching	Nucleic acid (RNA)

ν = stretching vibrations, δ = bending vibrations, s = symmetric vibrations, as = asymmetric vibrations.

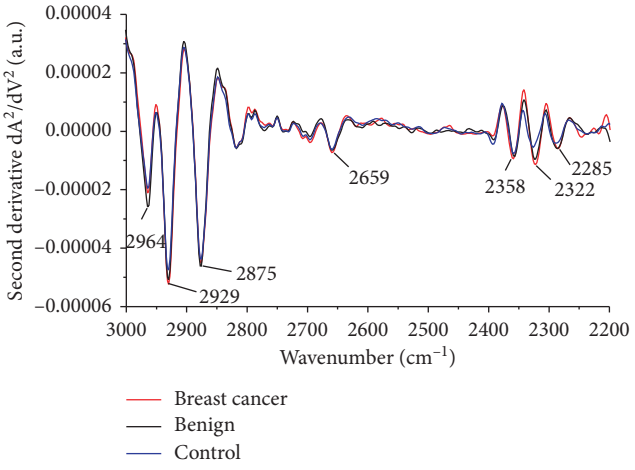

(a)

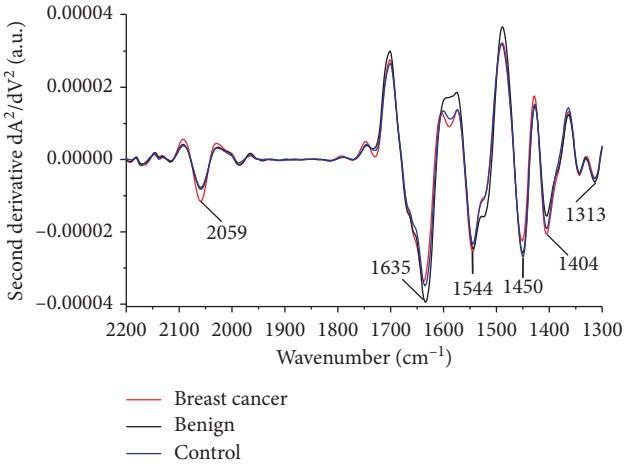

(b)

Figure 2: Continued.

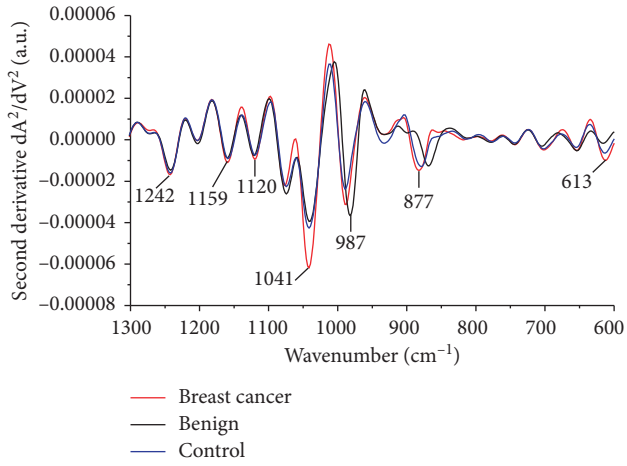

(c)

Figure 2: Detailed average second-derivative spectra and major wavenumbers. Average spectra between (a) 3000 cm^{-1} and 2200 cm^{-1}, (b) 2200 cm^{-1} and 1300 cm^{-1}, and (c) 1300 cm^{-1} and 600 cm^{-1} for breast cancer (red line), benign breast disease (black line), and control saliva (blue line).

Table 4: Assignments of FTIR peaks of the average second-derivative spectra and assignments based on different references [45–51].

2^{nd} derivative peak (cm^{-1})	Proposed vibrational mode	Molecular source
2964	CH_3 asymmetric stretching (ν_{as} (CH_3))	Lipid
2929	CH_2 asymmetric stretching (ν_{as} (CH_2))	Nucleic acid/Lipid
2875	CH_3 symmetric stretching (ν_s (CH_3))	Lipid
2659	Unassigned band	
2358	O=C=O stretching	Carbon dioxide
2322	Unassigned band	
2285	N=C=O stretching	Nitrile
2059	C-N stretching of thiocyanate anions (SCN^-)	Thiocyanate
1635	Amide I (β-sheet structure)	Protein
1544	Amide II	Protein
1450	CH_2 symmetric bending (δ_s (CH_2)) Methylene bending	Lipid and protein
1404	CH_3 symmetric bending (δ_s (CH_3))	Protein (methyl groups)
1313	Amide III	Protein
1242	Amide III PO_2^- asymmetric stretching (ν_{as} (PO_2^-))	Protein Nucleic acid
1159	C-O stretching (ν (C-O)) CO–O–C asymmetric stretching (ν_{as} (CO-O-C))	Protein/CarbohydrateLipid
1120	Phosphorylated saccharide residue Mannose-6-phosphate	Carbohydrate Protein (glycoprotein)
1041	PO_2^- symmetric stretching (ν_s (PO_2^-))	Nucleic acid (RNA/DNA) and glycogen
987	C=C bending	Monosaccharides and polysaccharides
877	C_3, *endo/anti A*-form helix	Nucleic acid
613	C-H out-of-plane bending	Cell membranes

ν = stretching vibrations, δ = bending vibrations, s = symmetric vibrations, as = asymmetric vibrations.

(AUC) (Figures 3(b) and 3(c)). The ROC curve analysis shows a reasonable accuracy of ATR-FTIR tool to discriminate breast cancer from benign and control patients, with an AUC of 0.770 for breast cancer vs. control and an AUC of 0.765 for breast cancer vs. benign patients. Using the ROC curve, it was possible to select the optimal cutoff that distinguished breast cancer patients. This yielded a sensitivity of 80% and a specificity of 70% for breast cancer vs. control and a sensitivity of 70% and a specificity of 70% for breast cancer vs. benign patients.

Considering the difference of the salivary original spectra in the region between 1433 cm^{-1} and 1302.9 cm^{-1}, we performed quantitative analysis in breast cancer, benign, and control patients (Figure 4). The 1433–1302.9 cm^{-1} salivary wavenumber range was higher in breast cancer than in benign patients ($P = 0.0451$) and matched control ($P = 0.0123$) patients. It is important to note that the vibrational mode was similar in benign patients and control ($P = 0.5656$) (Figure 4(a)). Since 1433–1302.9 salivary band area seems to be important for the discrimination of breast

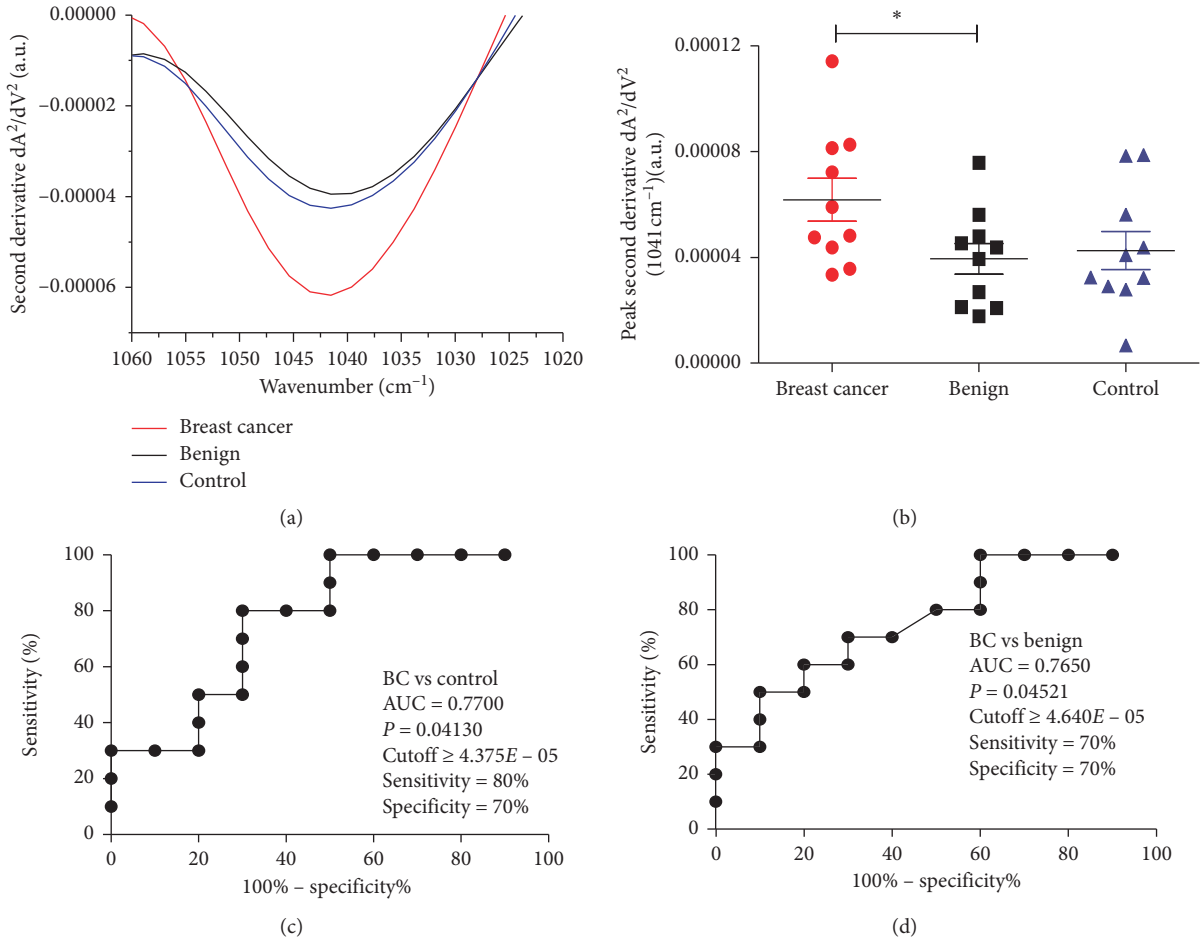

FIGURE 3: Comparison of the second-derivative absorbance of the statistically significant peak 1041 cm^{-1} between the three study groups. (a) Average second-derivative spectra between 1060–1020 cm^{-1} highlighting the wavenumber 1041 cm^{-1} for breast cancer (red line), benign breast disease (black line), and control saliva (blue line). (b) Scatter plot of the statistically significant wavenumber 1041 cm^{-1} for breast cancer (red), benign breast disease (black), and control saliva (blue). The line represents the mean, and the error bars (whiskers) represent the standard error of the mean (SEM) ($^*P < 0.05$, comparison of groups via the unpaired t-test with Welch's correction). ROC curves made from the wavenumber 1041 cm^{-1} for (c) breast cancer vs. control and (d) breast cancer vs. benign breast disease. Results about area under the curve (AUC), P value, cutoff, sensitivity, and specificity are being shown near the ROC curve. Statistically significant differences are represented by * ($^*P < 0.05$).

cancer from benign and control patients, we also evaluated the ROC curve between breast cancer and controls (Figure 4(b)) and between breast cancer and benign patients (Figure 4(c)). The ROC curve analysis shows a good accuracy of the ATR-FTIR tool to discriminate between breast cancer and the other groups of patients. The AUC of 1433–1302.9 salivary band area was 0.835 for breast cancer vs. control and 0.770 for breast cancer vs. benign patients. Using the ROC curve, it was possible to select the optimal cutoff that distinguished the groups of patients. This yielded a sensitivity of 90% and a specificity of 80% for breast cancer vs. control and a sensitivity of 90% and a specificity of 70% for breast cancer vs. benign patients.

4. Discussion

Our present data support our hypothesis that ATR-FTIR vibrational modes of saliva may discriminate breast cancer from benign and matched-control patients. Here, we have identified new salivary ATR-FTIR spectral biomarkers for breast cancer screening. The 1041 cm^{-1} salivary vibrational mode in the second-derivative spectra and the 1433–1302.9 cm^{-1} wavenumber region in the original spectra could potentially be used as salivary biomarkers to discriminate breast cancer from benign and matched-control patients with very good accuracy.

Our most potential spectral biomarker at 1433–1302.9 cm^{-1} was able to discriminate human BC from controls with sensitivity and specificity of 90% and 80%, respectively. Besides, it was able to differentiate BC from benign disease with sensitivity and specificity of 90% and 70%, respectively. Considering that mammography, ultrasound, and MRI, the conventional techniques used in clinical practice, show sensitivities of 67.8%, 83%, and 94.4% and specificities of 75%, 34%, and 26.4%, respectively [52], we believe that our results could improve the accuracy

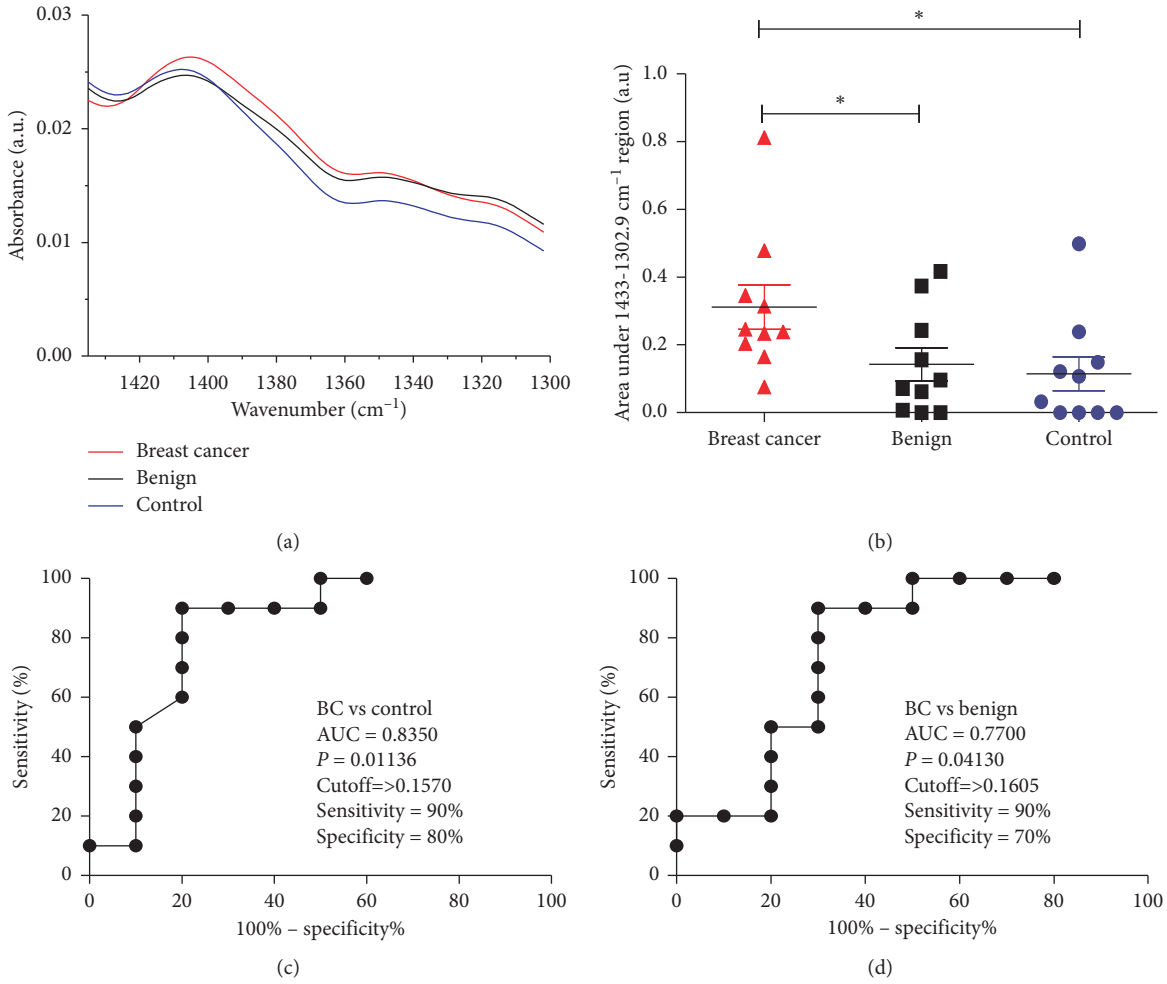

Figure 4: Comparison of the area under the 1433 cm^{-1} and 1302.9 cm^{-1} wavenumber region between the three study groups. (a) Average original spectra highlighting the 1433–1302.9 cm^{-1} region for breast cancer (red line), benign breast disease (black line), and control saliva (blue line). (b) Scatter plot of the 1433 cm^{-1} and 1302.9 cm^{-1} region for breast cancer (red), benign breast disease (black), and control saliva (blue). The line represents the mean, and the error bars (whiskers) represent the standard error of the mean (SEM) ($^*P < 0.05$, pairwise comparison of groups via the Mann–Whitney test). ROC curves made from area under the 1433 cm^{-1} and 1302.9 cm^{-1} region for (c) breast cancer vs. control and (d) breast cancer vs. benign breast disease. Results about area under the curve (AUC), P value, cutoff, sensitivity, and specificity are being shown near the ROC curve. Statistically significant differences are represented by * ($^*P < 0.05$).

obtained for breast cancer diagnosis. However, in order to perform the conventional diagnosis, high-end equipments and facilities are required with significant clinical costs. Furthermore, circulating biomarkers have also been used as indicators of breast cancer; however, none of them has reached adequate sensitivity and specificity, limiting their clinical applicability in breast cancer diagnosis [53]. Infrared spectroscopy allows analyzing the entire biochemical signature (including proteins, lipids, nucleic acids, and carbohydrates) of a biological sample rather than focusing on a single specific protein as a biomarker [25]. Therefore, the salivary ATR-FTIR spectra are highly desirable due to their speed, convenience, and cost effectiveness, strongly suggesting this diagnostic platform for breast cancer screening.

ROC curve analysis is widely considered to be the most objective and statistically valid method for biomarker performance evaluation. In the current study, the ROC curve analysis showed reasonable accuracy for the salivary 1041 cm^{-1} level of second-derivative ATR-FTIR spectra and good accuracy for the 1433–1302.9 band area. The salivary 1041 cm^{-1} level of second-derivative ATR-FTIR spectra was increased in breast cancer patients compared with benign patients. Surprisingly, despite the absence of significant difference between breast cancer patients and controls, this spectral biomarker candidate exhibited significant diagnostic value with an AUC of 0.7700 comparing breast cancer patients than controls. Additionally, it also exhibited significant diagnostic value with similar AUC to compare breast cancer and benign patients. Therefore, this salivary spectral ATR-FTIR biomarker is a compatible complementary alternative to improve diagnosis of breast cancer. The 1433–1302.9 band area was elevated in saliva of breast cancer patients as compared with control and benign patients, and this band area showed a high sensitivity and

specificity to discriminate breast cancer from both controls and benign patients, being prevalidated as a salivary ATR-FTIR biomarker of breast cancer by ROC curve analysis. The discriminatory power of this biomarker candidate for breast cancer reached 90% of specificity and 80% of sensitivity from matched controls and 90% of specificity and 70% of sensitivity from benign patients. As to potential for clinic application, these data strongly indicate that the salivary band area of the 1433–1302.9 cm^{-1} region had a high capacity do discriminate patients with breast cancer from healthy and benign patients. It is important to note that the salivary band area of the 1433–1302.9 cm^{-1} region was similar between benign and control, which is in concordance with blood test analysis [25].

It is known that increase in absorbance in each specific spectral vibrational mode represents increase in the presence of a specific biomolecule [44]. The increase in absorbance levels of breast cancer patients at the 1041 cm^{-1} vibrational mode is due to increased levels of PO_2^- symmetric stretching [ν_s (PO_2^-)], which is present in nucleic acids and glycogen. Previous studies on cancer cells and tissues using FTIR spectroscopy also reported many changes in the phosphate region, which corresponds mainly to nucleic acids and carbohydrates [25]. The increased level in the 1433–1302.9 cm^{-1} region is due to increased levels of COO^- symmetric stretching [ν_s (COO^-)], which is present in proteins and lipids.

Considering the higher expression of PO_2 symmetric stretching (ν_s (PO_2^-)) and COO^- symmetric stretching (ν_s (COO^-)) in saliva of breast cancer patients, we suggest that these molecules are originated from blood and access saliva by passive diffusion of lipophilic molecules (e.g., steroid hormones) or active transport of proteins via ligand-receptor binding [35]. Hence, saliva may present biomarkers that reflect the pathophysiological state of the body, such as, breast cancer. There are numerous putative salivary molecular biomarkers that are probably altered in the presence of breast cancer. Higher levels of some proteins [54–56], carbohydrates [52], and nucleic acids [47] have already been found in the saliva of breast cancer patients in comparison with normal controls, which corroborates with the results found in this study. In general, these biomarkers were evaluated by proteomic, immunological, and biomolecular techniques.

Higher levels of many proteins were observed in the saliva of breast cancer patients, such as (a) vascular endothelial growth factor (VEGF) and epidermal growth factor (EGF), which are potent angiogenic factors; (b) carcinoembryonic antigen (CEA) that is a glycoprotein and well-established serum tumor marker for breast cancer [54]; (c) soluble form of HER2 protein, that is a receptor tyrosine kinase, product of c-erbB-2 oncogene, and marker of poor prognosis [55]; and (d) p53 that is a tumor suppressor protein product of oncogene p53, it regulates target genes that induce cell cycle arrest, apoptosis, senescence, DNA repair, or changes in metabolism, and it is the indicator of poor clinical outcome [56].

One limitation of our study is the relatively small number of patients and the need for larger multicenter studies to confirm our results. Another limitation of this study is the lack of information about the specificity of this salivary ATR-FTIR spectral biomarker in breast cancer, especially considering that other cancers may also exhibit similar changes. Therefore, further studies are needed to evaluate the diagnostic performance of these spectral ATR-FTIR biomarkers of saliva in other cancers.

5. Conclusions

In conclusion, the present study showed for the first time that ATR-FTIR spectroscopy can be used in saliva samples to discriminate breast cancer patients than benign patients and healthy subjects. It was found absorbance levels significantly higher in saliva of breast cancer patients compared with benign patients at wavenumber 1041 cm^{-1} and the ROC curve analysis of this peak showed a reasonable accuracy to discriminate breast cancer from benign and control patients. In addition, we demonstrated that the 1433–1302.9 cm^{-1} wavenumber region was elevated in saliva of breast cancer patients as compared with control and benign patients. Our study highlighted this salivary spectral region as a biomarker with high accuracy to differentiate breast cancer from both control and benign patients. In summary, these innovative results suggest that salivary analysis by ATR-FTIR spectroscopy is a promising tool for breast cancer diagnosis.

Data Availability

The datasets generated and/or analyzed during the current study are available from the corresponding author on reasonable request.

Disclosure

The funders had no role in the design of the study; in the collection, analyses, or interpretation of data; in the writing of the manuscript; or in the decision to publish the results. The results presented in this manuscript are part of one patent application: Maia, Y. C. P.; Ferreira, I. C. C.; Goulart, L. R.; Silva, A. T. F.; Santos, L. L. D.; Aguiar, E. M. G.; Araujo, T. G.; Sousa, L. C.; and Silva, R. S. "Método para detecção de câncer de mama baseado em componentes salivares", 2018. Registration number: BR10201801530. Date of deposit: 07/26/2018."

Conflicts of Interest

There are no conflicts to declare.

Acknowledgments

The authors thank the Obstetric Division of the University Hospital of Uberlandia for help in sourcing the clinical samples and the volunteer women of this study and the Research Center for Biomechanics, Biomaterials, and Cell Biology of the Federal University of Uberlandia for allowing us to use the ATR-FTIR spectrometer Bruker VERTEX 70/

70v and acquire the spectral images. This research was funded by CNPq (#458143/2014 and #449938/2014-0); FAPEMIG (#APQ-02872-16 and #APQ-01154-14); National Institute of Science and Technology in Theranostics and Nanobiotechnology - INCT - Teranano (CNPq Process N.: 465669/2014-0); CAPES and FAU - Fundação de Apoio Universitário - Universidade Federal de Uberlândia.

Supplementary Materials

The supplementary material file includes Table S1 that shows a resume of statistical analysis (mean ± SD; *t*-test; ROC curve *P* value, sensitivity, and specificity) of all FTIR peaks of the second-derivative spectra shown in Figure 2. (*Supplementary Materials*)

References

[1] E.-H. Koh, Y.-W. Cho, Y.-J. Mun et al., "Upregulation of human mammaglobin reduces migration and invasion of breast cancer cells," *Cancer Investigation*, vol. 32, no. 1, pp. 22–29, 2014.

[2] S. Ghersevich and M. P. Ceballos, "Mammaglobin A," *Advances in Clinical Chemistry*, vol. 64, pp. 241–268, 2014.

[3] IARC, *World Cancer Report 2014*, B. W. Stewart and C. P. Wild, Eds., IARC Publications, Lyon, France, 2014.

[4] J. Depciuch, E. Kaznowska, I. Zawlik et al., "Application of Raman spectroscopy and infrared spectroscopy in the identification of breast cancer," *Applied Spectroscopy*, vol. 70, no. 2, pp. 251–263, 2016.

[5] M. Tria Tirona, "Breast cancer screening update," *American Family Physician*, vol. 87, no. 4, pp. 274–278, 2013.

[6] K. M. Elkins, "Rapid presumptive "fingerprinting" of body fluids and materials by ATR FT-IR spectroscopy," *Journal of Forensic Sciences*, vol. 56, no. 6, pp. 1580–1587, 2011.

[7] D. Simonova and I. Karamancheva, "Application of fourier transform infrared spectroscopy for tumor diagnosis," *Biotechnology & Biotechnological Equipment*, vol. 27, no. 6, pp. 4200–4207, 2013.

[8] A. A. Bunaciu, V. D. Hoang, and H. Y. Aboul-Enein, "Applications of FT-IR spectrophotometry in cancer diagnostics," *Critical Reviews in Analytical Chemistry*, vol. 45, no. 2, pp. 156–165, 2015.

[9] A. Barth, "Infrared spectroscopy of proteins," *Biochimica et Biophysica Acta (BBA)—Bioenergetics*, vol. 1767, no. 9, pp. 1073–1101, 2007.

[10] C. A. Lima, V. P. Goulart, L. Correa, T. M. Pereira, and D. M. Zezell, "ATR-FTIR spectroscopy for the assessment of biochemical changes in skin due to cutaneous squamous cell carcinoma," *International Journal of Molecular Sciences*, vol. 16, no. 4, pp. 6621–6630, 2015.

[11] R. Lane and S. S. Seo, "Attenuated total reflectance Fourier transform infrared spectroscopy method to differentiate between normal and cancerous breast cells," *Journal of Nanoscience and Nanotechnology*, vol. 12, no. 9, pp. 7395–7400, 2012.

[12] X. Zhang, Y. Xu, Y. Zhang et al., "Intraoperative detection of thyroid carcinoma by fourier transform infrared spectrometry," *Journal of Surgical Research*, vol. 171, no. 2, pp. 650–656, 2011.

[13] N. S. Eikje, K. Aizawa, and Y. Ozaki, "Vibrational spectroscopy for molecular characterisation and diagnosis of benign, premalignant and malignant skin tumours," *Biotechnology Annual Review*, vol. 11, pp. 191–225, 2005.

[14] M. Beekes, P. Lasch, and D. Naumann, "Analytical applications of Fourier transform-infrared (FT-IR) spectroscopy in microbiology and prion research," *Veterinary Microbiology*, vol. 123, no. 4, pp. 305–319, 2007.

[15] J. Depciuch, E. Kaznowska, S. Golowski et al., "Monitoring breast cancer treatment using a Fourier transform infrared spectroscopy-based computational model," *Journal of Pharmaceutical and Biomedical Analysis*, vol. 143, pp. 261–268, 2017.

[16] C. Krafft, L. Shapoval, S. B. Sobottka, G. Schackert, and R. Salzer, "Identification of primary tumors of brain metastases by infrared spectroscopic imaging and linear discriminant analysis," *Technology in Cancer Research & Treatment*, vol. 5, no. 3, pp. 291–298, 2006.

[17] P. Tian, W. Zhang, H. Zhao et al., "Intraoperative detection of sentinel lymph node metastases in breast carcinoma by Fourier transform infrared spectroscopy," *British Journal of Surgery*, vol. 102, no. 11, pp. 1372–1379, 2015.

[18] A. Benard, C. Desmedt, M. Smolina et al., "Infrared imaging in breast cancer: automated tissue component recognition and spectral characterization of breast cancer cells as well as the tumor microenvironment," *The Analyst*, vol. 139, no. 5, pp. 1044–1056, 2014.

[19] S. Rehman, Z. Movasaghi, J. A. Darr, and I. U. Rehman, "Fourier transform infrared spectroscopic analysis of breast cancer tissues; identifying differences between normal breast, invasive ductal carcinoma, and ductal carcinoma in situ of the breast," *Applied Spectroscopy Reviews*, vol. 45, no. 5, pp. 355–368, 2010.

[20] D. C. Malins, N. L. Polissar, K. Nishikida, E. H. Holmes, H. S. Gardner, and S. J. Gunselman, "The etiology and prediction of breast cancer. Fourier transform-infrared spectroscopy reveals progressive alterations in breast DNA leading to a cancer-like phenotype in a high proportion of normal women," *Cancer*, vol. 75, no. 2, pp. 503–517, 1995.

[21] C. M. Krishna, G. Kegelaer, I. Adt et al., "Combined Fourier transform infrared and Raman spectroscopic approach for identification of multidrug resistance phenotype in cancer cell lines," *Biopolymers*, vol. 82, no. 5, pp. 462–470, 2006.

[22] A. Mignolet and E. Goormaghtigh, "High throughput absorbance spectra of cancerous cells: a microscopic investigation of spectral artifacts," *The Analyst*, vol. 140, no. 7, pp. 2393–2401, 2015.

[23] S. Kumar, C. Desmedt, D. Larsimont, C. Sotiriou, and E. Goormaghtigh, "Change in the microenvironment of breast cancer studied by FTIR imaging," *The Analyst*, vol. 138, no. 14, pp. 4058–4065, 2013.

[24] I. Zawlik, E. Kaznowska, J. Cebulski et al., "FPA-FTIR microspectroscopy for monitoring chemotherapy efficacy in triple-negative breast cancer," *Scientific Reports*, vol. 6, no. 1, p. 37333, 2016.

[25] U. Zelig, E. Barlev, O. Bar et al., "Early detection of breast cancer using total biochemical analysis of peripheral blood components: a preliminary study," *BMC Cancer*, vol. 15, no. 1, p. 408, 2015.

[26] S. H. Chen, W. W. Lao, Z. X. Xu, Q. Liu, H. Wen, and H. Deng, "Fourier transform infrared spectroscopy in detection of breast cancer," *Zhejiang Da Xue Xue Bao Yi Xue Ban*, vol. 43, no. 4, pp. 494–500, 2014.

[27] J. Backhaus, R. Mueller, N. Formanski et al., "Diagnosis of breast cancer with infrared spectroscopy from serum samples," *Vibrational Spectroscopy*, vol. 52, no. 2, pp. 173–177, 2010.

[28] M. Khanmohammadi, F. H. Rajabi, A. B. Garmarudi, R. Mohammadzadeh, and R. Mohammadzadeh, "Chemometrics assisted investigation of variations in infrared spectra of blood samples obtained from women with breast cancer: a new approach for cancer diagnosis," *European Journal of Cancer Care*, vol. 19, no. 3, pp. 352–359, 2010.

[29] M. Verdonck, A. Denayer, B. Delvaux et al., "Characterization of human breast cancer tissues by infrared imaging," *The Analyst*, vol. 141, no. 2, pp. 606–619, 2016.

[30] R. Mehrotra, A. Gupta, A. Kaushik, N. Prakash, and H. Kandpal, "Infrared spectroscopic analysis of tumor pathology," *Indian Journal of Experimental Biology*, vol. 45, no. 1, pp. 71–76, 2007.

[31] H. Fabian, N. A. N. Thi, M. Eiden, P. Lasch, J. Schmitt, and D. Naumann, "Diagnosing benign and malignant lesions in breast tissue sections by using IR-microspectroscopy," *Biochimica et Biophysica Acta (BBA)—Biomembranes*, vol. 1758, no. 7, pp. 874–882, 2006.

[32] B. B. Wu, Y. P. Gong, X. H. Wu et al., "Fourier transform infrared spectroscopy for the distinction of MCF-7 cells treated with different concentrations of 5-fluorouracil," *Journal of Translational Medicine*, vol. 13, no. 1, p. 108, 2015.

[33] E. Gavgiotaki, G. Filippidis, H. Markomanolaki et al., "Distinction between breast cancer cell subtypes using third harmonic generation microscopy," *Journal of Biophotonics*, vol. 10, no. 9, pp. 1152–1162, 2016.

[34] R. Pink, J. Simek, J. Vondrakova et al., "Saliva as a diagnostic medium," *Biomedical Papers*, vol. 153, no. 2, pp. 103–110, 2009.

[35] T. Pfaffe, J. Cooper-White, P. Beyerlein, K. Kostner, and C. Punyadeera, "Diagnostic potential of saliva: current state and future applications," *Clinical Chemistry*, vol. 57, no. 5, pp. 675–687, 2011.

[36] A. Wang, C. P. Wang, M. Tu, and D. T. Wong, "Oral biofluid biomarker research: current status and emerging frontiers," *Diagnostics*, vol. 6, no. 4, 2016.

[37] C.-Z. Zhang, X.-Q. Cheng, J.-Y. Li et al., "Saliva in the diagnosis of diseases," *International Journal of Oral Science*, vol. 8, no. 3, pp. 133–137, 2016.

[38] A. L. P. Abrão, D. P. Falcao, R. F. B. de Amorim et al., "Salivary proteomics: a new adjuvant approach to the early diagnosis of familial juvenile systemic lupus erythematosus," *Medical Hypotheses*, vol. 89, pp. 97–100, 2016.

[39] D. Malamud, "Saliva as a diagnostic fluid," *Dental Clinics of North America*, vol. 55, no. 1, pp. 159–178, 2011.

[40] L. R. Bigler, C. F. Streckfus, and W. P. Dubinsky, "Salivary biomarkers for the detection of malignant tumors that are remote from the oral cavity," *Clinics in Laboratory Medicine*, vol. 29, no. 1, pp. 71–85, 2009.

[41] F. Agha-Hosseini, I. Mirzaii-Dizgah, and A. Rahimi, "Correlation of serum and salivary CA15-3 levels in patients with breast cancer," *Medicina Oral Patología Oral y Cirugia Bucal*, vol. 14, no. 10, pp. 521–524, 2009.

[42] A. E. Giuliano, J. L. Connolly, S. B. Edge et al., "Breast Cancer-Major changes in the American Joint Committee on Cancer eighth edition cancer staging manual," *CA: A Cancer Journal for Clinicians*, vol. 67, no. 4, pp. 290–303, 2017.

[43] S. Khaustova, M. Shkurnikov, E. Tonevitsky, V. Artyushenko, and A. Tonevitsky, "Noninvasive biochemical monitoring of physiological stress by Fourier transform infrared saliva spectroscopy," *The Analyst*, vol. 135, no. 12, pp. 3183–3192, 2010.

[44] P. D. Lewis, K. E. Lewis, R. Ghosal et al., "Evaluation of FTIR Spectroscopy as a diagnostic tool for lung cancer using sputum," *BMC Cancer*, vol. 10, no. 1, p. 640, 2010.

[45] B. H. Stuart, "Biological applications," in *Infrared Spectroscopy: Fundamentals and Applications*, pp. 137–165, John Wiley & Sons, Hoboken, NJ, USA, 2005.

[46] Z. Movasaghi, S. Rehman, and D. I. ur Rehman, "Fourier transform infrared (FTIR) spectroscopy of biological tissues," *Applied Spectroscopy Reviews*, vol. 43, no. 2, pp. 134–179, 2008.

[47] G. Bellisola and C. Sorio, "Infrared spectroscopy and microscopy in cancer research and diagnosis," *American Journal of Cancer Research*, vol. 2, no. 1, pp. 1–21, 2012.

[48] C.-M. Orphanou, L. Walton-Williams, H. Mountain, and J. Cassella, "The detection and discrimination of human body fluids using ATR FT-IR spectroscopy," *Forensic Science International*, vol. 252, pp. e10–e16, 2015.

[49] B. H. Stuart, "Infrared spectroscopy of biological applications: an overview," in *Encyclopedia of Analytical Chemistry*, John Wiley & Sons, Hoboken, NJ, USA, 2012.

[50] C. P. Schultz, M. K. Ahmed, C. Dawes, and H. H. Mantsch, "Thiocyanate levels in human saliva: quantitation by Fourier transform infrared spectroscopy," *Analytical Biochemistry*, vol. 240, no. 1, pp. 7–12, 1996.

[51] L. M. Rodrigues, T. D. Magrini, C. F. Lima, J. Scholz, H. da Silva Martinho, and J. D. Almeida, "Effect of smoking cessation in saliva compounds by FTIR spectroscopy," *Spectrochimica Acta Part A: Molecular and Biomolecular Spectroscopy*, vol. 174, pp. 124–129, 2017.

[52] L. Wang, "Early diagnosis of breast cancer," *Sensors*, vol. 17, no. 7, p. 1572, 2017.

[53] C. Van Poznak, M. R. Somerfield, R. C. Bast et al., "Use of biomarkers to guide decisions on systemic therapy for women with metastatic breast cancer: American society of clinical oncology clinical practice guideline," *Journal of Clinical Oncology*, vol. 33, no. 24, pp. 2695–2704, 2015.

[54] M. N. Brooks, J. Wang, Y. Li, R. Zhang, D. Elashoff, and D. T. Wong, "Salivary protein factors are elevated in breast cancer patients," *Molecular Medicine Reports*, vol. 1, no. 3, pp. 375–378, 2008.

[55] C. Streckfus, L. Bigler, T. Dellinger, X. Dai, A. Kingman, and J. T. Thigpen, "The presence of soluble c-erbB-2 in saliva and serum among women with breast carcinoma: a preliminary study," *Clinical Cancer Research*, vol. 6, no. 6, pp. 2363–2370, 2000.

[56] C. Streckfus, L. Bigler, M. Tucci, and J. T. Thigpen, "A preliminary study of CA15-3, c-erbB-2, epidermal growth factor receptor, cathepsin-D, and p53 in saliva among women with breast carcinoma," *Cancer Investigation*, vol. 18, no. 2, pp. 101–109, 2000.

Hindawi
Journal of Oncology
Volume 2019, Article ID 1781762, 8 pages
https://doi.org/10.1155/2019/1781762

Research Article

Exploring the Role of Breast Density on Cancer Prognosis among Women Attending Population-Based Screening Programmes

Laia Domingo,[1,2] Maria Sala,[1,2] Javier Louro,[1,2] Marisa Baré,[2,3,4] Teresa Barata,[5] Joana Ferrer,[6] Maria Carmen Carmona-Garcia,[7,8,9] Mercè Comas,[1,2] Xavier Castells,[1,2,3] and CAMISS Study Group[10]

[1]*Department of Epidemiology and Evaluation, IMIM (Hospital del Mar Medical Research Institute), Passeig Marítim, 25-29, 08003 Barcelona, Spain*
[2]*Research Network on Health Services in Chronic Diseases (REDISSEC), Barcelona, Spain*
[3]*Department of Paediatrics, Obstetrics and Gynaecology, Preventive Medicine and Public Health, Universitat Autònoma de Barcelona (UAB), 08193 Bellaterra, Barcelona, Spain*
[4]*Cancer Screening and Clinical Epidemiology, Corporació Sanitària Parc Taulí, 08208 Sabadell, Spain*
[5]*General Directorate of Health Care Programmes, Canary Islands Health Service, C/Juan XXIII, 13 35005, Las Palmas de Gran Canaria, Spain*
[6]*Department of Radiology, Hospital de Santa Caterina, C/Dr. Castany, s/n, 17190 Salt, Girona, Spain*
[7]*Epidemiology Unit and Girona Cancer Registry, Oncology Coordination Plan, Department of Health, Catalan Institute of Oncology, C/Sol, 15, Barcelona 17004, Girona, Spain*
[8]*Girona Biomedical Research Institute (IDIBGI), C/Dr Castany s/n, 17190 Salt, Girona, Spain*
[9]*Department of Medical Oncology, Catalan Institute of Oncology, University Hospital Dr. Josep Trueta, Av França s/n, 17007, Barcelona, Girona, Spain*
[10]*IMIM (Hospital del Mar Medical Research Institute), Passeig Marítim, 25-29, 08003 Barcelona, Spain*

Correspondence should be addressed to Maria Sala; 92601@parcdesalutmar.cat

Received 26 April 2019; Accepted 5 August 2019; Published 27 November 2019

Guest Editor: Chia-Jung Li

Background. Our aim was to assess the role of breast density on breast cancer mortality and recurrences, considering patient and tumour characteristics and the treatments received among women attending population-based screening programmes. *Methods*. We conducted a retrospective cohort study among women aged 50–69 years attending population-based screening programmes, diagnosed with invasive breast cancer between 2000 and 2009, and followed up to 2014. Breast density was categorised as low density (≤25% dense tissue), intermediate density (25–50%), and high density (≥50%). Cox proportional hazards regression models were fitted to estimate the adjusted hazard ratios (aHR) and 95% confidence intervals (95% CI) for death and recurrences, adjusting by patient characteristics, mode of detection (screen-detected vs. interval cancer), and tumour features. *Results*. The percentage of deaths and recurrences was higher among women with intermediate- and high-density breasts than among women with low-density breasts ($p = 0.011$ for death; $p = 0.037$ for recurrences). Adjusted Cox proportional hazards regression models revealed that women with intermediate- and high-density breasts had a higher risk of death than women with low-density breasts, being statistically significant for intermediate densities (aHR = 2.19 [95% CI: 1.16–4.13], aHR = 1.44 [95% CI: 0.67–3.1], respectively). No association was found between breast density and recurrences. *Conclusions*. Breast density was associated with a higher risk of death, but not of recurrences, among women participating in breast cancer screening. These findings reinforce the need to improve screening sensitivity among women with dense breasts and to routinely assess breast density, not only for its role as a risk factor for breast cancer but also for its potential influence on cancer prognosis.

1. Introduction

Mammographic breast density is defined as the relative amount of radiolucent elements (fatty tissue) and radiopaque elements of the breast (fibroglandular tissue). It has become a key element in breast cancer screening because of its dual effect on breast cancer risk: high breast density impairs the detection of abnormalities in the breast, decreasing the sensitivity of mammography [1], and is also an independent risk factor for breast cancer, as most cancers develop in the glandular parenchyma [2]. More recently, breast density has been postulated as a robust candidate for tailoring screening intervals, suggesting that annual screening may be more effective than biennial screening for women at high risk due to dense breasts in combination with other risk factors [3]. However, such an approach has not been implemented in any screening programme, since it requires more individual-level data, among many other unresolved issues and challenges [4].

Variations in breast density during a woman's lifetime may be influenced by several internal and external factors related to the hormonal environment. Breast density is inversely associated with age, with premenopausal women younger than 50 years being more likely to have dense breasts [5, 6]. The use of hormone replacement therapy slows the age-related trend to fatty tissue, especially for those women taking a combination of oestrogen and progestin components [7]. In addition, some studies have reported that tumours developing in dense breasts are more likely to express hormone receptors such as oestrogen receptor (ER) and progesterone receptor (PR) [8, 9], suggesting a positive association with stromal composition and the oestrogenic microenvironment.

However, whereas increased breast density is a well-recognised risk factor for breast cancer, the relationship between breast density and breast cancer prognosis is still controversial. Some studies have reported an increased risk of death for women with dense breasts [10, 11], while others have found an inverse association [12] or no relationship [13]. In addition, only few studies have been restricted to the context of mammography screening [14–16], also with contradictory results. Because this population has particular characteristics (e.g., average-risk women, women over 45/50 years, mostly postmenopausal), performing studies focused on this population may provide useful information to better understand the relationship between breast density and cancer prognosis and to eventually provide individually tailored screening strategies.

Our aim was to assess the role of breast density on mortality and recurrences, taking into account patient and tumour characteristics and the treatments received among women attending population-based screening programmes.

2. Materials and Methods

2.1. Setting and Study Population. This study was carried out among a retrospective cohort of 1,086 women with breast cancer, aged between 50 and 69 years, who underwent breast cancer screening in two Spanish regions (Catalonia and the Canary Islands; CAMISS retrospective cohort). All of them were diagnosed with breast cancer between 2000 and 2009 and were followed up until June 2014. The study included asymptomatic women with cancers detected in routine screening mammograms and symptomatic women with cancers detected between two screening mammograms (interval cancers).

Mammography screening in Spain follows the recommendations of the European Guidelines for quality assurance in breast cancer screening and diagnosis [17], offering all women aged 50 to 69 years free biennial screening. Two mammographic projections (mediolateral oblique and craniocaudal views) are made, using the BI-RADS (Breast Imaging Reporting and Data System) classification for mammogram reading [18].

As breast density is not routinely recorded by all participating screening programmes, we determined breast density for a subsample of cases. Sample size was calculated to estimate a hazard ratio of 2.5 [15], with a mortality rate of 14.5% (from the whole CAMISS cohort). With 5% significance level and 80% power, 55 subjects were needed in the high-density group. The subsample included all interval cancers with available screening and diagnostic mammograms and a random sample of screen-detected cancers, matched by screening programme and year of cancer diagnosis. After the breast density assessment, this resulted in 375 invasive breast cancers, 79 of them assigned to the high-density group, thus assuring enough sample size for the analysis.

The study protocol was approved by the Ethics Committee of Parc de Salut Mar, Barcelona (CEIC Parc de Salut Mar). Specific patient consent was not required.

2.2. Breast Density Assessment. For the purpose of this study, breast density was retrospectively evaluated by three experienced radiologists who followed a consensus-based protocol, as detailed elsewhere [19]. In brief, each radiologist determined the breast density of the cancer-free breast at the moment of diagnosis using Boyd's scale, a semiquantitative score of six categories using percentages of density: A: 0%; B: 1–10%; C: 10–25%; D: 25–50%; E: 50–75%; F: 75–100% [20]. For statistical purposes, breast density was collapsed into low (≤25% density), intermediate (25–50% density), and high density (≥50% density).

2.3. Study Variables. Patient information, including age at diagnosis, menopausal status, hormone replacement therapy (ever/never), and first-degree family history of breast cancer, was obtained from the databases of the screening programmes. To obtain information on the burden of disease at diagnosis, we manually reviewed clinical records to identify the presence of comorbidities and construct the Charlson comorbidity index (CCI) [21]. The CCI was stratified into three categories: CCI = 0, CCI = 1, and CCI ≥ 2.

Information on mode of detection was obtained from the screening programme databases and by merging data with population-based cancer registries, the hospital minimum basic dataset, and hospital-based cancer registries. We

differentiated between breast cancers detected by routine screening mammograms (i.e., screen-detected cancers) and cancers detected between 2 screening mammograms, or within 24 months for women who reached the upper age limit (i.e., interval cancers). Further details on the identification of interval cancers are explained elsewhere [19]. Tumour-related information, including tumour size, lymph node involvement, focality, histological type, histological grade, and biomarker expression, was retrieved from the cancer registries, hospital-based registries, and clinical records. Biomarker expression included information on ER, PR, human epidermal growth factor receptor 2 (Her2), p53, and Ki67 status. The positivity criteria for biomarker expression followed international recommendations and their updates throughout the study period [22, 23]. Tumours were classified into the following four phenotypes based on the expression of ER, PR, and Her2: (1) luminal A: ER+/Her2− or PR+/Her2−; (2) luminal B: ER+/Her2+ or PR+/Her2+; (3) Her2: ER−/PR−/Her2+; and (4) triple-negative: ER−, PR−, Her2− [24].

From the review of the clinical records, we obtained information on the treatments received. We considered two types of surgery: radical (including all the mastectomies performed, whether radical or simple) and conservative. Information on breast surgery and axillary lymph node dissection (ALND) treatments was collapsed into a single explicative variable. Information on adjuvant treatment was categorised as follows: chemotherapy, radiotherapy, and hormonal therapy; radiotherapy and hormonal therapy; and other treatments.

2.4. Follow-Up Information. Information on recurrences (including locoregional and distant recurrences), second breast neoplasms, and vital status at the end of follow-up (alive or dead) was obtained from the cancer registries and clinical records. Locoregional recurrence was defined as disease recurrence within the ipsilateral breast or chest wall, in the ipsilateral axillary nodes, internal mammary nodes, or supraclavicular nodes. Distant recurrence was defined as disease recurrence in sites other than the breast or regional lymph nodes (bone, skin, or visceral metastasis). A second neoplasm was considered as a second primary carcinoma developing in the ipsilateral or contralateral breast.

Overall survival was computed from the date of breast cancer diagnosis to death from any cause. Patients were censored at the date of their last hospital visit. Recurrence-free survival was computed from the date of breast cancer diagnosis to the first locoregional or distant recurrence, whichever occurred first. Women lost to follow-up or those who died were censored either at the last visit or at death. The median follow-up period was 8.7 years (interquartile range (IQR): 7.2–10.6).

2.5. Statistical Analyses. Descriptive analyses of patient and tumour characteristics and the treatments received according to breast density categories were explored using contingency tables.

Survival curves for overall mortality and for recurrences were generated by using the Kaplan–Meier method and were compared by the log-rank test. Recurrence-free survival and overall survival were plotted by breast density categories. 5-year and 10-year survival rates and their 95% confidence intervals (95% CI) were computed.

We fitted two multivariate Cox proportional hazards regression models to estimate the hazard ratios (HR) and their 95% CI for death and recurrences using a stepwise backward variable selection approach. The initial model included all predictors. In the final models, we forced to include age, screening programme, and CCI as adjusting variables, although they were not statistically significant. The proportional hazards assumption was ascertained by assessment of log-log survival plots. To test the statistical significance of breast density variable as a whole, we performed a Wald test in both models.

All statistical tests were two-sided. p values <0.05 were considered statistically significant. Analyses were performed using the statistical software IBM SPSS Statistics version 23.0 (Armonk, NY, USA) and R statistical software version 3.3.2 (http://www.r-project.org).

3. Results

A total of 375 invasive breast cancers were included in this study, most of them detected among women with low-density breasts (51.2%, 27.7%, and 21.1% of tumours detected in women with low-, intermediate-, and high-density breasts).

Patient characteristics by breast density categories are summarized in Table 1. Percentages of women with low breast density were highest among older and post-menopausal women. No differences were observed between a family history of breast cancer, the use of hormone replacement therapy or comorbidities, and breast density categories.

Tumour characteristics according to breast density categories are shown in Table 2. Screen-detected cancers were more common among women with low-density breasts, whereas interval cancers were more frequent in intermediate- and high-density breasts. Tumours detected in low-density breasts showed a trend to be smaller, node-negative, unifocal, and triple-negative. No differences were observed among the treatments received, although the percentage of radical surgery tended to be higher among women with dense breasts.

Kaplan–Meier curves revealed poorer overall survival ($p = 0.010$) and poorer relapse-free survival ($p = 0.032$) among women with high-density breasts (Figure 1). 5-year overall survival rate for women with low breast density was 0.97 (95% CI: 0.94–1.00), whereas figures for women with high breast density were 0.83 (95% CI: 0.72–0.96). The same pattern was observed at 10 years of follow-up. Recurrence-free survival rate at 5 years was 0.97 (0.94–1.00) for women with low breast density and 0.81 (0.69–0.95) for women with high breast density (Table 3).

Adjusted Cox proportional hazards regression models revealed that breast density was statistically significant for

Table 1: Patient-related characteristics by breast density categories.

	Total $n = 375$ (%)	Low breast density (<25%) $n = 192$ (%)	Intermediate breast density (25–50%) $n = 104$ (%)	High breast density (>50%) $n = 79$ (%)
Age groups (years)				
50–54	106 (28.3)	34 (17.7)	33 (31.7)[a]	39 (49.4)
55–59	102 (27.2)	50 (26)	33 (31.7)	19 (24.1)
60–64	103 (27.5)	64 (33.3)	24 (23.1)	15 (19)
65–70	64 (17.1)	44 (22.9)	14 (13.5)	6 (7.6)
Menopausal status				
Premenopause	31 (13.3)	5 (4.7)	9 (12.3)	17 (32.1)
Menopause	202 (86.7)	102 (95.3)	64 (87.7)	36 (67.9)
Hormone replacement therapy				
No	192 (85)	86 (84.3)	60 (84.5)	46 (86.8)
Yes	34 (15)	16 (15.7)	11 (15.5)	7 (13.2)
Family history of breast cancer				
No	200 (86.6)	90 (85.7)	63 (86.3)	47 (88.7)
Yes	31 (13.4)	15 (14.3)	10 (13.7)	6 (11.3)
Charlson comorbidity index				
0	285 (76)	143 (74.5)	79 (76)	63 (79.7)
1	53 (14.1)	31 (16.1)	13 (12.5)	9 (11.4)
2	37 (9.9)	18 (9.4)	12 (11.5)	7 (8.9)

predicting mortality (Wald test p value = 0.050) but not for predicting recurrences (Wald test p value = 0.499). Women with intermediate- and high-density breasts had a higher risk of death than women with low-density breasts, reaching statistical significance for intermediate densities (Table 4) (aHR = 2.19 [95% CI: 1.16–4.13], aHR = 1.44 [95% CI: 0.67–3.10], for intermediate and high densities, respectively). Tumours arising as interval cancers (aHR = 1.96 [95% CI: 1.09–3.52] and node-positive tumours were also associated with a higher risk of death (aHR = 2.73 [95% CI: 1.55–4.81]) in the adjusted model (data not shown).

Breast density showed no association with the risk of recurrences (aHR = 1.43 [95% CI: 0.71–2.89]; aHR = 1.47 [95% CI: 0.71–3.08], for intermediate and high densities, respectively) (Table 5). Node-positive tumours showed an increased risk of recurrences in the adjusted analysis (aHR = 3.96 [95% CI: 2.12–7.39]) (data not shown).

4. Discussion

The results of the current study suggest that higher breast density is associated with a greater risk of death in women participating in breast cancer screening, while breast density showed no association with the risk of recurrences.

The positive association between dense tissue and risk of death is consistent with some [14, 15], but not all [16, 25], prior studies conducted among screened women. Based on the data of Swedish women, Chiu et al. found that dense tissue increased mortality from breast cancer in addition to increasing breast cancer risk and the likelihood of more aggressive tumours [14]. Based on Danish data, Olsen et al. also found a positive association between dense tissue and death, although they reported lower case fatality among tumours developing in dense breasts [15]. By contrast, a study carried out in the UK [25] reported no relationship between breast density and survival. In that study, however, the screening interval was 3 years, and the survival analyses were not adjusted. A recent study carried out among the Dutch population also reported no relationship between breast density and survival [16]. In this study, as pointed out by the authors, the lack of tumour-related information may confound the results shown. In addition, the definition for high density includes ≥25% of dense tissue, differing from most of the published studies. Other works conducted in nonscreening populations have also found contradictory results, some of them reporting positive associations between breast density and mortality [10, 11] and others finding no association [13] or even a negative association [12].

Some authors have hypothesized that the association between higher density and worse survival would be explained by the diagnosis delay due to the masking effect. In that sense, we do observe a higher percentage of larger, node-positive, and interval cancers among women with high-density breasts in the descriptive data. In the adjusted analyses, lymph node involvement and detection as an interval cancer were also associated with mortality, along with intermediate breast densities so that the current results would support this hypothesis, since breast density as well as other factors related to diagnostic delay remained associated with the risk of death. These findings reinforce the need to improve screening sensitivity among women with dense breasts, which is currently been proposed by means of shifting the conventional one-size-fits-all screening approach towards more personalized screening strategies based on the individual risk of breast cancer.

Other authors have postulated that the relationship between breast density and survival may be explained by the tumour characteristics of cancers arising in epithelial tissue. It has been suggested an increased proliferation and growth factors in dense tissue [26, 27] that may be involved in pathways that lead to more aggressive tumours. Nevertheless, the evidence supporting this hypothesis is not conclusive and

Table 2: Tumour characteristics by breast density categories.

	Total $n = 375$ (%)	Low breast density (<25%) $n = 192$ (%)	Intermediate breast density (25–50%) $n = 104$ (%)	High breast density (>50%) $n = 79$ (%)
Mode of detection				
Screen-detected cancers	195 (52)	113 (58.9)	45 (43.3)	37 (46.8)
Interval cancer	180 (48)	79 (41.1)	59 (56.7)	42 (53.2)
Tumour size				
<20 mm	199 (61.8)	108 (56.3)	53 (51)	38 (48.1)
≥20 mm	123 (38.2)	58 (30.2)	33 (31.7)	32 (40.5)
Lymph node involvement				
Negative	218 (66.1)	117 (60.9)	60 (57.7)	41 (51.9)
Positive	112 (33.9)	51 (26.6)	30 (28.8)	31 (39.2)
Focality				
Unifocal	301 (84.6)	155 (87.1)	80 (80)	66 (84.6)
Multifocal and/or multicentric	55 (15.4)	23 (12.9)	20 (20)	12 (15.4)
Histological type				
Ductal	303 (80.8)	152 (79.2)	86 (82.7)	65 (82.3)
Lobular	39 (10.4)	22 (11.5)	8 (7.7)	9 (11.4)
Others	33 (8.8)	18 (9.4)	10 (9.6)	5 (6.3)
Histological grade				
I	83 (23.9)	44 (22.9)	18 (17.3)	21 (26.6)
II	134 (38.5)	64 (33.3)	40 (38.5)	30 (38)
III	116 (33.3)	60 (31.3)	35 (33.7)	21 (26.6)
NA	15 (4.3)	9 (4.7)	3 (2.9)	3 (3.8)
Oestrogen receptor				
Negative	88 (23.5)	46 (24)	28 (26.9)	14 (17.7)
Positive	287 (76.5)	146 (76)	76 (73.1)	65 (82.3)
Progesterone receptor				
Negative	150 (40.1)	70 (36.5)	45 (43.3)	35 (44.3)
Positive	224 (59.9)	121 (63)	59 (56.7)	44 (55.7)
HER2				
Negative	261 (79.1)	133 (69.3)	70 (67.3)	58 (73.4)
Positive	69 (20.9)	35 (18.2)	21 (20.2)	13 (16.5)
Ki67				
Negative	114 (60.3)	62 (32.3)	29 (27.9)	23 (29.1)
Positive	75 (39.7)	49 (25.5)	15 (14.4)	11 (13.9)
Tumour phenotype				
Luminal A	155 (48)	79 (41.1)	38 (36.5)	38 (48.1)
Luminal B	93 (28.8)	46 (24)	26 (25)	21 (26.6)
HER2	31 (9.6)	11 (5.7)	12 (11.5)	8 (10.1)
Triple-negative	44 (13.6)	29 (15.1)	11 (10.6)	4 (5.1)
Treatment				
Conservative surgery only or with sentinel lymph node biopsy	97 (26.4)	50 (26.4)	28 (28)	19 (24.1)
Conservative surgery with axillary lymph node dissection	182 (49.5)	100 (52.9)	44 (44)	38 (48.1)
Radical surgery with or without lymphadenectomy	79 (21.5)	35 (18.5)	24 (24)	20 (25.3)
No surgery and/or adjuvant treatment	10 (2.7)	4 (2.1)	4 (4)	2 (2.5)
Adjuvant treatment after surgery				
Chemotherapy, radiotherapy, and hormonal therapy	122 (32.5)	54 (28.1)	36 (34.6)	32 (40.5)
Radiotherapy and hormonal therapy	123 (32.8)	68 (35.4)	35 (33.7)	20 (25.3)
Other treatments	130 (34.7)	70 (36.5)	33 (31.7)	27 (34.2)

seems contradictory to the overrepresentation (although nonsignificant) of triple-negative cancers in low-density breasts, observed in the current descriptive data and in previous works [19, 28]. Further studies conducted in larger cohorts, with information on breast density, tumour characteristics, and clinical outcomes, are warranted to elucidate the mechanisms through which breast density and prognosis are associated.

Contrasting with prior series, we did not find association between breast density and the risk of recurrences [29–31].

Table 3: 5-year and 10-year survival rates for overall survival and recurrence-free survival.

	5-year survival rate (95% CI)	10-year survival rate (95% CI)
Overall survival		
Low breast density (<25%)	0.97 (0.94–1.00)	0.95 (0.91–0.99)
Intermediate breast density (25–50%)	0.89 (0.80–0.99)	0.82 (0.71–0.96)
High breast density (>50%)	0.83 (0.72–0.96)	0.78 (0.65–0.93)
Recurrence-free survival		
Low breast density (<25%)	0.97 (0.94–1.00)	0.92 (0.85–0.98)
Intermediate breast density (25–50%)	0.93 (0.86–1.00)	0.88 (0.79–0.99)
High breast density (>50%)	0.81 (0.69–0.95)	0.78 (0.65–0.93)

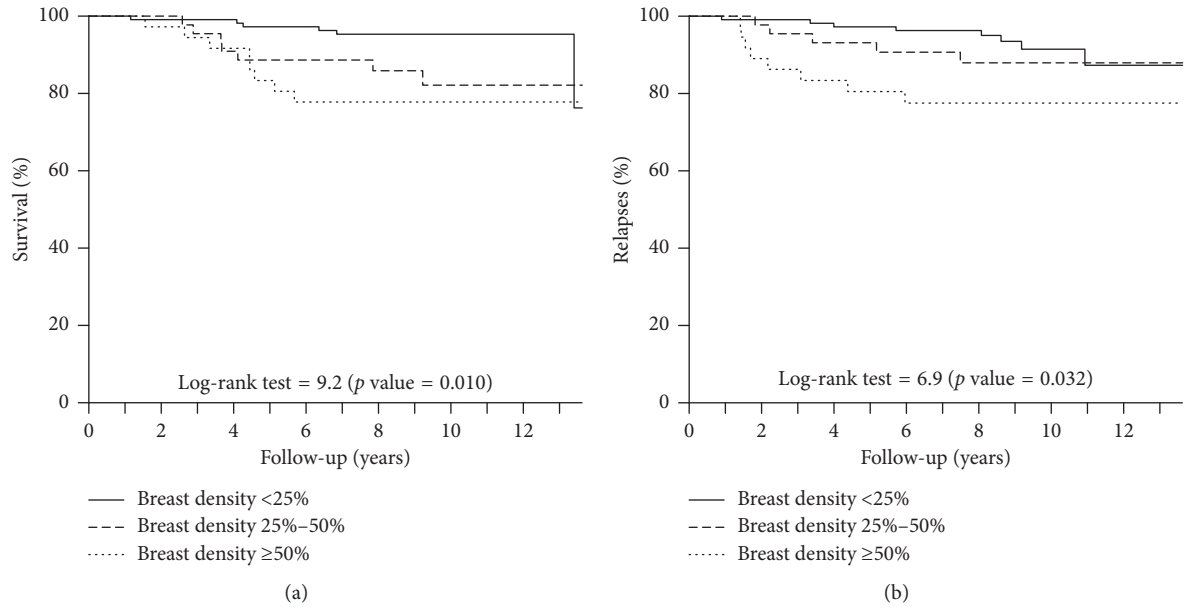

Figure 1: Survival and recurrence-free survival by breast density. (a) Overall survival; log-rank test = 0.010. (b) Recurrence-free survival; log-rank test = 0.032.

Table 4: Unadjusted and adjusted hazard ratios for death.

	Number of deaths	Unadjusted HR	Adjusted HR*
Breast density			
<25%	20	Ref.	Ref.
25–50%	24	2.48 (1.37–4.49)	2.19 (1.16–4.13)
>50%	15	1.89 (0.97–3.7)	1.44 (0.67–3.10)

*The final model included breast density, mode of detection, lymph node involvement, age, Charlson comorbidity index, and screening programme. HR: hazard ratio; aHR: adjusted hazard ratio.

Table 5: Unadjusted and adjusted hazard ratios for recurrences.

	Number of recurrences	Unadjusted HR	Adjusted HR*
Breast density			
≤25%	19	Ref.	Ref.
25–50%	16	1.72 (0.89–3.35)	1.43 (0.71–2.89)
≥50%	17	2.34 (1.21–4.5)	1.47 (0.71–3.08)

*Adjusted by breast density, progesterone receptor, lymph node involvement, age, Charlson comorbidity index, and screening programme. HR: hazard ratio; aHR: adjusted hazard ratio.

Those studies reported an increased risk of locoregional recurrences, but not for distant metastasis or death. Unfortunately, our study sample was not large enough to replicate the analysis for different types of recurrence. Besides, the populations considered in these works differed from ours, since they included study periods prior to ours, which could involve different treatment schemes. In addition, the study by Park et al. [30] only included patients undergoing breast-conserving surgery and radiotherapy, whereas we included both patients receiving and not receiving radiotherapy, which is strongly related to the risk of recurrences [29]. Our adjusted analyses revealed that the only factor associated with recurrences was the lymph node involvement at diagnosis.

Our study is limited by the relatively small number of events in some categories, which prevented us from including all breast density categories of Boyd's scale in the adjusted model. Nevertheless, most studies assessing the effect of breast density on mortality outcomes collapse breast density data into two or three categories, making our data more comparable with those of previous works. Second, we were not able to explore breast-specific cancer mortality. Previous studies exploring both breast-specific cancer

mortality and mortality from other causes found that the latter was not associated with breast density [11]. Therefore, the impact of analysing all causes of death together may lead to underestimation of the effect of breast density on mortality. Finally, we used a qualitative classification for breast density assessment, which is known to have moderate interobserver concordance [32]. However, to minimise misclassification, breast density assessment was centralised and performed by a panel of experienced radiologists, specially trained for the study [19].

The current study is strengthened by the homogeneity of the study population included. Restricting the study to screening participants allowed us to explore the effect of breast density on a relatively homogeneous group of patients in terms of age range and tumour stage. Thus, the conclusions drawn from the current work are robust and informative within the framework of population-based screening and are of interest for tailored screening strategies. In addition, the availability of data on comorbidities, patient and tumour characteristics, and the treatments received allowed us to control for important prognostic factors and to explore—for the first time among women participating in breast cancer screening—the effect of breast density on mortality considering both patient and tumour characteristics and treatments received.

5. Conclusion

In conclusion, our findings reveal that increased breast density was associated with worse survival outcomes among women participating in breast cancer screening. This association seems to be mainly explained as a result of the masking effect of dense tissue, although an underlying biological mechanism in the stroma composition may also play a role. These findings reinforce the need to improve screening sensitivity among women with dense breasts by means of more personalized screening approaches as well as the importance to routinely assess and record information on breast density during the screening process, both because of its utility as a predictive factor for breast cancer and because of its role in breast cancer prognosis.

Abbreviations

ALND: Axillary lymph node dissection
BI-RADS: Breast Imaging Reporting and Data System
CCI: Charlson comorbidity index
ER: Oestrogen receptor
Her2: Human epidermal growth factor receptor 2
HR: Hazard ratios
IQR: Interquartile range
PR: Progesterone receptor
TNM: Tumour-node-metastasis.

Data Availability

The retrospective observational data used to support the findings of this study are available from the corresponding author on reasonable request.

Conflicts of Interest

The authors declare that they have no conflicts of interest.

Acknowledgments

The authors acknowledge the contribution of Francesc Macià, Imma Collet, and the Hospital del Mar Tumour Registry (Barcelona) in providing tumour-related data. The authors also would like to acknowledge the dedication and support of the entire CAMISS Study Group (in alphabetical order): IMIM (Hospital del Mar Medical Research Institute), Barcelona: Xavier Castells, Mercè Comas, Laia Domingo, Francesc Macià, Marta Roman, Anabel Romero, Maria Sala; Canary Islands Health Service: Teresa Barata, Isabel Diez de la Lastra, Mariola de la Vega; Corporació Sanitaria Parc Taulí, Sabadell: Marisa Baré, Núria Torà; Hospital Santa Caterina, Girona: Joana Ferrer; Epidemiology Unit and Girona Cancer Registry: Maria Carmen Carmona-Garcia; Hospital Galdakao-Usansolo, Vizcaya: Susana García, Maximina Martín, Miren Orive, Maria Amparo Valverde; Canary Islands Foundation for Health Research: Jeanette Pérez, Amado Rivero, Cristina Valcárcel; Hospital Costa del Sol, University of Málaga: María del Carmen Padilla, Maximino Redondo, Teresa Téllez, Irene Zarcos; Hospital Universitario Donostia/Biodonostia: Cristina Churruca, Amaia Perales, Javier Recio, Irune Ruiz, Cristina Sarasqueta, Jose María Urraca; Instituto Oncológico de Guipúzcoa-Onkologikoa: Maria Jesús Michelena; Hospital Universitario Basurto: Julio Moreno; Hospital Universitario Cruces: Gaizka Mallabiabarrena, Patricia Cobos, Borja Otero; Hospital Universitario Txagorritxu: Javier Gorostiaga, Itsaso Troya. This study was supported by grants from Instituto de Salud Carlos III FEDER (grant numbers: PS09/01153, PI12/00387, PI11/01296, PI15/00098, and PI16/00244) and by the Research Network on Health Services in Chronic Diseases (Instituto de Salud Carlos III) (REDISSEC: RD12/0001/0015, RD12/0001/0007, and RD16/0001/0013).

References

[1] D. van der Waal, T. M. Ripping, A. L. M. Verbeek, and M. J. M. Broeders, "Breast cancer screening effect across breast density strata: a case-control study," *International Journal of Cancer*, vol. 140, no. 1, pp. 41–49, 2017.

[2] N. F. Boyd, H. Guo, L. J. Martin et al., "Mammographic density and the risk and detection of breast cancer," *New England Journal of Medicine*, vol. 356, no. 3, pp. 227–236, 2007.

[3] A. Trentham-Dietz, K. Kerlikowske, N. K. Stout et al., "Tailoring breast cancer screening intervals by breast density and risk for women aged 50 years or older: collaborative modeling of screening outcomes," *Annals of Internal Medicine*, vol. 165, no. 10, pp. 700–712, 2016.

[4] L. Rainey, D. van der Waal, A. Jervaeus et al., "Are we ready for the challenge of implementing risk-based breast cancer screening and primary prevention?," *The Breast*, vol. 39, pp. 24–32, 2018.

[5] C. M. Checka, J. E. Chun, F. R. Schnabel, J. Lee, and H. Toth, "The relationship of mammographic density and age: implications for breast cancer screening," *American Journal of Roentgenology*, vol. 198, no. 3, pp. W292–W295, 2012.

[6] M. E. Work, L. L. Reimers, A. S. Quante, K. D. Crew, A. Whiffen, and M. B. Terry, "Changes in mammographic density over time in breast cancer cases and women at high risk for breast cancer," *International Journal of Cancer*, vol. 135, no. 7, pp. 1740–1744, 2014.

[7] F. J. B. van Duijnhoven, P. H. M. Peeters, R. M. L. Warren et al., "Postmenopausal hormone therapy and changes in mammographic density," *Journal of Clinical Oncology*, vol. 25, no. 11, pp. 1323–1328, 2007.

[8] L. Yaghjyan, G. A. Colditz, L. C. Collins et al., "Mammographic breast density and subsequent risk of breast cancer in postmenopausal women according to tumor characteristics," *JNCI Journal of the National Cancer Institute*, vol. 103, no. 15, pp. 1179–1189, 2011.

[9] J. Ding, R. Warren, A. Girling, D. Thompson, and D. Easton, "Mammographic density, estrogen receptor status and other breast cancer tumor characteristics," *The Breast Journal*, vol. 16, no. 3, pp. 279–289, 2010.

[10] Å. Olsson, H. Sartor, S. Borgquist, S. Zackrisson, and J. Manjer, "Breast density and mode of detection in relation to breast cancer specific survival: a cohort study," *BMC Cancer*, vol. 14, p. 229, 2014.

[11] G. Maskarinec, I. S. Pagano, M. A. Little, S. M. Conroy, S.-Y. Park, and L. N. Kolonel, "Mammographic density as a predictor of breast cancer survival: the multiethnic cohort," *Breast Cancer Research*, vol. 15, no. 1, p. R7, 2013.

[12] A. Masarwah, P. Auvinen, M. Sudah et al., "Very low mammographic breast density predicts poorer outcome in patients with invasive breast cancer," *European Radiology*, vol. 25, no. 7, pp. 1875–1882, 2015.

[13] G. L. Gierach, L. Ichikawa, K. Kerlikowske et al., "Relationship between mammographic density and breast cancer death in the Breast Cancer Surveillance Consortium," *JNCI: Journal of the National Cancer Institute*, vol. 104, no. 16, pp. 1218–1227, 2012.

[14] S. Y. H. Chiu, S. Duffy, A. M. F. Yen, L. Tabar, R. A. Smith, and H. H. Chen, "Effect of baseline breast density on breast cancer incidence, stage, mortality, and screening parameters: 25-year follow-up of a Swedish mammographic screening," *Cancer Epidemiology Biomarkers & Prevention*, vol. 19, no. 5, pp. 1219–1228, 2010.

[15] A. H. Olsen, K. Bihrmann, M.-B. Jensen, I. Vejborg, and E. Lynge, "Breast density and outcome of mammography screening: a cohort study," *British Journal of Cancer*, vol. 100, no. 7, pp. 1205–1208, 2009.

[16] D. van der Waal, A. L. M. Verbeek, and M. J. M. Broeders, "Breast density and breast cancer-specific survival by detection mode," *BMC Cancer*, vol. 18, 2018.

[17] European Commission and Directorate-General for Health and Consumer Protection, *European Guidelines for Quality Assurance in Breast Cancer Screening and Diagnosis*, N. Perry and E. Puthaar, Eds., Office for Official Publications of the European Communities, Brussels, Belgium, 2006.

[18] E. A. Sickles and C. J. B. L. D'Orsi, "ACR BI-RADS® mammography," in *ACR BI-RADS® Atlas, Breast Imaging Reporting and Data System*, American College of Radiology, Reston, VA, USA, 2013.

[19] L. Domingo, D. Salas, R. Zubizarreta et al., "Tumor phenotype and breast density in distinct categories of interval cancer: results of population-based mammography screening in Spain," *Breast Cancer Research*, vol. 16, no. 1, p. R3, 2014.

[20] N. F. Boyd, J. W. Byng, R. A. Jong et al., "Quantitative classification of mammographic densities and breast cancer risk: results from the Canadian National Breast Screening Study," *JNCI Journal of the National Cancer Institute*, vol. 87, no. 9, pp. 670–675, 1995.

[21] M. E. Charlson, P. Pompei, K. L. Ales, and C. R. MacKenzie, "A new method of classifying prognostic comorbidity in longitudinal studies: development and validation," *Journal of Chronic Diseases*, vol. 40, no. 5, pp. 373–383, 1987.

[22] A. C. Wolff, M. E. H. Hammond, J. N. Schwartz et al., "American Society of Clinical Oncology/College of American Pathologists guideline recommendations for human epidermal growth factor receptor 2 testing in breast cancer," *Journal of Clinical Oncology*, vol. 25, no. 1, pp. 118–145, 2006.

[23] M. E. H. Hammond, D. F. Hayes, M. Dowsett et al., "American Society of Clinical Oncology/College of American Pathologists guideline recommendations for immunohistochemical testing of estrogen and progesterone receptors in breast cancer (unabridged version)," *Archives of Pathology & Laboratory Medicine*, vol. 134, pp. e48–e72, 2010.

[24] A. Goldhirsch, W. C. Wood, A. S. Coates et al., "Strategies for subtypes-dealing with the diversity of breast cancer: highlights of the St Gallen international expert consensus on the primary therapy of early breast cancer 2011," *Annals of Oncology*, vol. 22, no. 8, pp. 1736–1747, 2011.

[25] G. J. R. Porter, A. J. Evans, E. J. Cornford et al., "Influence of mammographic parenchymal pattern in screening-detected and interval invasive breast cancers on pathologic features, mammographic features, and patient survival," *American Journal of Roentgenology*, vol. 188, no. 3, pp. 676–683, 2007.

[26] N. F. Boyd, L. J. Martin, M. J. Yaffe, and S. Minkin, "Mammographic density and breast cancer risk: current understanding and future prospects," *Breast Cancer Research*, vol. 13, p. 223, 2011.

[27] M. Ellingjord-Dale, E. Lee, E. Couto et al., "Polymorphisms in hormone metabolism and growth factor genes and mammographic density in Norwegian postmenopausal hormone therapy users and non-users," *Breast Cancer Research*, vol. 14, no. 5, p. R135, 2012.

[28] V. A. Kirsh, A. M. Chiarelli, S. A. Edwards et al., "Tumor characteristics associated with mammographic detection of breast cancer in the Ontario breast screening program," *JNCI Journal of the National Cancer Institute*, vol. 103, no. 12, pp. 942–950, 2011.

[29] T. Cil, E. Fishell, W. Hanna et al., "Mammographic density and the risk of breast cancer recurrence after breast-conserving surgery," *Cancer*, vol. 115, no. 24, pp. 5780–5787, 2009.

[30] C. C. Park, J. Rembert, K. Chew, D. Moore, and K. Kerlikowske, "High mammographic breast density is independent predictor of local but not distant recurrence after lumpectomy and radiotherapy for invasive breast cancer," *International Journal of Radiation Oncology · biology · physics*, vol. 73, no. 1, pp. 75–79, 2009.

[31] L. Eriksson, K. Czene, L. U. Rosenberg, S. Törnberg, K. Humphreys, and P. Hall, "Possible influence of mammographic density on local and locoregional recurrence of breast cancer," *Breast Cancer Research*, vol. 15, no. 4, 2013.

[32] R. R. Winkel, M. von Euler-Chelpin, M. Nielsen et al., "Inter-observer agreement according to three methods of evaluating mammographic density and parenchymal pattern in a case control study: impact on relative risk of breast cancer," *BMC Cancer*, vol. 15, p. 274, 2015.

Hindawi
Journal of Oncology
Volume 2019, Article ID 7512632, 8 pages
https://doi.org/10.1155/2019/7512632

Review Article

CD133 in Breast Cancer Cells: More than a Stem Cell Marker

Federica Brugnoli,[1] Silvia Grassilli,[1] Yasamin Al-Qassab,[1,2] Silvano Capitani,[1] and Valeria Bertagnolo[1]

[1]*Department of Morphology, Surgery and Experimental Medicine, University of Ferrara, Ferrara, Italy*
[2]*College of Medicine, University of Baghdad, Baghdad, Iraq*

Correspondence should be addressed to Valeria Bertagnolo; bgv@unife.it

Received 26 April 2019; Accepted 10 August 2019; Published 16 September 2019

Guest Editor: Chia-Jung Li

Initially correlated with hematopoietic precursors, the surface expression of CD133 was also found in epithelial and nonepithelial cells from adult tissues in which it has been associated with a number of biological events. CD133 is expressed in solid tumors as well, including breast cancer, in which most of the studies have been focused on its use as a surface marker for the detection of cells with stem-like properties (i.e., cancer stem cells (CSCs)). Differently with other solid tumors, very limited and in part controversial are the information about the significance of CD133 in breast cancer, the most common malignancy among women in industrialized countries. In this review, we summarize the latest findings about the implication of CD133 in breast tumors, highlighting its role in tumor cells with a triple negative phenotype in which it directly regulates the expression of proteins involved in metastasis and drug resistance. We provide updates about the prognostic role of CD133, underlining its value as an indicator of increased malignancy of both noninvasive and invasive breast tumor cells. The molecular mechanisms at the basis of the regulation of CD133 levels in breast tumors have also been reviewed, highlighting experimental strategies capable to restrain its level that could be taken into account to reduce malignancy and/or to prevent the progression of breast tumors.

1. Introduction

CD133/prominin 1 (PROM1) is a pentaspan transmembrane single-chain glycoprotein (Figure 1(a)) mainly localized into protrusions of cellular plasma membrane and particularly in the cholesterol-based lipid microdomains, indicative of its involvement in membrane organization [1]. Transcription of human CD133 is driven by five tissue-specific promoters, three of which located in CpG islands and partially regulated by methylation (Figure 1(b)), leading to spliced mRNAs which results in CD133 isoforms with possibly distinct roles [2].

CD133 was firstly revealed as the target of a monoclonal antibody directed against the AC133 epitope expressed by a subpopulation of $CD34^+$ hematopoietic stem cells from the human fetal liver and bone marrow [3]. Despite the initial correlation of CD133 expression with progenitor cells [4, 5], accumulating evidence demonstrated that this surface antigen also characterizes adult tissues, including mammary gland [6–10]. In normal breast tissue, CD133 is not a stem cell marker and plays a role in morphogenesis, regulating ductal branching and the ratio of luminal to basal cells [10]. Even though CD133 has been variously associated with proliferation, cell survival, and autophagy, in precursors and/or mature cells [11], its exact role is not well defined and a specific ligand was not discovered.

The expression of CD133 is deregulated in various solid tumors; however, despite numerous studies, the role of this surface antigen in tumorigenesis and tumor progression is largely unknown [12]. In particular, it is not clear, and in part controversial, the role of CD133 in breast tumors, the most common malignancy and the second cause of cancer-related death among women in industrialized countries. The aim of this review is to summarize the latest findings about the meaning of CD133 in breast cancer, focusing on its relationship with the malignant evolution of the neoplasia.

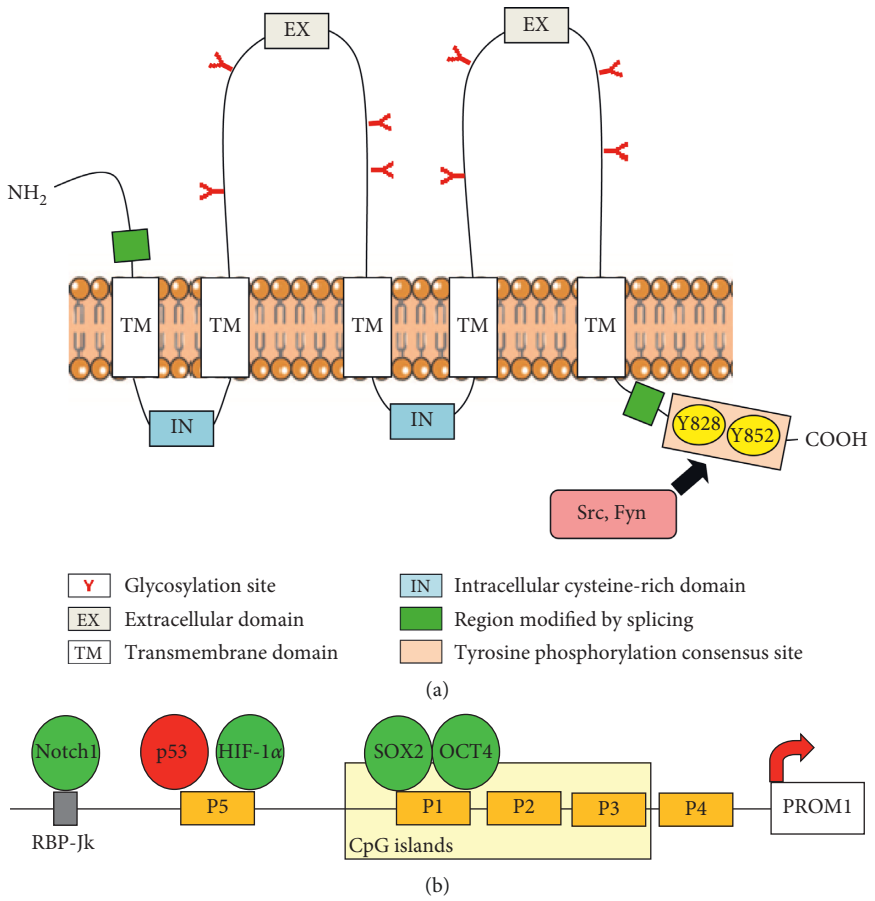

Figure 1: Structure and regulation of CD133. (a) CD133 protein structure in which the C-terminal tyrosine-phosphorylation consensus site, which comprises 5 tyrosine residues including Y828 and Y852, and the splice variants regions are indicated. (b) Schematic representation of the 5′ untranslated region of the CD133 gene. Transcription factors that positively (green circles) or negatively (red circles) regulate CD133 expression by direct binding to the different promoters are reported. The direct binding of Notch1 to the site for RBP-Jk located upstream P1–P5 promoters is also indicated.

2. CD133 as a Cancer Stem Cell Marker

Most of the studies in solid tumors have been focused on its use as a surface marker for the detection of cells with stem-like properties (i.e., cancer stem cells (CSCs)) [2, 13]. Due to its more restricted expression compared with other CSC markers such as CD44 and aldehyde dehydrogenase (ALDH), CD133 has long been considered the most rigorous indicator of malignant precursors in different solid tumors, including breast cancer [14].

In breast tumors, the role of CD133 as a CSC marker was firstly demonstrated in cell lines derived from BRCA1-associated murine mammary tumors, in which $CD133^+$ cells were shown to have a greater colony-forming efficiency, higher proliferative rate, and greater capability to form tumors in NOD/SCID mice [15]. In human invasive breast cancer cell lines, Croker et al. [16] firstly identified subpopulations of cells expressing CD133 together with the putative CSC markers CD44/CD24 and ALDH. When isolated by fluorescence-activated cell sorting and subjected to functional assays, these subpopulations showed increased growth, colony formation ability, migration, invasion, and induced tumorigenesis and metastasis in mice. In particular, $ALDH^{high}CD44^+CD133^+$ cells isolated from MDA-MB-231 and MDA-MB-468 cell lines, displaying a triple negative phenotype (ER-, PR-, and HER2-), showed enhanced malignant/metastatic behavior both *in vitro* and *in vivo* [16]. Furthermore, a subpopulation of $CD44^+CD49^{high}CD133/2^{high}$ cells isolated from ER-negative tumors was demonstrated to be enriched for xenograft-initiating cells capable of giving rise to triple negative and ER-negative/HER2-positive tumors [17], endorsing CD133 as a suitable molecule for the identification of CSCs in the most aggressive subtypes of breast cancer. Indeed, when the expression of CD133 was evaluated in breast tumor cell lines with different phenotypes, a strong variability was found. In fact, the number of $CD133^+$ cells ranged between 1 and 10% in claudin-low cells, reached 80% in basal-like cell lines, and were between 1 and 2% in both luminal and $HER2^+$ cells, questioning the equivalence between CD133 levels and stem-like properties

in breast tumor cells [18]. For this reason, although also recently it was used as the sole marker of CSCs [19], CD133 belongs to a well-known panel of molecules that, when properly combined, can actually identify cells with a stem-like phenotype in breast cancer cell lines and primary tumors with different phenotypes [13, 20].

3. CD133 as a Prognostic Marker

Although the data concerning the use of the only CD133 to identify CSCs are contradictory, the majority of the studies so far report for CD133 a significant predictive value [21]. Anyway, since CSCs generally express CD133, the prognostic significance of this surface antigen is generally correlated with the stem-like properties of $CD133^+$ cells [13].

The role for CD133 as a prognostic marker in breast cancer was firstly demonstrated by Liu et al., who revealed that high PROM1 expression in invasive ductal carcinoma positively correlates with adverse clinic-pathological factors, as tumor size and lymph node metastasis [22]. More recently, it was demonstrated that both CD133 mRNA and protein expression are important biomarkers for prognosis as they positively correlate with higher tumor grade, occurrence of lymph node metastasis, negative PR and ER and positive HER2 status, advanced TNM stage, and poor overall survival (OS) [23–25]. While both cytoplasmic and membrane CD133 were linked to shorter survival, membrane positivity only seems to confer the worst patient outcome. Furthermore, high membrane expression of CD133 was significantly associated with younger age at diagnosis and premenopausal status [26].

Despite the general relationship between CD133 and breast tumor malignancy, some controversies concern the significance of CD133 in tumors with a triple negative phenotype (TNBC), in which *CD133* is strongly hypomethylated with respect to other breast cancer subtypes [27]. A strong negative correlation of CD133 levels with clinical stage of TNBC tumors was firstly observed by Zhao et al. [28], and the use of CD133 to detect circulating tumor cells in TNBC patients ratified its role in prognosis of this breast cancer subtype [29]. Still in TNBC, Cantile et al. suggested that poor prognosis is possibly due to a nuclear mislocalization of CD133, which normally shows a membrane, and more sporadically cytoplasmic, localization [30]. In contrast to all the previous experimental evidences, Collina et al., who described a prevalent cytoplasmic expression of CD133, failed to reveal statistical association of CD133 expression with TNBCs patients' survival [31]. This discordance may be at least in part ascribed to the well-known problem that concerns the different antibodies used to detect CD133 by cytofluorimetrical and immunohistochemical investigations [21], as well as to the absence of standardized criteria to define the scores used for the quantification of the glycoprotein at membrane, cytoplasm, and nuclear level.

A recent study performed with the Gene Expression-Based Outcome for Breast Cancer Online (GOBO) algorithm confirmed that CD133 mRNA is associated with distant metastasis-free survival (DMFS) in patients with all the subtypes of breast cancer [24]. More recently, the overexpression of both CD133 mRNA and protein were investigated in large well-characterized BC cohorts, resulting particularly high in TNBC and $HER2^+$ tumors and confirming the negative prognostic value of CD133 in all breast tumor subtypes [26].

In breast cancer, CD133 is also useful in predicting chemosensitivity to neoadjuvant chemotherapy (NAC) [32]. Interestingly, the treatment with NAC resulted in the enrichment of $CD133^+$ cells and in the positive correlation of the surface antigen with prognosis, contrarily to its negative significance in pre-NAC tumors [32]. The potential role of CD133 as a marker of chemoresistance in nonluminal breast cancer subtypes was also proposed, on the basis of the relative enrichment of CSCs expressing the surface antigen after systemic therapy [29].

3.1. CD133 Regulates Invasive Potential of TNBC-Derived Cells. Various signaling pathways, all directly involved in the acquisition of malignant properties, have been correlated with CD133 levels in solid tumors, supporting its role in different stages of cancer development, including initiation, progression, and metastasis [12]. The identification of CD133 as a substrate for Src and Fyn families of tyrosine kinases suggests that its cytoplasmic domain could play an important role in the regulation of its functions (Figure 1(a)). In particular, the phosphorylation of tyrosine-828 and tyrosine-852 may regulate interaction of CD133 with SH2-domain containing proteins, which may be involved in a number of intracellular signaling events [33], including the activation of PI3K/Akt pathway [34–37].

At variance with other solid tumors, little is known about the signaling associated to CD133 in breast cancer cells (Figure 2). Interestingly, the almost totality of the data on breast tumors correlate CD133 with molecules involved in cell motility and invasion, suggesting a direct role of PROM1 in modulating the potential malignancy of breast tumors. A role of CD133 in regulating the migration rate of breast cancer cells was firstly revealed in a murine model and involved c-Met and STAT3, both downstream to the Wnt signaling and responsible of cancer invasion and metastasis [38]. A peculiar role of CD133 in the direct modulation of motility and invasive potential of breast tumor cells was demonstrated in the TNBC-derived MDA-MB-231 cell line that comprises a small cellular subset expressing high levels of CD133 at both membrane and cytoplasm levels. Remarkably, the CD133 high cells showed lower proliferation [39], in accordance with the evidence of Di Bonito et al., indicating that only in TNBC, both CD133 mRNA and protein positively correlate with geminin, an inhibitor of cell cycle progression [40]. CD133 high cells also showed a larger adhesion area, consistent with a more differentiated phenotype [39], according to the described role of CD133 in regulating differentiation of normal mammary gland [10]. On the other hand, CD133 high cells exhibited greater invasion capability, suggestive of higher metastatic potential, in accordance with the positive correlation between CD133 and poor prognosis in breast cancer. At variance with other

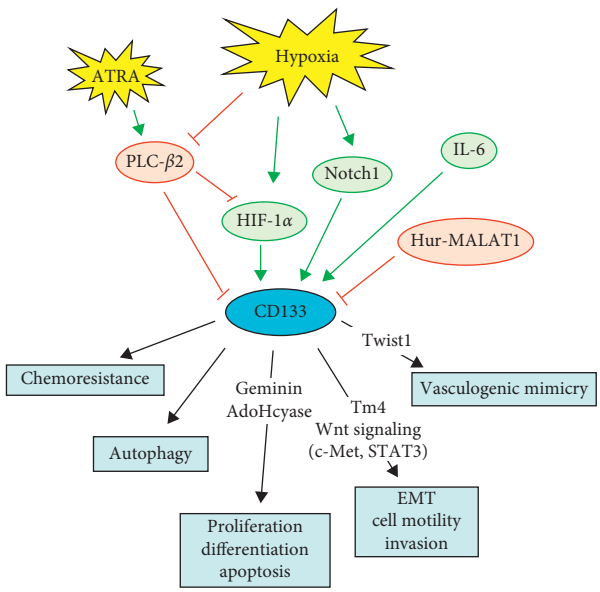

Figure 2: Regulation and functional roles of CD133 in breast cancer. Schematic summary of the main mechanisms regulating CD133 gene expression in breast cancer cells (green circles: positive regulators; red circles: negative regulators) and of cellular events directly targeted by CD133 and involved in breast cancer progression.

studies, these data highlight the value of both the number of $CD133^+$ cells and the expression levels of the surface antigen, which at least in part may justify some discrepancies on the described prognostic role of CD133 in breast tumors.

When MDA-MB-231 subpopulations expressing different levels of CD133 were subjected to two-dimensional electrophoresis followed by mass spectrometry, specific protein signatures were found, including proteins known to be deregulated and to play crucial roles in breast cancer [39]. As expected, the fastest CD133 low cells expressed lower levels of proteins involved in cell cycle and apoptosis, and the most invasive CD133 high cells showed higher expression of proteins with an oncogenic/metastatic role. The CD133-related proteins included the actin-binding protein tropomyosin4 (Tm4), upregulated in highly metastatic breast cancer cell lines and associated with lymph node metastasis of breast tumors [41] and AdoHcyase (Figure 2), known to play a key role in the control of DNA methylation [42] and in the regulation of cell cycle, apoptosis, and cellular differentiation of breast tumor cells [43]. Of note, the silencing of CD133 in CD133 high cells reduced invasiveness and expression of Tm4, ascertaining the existence of direct mechanisms by which CD133 can promote invasiveness of TNBC-derived cells [39].

A relationship between CD133 and EMT markers was demonstrated in tumors cells from metastatic breast cancer patients. In particular, the concomitant overexpression of N-cadherin and CD133 was revealed in both circulating tumor cells [44, 45] and breast cancer specimens [46], even if a significant correlation between the two molecules and patient's prognosis was not fully demonstrated.

4. CD133 as a Marker of Malignant Progression Induced by Low Oxygen Availability

A crucial driving force in the progression towards a more aggressive and resistant tumor phenotype is the adaptation of neoplastic cells to a state of reduced oxygen availability defined as hypoxia [47–52]. At least half of all solid tumors, including breast cancer, enclose hypoxic regions varying in amount and size, and recurring tumors often exhibit a hypoxic fraction higher than primary tumors [53]. Intratumoral hypoxia has been identified as an adverse prognostic indicator independent of all the histopathological parameters and, in breast cancer, as in many other solid cancers, low oxygen availability has been reported as associated with a clinically aggressive tumor behavior [54].

In solid tumors, including breast cancer, CD133 is generally induced by low oxygen availability via upregulation HIF-1α (Figures 1(b) and 2), even though only in colon cancer cells a physical interaction of HIF-1α with the *CD133* promoter was demonstrated [55–58]. Once again, the almost totality of the studies correlating CD133 with low oxygen availability looked at PROM1 as a marker of CSCs, known to increase under hypoxia [50].

In breast tumors, Currie et al. firstly associated the expression of CD133 with markers of hypoxia and/or tumor microvasculature in invasive and noninvasive breast carcinoma [23] although most of the further studies correlating CD133 to low oxygen availability were performed in TNBC. In MDA-MB-231-derived xenografts, $CD133^+$ cells with cancer stem cell characteristics were related to vasculogenic mimicry (VM) (Figure 2) and hypoxia induced by the antiangiogenic agent sunitinib [59]. In the same cell model, only $CD133^+$ cells formed VM channels in Matrigel after reoxygenation, suggesting that hypoxia accelerates VM by stimulating the CSC population [60]. Again in TNBCs, chemoresistance was associated with higher numbers of CD133/ALDH1 or CD133/CD146 coexpressing cells that were in a quiescent autophagic state related to hypoxia [61]. A further correlation of CD133 with autophagy induced by low oxygen availability was performed in patient-derived TNBC xenografts, in which hypoxia increased drug resistance of $CD133^+$ cells, and the inhibition of the autophagic pathway reversed chemoresistance [61].

More recent *in vitro* studies suggest that the effects of hypoxia on the expression of CD133 in breast tumor cells are closely related to their phenotype, and particularly to their ER status. In fact, low oxygen availability seems to induce CD133 only in ER^+ cells and mostly in cells belonging to the luminal A subtype [62]. At variance with experiments in which hypoxia was pharmacologically induced in xenografts [60], no significant modifications of CD133 were revealed in TNBC-derived cells cultured under low oxygen [62]. At the basis of this discrepancy could be the change of the glycosylation status of CD133 induced by hypoxia, in turn responsible of abnormal detection of the extracellular glycosylated AC133 epitope, as observed in glioma cells [63].

Since hypoxia improves both the number of cells expressing high levels of CD133 and the malignant potential

of the noninvasive MCF10DCIS cells [64], the increase of CD133 was considered a marker of malignant evolution induced by low oxygen availability in both noninvasive and low-invasive breast tumors.

5. Regulation of CD133 Levels

The expression of CD133 is controlled by many extracellular and intracellular agents, and hypoxic tumor microenvironment and mitochondria dysfunctions seem to be the main events modulating CD133 levels [2, 11]. In particular, hypoxia can improve the levels of the CD133 mRNA by acting at transcriptional level and can increase the recovery of the AC133 epitope, by regulating its glycosylation status [58, 63].

Apart from the hypoxia-related role of HIF-1α, there is a general agreement that the transcription factors that interact with CD133 promoters are tumor dependent [12]. For this reason, although substantial evidence assigns to the increase of CD133 levels a crucial role in the malignant potential of various solid tumors, the regulatory mechanisms that promote CD133 expression are still largely unknown in breast cancer. The relationship between $CD133^+$ cancer stem cells and the Notch signaling was shown in several tumors, including breast cancer [65, 66], but only in gastric cancer cells, the direct binding of Notch 1 with the promoter region of *CD133* was demonstrated [67]. In colon cancer and osteosarcoma, CD133 expression is negatively regulated by direct binding of p53 to a noncanonical p53-binding sequence in the *CD133* promoter [68]. Moreover, TGFβ1 is able to regulate CD133 expression in hepatocellular carcinoma through inhibition of DNMT1 and DNMT3β expression [69] (Figure 1(b)).

Abnormal DNA methylation, usually reported in many human cancers, seems to play a critical role in CD133 expression, and deregulation of the methylation status was proposed to be at the basis of increased CD133 expression in breast cancer. In particular, D'Anello and colleagues [70] reported that IL-6 induced loss of methylation at *CD133* promoter enhancing CD133 gene transcription in basal-like breast cancer via an autocrine loop triggered by the inactivation of p53. Moreover, in cells with a luminal A phenotype, but not in TNBC-derived cells, the expression of CD133 was linked to MALAT1, one of the most widely studied long coding RNA in cancer development and progression, and to the RNA binding protein HuR (Figure 1(b)). HuR/MALAT1 impact on CD133 gene expression can regulate EMT features, suggesting that the specific regulation of these molecules could control, at least in part, the CD133-related tumor progression [71].

5.1. PLC-β2 Regulates CD133 in Breast Cancer Cells. An unexpected role in the regulation of CD133 mRNA in breast tumor cells was reported for the beta-2 isoform of PLC (PLC-β2) (Figure 2), poorly expressed in normal breast tissues and upregulated in tumor cells, in which sustains motility of invasive cells [72, 73]. The first evidence of a direct regulation of CD133 by PLC-β2 was obtained in MDA-MB-231 cells, in which overexpression of the PLC significantly reduced both membrane-associated and cytoplasmic levels of CD133, in parallel with the CD133-related invasion capability [46]. In the same cell model, PLC-β2 regulates the amount of $CD133^+$ cells with stem-like features. In particular, overexpression of PLC-β2 reduced the number of $CD44^+/CD133^+/EpCAM^+$ cells and proliferation and invasion capability of the $CD133^+/EpCAM^+$ cellular subset [74].

A role of PLC-β2 in modulating CD133 expression was also demonstrated in breast tumor derived cells under hypoxia. In particular, culture at low oxygen availability reduced PLC-β2 amount and increased CD133 expression in ER^+ breast tumor cells. Counteracting the decrease of PLC-β2 prevented the increase of CD133 induced by hypoxia and significantly reduced the hypoxia-related accumulation of HIF-1α (Figure 2), a putative regulator of CD133 in this cell model [62]. The same study demonstrated that PLC-β2 is not modified by hypoxia in TNBC-derived cells, in which low oxygen availability fails to induce CD133. On the other hand, its forced expression induced a decrease of the number of $CD133^+$ cells, confirming, also in this breast tumor subtype, the role of PLC-β2 in downregulating CD133 [62].

PLC-β2 is ectopically expressed and regulates the number of cells expressing CD133 also in the noninvasive MCF10DCIS cells [75]. In the same cell model, the administration of all *trans* retinoic acid (ATRA), currently used in the management of acute promyelocytic leukemia [76] in which it induces the expression of PLC-β2 [77], counteracts the effects of hypoxia on CD133 expression by up-modulating the PLC isozyme [64]. These data constitute the first evidence that CD133 levels can be modulated by acting on specific signaling molecules and suggest that agonists able to upmodulate PLC-β2 could counteract the CD133-related malignant properties in noninvasive and invasive breast tumor cells.

6. Conclusion

This review collects the data concerning the expression of CD133 in breast cancer in which this surface antigen is generally associated with a stem cell-like phenotype. In parallel with the role as a cancer stem cell marker, we reviewed the value of CD133 as a prognostic factor and indicator of malignant progression of breast tumors, highlighting its direct role in modulating invasive potential of breast tumor cells with a triple negative phenotype. We also revised the mechanisms regulating CD133 gene expression in both noninvasive and invasive breast tumor cells, underlining experimental strategies capable to limit its expression level that could constitute the basis for new therapeutic approaches to reduce malignancy and/or to prevent progression of breast tumors.

Conflicts of Interest

The authors declare that there are no conflicts of interest regarding the publication of this paper.

Authors' Contributions

Federica Brugnoli and Silvia Grassilli contributed equally to this article.

Acknowledgments

This work was supported by grants from the University of Ferrara (Italy) to VB and SC and from Unife-CCIAA (Ferrara, Italy) to VB.

References

[1] D. Corbeil, K. Roper, C. A. Fargeas, A. Joester, and W. B. Huttner, "Prominin: a story of cholesterol, plasma membrane protrusions and human pathology," *Traffic*, vol. 2, no. 2, pp. 82–91, 2001.

[2] P. M. Glumac and A. M. LeBeau, "The role of CD133 in cancer: a concise review," *Clinical and Translational Medicine*, vol. 7, no. 1, p. 18, 2018.

[3] A. H. Yin, S. Miraglia, E. D. Zanjani et al., "AC133, a novel marker for human hematopoietic stem and progenitor cells," *Blood*, vol. 90, no. 12, pp. 5002–5012, 1997.

[4] P. Salven, S. Mustjoki, R. Alitalo, K. Alitalo, and S. Rafii, "VEGFR-3 and CD133 identify a population of CD34+ lymphatic/vascular endothelial precursor cells," *Blood*, vol. 101, no. 1, pp. 168–172, 2003.

[5] C. A. Fargeas, A.-V. Fonseca, W. B. Huttner, and D. Corbeil, "Prominin-1 (CD133): from progenitor cells to human diseases," *Future Lipidology*, vol. 1, no. 2, pp. 213–225, 2006.

[6] C. A. Fargeas, A. Joester, E. Missol-Kolka, A. Hellwig, W. B. Huttner, and D. Corbeil, "Identification of novel Prominin-1/CD133 splice variants with alternative C-termini and their expression in epididymis and testis," *Journal of Cell Science*, vol. 117, no. 18, pp. 4301–4311, 2004.

[7] G. D. Richardson, C. N. Robson, S. H. Lang, D. E. Neal, N. J. Maitland, and A. T. Collins, "CD133, a novel marker for human prostatic epithelial stem cells," *Journal of Cell Science*, vol. 117, no. 16, pp. 3539–3545, 2004.

[8] M. Florek, M. Haase, A.-M. Marzesco et al., "Prominin-1/CD133, a neural and hematopoietic stem cell marker, is expressed in adult human differentiated cells and certain types of kidney cancer," *Cell and Tissue Research*, vol. 319, no. 1, pp. 15–26, 2005.

[9] H. T. Hassan, X. Zhai, and J. A. Goodacre, "CD133 stem cells in adult human brain," *Journal of Neuro-Oncology*, vol. 89, no. 2, pp. 247-248, 2008.

[10] L. H. Anderson, C. A. Boulanger, G. H. Smith, P. Carmeliet, and C. J. Watson, "Stem cell marker prominin-1 regulates branching morphogenesis, but not regenerative capacity, in the mammary gland," *Developmental Dynamics*, vol. 240, no. 3, pp. 674–681, 2011.

[11] A. Barzegar Behrooz, A. Syahir, and S. Ahmad, "CD133: beyond a cancer stem cell biomarker," *Journal of Drug Targeting*, vol. 17, pp. 1–13, 2018.

[12] G. Y. Liou, "CD133 as a regulator of cancer metastasis through the cancer stem cells," *The International Journal of Biochemistry & Cell Biology*, vol. 106, pp. 1–7, 2019.

[13] M. Najafi, B. Farhood, and K. Mortezaee, "Cancer stem cells (CSCs) in cancer progression and therapy," *Journal of Cellular Physiology*, vol. 234, no. 6, pp. 8381–8395, 2019.

[14] A. Lorico and G. Rappa, "Phenotypic heterogeneity of breast cancer stem cells," *Journal of Oncology*, vol. 2011, Article ID 135039, 6 pages, 2011.

[15] M. H. Wright, A. M. Calcagno, C. D. Salcido, M. D. Carlson, S. V. Ambudkar, and L. Varticovski, "Brca1 breast tumors contain distinct $CD44^+/CD24^-$ and $CD133^+$ cells with cancer stem cell characteristics," *Breast Cancer Research*, vol. 10, no. 1, p. R10, 2008.

[16] A. K. Croker, D. Goodale, J. Chu et al., "High aldehyde dehydrogenase and expression of cancer stem cell markers selects for breast cancer cells with enhanced malignant and metastatic ability," *Journal of Cellular and Molecular Medicine*, vol. 13, no. 8b, pp. 2236–2252, 2009.

[17] M. J. Meyer, J. M. Fleming, A. F. Lin, S. A. Hussnain, E. Ginsburg, and B. K. Vonderhaar, "$CD44^{pos}CD49f^{hi}CD133/2^{hi}$ defines xenograft-initiating cells in estrogen receptor-negative breast cancer," *Cancer Research*, vol. 70, no. 11, pp. 4624–4633, 2010.

[18] S. Borgna, M. Armellin, A. di Gennaro, R. Maestro, and M. Santarosa, "Mesenchymal traits are selected along with stem features in breast cancer cells grown as mammospheres," *Cell Cycle*, vol. 11, no. 22, pp. 4242–4251, 2012.

[19] W. Zheng, B. Duan, Q. Zhang et al., "Vitamin D-induced vitamin D receptor expression induces tamoxifen sensitivity in MCF-7 stem cells via suppression of Wnt/β-catenin signaling," *Bioscience Reports*, vol. 38, no. 6, Article ID BSR20180595, 2018.

[20] R. V. Oliveira, V. B. Souza, P. C. Souza et al., "Detection of putative stem-cell markers in invasive ductal carcinoma of the breast by immunohistochemistry: does it improve prognostic/predictive assessments?," *Applied Immunohistochemistry & Molecular Morphology*, vol. 26, no. 10, pp. 760–768, 2018.

[21] P. Grosse-Gehling, C. A. Fargeas, C. Dittfeld et al., "CD133 as a biomarker for putative cancer stem cells in solid tumours: limitations, problems and challenges," *The Journal of Pathology*, vol. 229, no. 3, pp. 355–378, 2013.

[22] Q. Liu, J. G. Li, X. Y. Zheng, F. Jin, and H. T. Dong, "Expression of CD133, PAX2, ESA, and GPR30 in invasive ductal breast carcinomas," *Chinese Medical Journal*, vol. 122, no. 22, pp. 2763–2769, 2009.

[23] M. J. Currie, B. E. Beardsley, G. C. Harris et al., "Immunohistochemical analysis of cancer stem cell markers in invasive breast carcinoma and associated ductal carcinoma in situ: relationships with markers of tumor hypoxia and microvascularity," *Human Pathology*, vol. 44, no. 3, pp. 402–411, 2013.

[24] P. Xia, "CD133 mRNA may be a suitable prognostic marker for human breast cancer," *Stem Cell Investigation*, vol. 4, no. 11, p. 87, 2017.

[25] L. Han, X. Gao, X. Gu et al., "Prognostic significance of cancer stem cell marker CD133 expression in breast cancer," *International Journal of Clinical and Experimental Medicine*, vol. 10, no. 3, pp. 4829–4837, 2017.

[26] C. Joseph, M. Arshad, S. Kurozomi et al., "Overexpression of the cancer stem cell marker CD133 confers a poor prognosis in invasive breast cancer," *Breast Cancer Research and Treatment*, vol. 174, no. 2, pp. 387–399, 2019.

[27] N. Kagara, K. T. Huynh, C. Kuo et al., "Epigenetic regulation of cancer stem cell genes in triple-negative breast cancer," *The American Journal of Pathology*, vol. 181, no. 1, pp. 257–267, 2012.

[28] P. Zhao, Y. Lu, X. Jiang, and X. Li, "Clinicopathological significance and prognostic value of CD133 expression in triple-negative breast carcinoma," *Cancer Science*, vol. 102, no. 5, pp. 1107–1111, 2011.

[29] R. Nadal, F. G. Ortega, M. Salido et al., "CD133 expression in circulating tumor cells from breast cancer patients: potential

role in resistance to chemotherapy," *International Journal of Cancer*, vol. 133, no. 10, pp. 2398–2407, 2013.

[30] M. Cantile, F. Collina, M. D'Aiuto et al., "Nuclear localization of cancer stem cell marker CD133 in triple-negative breast cancer: a case report," *Tumori Journal*, vol. 99, no. 5, pp. e245–e250, 2013.

[31] F. Collina, M. Di Bonito, V. Li Bergolis et al., "Prognostic value of cancer stem cells markers in triple-negative breast cancer," *BioMed Research International*, vol. 2015, Article ID 158682, 10 pages, 2015.

[32] N. Aomatsu, M. Yashiro, S. Kashiwagi et al., "CD133 is a useful surrogate marker for predicting chemosensitivity to neoadjuvant chemotherapy in breast cancer," *PLoS One*, vol. 7, no. 9, Article ID e45865, 2012.

[33] D. Boivin, D. Labbé, N. Fontaine et al., "The stem cell marker CD133 (Prominin-1) is phosphorylated on cytoplasmic tyrosine-828 and tyrosine-852 by Src and Fyn tyrosine kinases," *Biochemistry*, vol. 48, no. 18, pp. 3998–4007, 2009.

[34] A. Dubrovska, S. Kim, R. J. Salamone et al., "The role of PTEN/Akt/PI3K signaling in the maintenance and viability of prostate cancer stem-like cell populations," *Proceedings of the National Academy of Sciences*, vol. 106, no. 1, pp. 268–273, 2009.

[35] H. Sartelet, T. Imbriglio, C. Nyalendo et al., "CD133 expression is associated with poor outcome in neuroblastoma via chemoresistance mediated by the AKT pathway," *Histopathology*, vol. 60, no. 7, pp. 1144–1155, 2012.

[36] Y. Wei, Y. Jiang, F. Zou et al., "Activation of PI3K/Akt pathway by CD133-p85 interaction promotes tumorigenic capacity of glioma stem cells," *Proceedings of the National Academy of Sciences*, vol. 110, no. 17, pp. 6829–6834, 2013.

[37] J. U. Schmohl and D. A. Vallera, "CD133, selectively targeting the root of cancer," *Toxins*, vol. 8, 2016.

[38] J. Sun, C. Zhang, G. Liu et al., "A novel mouse CD133 binding-peptide screened by phage display inhibits cancer cell motility in vitro," *Clinical & Experimental Metastasis*, vol. 29, no. 3, pp. 185–196, 2012.

[39] F. Brugnoli, S. Grassilli, M. Piazzi et al., "In triple negative breast tumor cells, PLC-β2 promotes the conversion of $CD133^{high}$ to $CD133^{low}$ phenotype and reduces the CD133-related invasiveness," *Molecular Cancer*, vol. 12, no. 1, p. 165, 2013.

[40] M. Di Bonito, M. Cantile, F. Collina et al., "Overexpression of cell cycle progression inhibitor geminin is associated with tumor stem-like phenotype of triple-negative breast cancer," *Journal of Breast Cancer*, vol. 15, no. 2, pp. 162–171, 2012.

[41] H. Li, F. Li, Z. M. Qian, and H. Sun, "Structure and topology of the transmembrane domain 4 of the divalent metal transporter in membrane-mimetic environments," *European Journal of Biochemistry*, vol. 271, no. 10, pp. 1938–1951, 2004.

[42] H. Gellekink, M. d. Heijer, L. A. J. Kluijtmans, and H. J. Blom, "Effect of genetic variation in the human S-adenosylhomocysteine hydrolase gene on total homocysteine concentrations and risk of recurrent venous thrombosis," *European Journal of Human Genetics*, vol. 12, no. 11, pp. 942–948, 2004.

[43] A. Hayden, P. W. M. Johnson, G. Packham, and S. J. Crabb, "S-adenosylhomocysteine hydrolase inhibition by 3-deazaneplanocin A analogues induces anti-cancer effects in breast cancer cell lines and synergy with both histone deacetylase and HER2 inhibition," *Breast Cancer Research and Treatment*, vol. 127, no. 1, pp. 109–119, 2011.

[44] B. Aktas, M. Tewes, T. Fehm, S. Hauch, R. Kimmig, and S. Kasimir-Bauer, "Stem cell and epithelial-mesenchymal transition markers are frequently overexpressed in circulating tumor cells of metastatic breast cancer patients," *Breast Cancer Research*, vol. 11, no. 4, p. R46, 2009.

[45] A. J. Armstrong, M. S. Marengo, S. Oltean et al., "Circulating tumor cells from patients with advanced prostate and breast cancer display both epithelial and mesenchymal markers," *Molecular Cancer Research*, vol. 9, no. 8, pp. 997–1007, 2011.

[46] C. Bock, C. Kuhn, N. Ditsch et al., "Strong correlation between N-cadherin and CD133 in breast cancer: role of both markers in metastatic events," *Journal of Cancer Research and Clinical Oncology*, vol. 140, no. 11, pp. 1873–1881, 2014.

[47] L. Schito and G. L. Semenza, "Hypoxia-Inducible factors: master regulators of cancer progression," *Trends in Cancer*, vol. 2, no. 12, pp. 758–770, 2016.

[48] K. R. Luoto, R. Kumareswaran, and R. G. Bristow, "Tumor hypoxia as a driving force in genetic instability," *Genome Integrity*, vol. 4, no. 1, p. 5, 2013.

[49] S. Chouaib, M. Z. Noman, K. Kosmatopoulos, and M. A. Curran, "Hypoxic stress: obstacles and opportunities for innovative immunotherapy of cancer," *Oncogene*, vol. 36, no. 4, pp. 439–445, 2017.

[50] A. Mohyeldin, T. Garzón-Muvdi, and A. Quiñones-Hinojosa, "Oxygen in stem cell biology: a critical component of the stem cell niche," *Cell Stem Cell*, vol. 7, no. 2, pp. 150–161, 2010.

[51] E. B. Rankin, J.-M. Nam, and A. J. Giaccia, "Hypoxia: signaling the metastatic cascade," *Trends in Cancer*, vol. 2, no. 6, pp. 295–304, 2016.

[52] S. Marx, M. Van Gysel, A. Breuer et al., "Potentialization of anticancer agents by identification of new chemosensitizers active under hypoxia," *Biochem Pharmacol*, vol. 162, pp. 224–236, 2019.

[53] V. Bhandari, C. Hoey, L. Y. Liu et al., "Molecular landmarks of tumor hypoxia across cancer types," *Nature Genetics*, vol. 51, no. 2, pp. 308–318, 2019.

[54] J. C. Walsh, A. Lebedev, E. Aten, K. Madsen, L. Marciano, and H. C. Kolb, "The clinical importance of assessing tumor hypoxia: relationship of tumor hypoxia to prognosis and therapeutic opportunities," *Antioxidants & Redox Signaling*, vol. 21, no. 10, pp. 1516–1554, 2014.

[55] A. Soeda, M. Park, D. Lee et al., "Hypoxia promotes expansion of the CD133-positive glioma stem cells through activation of HIF-1α," *Oncogene*, vol. 28, no. 45, pp. 3949–3959, 2009.

[56] L. P. Schwab, D. L. Peacock, D. Majumdar et al., "Hypoxia-inducible factor 1α promotes primary tumor growth and tumor-initiating cell activity in breast cancer," *Breast Cancer Research*, vol. 14, no. 1, p. R6, 2012.

[57] K. Maeda, Q. Ding, M. Yoshimitsu et al., "CD133 modulate HIF-1alpha expression under hypoxia in emt phenotype pancreatic cancer stem-like cells," *International Journal of Molecular Sciences*, vol. 17, no. 7, Article ID E1025, 2016.

[58] S. Ohnishi, O. Maehara, K. Nakagawa et al., "hypoxia-inducible factors activate CD133 promoter through ETS family transcription factors," *PLoS One*, vol. 8, no. 6, Article ID e66255, 2013.

[59] T. J. Liu, B. C. Sun, X. L. Zhao et al., "$CD133^+$ cells with cancer stem cell characteristics associates with vasculogenic mimicry in triple-negative breast cancer," *Oncogene*, vol. 32, no. 5, pp. 544–553, 2013.

[60] D. Zhang, B. Sun, X. Zhao et al., "Twist1 expression induced by sunitinib accelerates tumor cell vasculogenic mimicry by increasing the population of $CD133^+$ cells in triple-negative breast cancer," *Molecular Cancer*, vol. 13, no. 1, p. 207, 2014.

[61] G. Bousquet, M. El Bouchtaoui, T. Sophie et al., "Targeting autophagic cancer stem-cells to reverse chemoresistance in

human triple negative breast cancer," *Oncotarget*, vol. 8, no. 21, pp. 35205–35221, 2017.

[62] F. Brugnoli, S. Grassilli, Y. Al-Qassab, S. Capitani, and V. Bertagnolo, "PLC-β2 is modulated by low oxygen availability in breast tumor cells and plays a phenotype dependent role in their hypoxia-related malignant potential," *Molecular Carcinogenesis*, vol. 55, no. 12, pp. 2210–2221, 2016.

[63] K. S. Lehnus, L. K. Donovan, X. Huang et al., "CD133 glycosylation is enhanced by hypoxia in cultured glioma stem cells," *International Journal of Oncology*, vol. 42, no. 3, pp. 1011–1017, 2013.

[64] Y. Al-Qassab, S. Grassilli, F. Brugnoli, F. Vezzali, S. Capitani, and V. Bertagnolo, "Protective role of all-trans retinoic acid (ATRA) against hypoxia-induced malignant potential of non-invasive breast tumor derived cells," *BMC Cancer*, vol. 18, no. 1, p. 1194, 2018.

[65] P. Sansone, M. Berishaj, V. K. Rajasekhar et al., "Evolution of cancer stem-like cells in endocrine-resistant metastatic breast cancers is mediated by stromal microvesicles," *Cancer Research*, vol. 77, no. 8, pp. 1927–1941, 2017.

[66] S. K. Saha, H. Y. Choi, B. W. Kim et al., "KRT19 directly interacts with β-catenin/RAC1 complex to regulate NUMB-dependent NOTCH signaling pathway and breast cancer properties," *Oncogene*, vol. 36, no. 3, pp. 332–349, 2017.

[67] H. Konishi, N. Asano, A. Imatani et al., "Notch1 directly induced CD133 expression in human diffuse type gastric cancers," *Oncotarget*, vol. 7, pp. 56598–56607, 2016.

[68] E. K. Park, J. C. Lee, J. W. Park et al., "Transcriptional repression of cancer stem cell marker CD133 by tumor suppressor p53," *Cell Death & Disease*, vol. 6, no. 11, Article ID e1964, 2015.

[69] H. You, W. Ding, and C. B. Rountree, "Epigenetic regulation of cancer stem cell marker CD133 by transforming growth factor-β," *Hepatology*, vol. 51, no. 5, pp. 1635–1644, 2010.

[70] L. D'Anello, P. Sansone, G. Storci et al., "Epigenetic control of the basal-like gene expression profile via Interleukin-6 in breast cancer cells," *Molecular Cancer*, vol. 9, no. 1, p. 300, 2010.

[71] E. Latorre, S. Carelli, I. Raimondi et al., "The ribonucleic complex hur-MALAT1 represses CD133 expression and suppresses epithelial-mesenchymal transition in breast cancer," *Cancer Research*, vol. 76, no. 9, pp. 2626–2636, 2016.

[72] V. Bertagnolo, M. Benedusi, P. Querzoli et al., "PLC-beta2 is highly expressed in breast cancer and is associated with a poor outcome: a study tissue microarrays," *International Journal of Oncology*, vol. 28, no. 4, pp. 863–872, 2006.

[73] V. Bertagnolo, M. Benedusi, F. Brugnoli et al., "Phospholipase C-β2 promotes mitosis and migration of human breast cancer-derived cells," *Carcinogenesis*, vol. 28, no. 8, pp. 1638–1645, 2007.

[74] F. Brugnoli, S. Grassilli, P. Lanuti et al., "Up-modulation of PLC-β2 reduces the number and malignancy of triple-negative breast tumor cells with a $CD133^+/EpCAM^+$ phenotype: a promising target for preventing progression of TNBC," *BMC Cancer*, vol. 17, no. 1, p. 617, 2017.

[75] V. Bertagnolo, S. Grassilli, S. Volinia et al., "Ectopic expression of PLC-β2 in non-invasive breast tumor cells plays a protective role against malignant progression and is correlated with the deregulation of miR-146a," *Molecular Carcinogenesis*, vol. 58, no. 5, 2018.

[76] S. Kayser, R. F. Schlenk, and U. Platzbecker, "Management of patients with acute promyelocytic leukemia," *Leukemia*, vol. 32, no. 6, pp. 1277–1294, 2018.

[77] V. Bertagnolo, M. Marchisio, S. Pierpaoli et al., "Selective up-regulation of phospholipase C-β2 during granulocytic differentiation of normal and leukemic hematopoietic progenitors," *Journal of Leukocyte Biology*, vol. 71, pp. 957–965, 2002.

Hindawi
Journal of Oncology
Volume 2019, Article ID 3860426, 11 pages
https://doi.org/10.1155/2019/3860426

Research Article

N-Acetyltransferase 1 Knockout Elevates Acetyl Coenzyme A Levels and Reduces Anchorage-Independent Growth in Human Breast Cancer Cell Lines

Marcus W. Stepp, Raúl A. Salazar-González, Kyung U. Hong, Mark A. Doll, and David W. Hein

Department of Pharmacology & Toxicology and James Graham Brown Cancer Center, University of Louisville, Louisville, KY 40202, USA

Correspondence should be addressed to David W. Hein; d.hein@louisville.edu

Received 16 June 2019; Accepted 31 July 2019; Published 20 August 2019

Guest Editor: Chia-Jung Li

Elevated expression of *N*-acetyltransferase 1 (NAT1) is associated with invasive and lobular breast carcinomas as well as with bone metastasis following an epithelial-to-mesenchymal transition. We investigated the effect of NAT1 gene deletion in three different human breast cancer cell lines, MDA-MB-231, MCF-7, and ZR-75-1. Human NAT1 was knocked out using CRISPR/Cas9 technology and two different guide RNAs. None of the NAT1 knockout (KO) cell lines exhibited detectable NAT1 activity when measured using its selective substrate *p*-aminobenzoic acid (PABA). Endogenous acetyl coenzyme A levels (cofactor for acetylation pathways) in NAT1 KO cell lines were significantly elevated in the MDA-MB-231 ($p < 0.001$) and MCF-7 ($p = 0.0127$) but not the ZR-75-1 ($p > 0.05$). Although the effects of NAT1 KO on cell-doubling time were inconsistent across the three breast cancer cell lines, the ability of the NAT1 KO cell lines to form anchorage-independent colonies in soft agar was dramatically and consistently reduced in each of the breast cancer cell lines. The NAT1 KO clones for MDA-MB-231, MCF-7, and ZR-75-1 had a reduction greater than 20-, 6-, and 7- folds in anchorage-independent cell growth, respectively, compared to their parental cell lines ($p < 0.0001$, $p < 0.0001$, and $p < 0.05$, respectively). The results indicate that NAT1 may be an important regulator of cellular acetyl coenzyme A levels and strongly suggest that elevated NAT1 expression in breast cancers contribute to their anchorage-independent growth properties and ultimately metastatic potential.

1. Introduction

Human arylamine *N*-acetyltransferase 1 (NAT1) catalyzes the transfer of an acetyl group from acetyl coenzyme A (AcCoA) to arylamine and hydrazine substrates [1, 2]. Human NAT1 also catalyzes hydrolysis of AcCoA in the presence of folate [3, 4]. NAT1 has a ubiquitous expression regulated by multiple mechanisms [5]. Elevated NAT1 expression is associated with invasive and lobular breast carcinomas [6]. Additional studies have reported elevated NAT1 expression in estrogen receptor-positive tumors [7–9] as well as with bone metastasis following an epithelial-to-mesenchymal transition (EMT) [10, 11].

A recent report demonstrated that congenic rats expressing high levels of rat *N*-acetyltransferase 2 (NAT2; ortholog to human NAT1) activity exhibited more mammary tumors, and this finding was independent of carcinogen metabolism [12]. The effects of inhibition or overexpression of human NAT1 has been the focus of previous studies [13–17]. Interestingly, MDA-MB-231 cells with increased NAT1 activity showed lower endogenous AcCoA levels, compared to the parental cell line [17]. These observations, together with the wide-spread tissue distribution of NAT1 and its presence in almost all species [18] and its ability to catalyze the hydrolysis of AcCoA, suggest the role of NAT1 in carcinogenesis might be related to the regulation of AcCoA.

In the present study, we utilized CRISPR/Cas9 to investigate the effects of NAT1 knockout (KO) on endogenous AcCoA levels and the cell growth properties in three human

breast cancer cell lines that originate from separate pleural effusions of different malignant breast cancer patients frequently used in breast cancer research.

2. Materials and Methods

2.1. Construction of NAT1 KO Cell Lines. MDA-MB-231, MCF-7, and ZR-75-1 breast cancer cell lines were obtained from ATCC (Manassas, Virginia, USA). MDA-MB-231 is estrogen receptor-negative, progesterone receptor-negative, and HER2-negative. MCF-7 is estrogen receptor-positive, progesterone receptor-positive, and HER2-negative. ZR-75-1 is estrogen receptor-positive, progesterone receptor-positive, and HER2-positive. A MDA-MB-231 breast cancer cell line with a single FRT site (Life Technologies, Grand Island, NY) and a nonspecific scrambled shRNA inserted in the FRT site was used as the parent MDA-MB-231 cell line. The construction of this cell line was described previously [16]. MDA-MB-231 and MCF-7 cells were cultured in DMEM media, high glucose (4.5 g/L) with the addition of fetal bovine serum (10%), glutamine (2 mM), and Pen/Strep (1%). ZR-75-1 cells were cultured in RPMI-1640 with the addition of fetal bovine serum (10%), glutamine (2 mM), and Pen/Strep (1%). The cell lines were grown in a humidified incubator set at 37°C with 5% CO_2. Horizon Discovery Group (Cambridge, UK) designed 5 different gRNAs for NAT1, and DNA 2.0 Inc (Menio Park, CA, USA) cloned the gRNAs into a Cas9 expressing vector expressing a dasher-GFP tag. Initially, each of the 5 gRNA/Cas9 vectors was transiently transfected in each cell line using the Amaxa Nucleofector II (Lonza, Allendale, NJ, USA). After forty-eight hours, transfection cells were harvested and DNA isolated. The SURVEYOR Mutation Detection Kit (Transgenomics, Omaha, NE, USA) was used to determine the effectiveness of each gRNA's ability to induce DNA strand breaks effectively. The gRNAs #2 and #5 were the most effective at inducing DNA strand breaks and were chosen to separately KO NAT1 as described below. The selected gRNA sequences were the following: gRNA #2, **CCA** *GATCCGAGCTGTTCCCTTTG* (protospacer adjacent motif is shown in bold face font; positions 93–112 from start shown in italic font) or gRNA #5, GAAAGAATTGGCTATAAGAAGTCT**AGG** (protospacer adjacent motif is shown in bold face font; positions 26–45 from start shown in italic font).

The parent MDA-MB-231 cell line described above was transfected with either #2 or #5 gRNA/Cas9 vectors separately as above and 48 hr after transfection cells were sorted for GFP fluorescence (MoFlo XDP, Beckman Coulter Inc. Kendall, FL, USA). MCF-7 and ZR-75-1 cells were transfected with #2 or #5 gRNA/Cas9 separately with Lipofectamine 3000 (Invitrogen, CA, USA), and 48 hr after transfection cells were sorted for GFP fluorescence as previously described. The GFP-positive cells were collected and plated at a low cell density so that individual unique clones could be isolated. After several weeks, individual cells grew into large enough colonies to utilize cloning cylinders to trypsin cells off the plate and transfer to a 96-well culture plate. Approximately 25 to 50 separate clones, chosen at random, for each cell gRNA, were passaged until nearly confluent in a 6-well plate and then were tested for PABA NAT1 activity. GFP-positive clones with undetectable PABA NAT1 activity were selected for further characterization. The NAT1 open reading frame was sequenced. We chose transient transfection of the gRNA/Cas9 protein to minimize off-target effects; thus; the gRNA/Cas9 plasmid was only present in the cell for a short time (48–96 hr) as opposed to stable long-term expression of gRNA/Cas9 where the editing machinery would be present indefinitely.

2.2. Sequencing of the NAT1 Gene in the gRNAs #2 and #5 KO Clones. Genomic DNA was isolated from MDA-MB-231, MCF-7, and ZR-75-1 NAT1 KO cell lines. The NAT1 open reading frame was amplified by PCR and cloned into pcDNA™3.1/V5-His-TOPO® (Invitrogen, CA, USA) following manufacturer's recommendations. TOPO cloning reaction for the individual cell lines was transformed into One Shot TOP10 chemically competent *E. coli*. For each NAT1 KO cell line, five transformed *E. coli* colonies were selected and grown overnight. Cultures of bacteria were then harvested for plasmid purification. Purified plasmids and primers were sent for DNA sequencing (Eurofins, Louisville, KY, USA) to determine base changes caused by gRNA/Cas9.

2.3. Cell Line Authentication. The genetically engineered MDA-MB-231 MCF-7 and ZR-75-1 cell lines described above were authenticated by the ATCC Short Tandem Repeat (STR) profiling authentication service.

2.4. In Vitro and In Situ N-Acetylation. *In vitro* *N*-acetylation assays using the NAT1-selective substrate PABA were conducted, and *N*-acetyl-PABA was separated and quantitated by high-performance liquid chromatography (HPLC) as previously described [16]. Briefly, enzymatic reactions containing 50 μL suitably diluted cell lysate, PABA (300 μM), and AcCoA (1 mM) were incubated at 37°C for 10 min. Three independent measurements ($n = 3$) performed in triplicate were completed for each cell line. In vitro *N*-acetylation assays using the NAT2-selective substrate sulfamethazine enzymatic assays were conducted as described previously [19]. Briefly, reactions containing lysate from parental and NAT1 KO cells lines for all cell lines, 300 μM sulfamethazine, and 1 mM AcCoA were incubated at 37°C for 120 min. Reactions were terminated by the addition of 1/10 volume of 1 M acetic acid. The reaction tubes were centrifuged to remove precipitated protein. Sulfamethazine and *N*-acetyl-sulfamethazine were separated and quantified by reverse-phase HPLC. Three independent measurements ($n = 3$) performed in triplicate were completed for each cell line. Under the conditions of this assay, the limit of detection was 0.005 nmoles/min/mg protein.

Measurement of NAT1-catalyzed *N*-acetylation *in situ* was determined by spiking media with a known concentration of PABA as previously described [20]. Briefly, the cells were incubated at 37°C for 48 hr with media containing 500 μM PABA. *N*-acetyl-PABA was separated and quantitated by HPLC as previously described [16]. The number of

separate determinations for MDA-MB-231, MCF-7, and ZR-75-1 was 3, 4, and 4, respectively.

2.5. NAT1 and NAT2 In-Cell Western Staining. Cells (1.5×10^5) were plated into 96-well black/clear bottom plates (Thermo Fisher Scientific, Waltham, MA, USA) and incubated overnight at 37°C and 5% CO_2. Once attached to the plate, cells were washed with PBS and then fixed to the plate with 3.7% formaldehyde in PBS for 20 min at room temperature. After fixing, cells were permeabilized using 0.1% Triton-X100 in PBS for 5 min with constant agitation, and the process was repeated 4 times. Cells were blocked with Odyssey® Blocking Buffer in PBS (LI-COR Biosciences, Lincoln, NE, USA) for 1.5 hours with constant agitation. After blocking, cells were incubated with rabbit anti-NAT1 (ab109114 (1:200), Abcam, Cambridge, UK) or rabbit NAT2 (ab194114 (1:100) Abcam) and β-actin (A2228 (1:200), Sigma-Aldrich, St. Louis, MO, USA) overnight at 4°C with constant agitation. Due to the high similarity between human NAT1 and NAT2, we evaluated the specificity of the primary antibodies against human NAT1 and NAT2. The specificity of ab109114 was about 4-fold greater for human NAT1 than NAT2, and the specificity of ab194114 was about 7-fold greater for human NAT2 than NAT1 (manuscript in preparation). After primary antibodies incubation, plates were washed 5 times with 0.1% Tween 20 in PBS for 5 min. Secondary detection was carried out using IRDye® 800CW Goat anti-Rabbit IgG (1:1200) or IRDye® 680RD Goat anti-Mouse IgG (1:1200), (LI-COR Biosciences, Lincoln, NE, USA) by incubation for 60 min. Finally, cells were washed with 0.1% Tween 20 in PBS. NAT1 or NAT2 and β-actin were simultaneously visualized using an Odyssey infrared imaging Scanner (LI-COR Biosciences) using the 680 nm channel and 800 nm channel. Relative fluorescence units (RFUs) allowed a quantitative analysis. Relative protein expression was calculated by dividing RFU for NAT1 or NAT2 (800 nm channel) by the RFU of β-actin (680 nm channel). Protein expression in NAT1 KO cells was divided by the protein expression in the parental cell line to determine fold change. The data was generated from 4 independent measurements for MDA-MB-231, MCF-7, and ZR-75-1 parental and their NAT1 KO cell lines.

2.6. Endogenous AcCoA Levels. Endogenous AcCoA levels within MDA-MB-231, MCF-7, and ZR-75-1 parental and NAT1 KO cell lines were measured by HPLC as previously described [16] with minor modifications. MDA-MB-231, MCF-7, and ZR-75-1 cell lines were plated in triplicate at a density of 1×10^6 cells per 10 cm plate and allowed to grow. After seventy-two hr, plating cells were washed once with 1X PBS and dissociated from the plate with 1.0 mL trypsin. Cells from 3, 10 cm plates were combined, resuspended in complete media, and counted. In the subsequent steps all cells and lysates were kept on ice. Collected cells were washed once in ice-cold PBS and transferred to a 1.5 ml microcentrifuge tubes. The suspended cells were collected by centrifugation and the supernatants discarded. Having removed any residual PBS, the cells were completely resuspended in 50 μL of ice-cold 1X PBS and then immediately lysed by addition of 50 μL of cold 10% 5-sulfosalicylic acid with vortexing for 15 sec. Lysed cells were incubated on ice for 10 min before centrifugation at 13,000 ×g for 10 min. Supernatant was injected on a C18 reverse-phase HPLC column (250 mm × 4 mm; 5 μm pore size) (Merck, Darmstadt, GER). HPLC separation and quantitation of AcCoA were achieved as previously described [16]. The data was generated from 8, 12, and 3 independent measurements for MDA-MB-231, MCF-7, and ZR-75-1 parental and NAT1 KO cell lines, respectively.

2.7. Cell Doubling Time. Doubling time for each parental and NAT1 KO cell line was determined by plating each cell line to a confluence level that would give the cell lines ample room to grow for at least 7 days or 168 hr. The same number of cells were plated for parental and NAT1 KO cell lines for each cell line. Cells were plated in 6-well plates in triplicate and allowed to grow for 7 days (168 hr). Cells were counted and doubling time calculated using the online calculator (http://www.doubling-time.com/compute.php). The number of separate doubling time determinations for MDA-MB-231, MCF-7, and ZR-75-1 cells was 3, 3, and 4, respectively.

2.8. Anchorage-Dependent and Anchorage-Independent Growth Assays. Anchorage-*dependent* growth assays were performed as described previously [16]. Briefly, cells (300 cells/well) were plated in triplicate in 6-well plates and allowed to grow for 2 weeks. Visible colonies were counted manually following staining with crystal violet. The data were generated from 6, 3, and 3 independent measurements for MDA-MB-231, MCF-7, and ZR-75-1 parental and NAT1 KO cell lines, respectively. The anchorage-*independent* growth assays were performed as described previously [16]. Briefly, the anchorage-independent growth assays were performed by plating the cells (6000 cells/well) in 1.5 mL of low-melting temperature agarose (0.3%) in complete media over a base layer of 1.5 mL noble agar (0.5%) in complete media. The total volume was 3 mL in each well of a 6-well plate. Cells were plated in triplicate and grown for 2 weeks. Colonies (containing >4 individual cells) were counted manually following staining with crystal violet. The data was generated from 3 independent measurements for MDA-MB-231, MCF-7, and ZR-75-1 parental and NAT1 KO cell lines.

2.9. Statistical Analyses. Differences between the MDA-MB-231 and MCF-7 parental and NAT1 KO cell lines were analyzed for significance by ANOVA followed by Bonferroni post hoc test. Differences between the ZR-75-1 parental and NAT1 KO cell lines were analyzed for significance by Student's *t*-test. All statistical analyses were performed using GraphPad Prism v6.0c (GraphPad Software, La Jolla, CA, USA). The results are expressed as the mean ± the standard error of the mean (SEM). Values of $p < 0.05$ were considered statistically significant.

3. Results

3.1. NAT1 Genomic and Amino Acid Sequences. Sequencing the NAT1 gene of MDA-MB-231 gRNA #2 (clone 2–19) KO cell line revealed a deletion of a single cytosine at 96 bases (bp) from the translation start codon (Table 1). This single-nucleotide deletion resulted in a frameshift mutation causing a premature stop codon after amino acid 49 of 290 (Table 2). The MDA-MB-231 gRNA #5 (clone 5–50) KO cell line had two nucleotides deleted at 43 and 44 bp from the translation start codon (Table 1). This deletion resulted in a premature stop codon after amino acid codon 14 of 290, which immediately terminates translation of NAT1 (Table 2).

Sequencing the NAT1 gene of MCF-7 gRNA #2 (clone 2–4) KO cell line showed a 34 bp deletion in the open reading frame, which spans from 95 to 129 bp (Table 1). This deleted segment of DNA resulted in a frameshift mutation causing a premature stop codon after 38 amino acids (Table 2). The MCF-7 gRNA #5 (clone 5–20) KO cell line had two different deletions (Table 1). The first deletion was a single nucleotide deletion at 42 bp, and the other was a deletion of 43 to 48 bp with an additional adenosine insertion in the same region. These deletions and insertions resulted in a premature stop codon after amino acid codon 23 for both sequences (Table 2).

Sequencing the NAT1 gene of ZR-75-1 gRNA #2 (clone 2–10) KO cell line showed a single adenosine insertion at 95 bp in the open reading frame (Table 1). This insertion results in a frameshift mutation causing a premature stop codon after 37 amino acids (Table 2).

3.2. In Vitro and In Situ PABA N-Acetylation. The *in vitro N*-acetylation of PABA in the parental cell line was 14.4 ± 2.8, 39.0 ± 5.9, and 121 ± 19 nmoles/min/mg for MDA-MB-231, MCF-7, and ZR-75-1 cell lines, respectively (Figure 1(a)). The gRNA #2 and #5 clones for all cell lines reduced levels of activity to below the limit of detection (0.05 nmoles/min/mg; Figure 1(a)). The *N*-acetylation of PABA *in situ* followed the same pattern as that for *in vitro* activity. *N*-acetylation activity of PABA in the parental cell lines was 1.13 ± 0.01, 2.20 ± 0.35, and 6.56 ± 0.87 nmoles/hr/million cells for MDA-MB-231, MCF-7, and ZR-75-1 cell lines, respectively (Figure 1(b)). In the gRNA #2 and #5 clones, levels of PABA *N*-acetylation *in situ* were reduced to below the limit of detection (0.20 nmoles/hr/million cells Figure 1(b)).

3.3. Human NAT1 and NAT2 Protein Levels. Relative NAT1 and NAT2 protein expression was evaluated following an in-cell western staining protocol as described in Materials and Methods. NAT1 protein expression was significantly (ANOVA, $p < 0.0001$) decreased in the MDA-MB-231 gRNA #2 and gRNA #5, the MCF-7 gRNA #2 and gRNA #5, and the ZR-75-1 gRNA #2 NAT1 KO cells compared to their respective parental cells (Figure 2(a)). Relative NAT2 protein expression in MDA-MB-231 gRNA #2 and gRNA #5 and in MCF-7 gRNA #2 and gRNA #5 NAT1 KO cells were increased significantly (ANOVA, $p < 0.0001$) compared to their respective parental cell line whereas no significant changes ($p > 0.05$) in NAT2 protein expression were observed in ZR-75-1 gRNA #2 NAT1 KO cells compared to the parental (Figure 2(b)). Following detection of increased NAT2 protein, sulfamethazine NAT2 enzymatic assays were conducted as described in Materials and Methods, but NAT2 activity was below the limit of detection (0.005 nmoles/min/mg protein) in all cell lines tested.

3.4. Endogenous AcCoA Levels. The endogenous level of AcCoA within the MDA-MB-231 parental cell line was 17.8 ± 1.1 pmoles/million cells, whereas the endogenous level of AcCoA within the cells of the gRNA #2 and #5 NAT1 KO clones was 33.1 ± 1.8 and 35.5 ± 2.6 pmoles/million cells, respectively, both of which were significantly elevated compared to the MDA-MB-231 parental cell line ($n = 8$; ANOVA, $p < 0.0001$) (Figure 3).

The MCF-7 parental cell line had an endogenous AcCoA level of 18.7 ± 0.9 pmoles/million cells, whereas the endogenous levels of AcCoA within the cells of the gRNA #2 and #5 NAT1 KO clones were 27.6 ± 2.6 and 27.0 ± 2.7 pmoles/million cells, respectively, both of which were significantly elevated compared to their MCF-7 parental cell line ($n = 12$; ANOVA, $p < 0.05$) (Figure 3).

The ZR-75-1 parental cell line had an endogenous AcCoA level of 43.2 ± 3.6 pmoles/million cells, whereas the endogenous levels of AcCoA within the cells of the gRNA #2 NAT1 KO was 33.6 ± 8.4 pmoles/million cells ($n = 3$; Student's *t*-test, $p > 0.05$) (Figure 3).

3.5. Cell Doubling Time. The doubling times for the MDA-MB-231 parental and gRNA #2 and #5 NAT1 KO cell lines were 24.8 ± 0.3, 30.3 ± 0.4, and 30.9 ± 0.3 hr, respectively ($n = 3$). Both MDA-MB-231 NAT1 KO cell lines had a significant (ANOVA, $p < 0.0001$) increase in doubling time compared to the parental MDA-MB-231 cell line (Figure 4(a)).

The doubling times for the MCF-7 parental cell line and gRNA #2 and #5 NAT1 KO cell lines were 41.4 ± 0.4, 45.3 ± 6.2, and 38.8 ± 8.5 hr, respectively ($n = 3$), which did not differ significantly (ANOVA, $p > 0.05$) compared to the parental MCF-7 cell line (Figure 4(a)).

The doubling times for the ZR-75-1 parental cell line and gRNA #2 NAT1 KO cell line were 37.0 ± 2.8, and 63.1 ± 2.9 hr, respectively ($n = 4$). The doubling time of the ZR-75-1 gRNA #2 NAT1 KO cell line was significantly (Student's *t*-test, $p = 0.0006$) elevated compared to the parental ZR-75-1 cell line (Figure 4(a)).

3.6. Anchorage-Dependent Colony Formation. Anchorage-*dependent* colony formation assay allows the determination of cancer cell ability to form colonies when attached to a surface. Results of the anchorage-*dependent* colony formation assay showed the number of colonies formed for MDA-MB-231 parental colonies, gRNA #2, and gRNA #5 NAT1

Table 1: Genomic DNA sequences of the reference (*NAT1*4*) and mutated *NAT1* from each NAT1 KO clone.

Cell line	KO clone	No. of bp from start codon	Genomic sequence	No. of bp from start codon
	Reference (*NAT1*4*)		1 ATGGACATTGAAGCATATCTTGAAAGAATTGGCTATAAGA 41 AGTCTAGGAACAAATTGGACTTGGAAACATTAACTGACAT 81 TCTTCAACACCAGATCCGAGCTGTTCCCTTTGAGAACCTT 121 AACATCCATTGTGGGGATGCCATGGACTTAGGCTTAGAGG 161 CCATTTTTGATCAAGTTGTGAGAAGAAATCGGGGTGGATG 201 GTGTCTCCAGGTCAATCATCTTCTGTACTGGGCTCTGACC 241 ACTATTGGTTTTGAGACCACGATGTTGGGAGGGTATGTTT 281 ACAGCACTCCAGCCAAAAAATACAGCACTGGCATGATTCA 321 CCTTCTCCTGCAGGTGACCATTGATGGCAGGAACTACATT 361 GTCGATGCTGGGTTTGGACGCTCATACCAGATGTGGCAGC 401 CTCTGGAGTTAATTTCTGGGAAGGATCAGCCTCAGGTGCC 441 TTGTGTCTTCCGTTTGACGGAAGAGAATGGATTCTGGTAT 481 CTAGACCAAATCAGAAGGGAACAGTACATTCCAAATGAAG 521 AATTTCTTCATTCTGATCTCCTAGAAGACAGCAAATACCG 561 AAAAATCTACTCCTTTACTCTTAAGCCTCGAACAATTGAA 601 GATTTTGAGTCTATGAATACATACCTGCAGACATCTCCAT 641 CATCTGTGTTTACTAGTAAATCATTTTGTTCCTTGCAGAC 681 CCCAGATGGGGTTCACTGTTTGGTGGGCTTCACCCTCACC 721 CATAGGAGATTCAATTATAAGGACAATACAGATCTAATAG 761 AGTTCAAGACTCTGAGTGAGGAAGAAATAGAAAAAGTGCT 801 GAAAAATATATTTAATATTTCCTTGCAGAGAAAGCTTGTG 841 CCCAAACATGGTGATAGATTTTTTACTATTTAG	
MDA-MB-231	gRNA #2	76	GACATTCTTCAACACCAGATC-GAGCTGTT	105
MDA-MB-231	gRNA #5	21	TGAAAGAATTGGCTATAAGAAG--TAGGAA	50
MCF-7	gRNA #2	91	CAGA----------TGTGGG	135
MCF-7	gRNA #5	31	GGCTATAAGAA-TCTAGGAACAAATTGGAC	60
MCF-7	gRNA #5	31	GGCTATAAGAAGA-----AACAAATTGGAC	60
ZR-75-1	gRNA #2	76	GACATTCTTCAACACCAGAT**A**CCGAGCTGTT (mutated nucleotide in bold face font)	105

KO cell lines was 40.7 ± 2.5, 51.3 ± 1.6, and 54.8 ± 6.8 colonies, respectively. Anchorage-*dependent* colonies among the MDA-MB-231 and NAT1 KO cell lines did not differ statistically from each other (ANOVA, $p > 0.05$; $n = 6$) (Figure 4(b)).

MCF-7 parental and gRNA #2 and #5 NAT1 KO cell line anchorage-*dependent* colony formation was 68.2 ± 8.6, 86.2 ± 9.9, and 96.7 ± 9.1 colonies, respectively, which did not differ statistically from each other (ANOVA, $p > 0.05$; $n = 3$) (Figure 4(b)).

ZR-75-1 parental and gRNA #2 NAT1 KO cell anchorage-*dependent* colony formation was 102 ± 5, and 39.4 ± 6.5 colonies, which differed statistically from each other (Student's *t*-test, $p < 0.001$; $n = 3$) (Figure 4(b)).

3.7. Anchorage-Independent Colony Formation. Anchorage-*independent* colony formation assays (also known as "soft agar assays") allows the determination of cancer cell ability to form colonies in the absence of cellular attachment to a surface. The MDA-MB-231 parental cell line formed anchorage-*independent* colonies at markedly higher levels than the NAT1 KO clones (Figure 4(c)). The number of colonies formed by MDA-MB-231 parental and gRNA #2 and #5 NAT1 KO cell lines were 1070 ± 76, 48.3 ± 17.2, and 23.4 ± 7.0 colonies, respectively (ANOVA, $p < 0.0001$; $n = 3$). The number of colonies formed by the two NAT1 KO cell lines were not statistically different from each other ($p > 0.05$).

The MCF-7 parental cell line formed anchorage-*independent* colonies at a higher level than the MCF-7 NAT1 KO clones (Figure 4(c)). The number of colonies formed by MCF-7 parental and gRNA #2 and #5 NAT1 KO cell lines were 195 ± 9, 33.7 ± 6.8, and 13.8 ± 6.6, respectively. Anchorage-*independent* colonies formed by the MCF-7 parental cell line were significantly higher than gRNA #2 and #5 NAT1 KO clones (ANOVA $p < 0.0001$; $n = 4$). The MCF-7 gRNA #2 and #5 NAT1 KO clones were not statistically ($p > 0.05$) different from each other.

The ZR-75-1 parental cell line formed anchorage-*independent* colonies at a higher level than the NAT1 KO cell line clone (Figure 4(c)). The number of colonies formed by ZR-75-1 parental and gRNA #2 NAT1 KO cell line was 45.6 ± 13.4, and 6.00 ± 1.84, respectively. Anchorage-*independent* colonies formed by the ZR-75-1 parental cell line were significantly higher than gRNA #2 NAT1 KO clone (Student's *t*-test, $p < 0.05$; $n = 3$).

4. Discussion

We investigated the effect of NAT1 gene deletion in three different human breast cancer cell lines, MDA-MB-231,

Table 2: Amino acid sequences of reference (NAT1 4) and mutated NAT1 from each NAT1 KO clone.

Cell line	KO clone	Amino acid sequence	No. of total amino acids
	NAT1 4 (Reference)	MDIEAYLERIGYKKS RNKLDLETLTDILQHQIRA VPFENLNIHCGD AMDLGLEAIFDQVVRRNRGGWCLQVNHLLY WALTTIGFETTMLGGYVY STPAKKYSTGMIHLLLQVTIDGRNYI VDAGFGRSYQMWQPLELISGKDQP QVPCVFRLTEENGFWYLDQIRREQYI PNEEFLHSDLLEDSKYRKIYSFTLK PRTIEDFESMNTYLQTSPSSVFTSKSF CSLQTPDGVHCLVGFTLTHRRFNYKDNTDLIEF KTLSEEEIEKVLKNIFNISLQRKL VPKHGDRFFTI stop	290
MB-MDA-231	gRNA #2 clone	MDIEAYLERIGYKKSRNKLDLETLTDIL QHQIELFPLRTLTSIVGMPWT stop	49
MB-MDA-231	gRNA #5 clone	MDIEAYLERIGYKK stop	14
MCF-7	gRNA #2 clone	MDIEAYLERIGYKKSRNK LDLETLTDILQHQIVGMPWT stop	38
MCF-7	gRNA #5 clone (allele 1)	MDIEAYLERIGYKNLGTNWTW KH stop	23
MCF-7	gRNA #5 clone (allele 2)	MDIEAYLERIGYKKKQIGLGNIN stop	23
ZR-75-1	gRNA #2 clone	MDIEAYLERIGYKKSRNKL DLETLTDILQHQIPSCSL stop	37

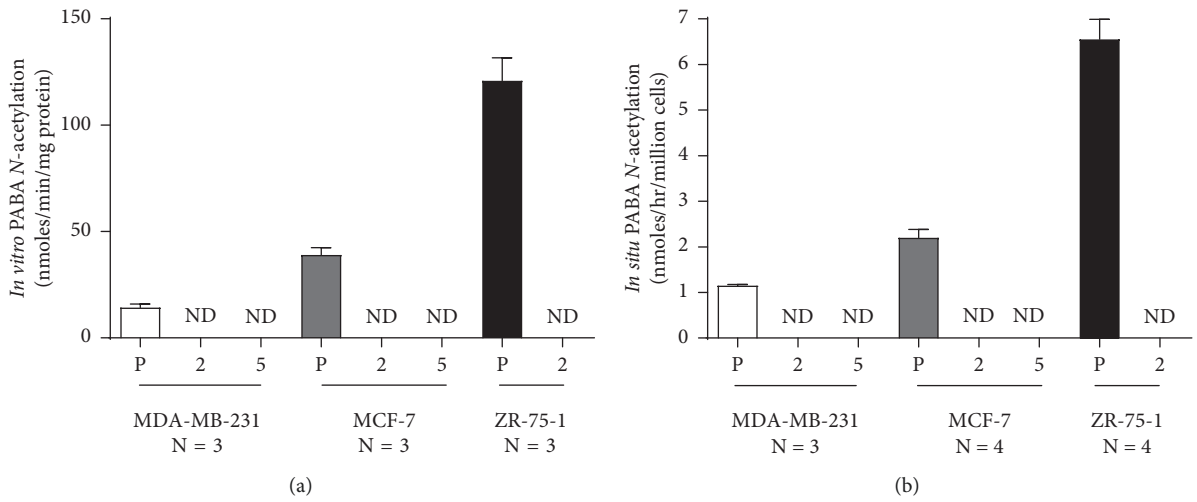

Figure 1: *In vitro* and *in situ* PABA (N)-acetylation activity of parental and NAT1 KO clones for MDA-MB-231, MCF-7, and ZR-75-1 cell lines. (a) The in vitro PABA N-acetyltransferase activity in MDA-MB-231, MCF-7, and ZR-75-1 parental (P) and gRNA #2 (2) and #5 (5) clones NAT1 KO cell lines are shown. (b) The *in situ* PABA *N*-acetylation in MDA-MB-231, MCF-7, and ZR-75-1 parental (P) and gRNA #2 (2) and #5 (5) clones NAT1 KO cell lines are shown. Each bar illustrates mean ± SEM. Three or four separate determinations were performed in triplicate. ND is nondetectable ((a) <0.05 nmoles/min/mg; (b) <0.20 nmoles/hr/million cells).

MCF-7, and ZR-75-1. Human NAT1 was knocked out using CRISPR/Cas9 technology and two different guide RNAs. None of the NAT1 KO cell lines exhibited detectable NAT1 activity when measured using their selective substrate PABA. Endogenous AcCoA levels (cofactor for acetylation pathways) in NAT1 KO cell lines were significantly elevated in the MDA-MB-231 ($p < 0.001$) and MCF-7 ($p = 0.0127$) but not the ZR-75-1 ($p > 0.05$). Although the effects of NAT1 KO on cell doubling time were inconsistent across the three breast cancer cell lines, the ability of the NAT1 KO cell lines to form anchorage-independent colonies in soft agar was dramatically and consistently reduced in each of the breast cancer cell lines. The NAT1 KO clones for MDA-MB-231, MCF-7, and ZR-75-1 had a reduction greater than 20-, 6-, and 7-folds in anchorage-independent cell growth, respectively, compared to their parental cell lines ($p < 0.0001$, $p < 0.0001$ and $p < 0.05$, respectively).

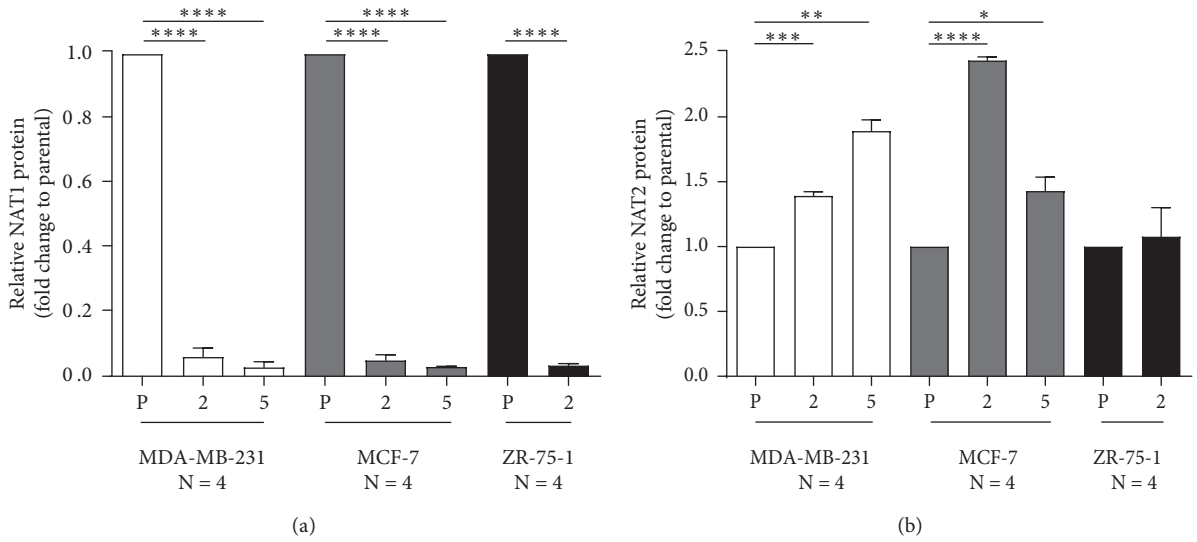

Figure 2: NAT1 and NAT2 protein expression in breast cancer cell lines. (a). Relative NAT1 protein expression was evaluated following an in-cell western staining protocol as described in Materials and Methods. NAT1 protein expression was significantly ($p < 0.0001$) decreased in MDA-MB-231 gRNA #2 (2) and gRNA #5 (5) NAT1 KO cells compared to the parental (P); MCF-7 gRNA #2 (2) and gRNA #5 (5) and ZR-75-1 gRNA #2 (2) NAT1 KO cells compared to the respective parental (P) cells. (b). Relative NAT2 protein expression in MDA-MB-231 gRNA #2 (2) and gRNA #5 (5) KO cells was significantly ($p < 0.0001$) increased compared to the parental (P) cells, the same phenomenon was observed for MCF-7 gRNA #2 (2) and gRNA #5 (5) KO cells ($p < 0.0001$) compared to the parental (P); however, no significant ($p > 0.05$) changes in the relative NAT2 protein expression were observed in ZR-75-1 gRNA #2 (2) NAT1 KO cells compared to the parental (P). Data expressed as mean ± SEM for 4-different determinations $^{*}p < 0.05$, $^{**}p < 0.01$, $^{***}p < 0.001$, $^{****}p < 0.0001$.

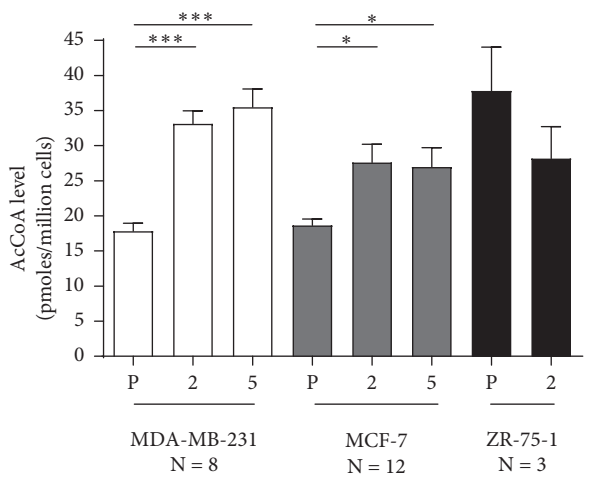

Figure 3: Intracellular AcCoA levels in parental and NAT1 KO clones for MDA-MB-231, MCF-7, and ZR-75-1 cell lines. AcCoA levels were measured in parental (P) and NAT1 KO cell lines for MDA-MB-231, MCF-7, and ZR-75-1. Each bar illustrates mean ± SEM for number of replicates (N). AcCoA levels differed significantly between parental and NAT1 KO cells for MDA-MB-231 ($p < 0.0001$) and MCF-7 ($p < 0.05$) cell lines.

CRISPR/Cas9 was used to make stable NAT1 KO human MDA-MB-231, MCF-7, and ZR-75-1 breast cancer cell lines. We used two different gRNA's to allow us to distinguish between specific NAT1 KO effects versus off-target effects caused by gRNA binding and mutating at nonspecific site (s). We also used a MDA-MB-231 breast cancer cell line with a single FRT site and a nonspecific scrambled shRNA inserted in the FRT site as the MDA-MB-231 parental cell line. This cell line was transfected with gRNA #2 and #5 to facilitate comparison of the results of NAT1 KO with those previously described for NAT1 knockdown [16].

We isolated single clones from MDA-MB-231 and MCF-7 cells lines with both gRNA #2 and #5. We were not able to isolate a NAT1 KO clone using gRNA #5 in the ZR-75-1 cell line, likely due to reduced growth rate of ZR-75-1 NAT1 KO cell lines. Other groups have also investigated NAT1 KO in MDA-MB-231 and other cell lines by CRISPR/Cas9 [21, 22]. The knockout strategy of the previous studies was different from ours in the following regards: (1) different gRNA sequences were employed to cause DNA breaks and (2) previous studies used a linear donor plasmid carrying a selection marker stably integrated into the DNA breakage site. We chose transient transfection to minimize off-target effects, so the gRNA/Cas9 plasmid was present in the cell for a short time (72–96 hr). We also attempted to assess the effects of NAT1 rescue of gRNA #2 and #5 NAT1 KO in MDA-MB-231 and MCF-7 cells. Although we initially measured PABA NAT1 activity confirming successful NAT1 rescue, the NAT1 activity was no longer detectable during experiments to measure AcCoA levels or cell growth properties, and thus we were not able to characterize the effects of NAT1 rescue.

NAT1 KO in MDA-MB-231, MCF-7, and ZR-75-1 reduced levels of PABA *N*-acetylation below limits of detection both *in vitro* and *in situ*. Despite this functional validation of the NAT1 KO, the effects on endogenous levels of AcCoA and cancer cell growth were not completely consistent across different cell lines. The KO of NAT1 activity by both gRNA #2 and gRNA #5 in MDA-MB-231 breast cancer cells caused a

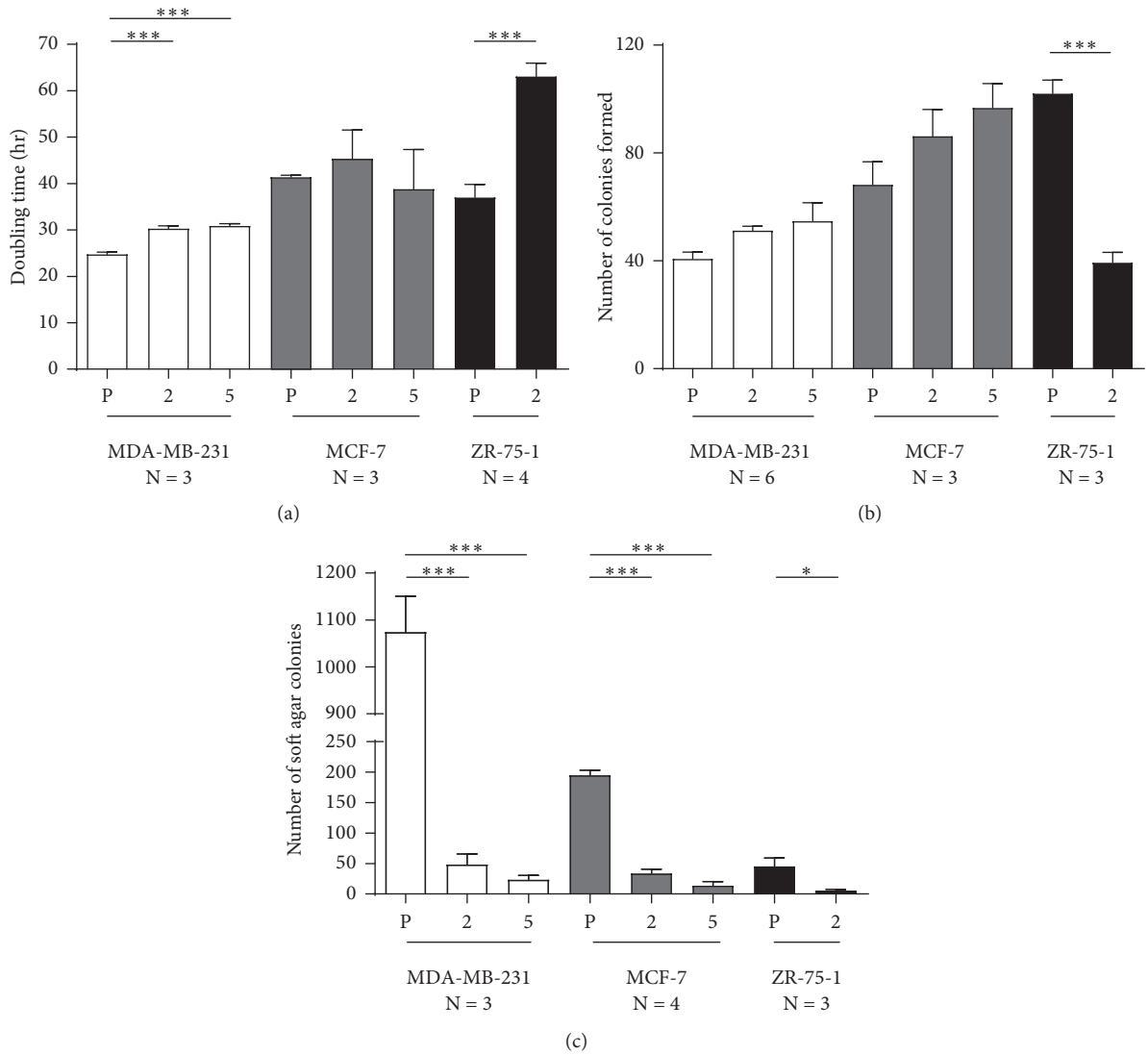

Figure 4: Doubling time and anchorage-dependent and anchorage-independent colony formation of parental and NAT1 KO clones for MDA-MB-231, MCF-7, and ZR-75-1 cell lines. (a) Doubling time was determined in MDA-MB-231, MCF-7, and ZR-75-1 parental (P) and gRNA #2 (2) and #5 (5) NAT1 KO clones. Each bar illustrates mean ± SEM for number of replicates (*N*). Doubling times differed significantly between parental and NAT1 KO cell lines for MDA-MB-231 ($p < 0.0001$), and ZR-75-1 ($p = 0.0006$) cell lines. (b) Anchorage-*dependent* growth/colony formation was determined in MDA-MB-231, MCF-7, and ZR-75-1 parental (P) and NAT1 KO cell lines. Cells (300) were plated on plastic in triplicate and allowed to grow for 14 days before staining. Anchorage-*dependent* growth/colony formation between parental and NAT1 KO cells were not significantly different ($p > 0.05$) for all cell lines, except for ZR-75-1. (c) Anchorage-*independent*/soft agar assays were completed in MDA-MB-231, MCF-7, and ZR-75-1 parental (P) and NAT1 KO cell lines. Cells (6000) plated in triplicate in soft agar were allowed to grow for 14 days before staining. The number of colonies formed in soft agar were significantly higher in parental MDA-MB-231 ($p < 0.0001$) MCF-7 ($p < 0.0001$) and ZR-75-1 ($p < 0.05$) than their respective NAT1 KO cell lines.

modest but significant ($p < 0.0001$) elevation in doubling time but neither gRNA #2 or gRNA #5 caused significant ($p > 0.05$) elevation in doubling time for the MCF-7 breast cancer cell line. NAT1 KO in ZR-75-1 cells using gRNA #2 resulted in a 1.7-fold ($p < 0.001$) elevation in doubling time. Previous studies in our laboratory found that knockdown of NAT1 in MDA-MB-231 by approximately 40% did not significantly change the doubling time [16]. Knockdown of NAT1 by 85% in HT-29 cells showed similar exponential growth; however, the NAT1 knockdown cells reached saturation density earlier than control cells [15]. With NAT1 KO cells, cell death increased when cells were at confluence [15]. Wang et al. demonstrated that growth in low glucose (1 mM) was enhanced in HT29 cells following NAT1 KO [21]. We performed experiments with both MDA-MB-231 and ZR-75-1 parental and NAT1 KO cells in the presence of low (1 g/L or 5.5 mM) or no glucose supplemented with 10 mM galactose to determine whether NAT1 KO would alter the cell doubling time under these nutrient conditions. Cells grown in the presence of low (1 g/L or 5.5 mM) or no glucose supplemented with 10 mM galactose grew more slowly; however, the relationship

between the parental and NAT1 KO cell lines did not differ from cells grown in standard media.

The level of NAT1 was substantially and significantly ($p < 0.0001$) reduced in each of the NAT1 KO cells lines. In MDA-MB-231 and MCF-7 cells, NAT1 KO was associated with a significant increase ($p < 0.0001$) in NAT2 protein. However, NAT2 enzymatic activity in the parental or NAT1 KO cell lines was below the limit of detection.

Human NAT1 has the capacity to hydrolyze AcCoA [3, 4] and partial knockdown of NAT1 in MDA-MB-231 cells has been reported to increase endogenous AcCoA levels [16]. In the present study, we measured the endogenous level of AcCoA in MDA-MB-231, MCF-7, and ZR-75-1 parental and NAT1 KO cell lines. The MDA-MB-231 and MCF-7 NAT1 KO with both the gRNA #2 and gRNA #5 showed significant ($p < 0.05$) increases in AcCoA levels relative to their respective parental cell lines. However, the ZR-75-1 NAT1 KO cell line did not show the same increase in AcCoA compared to the parental cell line as did the MDA-MB-231 and MCF-7 cell lines. The results for MDA-MB-231 and MCF-7 NAT1 KO cell lines are similar to what was observed when NAT1 was knocked down by shRNA in MDA-MB-231 cells [16].

AcCoA is considered a central metabolic intermediate whose level reflects the general energetic state of the cell [23]. In addition, AcCoA concentrations not only influence the activity or specificity of multiple enzymes but also influence the acetylation profiles of proteins, including histones. For instance, it is well known that the N^{ϵ} amino group of lysine residues can be posttranslationally modified via acetylation, the process by which numerous key cellular processes, including energy metabolism, mitosis, and autophagy, are known to be regulated [23, 24]. Notably, many lysine acetyltransferases have a relatively high K_D (low affinity) for AcCoA [25], and thus changes in cellular AcCoA levels likely affect their enzymatic activity and subsequently the acetylation profile of their substrate proteins. Interestingly, in two of the cell lines tested in the current study, NAT1 deficiency led to a significant increase in the cellular level of AcCoA, which suggests that cellular level of AcCoA is, at least in part, dependent on NAT1 activity in these cell lines. In support of this, we also have previously reported that rat embryonic fibroblasts from rapid acetylator congenic rats (high levels of rat NAT2 which is orthologous to human NAT1) have lower levels of AcCoA than those derived from slow acetylator congenic rats, which have low levels of rat Nat2 [12]. NAT1 uses AcCoA during *N*-acetylation of endogenous and exogenous substrates, but also catalyzes the hydrolysis of AcCoA to CoA in the presence of folate [3, 4]. It is possible that the cellular levels of AcCoA are negatively affected by NAT1 activity. Based on this, we can speculate that depletion of NAT1 could in turn lead to increased levels of AcCoA, which occurred in two of the three cancer cell lines investigated in our study. Depletion of NAT1 in ZR-75-1 cells did not result in an increase in the AcCoA level despite the fact that they exhibit the highest NAT1 activity among the three breast cancer cell lines tested. Alternatively, the elevated levels of AcCoA in two KO cell lines (i.e., MDA-MB-231 and MCF-7) may not be a direct effect of NAT1 depletion but rather reflect changes in their metabolic status. Whether or not elevated levels of AcCoA in NAT1 KO cell lines translate into alterations in protein acetylation profile within these cells remains unknown. Furthermore, the significant reductions in cell growth rate as well as anchorage-dependent and anchorage-independent growth observed in NAT1 KO ZR-75-1 cells occurred in the absence of concomitant changes in AcCoA levels. Thus, the relationship of AcCoA levels to alterations in cancer growth properties observed in NAT1 KO cells requires further investigation.

Anchorage-dependent colony formation in human MDA-MB-231 and MCF-7 did not show a significant difference ($p > 0.05$) between parental and NAT1 KO cell lines. These results agree with previous studies where knockdown of NAT1 in MDA-MB-231 cells by shRNA did not alter the ability of the cells to form anchorage-dependent colonies [16]. Although NAT1 KO in the ZR-75-1 cell line formed fewer colonies than the parental ZR-75-1, this difference may be due to the fact that the ZR-75-1 KO cells grew more slowly than the ZR-75-1 parental cell line.

The ability of the NAT1 KO cell lines to form anchorage-independent colonies in soft agar was dramatically and consistently reduced in each of the MDA-MB-231, MCF-7, and ZR-75-1 breast cancer cell lines. This data is consistent with previous results following knockdown of NAT1 by shRNA in MDA-MB-231 [16] and HT-29 [14, 15] cells. Although the significant decline in the ability of ZR-75-1 NAT1 KO cells to form anchorage-independent colonies may be partially attributed to its slower growth rate (i.e., a higher cell doubling time; Figure 4(a)), the magnitude of the decline (from 45.6 ± 13.4 colonies in parental cells to 6.00 ± 1.84 colonies in NAT1 KO cells; an approximately 7.6-fold decrease) was greater than that observed with anchorage-dependent colony formation (from 102 ± 5 colonies in parental cells to 39.4 ± 6.5 colonies in NAT1 KO cells; an approximately 2.6-fold decrease). Based on this, it seems that the ability of ZR-75-1 cells to form colonies in an anchorage-independent manner is further compromised in the absence of NAT1.

Anchorage-independent growth is one of the hallmarks of metastatic tumors. Tumor cells often lose epithelial features and acquire mesenchymal properties via a complex and dynamic EMT. Through EMT, the tumor cells are believed to acquire increased motility and resistance to apoptosis, ultimately leading to metastasis [26]. Savci-Heijink and colleagues analyzed gene expression signatures specifically associated with the development of bone metastases of breast cancer using primary breast tumor samples and reported NAT1 as one of three genes whose increased expression levels were highly correlated to EMT-activated breast tumor [27]. In a follow-up study, they also demonstrated a high correlation between positive immunostaining for NAT1 and expression of EMT signature genes in breast cancer [10], suggesting that increased NAT1 expression may contribute to the EMT of breast cancers and subsequently their metastatic potential. In support of this notion, we found that NAT1 KO reduced anchorage-independent growth in all three breast cancer cell lines tested. Similarly, Tiang et al. have previously reported that RNAi-mediated knockdown of NAT1 in the colon adenocarcinoma cell line, HT-29, leads to increased growth inhibition by cell-cell contact and attenuation of anchorage-independent growth in soft agar

[15]. In a later study, the same group silenced NAT1 in the triple-negative breast cancer cell lines and tested the invasiveness of the cells in both *in vitro* and *in vivo*. Importantly, NAT1 knockdown in MDA-MB-231 cells resulted in a significant reduction in their ability to metastasize to and colonize in the lungs when injected into nude mice [14], suggesting that increased NAT1 level in breast cancer cells can contribute to their metastatic properties *in vivo*.

In conclusion, we knocked out human NAT1 with CRISPR/Cas9 technology using two different gRNA's in three different breast cancer cells lines. We verified complete NAT1 KO by measurement of PABA *N*-acetylation *in vitro* and *in situ* and measurement of NAT1-specific immunoreactive protein. KO of NAT1 caused a significant decrease in cell growth for MDA-MB-231 and ZR-75-1, but not for MCF-7 NAT1 KO cells relative to their respective parental cell lines. NAT1 KO caused a significant increase in cellular AcCoA levels in MDA-MB-231 and MCF-7 cells but not for ZR-75-1 cells relative to the parental cell lines. Each NAT1 KO cell line showed a dramatic decrease in the number of colonies that formed in an anchorage-independent manner relative to their respective parental cell line. Although it appears that NAT1 KO can influence the cell morphology and cell-cell interactions in cancer cell lines, further investigation is needed into whether or not NAT1 depletion ultimately alters metastatic potential *in vivo*.

Abbreviations

AcCoA: Acetyl-Coenzyme A
NAT1: *N*-acetyltransferase 1
NAT2: *N*-acetyltransferase 2
PABA: *para*-aminobenzoic acid
EMT: Epithelial-to-mesenchymal transition
gRNA: Guide RNA
KO: Knockout
PBS: Phosphate-buffered saline
EDTA: Ethylenediaminetetraacetic acid
DMEM: Dulbecco's modified eagles medium
RFU: Relative fluorescence units
HPLC: High-performance liquid chromatography.

Data Availability

The data that support the findings of this study are available from the corresponding author upon reasonable request.

Disclosure

Portions of this work constituted partial fulfilment by Marcus W. Stepp for the PhD in pharmacology and toxicology at the University of Louisville, whose current address is Charles River, Ashland, Ohio 44805.

Conflicts of Interest

The authors declare that they have no conflicts of interest.

Authors' Contributions

Marcus W. Stepp, Raúl A. Salazar-González, Kyung U. Hong, Mark A. Doll, and David W. Hein participated in research design. Marcus W. Stepp, Raúl A. Salazar-González, and Mark A. Doll conducted experiments. Marcus W. Stepp and Mark A. contributed new reagents or analytic tools. Marcus W. Stepp and Mark A. Doll performed data analysis. Marcus W. Stepp, Raúl A. Salazar-González, Kyung U. Hong, Mark A. Doll, and David W. Hein wrote or contributed to the writing of the manuscript. All authors read and approved the final manuscript.

Acknowledgments

This work was supported in part by the National Institute of Environmental Sciences (grant USPHS T32-ES011564).

References

[1] D. W. Hein, "Molecular genetics and function of NAT1 and NAT2: role in aromatic amine metabolism and carcinogenesis," *Mutation Research/Fundamental and Molecular Mechanisms of Mutagenesis*, vol. 506-507, pp. 65–77, 2002.

[2] D. W. Hein, M. A. Doll, A. J. Fretland et al., "Molecular genetics and epidemiology of the NAT1 and NAT2 acetylation polymorphisms," *Cancer epidemiology, Biomarkers & Prevention*, vol. 9, no. 1, pp. 29–42, 2000.

[3] M. W. Stepp, G. Mamaliga, M. A. Doll, J. C. States, and D. W. Hein, "Folate-dependent hydrolysis of acetyl-coenzyme A by recombinant human and rodent arylamine *N*-acetyltransferases," *Biochemistry and Biophysics Reports*, vol. 3, pp. 45–50, 2015.

[4] N. Laurieri, J. Dairou, J. E. Egleton et al., "From arylamine *N*-acetyltransferase to folate-dependent acetyl CoA hydrolase: impact of folic acid on the activity of (HUMAN)NAT1 and its homologue (MOUSE)NAT2," *PLoS One*, vol. 9, no. 5, Article ID e96370, 2014.

[5] N. Butcher, J. Tiang, and R. Minchin, "Regulation of arylamine *N*-acetyltransferases," *Current Drug Metabolism*, vol. 9, no. 6, pp. 498–504, 2008.

[6] P. J. Adam, J. Berry, J. A. Loader et al., "Arylamine *N*-acetyltransferase-1 is highly expressed in breast cancers and conveys enhanced growth and resistance to etoposide in vitro," *Molecular Cancer Research*, vol. 1, no. 11, pp. 826–835, 2003.

[7] M. C. Abba, Y. Hu, H. Sun et al., "Gene expression signature of estrogen receptor alpha status in breast cancer," *BMC Genomics*, vol. 6, p. 37, 2005.

[8] Y. Endo, T. Toyama, S. Takahashi et al., "miR-1290 and its potential targets are associated with characteristics of estrogen receptor α-positive breast cancer," *Endocrine-Related Cancer*, vol. 20, no. 1, pp. 91–102, 2013.

[9] S. M. Carlisle and D. W. Hein, "Retrospective analysis of estrogen receptor 1 and *N*-acetyltransferase gene expression in normal breast tissue, primary breast tumors, and established breast cancer cell lines," *International Journal of Oncology*, vol. 53, no. 2, pp. 694–702, 2018.

[10] C. D. Savci-Heijink, H. Halfwerk, G. K. J. Hooijer et al., "Epithelial-to-mesenchymal transition status of primary breast carcinomas and its correlation with metastatic behavior," *Breast Cancer Research and Treatment*, vol. 174, no. 3, pp. 649–659, 2019.

[11] M. Smid, Y. Wang, J. G. M. Klijn et al., "Genes associated with breast cancer metastatic to bone," *Journal of Clinical Oncology*, vol. 24, no. 15, pp. 2261–2267, 2006.

[12] M. W. Stepp, M. A. Doll, D. J. Samuelson, M. A. G. Sanders, J. C. States, and D. W. Hein, "Congenic rats with higher arylamine *N*-acetyltransferase 2 activity exhibit greater carcinogen-induced mammary tumor susceptibility independent of carcinogen metabolism," *BMC Cancer*, vol. 17, no. 1, p. 233, 2017.

[13] J. M. Tiang, N. J. Butcher, and R. F. Minchin, "Small molecule inhibition of arylamine *N*-acetyltransferase type I inhibits proliferation and invasiveness of MDA-MB-231 breast cancer cells," *Biochemical and Biophysical Research Communications*, vol. 393, no. 1, pp. 95–100, 2010.

[14] J. M. Tiang, N. J. Butcher, and R. F. Minchin, "Effects of human arylamine *N*-acetyltransferase I knockdown in triple-negative breast cancer cell lines," *Cancer Medicine*, vol. 4, no. 4, pp. 565–574, 2015.

[15] J. M. Tiang, N. J. Butcher, C. Cullinane, P. O. Humbert, and R. F. Minchin, "RNAi-mediated knock-down of arylamine *N*-acetyltransferase-1 expression induces E-cadherin up-regulation and cell-cell contact growth inhibition," *PLoS One*, vol. 6, no. 2, Article ID e17031, 2011.

[16] M. W. Stepp, M. A., S. M. Carlisle, J. C. States, and D. W. Hein, "Genetic and small molecule inhibition of arylamine *N*-acetyltransferase 1 reduces anchorage-independent growth in human breast cancer cell line MDA-MB-231," *Molecular Carcinogenesis*, vol. 57, no. 4, pp. 549–558, 2018.

[17] S. M. Carlisle, P. J. Trainor, X. Yin et al., "Untargeted polar metabolomics of transformed MDA-MB-231 breast cancer cells expressing varying levels of human arylamine *N*-acetyltransferase 1," *Metabolomics*, vol. 12, no. 7, p. 111, 2016.

[18] E. Vagena, G. Fakis, and S. Boukouvala, "Arylamine *N*-acetyltransferases in prokaryotic and eukaryotic genomes: a survey of public databases," *Current Drug Metabolism*, vol. 9, no. 7, pp. 628–660, 2008.

[19] D. W. Hein, M. A. Doll, D. E. Nerland, and A. J. Fretland, "Tissue distribution of *N*-acetyltransferase 1 and 2 catalyzing the *N*-acetylation of 4-aminobiphenyl and O-acetylation of N-hydroxy-4-aminobiphenyl in the congenic rapid and slow acetylator Syrian hamster," *Molecular Carcinogenesis*, vol. 45, no. 4, pp. 230–238, 2006.

[20] L. M. Millner, M. A. Doll, M. W. Stepp, J. C. States, and D. W. Hein, "Functional analysis of arylamine *N*-acetyltransferase 1 (NAT1) NAT1∗10 haplotypes in a complete NATb mRNA construct," *Carcinogenesis*, vol. 33, no. 2, pp. 348–355, 2012.

[21] L. Wang, R. F. Minchin, and N. J. Butcher, "Arylamine N-acetyltransferase 1 protects against reactive oxygen species during glucose starvation: role in the regulation of p53 stability," *PLoS One*, vol. 13, no. 3, Article ID e0193560, 2018.

[22] L. Wang, R. F. Minchin, P. J. Essebier, and N. J. Butcher, "Loss of human arylamine *N*-acetyltransferase I regulates mitochondrial function by inhibition of the pyruvate dehydrogenase complex," *The International Journal of Biochemistry & Cell Biology*, vol. 110, pp. 84–90, 2019.

[23] F. Pietrocola, L. Galluzzi, J. M. Bravo-San Pedro, F. Madeo, and G. Kroemer, "Acetyl coenzyme A: a central metabolite and second messenger," *Cell Metabolism*, vol. 21, no. 6, pp. 805–821, 2015.

[24] C. Choudhary, B. T. Weinert, Y. Nishida, E. Verdin, and M. Mann, "The growing landscape of lysine acetylation links metabolism and cell signalling," *Nature Reviews Molecular Cell Biology*, vol. 15, no. 8, pp. 536–550, 2014.

[25] M. R. Langer, C. J. Fry, C. L. Peterson, and J. M. Denu, "Modulating acetyl-CoA binding in the GCN5 family of histone acetyltransferases," *Journal of Biological Chemistry*, vol. 277, no. 30, pp. 27337–27344, 2002.

[26] A. Singh and J. Settleman, "EMT, cancer stem cells and drug resistance: an emerging axis of evil in the war on cancer," *Oncogene*, vol. 29, no. 34, pp. 4741–4751, 2010.

[27] C. D. Savci-Heijink, H. Halfwerkau, J. Koster, and M. J. van de Vijver, "A novel gene expression signature for bone metastasis in breast carcinomas," *Breast Cancer Research and Treatment*, vol. 156, no. 2, pp. 249–259, 2016.

Hindawi
Journal of Oncology
Volume 2019, Article ID 2024648, 14 pages
https://doi.org/10.1155/2019/2024648

Research Article

Dovitinib Triggers Apoptosis and Autophagic Cell Death by Targeting SHP-1/*p*-STAT3 Signaling in Human Breast Cancers

Yi-Han Chiu,[1,2] Yi-Yen Lee,[3] Kuo-Chin Huang,[4] Cheng-Chi Liu,[3] and Chen-Si Lin[3,5]

[1]*Department of Nursing, St. Mary's Junior College of Medicine, Nursing and Management, Yilan 26647, Taiwan*
[2]*Institute of Long-Term Care, Mackay Medical College, New Taipei City 25245, Taiwan*
[3]*Department of Veterinary Medicine, School of Veterinary Medicine, National Taiwan University, 1 Sec 4 Roosevelt Road, Taipei 10617, Taiwan*
[4]*Holistic Education Center, Mackay Medical College, New Taipei City 25245, Taiwan*
[5]*Animal Cancer Center, College of Bioresources and Agriculture, National Taiwan University, 1 Sec 4 Roosevelt Road, Taipei 10617, Taiwan*

Correspondence should be addressed to Chen-Si Lin; cslin100@ntu.edu.tw

Received 29 June 2019; Accepted 29 July 2019; Published 14 August 2019

Guest Editor: Chia-Jung Li

Breast cancer is the most common cancer and the leading cause of cancer deaths in women worldwide. The rising incidence rate and female mortality make it a significant public health concern in recent years. Dovitinib is a novel multitarget receptor tyrosine kinase inhibitor, which has been enrolled in several clinical trials in different cancers. However, its antitumor efficacy has not been well determined in breast cancers. Our results demonstrated that dovitinib showed significant antitumor activity in human breast cancer cell lines with dose- and time-dependent manners. Downregulation of phosphor-(*p*)-STAT3 and its subsequent effectors Mcl-1 and cyclin D1 was responsible for this drug effect. Ectopic expression of STAT3 rescued the breast cancer cells from cell apoptosis induced by dovitinib. Moreover, SHP-1 inhibitor reversed the downregulation of *p*-STAT3 induced by dovitinib, indicating that SHP-1 mediated the STAT3 inhibition effect of dovitinib. In addition to apoptosis, we found for the first time that dovitinib also activated autophagy to promote cell death in breast cancer cells. In conclusion, dovitinib induced both apoptosis and autophagy to block the growth of breast cancer cells by regulating the SHP-1-dependent STAT3 inhibition.

1. Introduction

Breast cancer is the most common cancer in women, and the mortality rate is in the rank of top five cancers [1]. In Taiwan, breast cancer is also the top diagnosed cancer in women. The incidence rate of breast cancer keeps climbing high in the last 30 years. Therefore, breast cancer is the critical public health issue in recent years. It was found that epidermal growth factor receptor- (EGFR-) positive breast cancer was more prevalent in Asian women diagnosed than Western women [2] and high expression of EGFR oncoprotein was associated with advanced stages of breast cancer [3]. The receptors of EGFR family regulate the transcription of molecules that control several cellular functions, including cell proliferation, differentiation, apoptosis, invasion, and angiogenesis [4]. Thus, EGFR is one of the first identified important targets of these novel anti-breast tumor agents in Asia. However, treatment of EGFR inhibitors on breast patients has been found to rapidly advance to resistance and disease progression [5, 6], implying that more effective therapeutic receptor tyrosine kinases (RTKs) inhibitors are required.

Fibroblast growth factors (FGFs) and FGF receptors (FGFRs) signaling network play essential roles to promote angiogenesis and tumor growth by binding to tyrosine kinase [7]. FGFR is reported to be overexpressed and potentially promote tumor growth and invasion in patients with breast cancer [8]. Recent studies reported that FGFR-dependent signaling contributes to a mechanism for intrinsic resistance to EGFR inhibitors in EGFR-dependent

cell lines [9, 10]. Taken together, FGFR inhibitors are considered one of the potential RTK inhibitors that can be used to treat patients with breast cancer.

Dovitinib (TKI258) is a small-molecule tyrosine kinase inhibitor targeting multiple RTKs, such as FGFRs [11], vascular endothelial growth factor receptor (VEGFR) [12], fetal liver tyrosine kinase receptor 3 (FLT-3) [13], and colony-stimulating factor receptor 1 (c-Fms) [14], which participates in tumor growth, survival, angiogenesis, and vascular development and is under clinical investigation in different malignancies [15]. According to previous studies, dovitinib exhibits potent tumor growth inhibition in a board range of preclinical animal models and clinical trials, including leukemia, advanced melanoma, endometrial cancer, brain neoplasm, digestive system neoplasm, breast cancer, etc. For example, dovitinib has been shown to have the antitumor effect in endometrial cancer beyond FGFR2-mutated cases [16]. In addition, a preclinical FGFR1-amplified xenograft model demonstrated that dovitinib showed antitumor activity in FGFR-amplified breast cancer cell lines [17]. Moreover, a phase I/II dose-escalation study revealed that dovitinib exhibited an acceptable safety profile at a dose of 400 mg/day and showed clinical benefit by specifically inhibiting FGFR and VEGFR in patients with advanced melanoma [18].

Although several studies have focused on the clinical efficacy of dovitinib in different cancers, comparatively few reports have looked at molecular mechanisms of dovitinib action in cancer cells, especially in breast cancer. In some human tumor models, dovitinib was shown to inhibit the STAT3/5, MAPK, PI3K/AKT/mTOR, and Wnt signaling pathways [19–21]. *In vivo* studies using both Huh-7 and PLC5 xenograft tumors model showed dovitinib down-regulated phospho-(*p*)STAT3 and subsequently reduced the expressions of its downstream-regulated proteins, Mcl-1, survivin, and cyclin D1 [22]. STAT3 plays a vital role in transcriptional regulation of genes involved in cell proliferation and tumor progression triggered by cytokines and growth factors such as EGFR and FGFR [23]. Many protein families act as negative regulators of the STAT3 signaling pathway, such as SH2-domain-containing cytosolic phosphatases, SHP-1 and SHP-2 [24]. SHP-1 belongs to a family of nonreceptor protein tyrosine phosphatases (PTP) and consists of 2 SH2 domains that bind phosphotyrosine, a catalytic PTP domain and a C-terminal tail [25]. Recently, studies identified that dovitinib acts as a SHP-1 agonist or SHP-1 mediator that enhances activation of protein tyrosine phosphatase SHP-1 and subsequent dephosphorylation of *p*-STAT3^{TYR705}, resulting in the downregulation of anti-apoptotic STAT3 target genes Mcl-1 and survivin and cyclin D1. However, dovitinib frequently reduced the activity of these signaling pathways while tyrosine kinase receptor-independent mechanisms of dovitinib also occur.

The mechanism of how breast tumor-suppressive role of dovitinib works is not fully known. Moreover, it is unclear whether dovitinib modulation using a pharmacologically relevant approach would yield similar activation of SHP-1 and subsequent inhibition of *p*-STAT3^{Tyr705} in breast cancer cells. Here, we report that dovitinib-mediated breast cancer cell death in both autophagic and apoptotic ways. To better understand the molecular mechanism of dovitinib in breast cancer therapy, we investigated the molecular events altered by dovitinib treatment in various breast cancer cells. The role of SHP-1 activity-mediated downregulation of *p*-STAT3 was also confirmed, thus providing novel mechanistic insight into this molecular target for breast cancer.

2. Materials and Methods

2.1. Reagents and Antibodies. Dovitinib (TKI258) was kindly provided by Novartis Pharmaceuticals. Bafilomycin A1 was purchased from Invivogen (California, USA). Thiazolyl blue tetrazolium bromide (3-(4,5-dimethylthiazol-2-yl)-2,5-diphe- nyltetrazolium bromide, MTT) and acridine orange were purchased from Sigma-Aldrich (Missouri, USA). SHP-1 inhibitor, the STAT3-specific inhibitor, was purchased from Merck Millipore (Massachusetts, USA). G418, being used for selecting transformed with STAT3 plasmid cell line, was purchased from Amresco (Ohio, USA). Antibody for immunoblotting, such as PARP, was purchased from Santa Cruz (Dallas, USA). Other antibodies, such as beclin 1, cyclin D1, Mcl-1, survivin, *p*-STAT3^{Tyr705}, STAT3, SQSTM1/*p*62, and SHP-1, were from Cell Signaling (Massachusetts, USA).

2.2. Cell Culture. The MCF-7, HCC1937, MDA-MB-231, MDA-MB-468, MDA-MB-453, and SK-BR-3 cell lines were acquired from American Type Culture Collection (Virginia, USA). The MDA-MB-468 with STAT3 overexpression cell line was generously provided by Dr. Liu CY, working in Division of Hematology and Oncology, Department of Medicine, Taipei Veterans General Hospital (Taipei, Taiwan). All cell lines were immediately expanded and frozen down immediately after acquiring. All cell lines could be restarted every 3 months from a frozen vial of the same batch of cells. Cells except for MDA-MB-468 with STAT3 overexpression were maintained as described culture medium by ATCC; MDA-MB-468 with STAT3 overexpression cells was maintained in L-15 medium with G418 700 μg/mL. All media were supplemented with 10% FBS (Caisson, USA), 100 units/mL penicillin, 100 mg/mL streptomycin, and 25 mg/mL amphotericin B (Caisson, USA). All human breast cancer cell lines were incubated in a humidified incubator at 37°C in an atmosphere of 5% CO_2 in air.

2.3. Cell Viability Analysis. The effect of individual test agents on cell viability was assessed by using the thiazolyl blue tetrazolium bromide (MTT). Human breast cancer cells were seeded in the density of 3,000 cells/well with 200 μL FBS-contained cultured medium in 96-well flat-bottom plate and incubated under 37°C and 5% CO_2 for 24 hours. The very next day, the medium with FBS was removed and 200 μL serum-free medium with various concentrations of dovitinib was added and dissolved in DMSO in serum-free medium, and human breast cancer cells were cocultured with dovitinib under 37°C and 5% CO_2 for different time intervals. Controls received DMSO

vehicle at a concentration equal to that in the highest dosage of drug-treated cells. After coculturing with dovitinib for a period of time, 20 μL of 0.5 mg/mL MTT (1/10 volume of the medium) was added and further incubated under 37°C and 5% CO_2 for 3 more hours. At the end of the incubation period, the medium was removed and 200 μL DMSO was added and then incubated in no-light condition at room temperature for 15 minutes with a gentle shake. After the incubation period, the 96-well plate was measured at a wavelength of 570 nm with background subtraction at 690 nm by using SpectraMax M5 multimode microplate readers (Molecular Devices, USA).

2.4. Autophagy Analysis. The following two methods were used to assess drug-induced autophagy: western blot analysis of microtubule-associated protein-1 light chain 3 (LC3 II) and immunofluorescence of acridine orange. Formation of acidic vesicular organelles (AVOs), a morphological characteristic of autophagy, was detected by acridine orange staining [26]. Cells were stained with 5 mg/mL acridine orange for 10 min at room temperature, and samples were observed under a Nikon Eclipse TS100-F fluorescence microscope (Nikon, Japan).

To quantify the percentage of cells with acidic vacuolar organelles (red-marked cells), human breast cancer cells treated with the indicated concentration of dovitinib were stained with acridine orange and incubated for 10 min in the dark at room temperature. The percentage of autophagic cells (containing the red-marked organelle in the cytoplasm) was analyzed with a FASCaliber flow cytometer.

2.5. Apoptosis Analysis. The following two methods were used to assess dovitinib-induced apoptotic cell death: measurement of apoptotic cells by flow cytometry (sub-G1) and western blot analysis for PARP caspases cleavage. For measurement of sub-G1 percentage, human breast cancer cells were treated with DMSO or dovitinib at the indicated dose for 24 hours. The human breast cancer cells were harvested and washed with ice-cold phosphate-buffered saline (PBS) solution twice. They were vortexed gently, and the ice-cold 70% EtOH was added for fixation of the sample lysate at the same time. They were stored at −20°C in a refrigerator for at least 1 day. The pellets were resuspended in PBS and then washed with PBS twice. Samples were incubated with 10 μg/mL DNase-free RNase A (Sigma-Aldrich, USA) and 83 μg/mL propidium iodide (Sigma-Aldrich, USA) at 37°C for 30 minutes. The percentage of apoptotic cells was shown by cell-cycle distribution using flow cytometry. The DNA content of individual cells was analyzed with the fluorescence-activated sorter. Cells with less DNA than that of G1/G0 cells were considered to be apoptotic cells.

2.6. Western Blot Analysis. Cell lysates of human breast cancer cells treated with drugs at the indicated concentration for certain periods of time were prepared for immunoblotting of *p*-STAT3, STAT3, cyclinD1, PARP, Mcl-1, survivin, LC3, p62, beclin 1, and α-actin. Human breast cancer cells treated with DMSO and other various concentrations of drugs were collected by trypsinization with Trypsin-EDTA solution and washed with ice-cold PBS. Then, the human breast cancer cell pellets were resuspended in 50–60 μL of RIPA lysis buffer (50 mM Tris-HCl (pH 7.4), 0.25% sodium deoxycholate, 1% Nonidet P-40, 150 mM sodium chloride (NaCl), 1 mM EDTA, 1 mM PMSF, 1 mM sodium orthovanadate (Na_3VO_4), 1 mM sodium fluoride (NaF), 1.5 μg/ml aprotinin, 1 μg/ml leupeptin and 1 μg/ml pepstatin) for 30 minutes and vortexed gently every 10 minutes. After incubation with RIPA lysis buffer, the physical disruption method was applied for lysis of the remaining pellets. The sonication was proceeded with a Misonix Sonicator S-4000 (New York, USA) as follows: Probe sonication performed to the lysates on ice with 6 cycles of 2-second bursts and 10-second rest at burst amplitude setting of 10. Soluble cell lysates were collected after centrifugation at 200*g* for 20 minutes. The supernatant was collected, and the protein concentrations of the lysates were determined by using a BCA Protein Assay Reagent (Thermo, USA), and the absorbance was measured at 595 nm by using SpectraMax M5 multi-mode microplate readers (Molecular Devices, USA). The lysates were aliquoted with 50 μg/mL in each eppendorf with the sample buffer (0.3 M Tris-HCl, 5% SDS, 50% glycerol, 100 mM dithiothreitol (DTT)) and stored in −80°C refrigerator. Each sample lysate was defrosted and boiled in sample buffer at 100°C for 5–10 minutes before running the gel. The stacking gel (DDW, 30% acrylamide, 1.0 M Tris (pH 6.8), 10% SDS, 10% ammonium persulfate, and TEMED) and 8%/12% resolving gel with DDW, 30% acrylamide, 1.5 M Tris (pH8.8), 10% SDS, 10% ammonium persulfate, and TEMED were prepared. The SDS-PAGE gel was prerun at 80 V for 10 minutes before loading the sample lysates. Equal amounts of protein were loaded into the wells along with molecular weight markers, and the stacking gel and resolving gel were run at 80 V and at 140 V, respectively. Then, the protein from the gel is transferred to the PVDF membrane (Millipore, USA) with the use of wet transfer cell (Bio-rad, USA). The membranes were washed twice with TBS (0.3% (wt/vol) Tris, 0.8% (wt/vol) NaCl, and 0.02% (wt/vol) KCl) containing 0.1% Tween 20 (TBST) and then incubated with TBST containing 5% bovine serum albumin (Sigma, USA) for 1 hour to block nonspecific antibody binding. Then, every PVDF membrane was incubated at 4°C overnight with a primary antibody in TBS containing 5% bovine serum albumin. The membranes were washed twice with TBST and then incubated at room temperature for one hour with horseradish peroxidase- (HRP-) conjugated goat anti-rabbit or anti-mouse immunoglobulin G (IgG) diluted 1 : 10,000 in TBS containing 5% bovine serum albumin at room temperature. The membranes were washed for three times with TBST, and bound antibody was visualized by chemiluminescent HRP substrate (Millipore, USA).

2.7. MDA-MB-468 Cells with Ectopic Expression of STAT3. The stable clone cells, MDA-MB-468 with STAT3 overexpression, were prepared for evaluating the major target of

dovitinib. MDA-MB-468 with STAT3 overexpression cells were cultured in the presence of G418 (0.7 mg/mL). MDA-MB-468 with STAT3 overexpression cells were treated with the indicated concentration of dovitinib for 24 hours. At the endpoint of treatment, the cell pellets were collected and aliquoted into two parts: one for sub-G1 population analysis and the other for protein immunoblotting analysis.

2.8. Statistical Analysis. Data are expressed as individual data or mean ± SD. Experiments were repeated at least three times with similar result. Analysis significance was performed using the Student's t-test (Microsoft Excel), and P-value < 0.05 was considered significant.

3. Results

3.1. Inhibition of Human Breast Cancer Cell Viability by Dovitinib in a Dose- and Time-Dependent Manner. The effect of dovitinib on cell viability in six human breast cancer cell lines (HCC1937, MCF-7, MDA-MB-231, MDA-MB-453, MDA-MB-468, and SK-BR-3) was evaluated for 24 h and 48 h by MTT assays. All the optical density (OD) values of dovitinib-treating groups were compared to the OD values of the control group, in which there was no dovitinib added. Dovitinib decreased the cell numbers in a dose-dependent manner in all tested cell lines (Figure 1), displaying a minor difference of IC_{50}. The inhibitory effects were similar in HCC1937 cells (estimated IC_{50}, $13.8 \pm 2.1\,\mu$mole/L), MCF-7 cells (estimated IC_{50}, $12.7 \pm 3.4\,\mu$mole/L), MDA-MB-231 cells (estimated IC_{50}, $11.9 \pm 3.8\,\mu$mole/L), MDA-MB-453 cells (estimated IC_{50}, $9.7 \pm 1.9\,\mu$mole/L), MDA-MB-468 cells (estimated IC_{50}, $10.1 \pm 2.4\,\mu$mole/L), and SK-BR-3 cells (estimated IC_{50}, $11.7 \pm 2.8\,\mu$mole/L). Therefore, the susceptibility of these cancer cells to dovitinib was considered to be similar. In addition, the drug effect was persistent even at 48 hours and the cell numbers reduced much lower than that at 24 hours to reveal that dovitinib inhibited cell growth in a time-dependent manner (Figure 1).

3.2. Dovitinib-Mediated Autophagic Cell Death and Induced Accumulation of Autophagic Markers. Recent studies indicate that chemotherapeutic drugs trigger autophagic but not apoptotic cell death in various cancer cells [27]. The process of autophagy starts with the autophagosome formation and subsequently fuses with an acidic lysosome to form an autolysosome [28]. In order to verify whether dovitinib induced the autophagic pathway, acridine orange staining was employed to visualize acidic vesicular organelles (AO-R positive cells) in control and dovitinib-treated MCF-7 cells. As shown in Figure 2(a), dovitinib treatment markedly elevated the amount of AO-R positive cells, indicating that dovitinib induced a high basal level of autophagic activities. We also evaluated the autophagic cell death by acridine orange staining with flow cytometry in three breast cancer cells treated with 0, 10, and 15 μmole/L dovitinib for 24 h. As shown in Figure 2(b), the percentage of the autophagic cell was 52.1 ± 2.5 and $63.9 \pm 1.4\%$ when exposed to 10 and 15 μmole/L dovitinib for 24 h in MCF-7 cells, 49.13 ± 2.6 and $67.2 \pm 6.1\%$ in MDA-MB-231 cells, and 47.2 ± 1.6 and $55.4 \pm 4.7\%$ in MDA-MB-468 cells. These results indicated that dovitinib induced the autophagy of various breast cancer cells in a dose-dependent manner.

To obtain better insight into the mechanism of dovitinib-induced autophagy, we next analyzed the effects of dovitinib on autophagy-related proteins by western blot analysis. As shown in Figure 2(c), the expression levels of p-STAT3, Mcl-1, and beclin 1 was decreased significantly in response to 5, 10, and 15 μmole/L dovitinib in both MDA-MB-468 and MCF-7 breast cell lines. It was reported Mcl-1 could inhibit autophagy by overexpression of beclin 1 [29]. The decreases in the expression levels of Mcl-1 and beclin 1 suggest that Mcl-1 regulates autophagy at least in part by downregulating the activity of beclin-1. We also observed the expression levels of the protein LC3B-I (an unprocessed form of LC3) and the cleaved protein LC3B-II (lipidated and autophagosome-associated form of LC3) were markedly increased in both MDA-MB-468 and MCF-7 breast cell lines following dovitinib treatment at various concentrations compared with the nontreated cells (Figure 2(c)). It was noted that when the expression of Mcl-1 was suppressed, the autophagy markers, LC3-II and p62, also responded to the changing of Mcl-1: LC3-II expression increased and p62 expression decreased (Figure 2(c)). In brief, dovitinib had induced autophagy in breast cancer cells through inhibiting STAT3/Mcl-1 axis and resulted in the formation of autophagy.

3.3. Blocking Autophagy Reduced the Antitumor Effects of Dovitinib. To determine the role of autophagy in dovitinib-treated breast cells, the present study cotreated with various concentrations of dovitinib and 20 μmole/L autophagy inhibitor, bafilomycin A1, in three breast cancer cells: MCF-7, MDA-MB-231, and MDA-MB-468 cells. The percentage of viable cells increased in the presence of bafilomycin A1 compared to that in the absence of bafilomycin A1. However, bafilomycin A1 exhibited the maximal autophagy inhibiting efficacy on MCF-7 cell line when compared to those in the MDA-MB-231 and MDA-MB-468 cell lines (Figure 3(a)). We further validated the inhibitory effects of bafilomycin A1 on dovitinib-induced activation of LC3B by western blotting. Bafilomycin A1 treatment reduced the accumulation of LC3B by 15 μmol/L dovitinib in MCF-7 breast cancer cells, whereas it caused the increased accumulation of LC3B in MDA-MB-468 cells (Figure 3(b)). Since bafilomycin A1 has been reported to block the fusion of autophagosomes with lysosomes [30], our results interestingly suggest that MCF-7 cells were relatively less activated to autophagosome marker LC3-II compared to MDA-MB-468 cells. As a result, an autophagy inhibitor, bafilomycin A1, blocked dovitinib-induced autophagy in various breast cancer cells, especially MCF-7, and reduced the anti-tumor effects of dovitinib.

3.4. Dovitinib Triggered Apoptotic Cell Death in Human Breast Cancer Cells. Recent studies reported that dovitinib showed antitumor activity by inhibiting cell proliferation

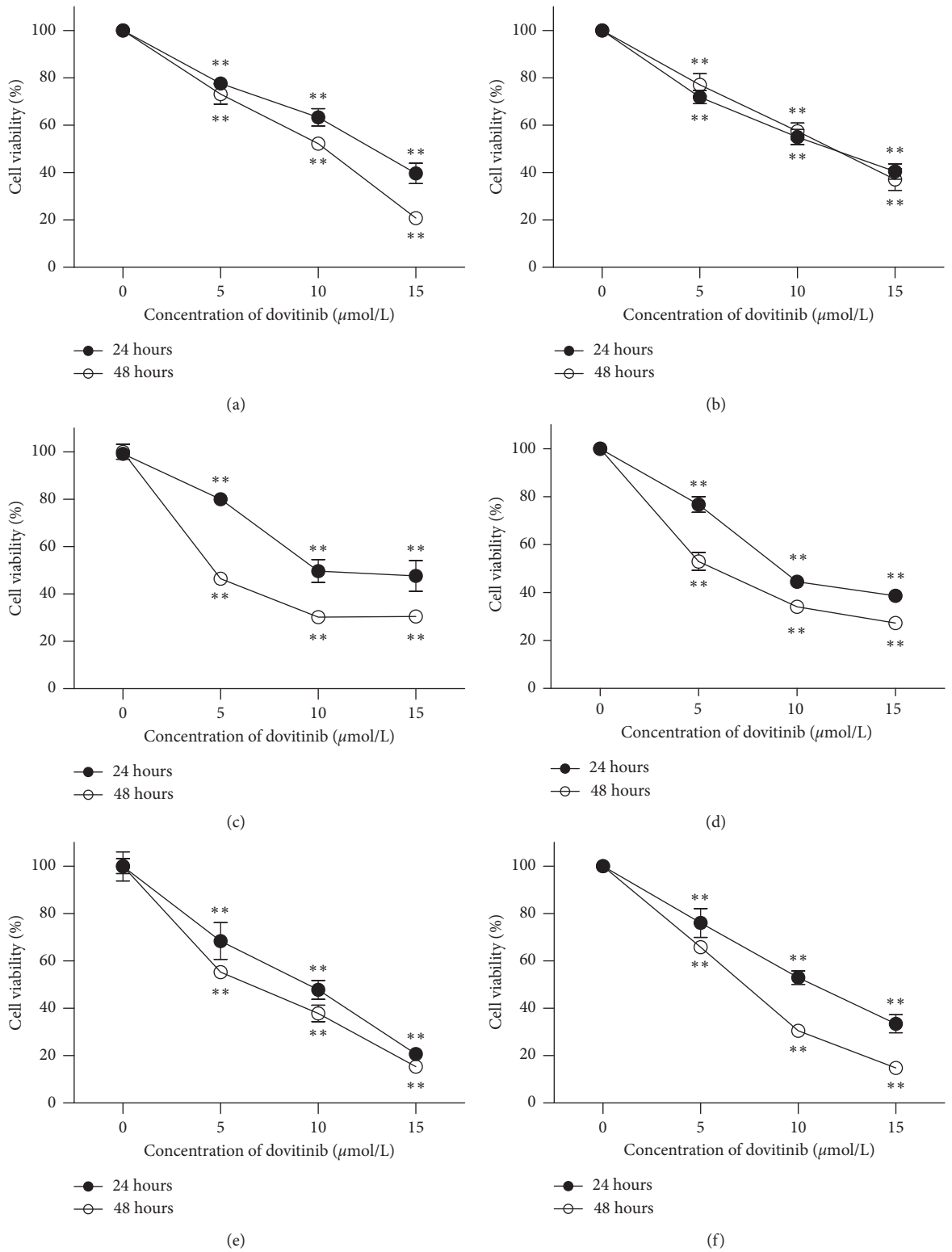

Figure 1: Dovitinib inhibited cell proliferation in a dose- and time-dependent manner. The breast cancer cell lines were treated with dovitinib at the indicated doses for 24 and 48 h, and cell viability was assessed by MTT assay. Points, mean; bars, SD ($N = 3$). $^{*}p < 0.05$; $^{**}p < 0.01$. (a) HCC1937. (b) MCF-7. (c) MDA-MB-231. (d) MDA-MB-453. (e) MDA-MB-468. (f) SK-BR-3.

and inducing apoptosis in breast and colorectal cancer cells [31, 32]. However, accumulated studies suggest that autophagy induces chemoresistance against chemotherapeutic agents by inhibiting apoptosis of cancer cells [33]. Our prior finding showed that dovitinib increased autophagy in various breast cancer cells, and the antitumor effect of dovitinib could

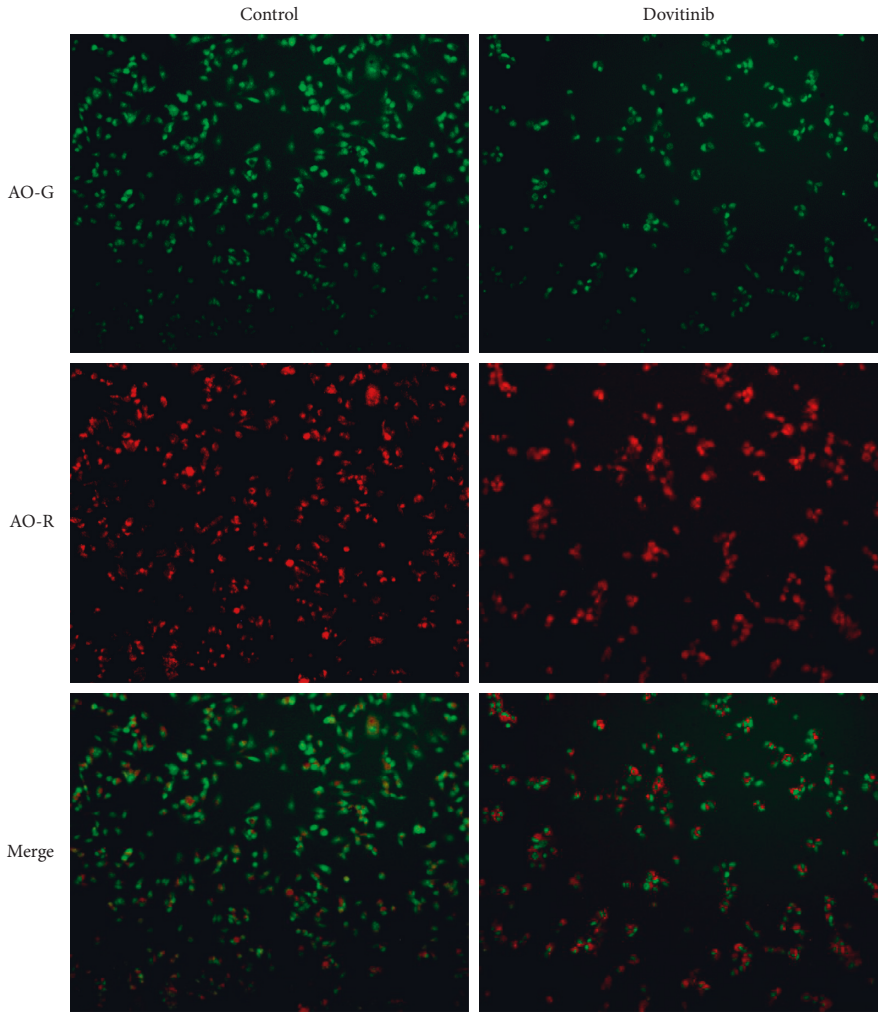

(a)

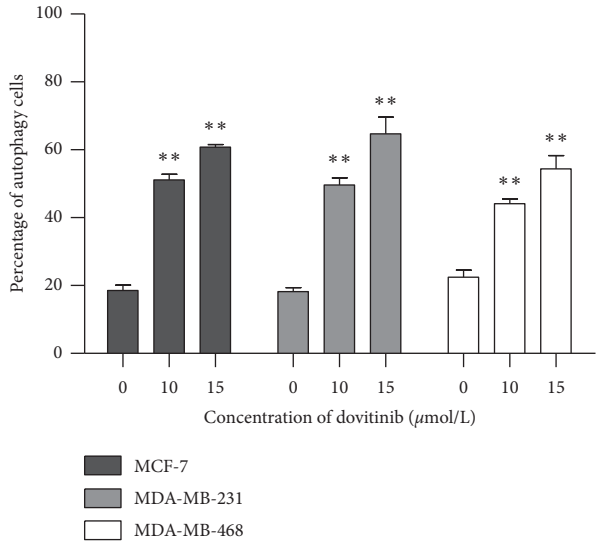

(b)

Figure 2: Continued.

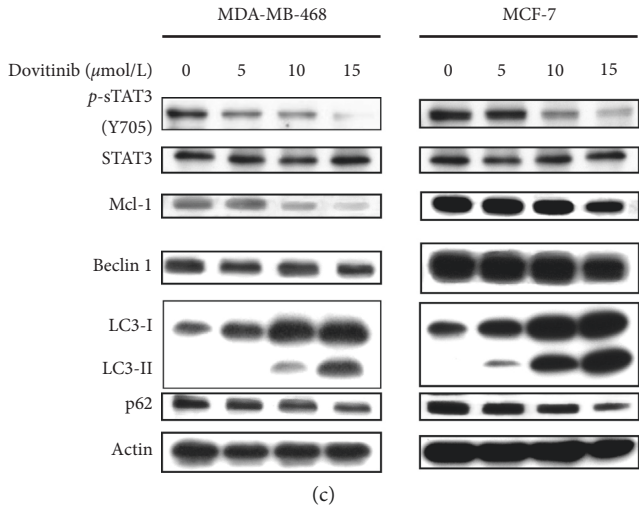

Figure 2: Dovitinib increased the autophagy-mediated cell death in the breast cancer cell. (a) MCF-7 cells were exposed to dovitinib (15 μmole/L) for 24 h. Detection of autophagy was performed by staining the cells with acridine orange for 15 minutes and examined by fluorescence microscopy. AO-R indicated the formation of acidic vesicular organelles. (b) Cells were treated with dovitinib (10 and 15 μmole/L) for 24 h, and the autophagic vacuoles were analyzed by staining of acridine orange. Columns, mean; bars, SD ($N = 3$). $^{*}p < 0.05$; $^{**}p < 0.01$. (c) The protein extracts from dovitinib-treated were subjected to immunoblot analysis for *p*-STAT3, STAT3, Mcl-1, beclin1, LC3B, p62, and actin.

be restricted by autophagic cell death. To determine whether autophagy is associated with the suppression of dovitinib-induced apoptotic cell death, the nucleic acid stain propidium iodide (PI) flow cytometric assay was used for the evaluation of the number of hypodiploid cells undergoing a late stage of apoptosis process (sub-G1) in the present study. MCF-7, MDA-MB-231, MDA-MB-468, and SK-BR-3 were exposed to dovitinib at the indicated concentration for 24 hours. Dovitinib increased apoptotic cell death in a dose-dependent manner on all tested cell lines. However, the percentages of dovitinib-induced apoptotic cells in 4 human breast cancer cells represented a significant difference. Treating 15 μmole/L dovitinib induced about 15%, 40%, 25%, and 17% cell apoptosis at 24 h for MCF-7, MDA-MB-231, MDA-MB-468, and SK-BR-3 cells, respectively (Figure 4). The data clearly show that increased dovitinib-induced autophagy led to decreased percentages of apoptotic cells on MCF-7 cells, whereas decreased dovitinib-induced autophagy led to increased percentages of apoptotic cells on MDA-MB-468 cells. Thus, we considered that the MCF-7 and MDA-MB-468 cell lines are better comparing the cell model in this experiment to reflect the true dovitinib-mediated apoptotic and autophagic cell death.

In order to provide a better understanding of the molecular mechanisms underlying dovitinib-induced apoptosis, the detection of apoptotic-related protein expression is required. Incubation with dovitinib using a range of concentrations (5–15 μmole/L) for 24 h resulted in a gradual and dose-dependent decrease in the level of *p*-STAT3^{Tyr705} and the downstream targets activated by STAT3, such as cyclin D1, and survivin in both MCF-7 and MDA-MB- 468 cells, whereas the total STAT3 protein was not influenced (Figure 5). Meanwhile, the protein expression levels of cleaved caspase-9 and cleaved poly (ADP-ribose) polymerase (PARP) were markedly increased by dovitinib in a dose-dependent manner. These observations suggested that dovitinib interferes with STAT3 signaling and downstream targets resulting in apoptosis in both MCF-7 and MDA-MB-468 cell lines.

3.5. Overexpression of STAT3 Rescued Dovitinib-Induced Apoptosis in Human Breast Cancer Cells. The previous research pointed out that dovitinib downregulates the *p*-STAT3 and subsequently reduced the levels of expression of STAT3-related proteins Mcl-1, survivin, and cyclin D1 in a time-dependent manner in human hepatocellular carcinoma (HCC) [22]. In our present study, the wild and overexpression of STAT3 MDA-MB-468 breast cancer cells were treated with dovitinib for 24 h and cell apoptosis and expression of STAT3/cyclin D1 axis were analyzed subsequently. The results indicated that 10 and 15 μmole/L dovitinib treatments in wild-type MDA-MB-468 cells cause $7.8 \pm 1.1\%$ and $20.7 \pm 2.8\%$ cell apoptosis, respectively. However, 10 and 15 μmole/L dovitinib induced $8.1 \pm 2.6\%$ and $8.9 \pm 2.7\%$ apoptotic cells, respectively, in overexpression of STAT3 MDA-MB-468 cells (Figure 6). The ratio of apoptotic cells in overexpression of STAT3 MDA-MB-468 cells significantly reduced after dovitinib treatment compared to that in the wild-type MDA-MB-468 cells. Furthermore, the expression levels of the protein *p*-STAT3, STAT3, and cyclin D1 were markedly increased in overexpression of STAT3 MDA-MB-468 cells following dovitinib treatment at various concentrations compared with the wild-type MDA-MB-468 cells.

Otherwise, since STAT3 has been demonstrated to be a target underlying dovitinib-induced cellular cytotoxicity and apoptosis, we are also interested in that if the other STAT3 negative regulator, SH2-domain-containing

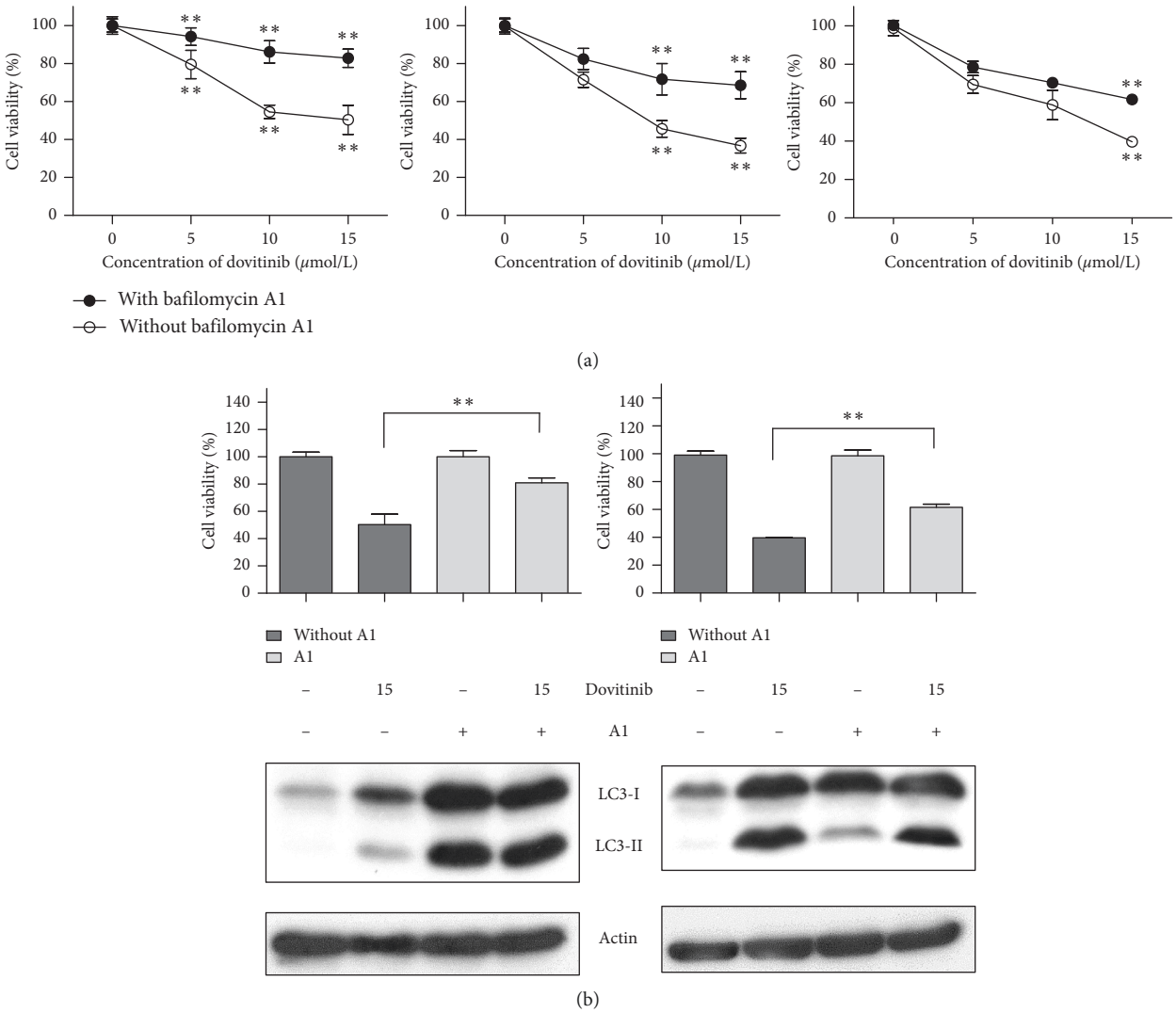

Figure 3: Blocking autophagy reduced the antitumor effects of dovitinib. (a) Cotreatment with the autophagy inhibitor, bafilomycin A1 (20 μmole/L), reduced the effect of dovitinib on cell death. Cells were treated with dovitinib at the indicated doses and/or bafilomycin A1 for 24 h. Cell viability was analyzed by MTT assay. Points, mean; bars, SD ($N = 3$). $^{*}p < 0.05$; $^{**}p < 0.01$. (b) MCF-7 cells were treated with dovitinib at 15 μmol/L and/or bafilomycin A1 for 24 h. Cell viability was analyzed by MTT assay. Cell extracts were subjected to immunoblot analysis for LC3B and actin. Columns, mean; bars, SD ($N = 3$). $^{*}p < 0.05$; $^{**}p < 0.01$.

phosphatase 1 (SHP-1), is involved in dovitinib-mediated downregulation of STAT3/cyclin D1 axis. SHP-1 is a nonreceptor protein tyrosine phosphatase (PTP) that notably has tumor-suppressive potential due to its negative regulation of STAT3 oncogenic signaling during tumor progression [34, 35]. The present study examined whether blocking SHP-1 affected the downregulation effect of dovitinib in the STAT3/cyclin D1 axis. As shown in Figure 7, the expression levels of *p*-STAT3 and cyclin D1 were decreased in response to dovitinib. However, the expression levels of *p*-STAT3 and cyclin D1 were markedly increased in response to dovitinib and SHP-1 inhibitor cotreatment compared with cells treated with dovitinib alone. Taken together, the SHP-1 inhibitor reversed the dovitinib-induced downregulation of *p*-STAT3, indicating that SHP-1 mediated the STAT3 inhibition effect of dovitinib.

4. Discussion

In this study, we showed that dovitinib inactivates STAT3 through SHP-1 to suppress the growth of human breast cancer via induction of both apoptosis and autophagy. Further analysis of the mechanisms discovered that downregulation of STAT3 and cell apoptotic status induced by dovitinib could be reversed by inhibiting the activity of SHP-1, the *p*-STAT3 phosphatase. Moreover, we also disclosed an interesting finding that autophagy was also involved in dovitinib-mediated cell death in human breast cancers. Decreased expression of Mcl-1, the downstream molecule of *p*-STAT3, was responsible for the dovitinib-induced autophagy since its low expression should free beclin-1 and result in the formation of autophagosome [36]. Autophagy induced by dovitinib was confirmed to play as an assassin to attack tumor cells when dovitinib triggered it.

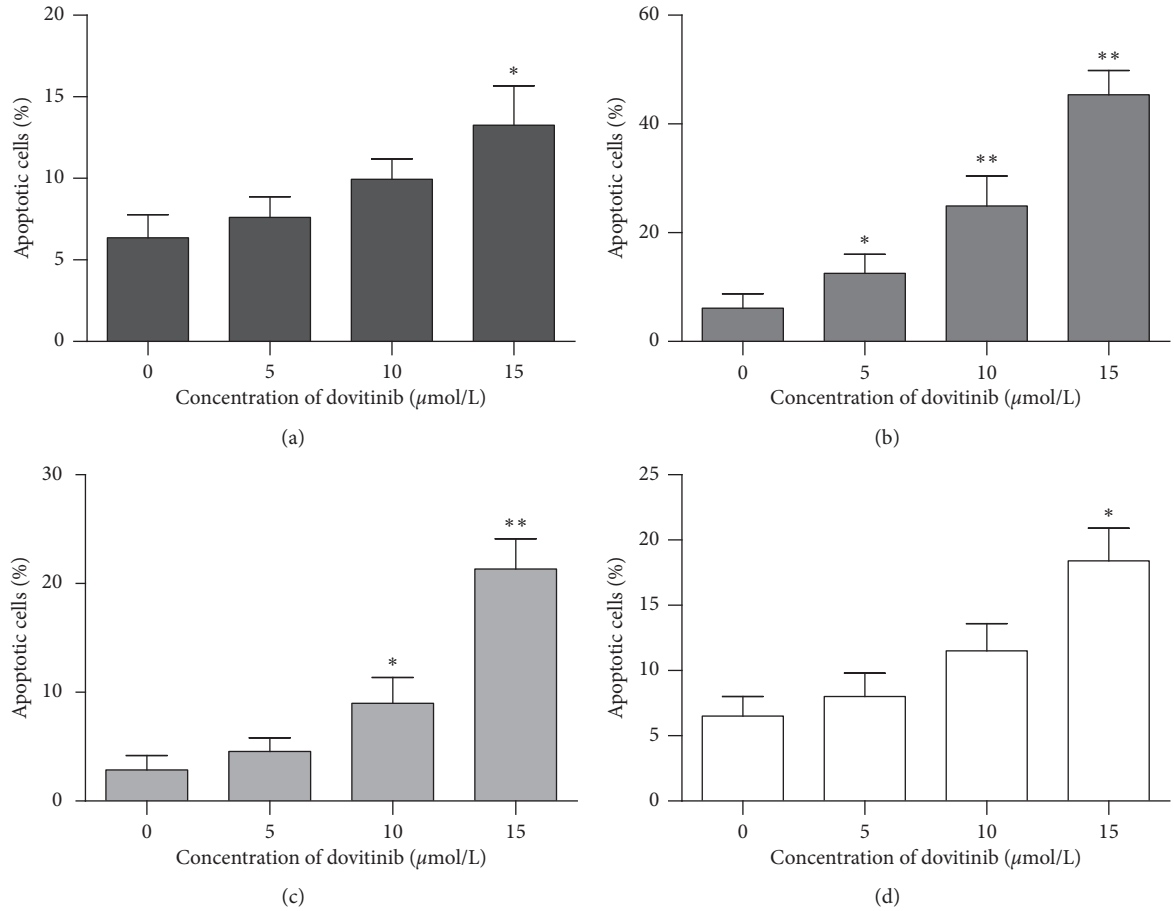

Figure 4: Dovitinib induced apoptosis in breast cancer cells. Human breast cancer cells were exposed to dovitinib at the indicated doses for 24 h. The cells were fixed by EtOH and stained with propidium iodide. Apoptotic cells were measured and determined by flow cytometry. Columns, mean; bars, SD ($N = 3$). $^{*}p < 0.05$; $^{**}p < 0.01$. (a) MCF-7. (b) MDA-MB-231. (c) MDA-MB-468. (d) SK-BR-3.

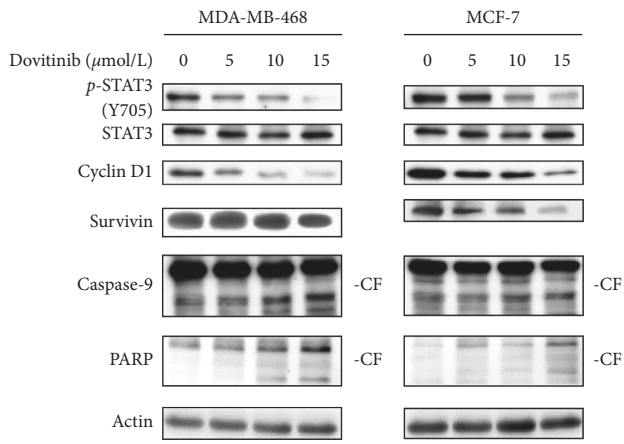

Figure 5: Dovitinib inhibited pSTAT3, apoptotic signaling pathway. Cells were exposed to drugs for 24 h. Cell extracts were subjected to immunoblot analysis for STAT3, pSTAT3, caspase 9, cyclin D1, PARP, survivin, LC3, and actin. CF: cleavage form.

These findings suggested that dovitinib could be a potential target therapy reagent for use in treating human breast cancer. In addition, the STAT3-associated molecular events pointed out a more specific application of dovitinib.

Dovitinib has shown a significant antitumor effect on human breast cancer cells. Dovitinib could downregulate *p*-STAT3 and subsequently influence the downstream STAT3-related proteins, such as Mcl-1 [37], PARP [38], cyclin D1 [39],

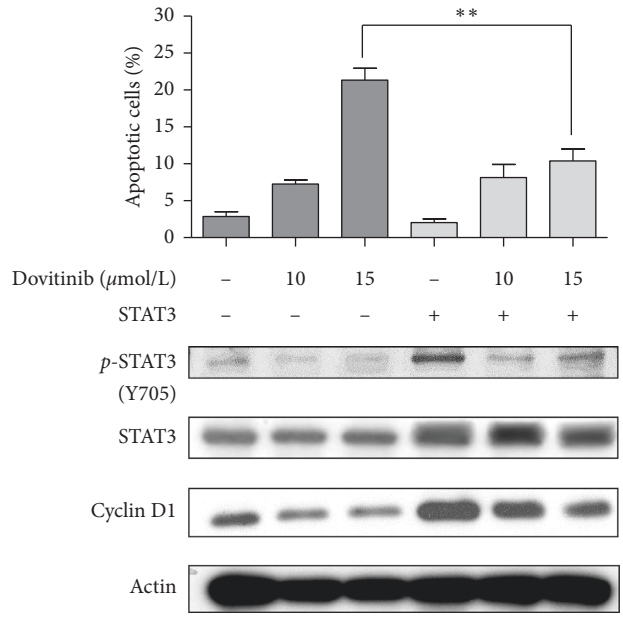

Figure 6: Overexpression of STAT3 rescued breast cancer cells from apoptosis. MDA-MB-468 cells (wild type or STAT3) were treated with dovitinib (10 μmole/L) for 24 h. Apoptotic cells (sub-G1) were analyzed by flow cytometry. Columns, mean; bars, SD ($N = 3$). $^{*}p < 0.05$; $^{**}p < 0.01$.

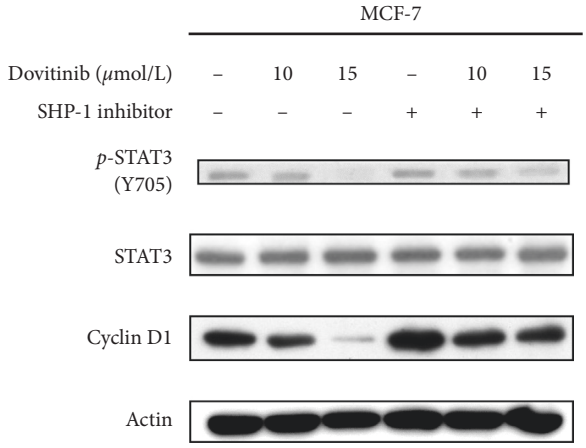

Figure 7: SHP-1 inhibitor decreased the STAT3-inactivating effect of dovitinib. MCF-7 cells were treated with dovitinib (10 and 15 μmole/L) for 24 h. Cell extracts were subjected to immunoblot analysis for STAT3, pSTAT3, cyclin D1, and actin.

and survivin [40]. These proteins are in charge of several major cellular events, including enhancing cell survival by apoptosis inhibition, DNA repairing, cell cycle progression, and regulating apoptosis [41]. There are many findings to prove the importance of STAT3 signaling in carcinogenesis and have contributed to the designs of new therapeutic targets [42, 43]. It has the ability to control the expression of the antiapoptotic and proliferative gene and also plays a part in creating the tumorigenic microenvironment, which is crucial for tumor progression in several human cancers [44–46]. In human breast cancer, STAT3 is critical in survival and proliferation of tumor-correlated cells, which are tumor-supporting cells [47] and, also, is a promoter in the human breast progression [44] and breast tumor progression [48]. Moreover, STAT3 has been proven to mediate the EGF-stimulating growth and survival effects of human breast cancer cells *in vitro* and, possibly, *in vivo* [49]. Clearly, this evidence indicates STAT3 is constitutively activated in the mammary tumors and contributes to cell transformation, progression, and survival in human breast cancer [50, 51]. Also, several STAT3-related proteins, such as survivin and cyclin D1, are found overexpressed in human breast cancer tissues [52–55]. The complicated involvement of STAT3 and its downstream molecules in cell fate determination has made STAT3 a convincible target in cancer therapy [22, 41, 56].

Dovitinib is a multitarget receptor tyrosine kinase inhibitor and has been reported with inhibition of fibroblast growth factor receptor (FGFR) on metastatic breast cancer patients [17]. Most of the reports about dovitinib are focused on exploring the clinical efficacy in different cancers [57]. There is little research discussing the detailed mechanism of dovitinib in cancer cells. We have shown dovitinib had significant antitumor effects in breast cancer cells with downregulation of *p*-STAT3 and its related molecules to result in cell apoptosis. Being consistent with the previous finding in hepatocellular carcinoma [22], the intrinsic apoptotic pathway (caspase 9) was involved in this dovitinib-mediated tumor cell death.

In addition, we firstly revealed it also caused autophagic cell death in human breast cancer. Autophagy is a vitally catabolic process which involves cell degradation of unneeded or dysfunctional cytosolic components with cooperation to lysosome digestion while cells are under survival stress or starvation [58]. The digested cellular materials will be recycled to maintain cell survival. However, once the cells experienced over or constitutively activated autophagy, the cells would be killed eventually, and this is the so-called autophagic programmed cell death or autophagic death [59]. Because of the dual role of autophagy, it becomes important in the cancer treatments [60–62]. Our data revealed dovitinib not only triggers apoptosis (Figure 4) but also conducts the autophagic death of human breast cancer cells (Figure 3). By simultaneously activating two

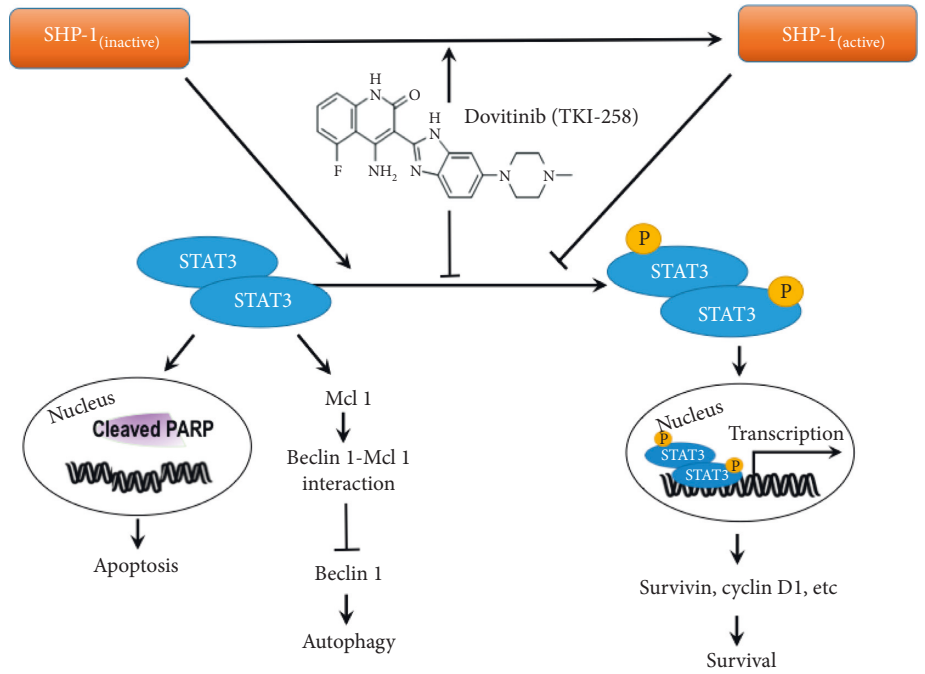

FIGURE 8: Proposed model of dovitinib-mediated autophagy and apoptosis with regard to the SHP-1/*p*-STAT3 pathway in breast cells. In breast cancer cells, dovitinib inhibit STAT3 phosphorylation and induced autophagy, in part, via releasing of beclin 1 from Mcl-1. Dovitinib also involved in SHP-1 activation and induced apoptotic cell death by downregulating of p-STAT3/cyclin D1 axis and increasing cleaved PARP expression. Accordingly, the present study may provide information regarding the association of autophagy and apoptosis with dovitinib chemotherapy in breast cancer cells, and the regulation of SHP-1/p-STAT3 pathway may be a promising strategy for treating breast cancer cells in response to RTKs inhibitors-based drugs, such as dovitinib.

of these significant cell death machinery, dovitinib could effectively decrease the proliferation of cancer cells.

There were several researches reporting that certain chemotherapy agents would induce autophagy, with pro-survival or pro-death effect [63–66]. One study also declared that autophagy facilitates the resistance to the breast cancer therapeutic agent, trastuzumab [67]. Our results showed dovitinib-induced autophagy to synergize with apoptosis and promote cell death in human breast cancer cells.

Shao et al. [68] also noticed that histone deacetylase (HDAC) inhibitors, both butyrate and suberoylanilide hydroxamic acid (SAHA), can induce apoptosis and caspase-independent autophagic cell death in several human cancer cells. HDAC is overexpressed in many cancers [69–71] and plays a role in transcriptional regulation, protein-DNA interaction, protein-protein interaction, and protein stability [72]. Butyrate and SAHA were designed to target HDAC in Shao's study to find the induction of both apoptosis and autophagy might serve as an efficient anticancer strategy. Dovitinib could induce apoptosis in human breast cancer via regulating survivin. As for the onset of autophagic cell death, Tai et al. noted that antitumor agents could induce the release of beclin-1 from Mcl-1 to induce autophagy [36]. Other reports also demonstrated that the decreased expression of cyclin D1 triggered the start of autophagy [73]. Therefore, it could be inferred that the downexpression of Mcl-1 and cyclin D1 was also involved in autophagic cell death in dovitinib-treated breast cancer cells.

5. Conclusions

The present study has proved that dovitinib induced a significant tumor-inhibitory effect through blockade of *p*-STAT3 via SHP-1 activation. Furthermore, the antitumor effects caused by dovitinib were mainly contributed by the activation of programmed cell death that includes both apoptosis and autophagy. The data represented here have provided the evidence for tumor cytotoxic effect of dovitinib to suggest it as a potential target for breast cancer therapy (Figure 8).

Data Availability

The data used to support the findings of this study are available from the corresponding author upon request.

Conflicts of Interest

The authors declare that they have no conflicts of interest.

Acknowledgments

The authors thank the grant support provided by the Ministry of Science and Technology of Taiwan, Republic of China (MOST 107-2313-B-002-044).

References

[1] C. E. DeSantis, J. Ma, A. Goding Sauer, L. A. Newman, and A. Jemal, "Breast cancer statistics, 2017, racial disparity in

mortality by state," *CA: A Cancer Journal for Clinicians*, vol. 67, no. 6, pp. 439–448, 2017.

[2] N. Pathmanathan, J.-S. Geng, W. Li et al., "Human epidermal growth factor receptor 2 status of breast cancer patients in Asia: results from a large, multicountry study," *Asia-Pacific Journal of Clinical Oncology*, vol. 12, no. 4, pp. 369–379, 2016.

[3] H. Masuda, D. Zhang, C. Bartholomeusz, H. Doihara, G. N. Hortobagyi, and N. T. Ueno, "Role of epidermal growth factor receptor in breast cancer," *Breast Cancer Research and Treatment*, vol. 136, no. 2, pp. 331–345, 2012.

[4] C. M. Connell and G. J. Doherty, "Activating HER2 mutations as emerging targets in multiple solid cancers," *ESMO Open*, vol. 2, no. 5, article e000279, 2017.

[5] D. Ercan, K. Zejnullahu, K. Yonesaka et al., "Amplification of EGFR T790M causes resistance to an irreversible EGFR inhibitor," *Oncogene*, vol. 29, no. 16, pp. 2346–2356, 2010.

[6] I. F. Tannock, C. M. Lee, J. K. Tunggal, D. S. M. Cowan, and M. J. Egorin, "Limited penetration of anticancer drugs through tumor tissue: a potential cause of resistance of solid tumors to chemotherapy," *Clinical Cancer Research*, vol. 8, no. 3, pp. 878–884, 2002.

[7] M. Katoh, "FGFR inhibitors: effects on cancer cells, tumor microenvironment and whole-body homeostasis (review)," *International Journal of Molecular Medicine*, vol. 38, no. 1, pp. 3–15, 2016.

[8] J. Perez-Garcia, E. Muñoz-Couselo, J. Soberino, F. Racca, and J. Cortes, "Targeting FGFR pathway in breast cancer," *The Breast*, vol. 37, pp. 126–133, 2018.

[9] M. T. Herrera-Abreu, A. Pearson, J. Campbell et al., "Parallel RNA interference screens identify EGFR activation as an escape mechanism in FGFR3-mutant cancer," *Cancer Discovery*, vol. 3, no. 9, pp. 1058–1071, 2013.

[10] S. A. Kono, M. E. Marshall, K. E. Ware, and L. E. Heasley, "The fibroblast growth factor receptor signaling pathway as a mediator of intrinsic resistance to EGFR-specific tyrosine kinase inhibitors in non-small cell lung cancer," *Drug Resistance Updates*, vol. 12, no. 4-5, pp. 95–102, 2009.

[11] S. H. Lee, D. Lopes de Menezes, J. Vora et al., "*In vivo* target modulation and biological activity of CHIR-258, a multitargeted growth factor receptor kinase inhibitor, in colon cancer models," *Clinical Cancer Research*, vol. 11, no. 10, pp. 3633–3641, 2005.

[12] C. Porta, P. Giglione, W. Liguigli, and C. Paglino, "Dovitinib (CHIR258, TKI258): structure, development and preclinical and clinical activity," *Future Oncology*, vol. 11, no. 1, pp. 39–50, 2015.

[13] D. E. Lopes de Menezes, J. Peng, E. N. Garrett et al., "CHIR-258: a potent inhibitor of FLT3 kinase in experimental tumor xenograft models of human acute myelogenous leukemia," *Clinical Cancer Research*, vol. 11, no. 14, pp. 5281–5291, 2005.

[14] J. Guo, P. A. Marcotte, J. O. McCall et al., "Inhibition of phosphorylation of the colony-stimulating factor-1 receptor (c-Fms) tyrosine kinase in transfected cells by ABT-869 and other tyrosine kinase inhibitors," *Molecular Cancer Therapeutics*, vol. 5, no. 4, pp. 1007–1013, 2006.

[15] P. A. Renhowe, S. Pecchi, C. M. Shafer et al., "Design, structure–activity relationships and *in vivo* characterization of 4-Amino-3-benzimidazol-2-ylhydroquinolin-2-ones: a novel class of receptor tyrosine kinase inhibitors," *Journal of Medicinal Chemistry*, vol. 52, no. 2, pp. 278–292, 2009.

[16] G. E. Konecny, T. Kolarova, N. A. O'Brien et al., "Activity of the fibroblast growth factor receptor inhibitors dovitinib (TKI258) and NVP-BGJ398 in human endometrial cancer cells," *Molecular Cancer Therapeutics*, vol. 12, no. 5, pp. 632–642, 2013.

[17] F. Andre, T. Bachelot, M. Campone et al., "Targeting FGFR with dovitinib (TKI258): preclinical and clinical data in breast cancer," *Clinical Cancer Research*, vol. 19, no. 13, pp. 3693–3702, 2013.

[18] K. B. Kim, J. Chesney, D. Robinson, H. Gardner, M. M. Shi, and J. M. Kirkwood, "Phase I/II and pharmacodynamic study of dovitinib (TKI258), an inhibitor of fibroblast growth factor receptors and VEGF receptors, in patients with advanced melanoma," *Clinical Cancer Research*, vol. 17, no. 23, pp. 7451–7461, 2011.

[19] H. J. Chon, Y. Lee, K. J. Bae, B. J. Byun, S. A. Kim, and J. Kim, "Traf2- and Nck-interacting kinase (TNIK) is involved in the anti-cancer mechanism of dovitinib in human multiple myeloma IM-9 cells," *Amino Acids*, vol. 48, no. 7, pp. 1591–1599, 2016.

[20] C. Zang, J. Eucker, P. Habbel et al., "Targeting multiple tyrosine kinase receptors with Dovitinib blocks invasion and the interaction between tumor cells and cancer-associated fibroblasts in breast cancer," *Cell Cycle*, vol. 14, no. 8, pp. 1291–1299, 2015.

[21] A. Chase, F. H. Grand, and N. C. P. Cross, "Activity of TKI258 against primary cells and cell lines with FGFR1 fusion genes associated with the 8p11 myeloproliferative syndrome," *Blood*, vol. 110, no. 10, pp. 3729–3734, 2007.

[22] W.-T. Tai, A.-L. Cheng, C.-W. Shiau et al., "Dovitinib induces apoptosis and overcomes sorafenib resistance in hepatocellular carcinoma through SHP-1-mediated inhibition of STAT3," *Molecular Cancer Therapeutics*, vol. 11, no. 2, pp. 452–463, 2012.

[23] E. Z. P. Chai, M. K. Shanmugam, F. Arfuso et al., "Targeting transcription factor STAT3 for cancer prevention and therapy," *Pharmacology & Therapeutics*, vol. 162, pp. 86–97, 2016.

[24] Z. Zhang, K. Shen, W. Lu, and P. A. Cole, "The role of C-terminal tyrosine phosphorylation in the regulation of SHP-1 explored via expressed protein ligation," *Journal of Biological Chemistry*, vol. 278, no. 7, pp. 4668–4674, 2003.

[25] T. T. Huang, J. C. Su, C. Y. Liu, C. W. Shiau, and K. F. Chen, "Alteration of SHP-1/p-STAT3 signaling: a potential target for anticancer therapy," *International Journal of Molecular Sciences*, vol. 18, no. 6, p. E1234, 2017.

[26] C. W. Elston and I. O. Ellis, "Pathological prognostic factors in breast cancer. I. The value of histological grade in breast cancer: experience from a large study with long-term follow-up," *Histopathology*, vol. 19, no. 5, pp. 403–410, 1991.

[27] A. Elliott and J. J. Reiners, "Suppression of autophagy enhances the cytotoxicity of the DNA-damaging aromatic amine p-anilinoaniline," *Toxicology and Applied Pharmacology*, vol. 232, no. 2, pp. 169–179, 2008.

[28] L. Yu, Y. Chen, and S. A. Tooze, "Autophagy pathway: cellular and molecular mechanisms," *Autophagy*, vol. 14, no. 2, pp. 207–215, 2018.

[29] M. C. Maiuri, G. Le Toumelin, A. Criollo et al., "Functional and physical interaction between Bcl-XL and a BH3-like domain in Beclin-1," *The EMBO Journal*, vol. 26, no. 10, pp. 2527–2539, 2007.

[30] J. J. Shacka, B. J. Klocke, and K. A. Roth, "Autophagy, bafilomycin and cell death: the "A-B-Cs" of plecomacrolide-induced neuroprotection," *Autophagy*, vol. 2, no. 3, pp. 228–230, 2006.

[31] S. Gaur, L. Chen, V. Ann et al., "Dovitinib synergizes with oxaliplatin in suppressing cell proliferation and inducing

apoptosis in colorectal cancer cells regardless of RAS-RAF mutation status," *Molecular Cancer*, vol. 13, no. 1, p. 21, 2014.

[32] A. Issa, J. W. Gill, M. R. Heideman et al., "Combinatorial targeting of FGF and ErbB receptors blocks growth and metastatic spread of breast cancer models," *Breast Cancer Research*, vol. 15, no. 1, p. R8, 2013.

[33] Y. H. Chiu, S. H. Hsu, H. W. Hsu et al., "Human non-small cell lung cancer cells can be sensitized to camptothecin by modulating autophagy," *International Journal of Oncology*, vol. 53, no. 5, pp. 1967–1979, 2018.

[34] P. Lopez-Ruiz, J. Rodriguez-Ubreva, A. Ernesto Cariaga, M. Alicia Cortes, and B. Colas, "SHP-1 in cell-cycle regulation," *Anti-Cancer Agents in Medicinal Chemistry*, vol. 11, no. 1, pp. 89–98, 2011.

[35] A. Witkiewicz, P. Raghunath, A. Wasik et al., "Loss of SHP-1 tyrosine phosphatase expression correlates with the advanced stages of cutaneous T-cell lymphoma," *Human Pathology*, vol. 38, no. 3, pp. 462–467, 2007.

[36] W.-T. Tai, C.-W. Shiau, H.-L. Chen et al., "Mcl-1-dependent activation of Beclin 1 mediates autophagic cell death induced by sorafenib and SC-59 in hepatocellular carcinoma cells," *Cell Death & Disease*, vol. 4, no. 2, p. e485, 2013.

[37] S. Bhattacharya, R. M. Ray, and L. R. Johnson, "STAT3-mediated transcription of Bcl-2, Mcl-1 and c-IAP2 prevents apoptosis in polyamine-depleted cells," *Biochemical Journal*, vol. 392, no. 2, pp. 335–344, 2005.

[38] A. H. Boulares, A. G. Yakovlev, V. Ivanova et al., "Role of poly (ADP-ribose) polymerase (PARP) cleavage in apoptosis," *Journal of Biological Chemistry*, vol. 274, no. 33, pp. 22932–22940, 1999.

[39] D. Sinibaldi, W. Wharton, J. Turkson, T. Bowman, W. J. Pledger, and R. Jove, "Induction of p21WAF1/CIP1 and cyclin D1 expression by the Src oncoprotein in mouse fibroblasts: role of activated STAT3 signaling," *Oncogene*, vol. 19, no. 48, pp. 5419–5427, 2000.

[40] T. Gritsko, A. Williams, J. Turkson et al., "Persistent activation of STAT3 signaling induces survivin gene expression and confers resistance to apoptosis in human breast cancer cells," *Clinical Cancer Research*, vol. 12, no. 1, pp. 11–19, 2006.

[41] H. Xiong, Z.-G. Zhang, X.-Q. Tian et al., "Inhibition of JAK1, 2/STAT3 signaling induces apoptosis, cell cycle arrest, and reduces tumor cell invasion in colorectal cancer cells," *Neoplasia*, vol. 10, no. 3, pp. 287–297, 2008.

[42] N. Jing and D. J. Tweardy, "Targeting STAT3 in cancer therapy," *Anti-Cancer Drugs*, vol. 16, no. 6, pp. 601–607, 2005.

[43] R. J. Leeman, V. W. Y. Lui, and J. R. Grandis, "STAT3 as a therapeutic target in head and neck cancer," *Expert Opinion on Biological Therapy*, vol. 6, no. 3, pp. 231–241, 2006.

[44] N. Li, S. I. Grivennikov, and M. Karin, "The unholy trinity: inflammation, cytokines, and STAT3 shape the cancer microenvironment," *Cancer Cell*, vol. 19, no. 4, pp. 429–431, 2011.

[45] J. Bollrath and F. R. Greten, "IKK/NF-κB and STAT3 pathways: central signalling hubs in inflammation-mediated tumour promotion and metastasis," *EMBO Reports*, vol. 10, no. 12, pp. 1314–1319, 2009.

[46] S. Pensa, C. J. Watson, and V. Poli, "STAT3 and the inflammation/acute phase response in involution and breast cancer," *Journal of Mammary Gland Biology and Neoplasia*, vol. 14, no. 2, pp. 121–129, 2009.

[47] J. Zhou, J. Wulfkuhle, H. Zhang et al., "Activation of the PTEN/mTOR/STAT3 pathway in breast cancer stem-like cells is required for viability and maintenance," *Proceedings of the National Academy of Sciences*, vol. 104, no. 41, pp. 16158–16163, 2007.

[48] R. Behera, V. Kumar, K. Lohite, S. Karnik, and G. C. Kundu, "Activation of JAK2/STAT3 signaling by osteopontin promotes tumor growth in human breast cancer cells," *Carcinogenesis*, vol. 31, no. 2, pp. 192–200, 2010.

[49] R. Garcia, T. L. Bowman, G. Niu et al., "Constitutive activation of STAT3 by the Src and JAK tyrosine kinases participates in growth regulation of human breast carcinoma cells," *Oncogene*, vol. 20, no. 20, pp. 2499–2513, 2001.

[50] C. Watson and W. Miller, "Elevated levels of members of the STAT family of transcription factors in breast carcinoma nuclear extracts," *British Journal of Cancer*, vol. 71, no. 4, pp. 840–844, 1995.

[51] R. Garcia, C. L. Yu, A. Hudnall et al., "Constitutive activation of STAT3 in fibroblasts transformed by diverse oncoproteins and in breast carcinoma cells," *Cell Growth & Differentiation: The Molecular Biology Journal of the American Association for Cancer Research*, vol. 8, no. 12, pp. 1267–1276, 1997.

[52] C. J. Ormandy, E. A. Musgrove, R. Hui, R. J. Daly, and R. L. Sutherland, "Cyclin D1, EMS1 and 11q13 amplification in breast cancer," *Breast Cancer Research and Treatment*, vol. 78, no. 3, pp. 323–335, 2003.

[53] K. Tanaka, S. Iwamoto, G. Gon, T. Nohara, M. Iwamoto, and N. Tanigawa, "Expression of survivin and its relationship to loss of apoptosis in breast carcinomas," *Clinical Cancer Research*, vol. 6, no. 1, pp. 127–134, 2000.

[54] S. M. Kennedy, L. O'Driscoll, R. Purcell et al., "Prognostic importance of survivin in breast cancer," *British Journal of Cancer*, vol. 88, no. 7, pp. 1077–1083, 2003.

[55] N. Diaz, S. Minton, C. Cox et al., "Activation of STAT3 in primary tumors from high-risk breast cancer patients is associated with elevated levels of activated SRC and survivin expression," *Clinical Cancer Research*, vol. 12, no. 1, pp. 20–28, 2006.

[56] H. Xin, C. Zhang, A. Herrmann, Y. Du, R. Figlin, and H. Yu, "Sunitinib inhibition of STAT3 induces renal cell carcinoma tumor cell apoptosis and reduces immunosuppressive cells," *Cancer Research*, vol. 69, no. 6, pp. 2506–2513, 2009.

[57] Y. J. Choi, H. S. Kim, S. H. Park et al., "Phase II study of dovitinib in patients with castration-resistant prostate cancer (KCSG-GU11-05)," *Cancer Research and Treatment*, vol. 50, no. 4, pp. 1252–1259, 2018.

[58] J. D. Rabinowitz and E. White, "Autophagy and metabolism," *Science*, vol. 330, no. 6009, pp. 1344–1348, 2010.

[59] A. L. Anding and E. H. Baehrecke, "Autophagy in cell life and cell death," *Current Topics in Developmental Biology*, vol. 114, pp. 67–91, 2015.

[60] Y. Kondo and S. Kondo, "Autophagy and cancer therapy," *Autophagy*, vol. 2, no. 2, pp. 85–90, 2006.

[61] Z. J. Yang, C. E. Chee, S. Huang, and F. A. Sinicrope, "The role of autophagy in cancer: therapeutic implications," *Molecular Cancer Therapeutics*, vol. 10, no. 9, pp. 1533–1541, 2011.

[62] Y. Kondo, T. Kanzawa, R. Sawaya, and S. Kondo, "The role of autophagy in cancer development and response to therapy," *Nature Reviews Cancer*, vol. 5, no. 9, pp. 726–734, 2005.

[63] W. Bursch, A. Ellinger, H. Kienzl et al., "Active cell death induced by the anti-estrogens tamoxifen and ICI 164 384 in human mammary carcinoma cells (MCF-7) in culture: the role of autophagy," *Carcinogenesis*, vol. 17, no. 8, pp. 1595–1607, 1996.

[64] T. Kanzawa, I. M. Germano, T. Komata, H. Ito, Y. Kondo, and S. Kondo, "Role of autophagy in temozolomide-induced

cytotoxicity for malignant glioma cells," *Cell Death & Differentiation*, vol. 11, no. 4, pp. 448–457, 2004.

[65] S. Paglin, T. Hollister, T. Delohery et al., "A novel response of cancer cells to radiation involves autophagy and formation of acidic vesicles," *Cancer Research*, vol. 61, no. 2, pp. 439–444, 2001.

[66] T. Kanzawa, Y. Kondo, H. Ito, S. Kondo, and I. Germano, "Induction of autophagic cell death in malignant glioma cells by arsenic trioxide," *Cancer Research*, vol. 63, no. 9, pp. 2103–2108, 2003.

[67] A. Vazquez-Martin, C. Oliveras-Ferraros, and J. A. Menendez, "Autophagy facilitates the development of breast cancer resistance to the anti-HER2 monoclonal antibody trastuzumab," *PLoS One*, vol. 4, no. 7, Article ID e6251, 2009.

[68] Y. Shao, Z. Gao, P. A. Marks, and X. Jiang, "Apoptotic and autophagic cell death induced by histone deacetylase inhibitors," *Proceedings of the National Academy of Sciences*, vol. 101, no. 52, pp. 18030–18035, 2004.

[69] B. H. Huang, M. Laban, C. H.-W. Leung et al., "Inhibition of histone deacetylase 2 increases apoptosis and p21Cip1/WAF1 expression, independent of histone deacetylase 1," *Cell Death & Differentiation*, vol. 12, no. 4, pp. 395–404, 2005.

[70] J. Song, J. H. Noh, J. H. Lee et al., "Increased expression of histone deacetylase 2 is found in human gastric cancer," *APMIS*, vol. 113, no. 4, pp. 264–268, 2005.

[71] J.-H. Choi, H. J. Kwon, B.-I. Yoon et al., "Expression profile of histone deacetylase 1 in gastric cancer tissues," *Japanese Journal of Cancer Research*, vol. 92, no. 12, pp. 1300–1304, 2001.

[72] S. Ropero and M. Esteller, "The role of histone deacetylases (HDACs) in human cancer," *Molecular Oncology*, vol. 1, no. 1, pp. 19–25, 2007.

[73] N. E. Brown, R. Jeselsohn, T. Bihani et al., "Cyclin D1 activity regulates autophagy and senescence in the mammary epithelium," *Cancer Research*, vol. 72, no. 24, pp. 6477–6489, 2012.

Hindawi
Journal of Oncology
Volume 2019, Article ID 6018432, 8 pages
https://doi.org/10.1155/2019/6018432

Research Article

Pregnancy Hypertension and a Commonly Inherited IGF1R Variant (rs2016347) Reduce Breast Cancer Risk by Enhancing Mammary Gland Involution

Mark J. Powell[1,2] **Suzanne M. Dufault**[3] **Jill E. Henry**[4] **Anna C. Allison**[5] **Renata Cora**[6] **and Christopher C. Benz**[1]

[1]*Buck Institute for Research on Aging, Novato, CA, USA*
[2]*Zero Breast Cancer, San Rafael, CA, USA*
[3]*Graduate Group in Biostatistics, University of California, Berkeley, School of Public Health, Berkeley, CA, USA*
[4]*Susan G. Komen for the Cure® Tissue Bank at the Indiana University Simon Cancer Center, Indianapolis, IN, USA*
[5]*Mission Analytics Group, San Francisco, CA, USA*
[6]*Care Mount Medical, Mount Kisco, NY, USA*

Correspondence should be addressed to Mark J. Powell; markp@zerobreastcancer.org

Received 12 April 2019; Revised 28 May 2019; Accepted 28 July 2019; Published 14 August 2019

Guest Editor: Chia-Jung Li

Background. Terminal duct lobular units (TDLUs) are the anatomic sites of breast cancer initiation, and breast tissue involution resulting in lower TDLU counts has been associated with decreased breast cancer risk. The insulin-like growth factor (IGF) pathway plays a role in breast involution, and systemic changes in this developmental pathway occur with hypertensive disorders of pregnancy (HDP), which have also been associated with lower breast cancer risk, especially in women carrying a functional variant of IGF1R SNP rs2016347. We proposed that this breast cancer protective effect might be explained by increased breast tissue involution. *Materials and Methods*. We conducted a retrospective cohort study utilizing the Komen Tissue Bank, which collects breast tissue core biopsies from women without a history of breast cancer. Eighty white non-Hispanic women with a history of HDP were selected along with 120 nonexposed participants, and after genotyping for rs2016347, TDLU parameters were histologically measured blinded to participant characteristics from fixed biopsy sections. *Results*. Stratified models by HDP status demonstrated that among HDP+ participants, those carrying two T alleles of rs2016347 had a decrease in TDLU counts of 53.2% when compared to those with no T alleles ($p = 0.049$). Trend analysis demonstrated a multiplicative decrease in counts of 31.6% per T allele ($p = 0.050$). Although no statistically significant interaction was seen between HDP status and T alleles, interaction terms showed increasingly negative values reaching a p value of 0.124 for HDP × 2T alleles. *Conclusions*. The observed statistically significant decrease in TDLU counts signifies increased breast epithelial involution in women with prior HDP who inherited the TT genotype of IGF1R SNP rs2016347. The increasing degree of breast involution with greater rs2016347 T allele copy number is consistent with the known progressive reduction in IGF1R expression in breast and other normal tissues.

1. Introduction

Terminal duct lobular units (TDLUs) are the main structures within the breast that produce milk and are recognized as the anatomic site of development of most breast cancers [1]. Aging and the completion of childbearing are accompanied by mammary gland involution, and lower TDLU counts at a single point in time have been independently associated with lower breast cancer risk in many studies [2–4]. In addition, longitudinal data have shown that women whose breast tissue demonstrates slower involution over time also have increased breast cancer risk [5]. The insulin-like growth factor (IGF) pathway has been implicated in playing a role in the involution process, and decreased levels of IGF-1 and increased levels of one of its binding proteins, IGFBP3, have been associated with lower TDLU counts [6–8].

Hypertensive disorders of pregnancy (HDP) are also associated with systemic changes in the IGF pathway and affect later-life breast cancer risk. HDP impact 5–8% of pregnancies and are characterized by the development of high blood pressure usually after the 20^{th} week of pregnancy. HDP include gestational hypertension (hypertension alone) and preeclampsia (hypertension accompanied by proteinuria). These pregnancies are characterized by inadequate cytotrophoblastic invasion of the myometrium and impaired transformation of the spiral arteries resulting in placental ischemia [9, 10] and alterations in many hormones and growth factors including lower levels of IGF-1 and increased levels of IGFBP3 [11–15]. Many studies have reported lower breast cancer rates in women who experience HDP, and although these findings have not been uniform, most larger cohort studies have reported a decrease in later-life breast cancer rates ranging from 15–20% for both gestational hypertension and preeclampsia [16–18].

The breast cancer protective effect of HDP may have been underestimated in subgroups of women in prior studies that did not study inherited gene variants potentially affecting the IGF axis. Recent findings from the California Teachers Study demonstrated that among women with a history of preeclampsia, those carrying the TT genotype of a specific functional IGF1R SNP (rs2016347) had a decrease in risk for estrogen receptor-positive breast cancer of 74% when compared to the GG genotype [19]. Similarly, earlier work in the Marin Women's Study had found that in women with a history of HDP, carrying the T allele (allele frequency 0.52) was associated with lower later-life breast density as well as decreased breast cancer risk [20, 21]. This SNP is located in the 3' UTR of the IGF1R gene, and T alleles have been shown to result in a progressive decrease in IGF1R mRNA expression levels in breast and other normal human tissues [22].

Since the IGF pathway plays an essential role in early mammary gland growth and development as well as later-life breast tissue involution [23] and overstimulation of the IGF axis plays a promoting role in breast cancer development [24], we proposed that the profound breast cancer protective effect of HDP associated with inheritance of the IGF1R SNP rs2016347 TT genotype might be explained by and associated with increased breast tissue involution, manifested as lower TDLU counts. To test this hypothesis, we performed a retrospective cohort study evaluating TDLU counts from normal breast core biopsy samples from a cohort of genotyped parous women with no history of breast cancer.

2. Materials and Methods

2.1. Study Population. This retrospective cohort study utilized participants from the Komen Tissue Bank (KTB) at the Indiana University Simon Cancer Center. The KTB is an annotated biobank that collects breast tissue core biopsies, questionnaire data, and blood from women with no prior history of breast cancer and to date has received tissue donations from over 5,000 women. Donors provide written informed consent and are recruited under a protocol approved by the Indiana University Institutional Review Board. KTB participants were asked if they developed hypertension, gestational hypertension, or preeclampsia during a pregnancy and also if they had hypertension prior to pregnancy.

Eighty white non-Hispanic women were selected with a history of HDP if they answered yes to any of the questions about pregnancy hypertension and no to having had hypertension prior to pregnancy. One-hundred and twenty nonexposed participants were then selected from white non-Hispanic parous women who answered no to all questions, and these participants were frequency matched for age. The KTB provided digitized slides of the formalin-fixed and hematoxylin and eosin- (H&E-) stained biopsy sections on all participants along with reproductive history details and relevant covariates. Core biopsy tissue acquisition from an upper outer breast quadrant was standardized, and processing details are well described in the KTB standard operating procedures [25].

2.2. Genotyping. Upon entry into the study, blood was drawn from participants into an EDTA tube and after plasma separation and removal was stored at −80°C. Buffy coat DNA extraction occurred at the Indiana CTSI Specimen Storage Facility using an AutogenFlex Star instrument and Flexigene AGF3000 kit for DNA extraction. Genotyping for rs2016347 was performed at the Beckman Research Institute of City of Hope using MGB TaqMan Probe Assays from Life Technologies. The overall call rate was 97.0%, and the T allele frequency was 0.53 across the entire cohort.

2.3. Histologic Assessment. Histologic evaluation was performed by an experienced cytotechnologist (R. Cora) with specific training and expertise in assessing TDLU parameters and who was blinded to all participant characteristics and genotyping. H&E-stained digital images were reviewed using the Aperio ImageScope software from Leica (version 12.3.3); no samples contained either preneoplastic or malignant cells, and samples without any obvious epithelial component were considered ineligible for review. The mean tissue area scored was 35.26 mm^2, and total counts of normal TDLUs were calculated per 100 mm^2 and included any TDLU with at least 2 acini associated with a discernable lumen. Ninety-one of our participants had TDLU counts independently determined for another KTB study by Mayo Clinic pathologist M. Sherman, MD; these results were made available to us after our counts were completed and the paired readings showed high correlation, $r = 0.89$.

Nine of the 200 participants were not included in the final analysis due to lack of detectable epithelium on their biopsy slide (3) or inconclusive rs2016347 genotyping (6), resulting in an analytical dataset of 191.

2.4. Statistical Analysis. We ran negative binomial generalized linear models (GLM-NB) with a log-link to estimate adjusted count ratios (CRs) per unit of tissue area to assess whether TDLU counts varied with HDP status and whether this association was modified by IGF1R SNP rs2016347 T

allele number. Models were adjusted for known confounders including age at first birth, age at time of biopsy, age at menarche, family history of a first-degree relative with breast cancer, body mass index (BMI), and parity. Different genotype parameterizations were used to test for trend and/or threshold effect on the TDLU counts. Multiplicative interaction was assessed via an interaction term in the GLM-NB between genotype and HDP at a significance threshold of 0.10.

Although there was a high percentage of zero TDLU counts (10%) despite presence of some epithelium, goodness-of-fit tests did not demonstrate improved fit for a zero-inflated or hurdle model when compared to the GLM-NB via the nested likelihood ratio test and the Vuong test for non-nested models, respectively. Additional nested goodness-of-fit testing compared the GLM-NB to the Poisson-GLM. This test returned evidence of improved model fit in the NB setting, suggesting overdispersion of TDLU counts. The model comparisons are summarized in supplementary Table S1.

All analyses were run using R version 3.5.0 "Joy in Playing" [26]. Estimation of the GLM-NB models was performed with the "glm.nb" function from the "MASS" package [27]. Zero-inflated models, hurdle models, and the Vuong goodness-of-fit test were estimated using "zeroinf," "hurdle," and "vuong" from the "pscl" package [28, 29]. All plots were made using the "ggplot2" package [30]. All code needed to recreate this analysis is available at https://github.com/sdufault15/tdlu-analysis.

Gail 5-year risk scores were calculated using the Breast Cancer Risk Assessment Tool located on the NIH website: https://bcrisktool.cancer.gov.

3. Results

3.1. Participant Characteristics. All participants were parous white non-Hispanic women by study design, and mean age at biopsy was 45.9 years. Characteristics of the major covariates are presented in Table 1.

HDP+ participants differed from HDP− participants only in having higher BMI ($p < 0.001$), with a mean BMI of 32.4 compared to 28.4 for HDP− participants. Obesity has been a frequently reported risk factor for HDP, and 55.2% of HDP+ participants in this study were obese (as defined by BMI >30) compared to 33.1% in the HDP− group [31, 32]. Mean values of all participants for parity, age at first birth, and age at menarche were 2.05, 27.0, and 12.5, respectively, and 26.7% reported a history of breast cancer in a first-degree relative.

3.2. Association of Breast Cancer Risk Characteristics and TDLU Counts. Relationships of major breast cancer risk factors with TDLU counts (adjusted for other covariates) are presented in Figure 1. Age at biopsy was inversely and significantly associated with TDLU counts, as would be expected. BMI was associated with lower TDLU counts, but this did not quite reach statistical significance ($p = 0.055$). Both parity and family history of breast cancer were associated with increased TDLU counts, while there was little evidence of an association for age at menarche or age at first birth. In addition, Gail 5-year risk scores demonstrated no significant correlation with TDLU counts, $r = -0.144$.

Table 1: Participant characteristics by HDP status[a].

Characteristic	HDP+ $N = 76$	HDP− $N = 115$	p value[b]
	N (%)		
Age at biopsy (years)			0.82
≤39	26 (34.2)	36 (31.2)	
40–49	24 (31.6)	33 (28.7)	
50–59	18 (23.7)	29 (25.2)	
≥60	8 (10.5)	17 (14.8)	
Age at menarche (years)			0.23
≤11	19 (25.0)	19 (16.5)	
12	18 (23.7)	40 (34.8)	
13	25 (32.9)	31 (27.0)	
≥14	14 (18.4)	25 (21.7)	
Parity			0.38
1	17 (22.4)	26 (22.6)	
2	36 (47.4)	64 (55.7)	
≥3	23 (30.2)	25 (21.7)	
Age at first birth (years)			0.89
≤24	25 (32.9)	35 (30.4)	
25–29	26 (34.2)	43 (37.4)	
≥30	25 (32.9)	37 (32.2)	
BMI (kg/m^2)			0.00
≤24.9	12 (15.8)	45 (39.1)	
25–29.9	22 (29.0)	32 (27.8)	
≥30	42 (55.2)	38 (33.1)	
Family history[c]			0.81
Yes	21 (27.6)	30 (26.1)	
No	55 (72.4)	85 (73.9)	
Rs2016347 genotype			0.83
GG	18 (23.7)	24 (20.9)	
GT	37 (48.7)	61 (53.0)	
TT	21 (27.6)	30 (26.1)	
Gail 5-year risk scores			0.44
Mean	1.50%	1.69%	

[a]All participants identify as non-Hispanic white. [b]p value is the chi-squared P value for differences in distribution between HDP+ and HDP− participants. [c]At least one first-degree relative with breast cancer.

3.3. Adjusted Negative Binomial Model for HDP and rs2016347 Genotype Interactions. When adjusted for multiple covariates associated with breast cancer risk, there were no statistically significant interactions between the effects of HDP status and the number of rs2016347 T alleles on TDLU count (Table 2), although Count Ratios (CRs) comparing the effects of 1 or 2 T alleles to 0 T alleles were, respectively, 0.734 ($p = 0.457$) and 0.477 ($p = 0.124$) times lower in the HDP+ stratum than in the HDP− stratum.

For women carrying no T alleles of rs2016347, the HDP+ exposure group has a TDLU count that is not significantly increased (CR = 1.23, $p = 0.546$) when compared to the HDP− group. For HDP− women, the CRs comparing rs2016347 genotypes of 1 and 2 T alleles to the reference genotype of 0 T alleles show no evidence of association as both CRs hover around the null (CR = 0.973, CR = 1.104, respectively) with relatively large p values ($p = 0.918$, $p = 0.747$, respectively).

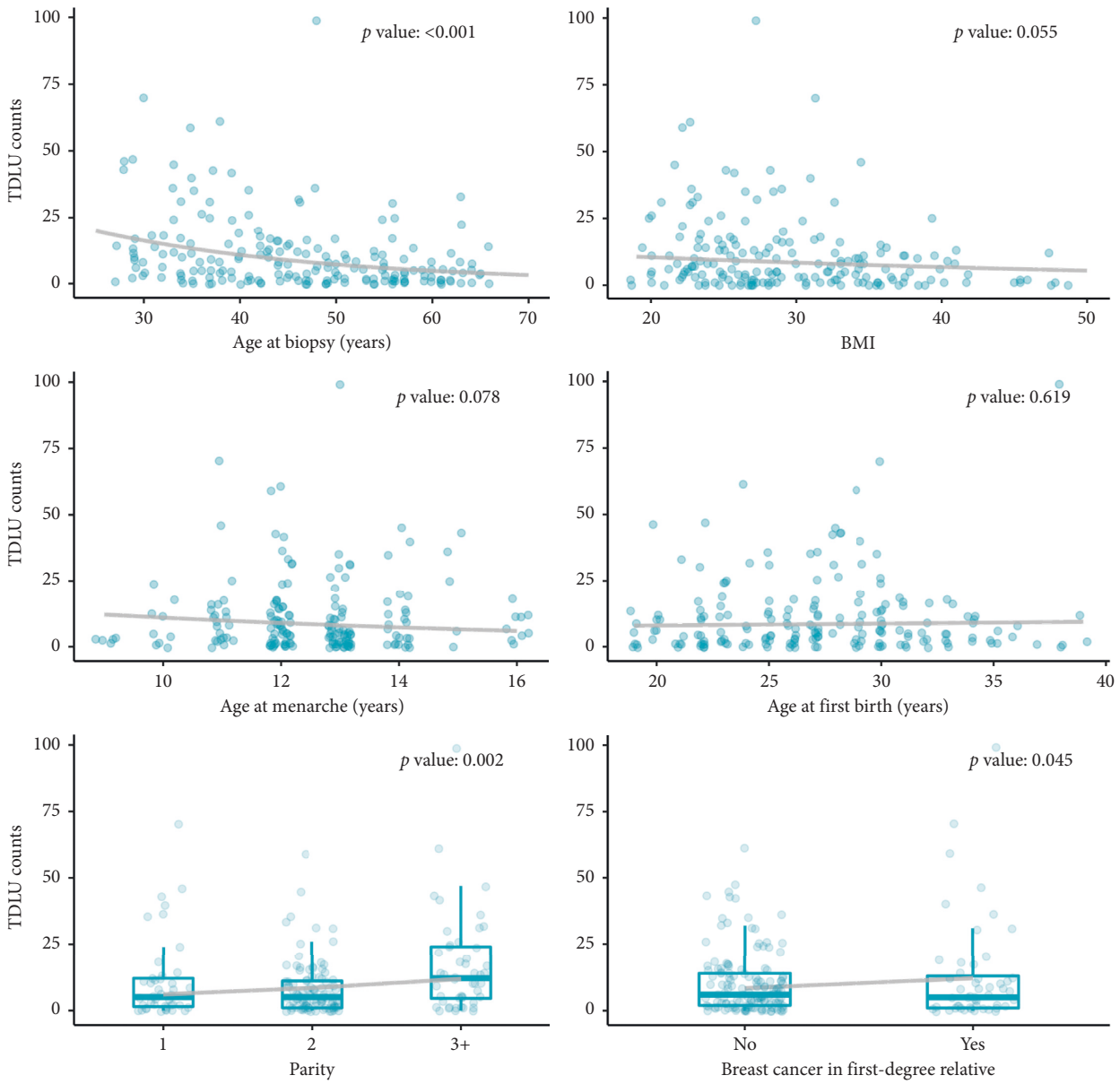

Figure 1: Adjusted bivariate TDLU relationships.

Table 2: Results of adjusted negative binomial model with interaction terms.

	Coefficient	Standard error	Z Value	p value	CR (95% CI)
HDP	0.208	0.345	0.604	0.546	1.231 (0.627, 2.419)
T alleles = 1	−0.027	0.268	−0.102	0.918	0.973 (0.575, 1.645)
T alleles = 2	0.099	0.307	0.322	0.747	1.104 (0.605, 2.016)
HDP × T alleles = 1	−0.310	0.417	−0.743	0.457	0.734 (0.324, 1.661)
HDP × T alleles = 2	−0.740	0.482	−1.536	0.124	0.477 (0.185, 1.227)

HDP compares HDP-postive women to HDP-negative women. T alleles are treated as a factor variable. The reference for T alleles is no T alleles (T alleles = 0). These results are adjusted for family history, age at biopsy, parity, age at menarche, age at first birth, and BMI. Full model covariates can be found in the supplemental material (Table S2).

3.4. Box Plots of Adjusted TDLU Counts by rs2016347 Genotype Stratified by HDP Status. The mean TDLU count across all participants was 11.01. Adjusted TDLU counts by rs2016347 genotypes stratified by HDP status are presented in Figure 2 (abbreviated model presented in Table 3 with full model in Table S3). TDLU count distributions within the HDP− group were statistically similar across all genotypes; by contrast, within the HDP+ group, there was a stepwise decrease in TDLU counts with increasing rs2016347 T allele number reaching significance for 2 T alleles compared to 0 T alleles.

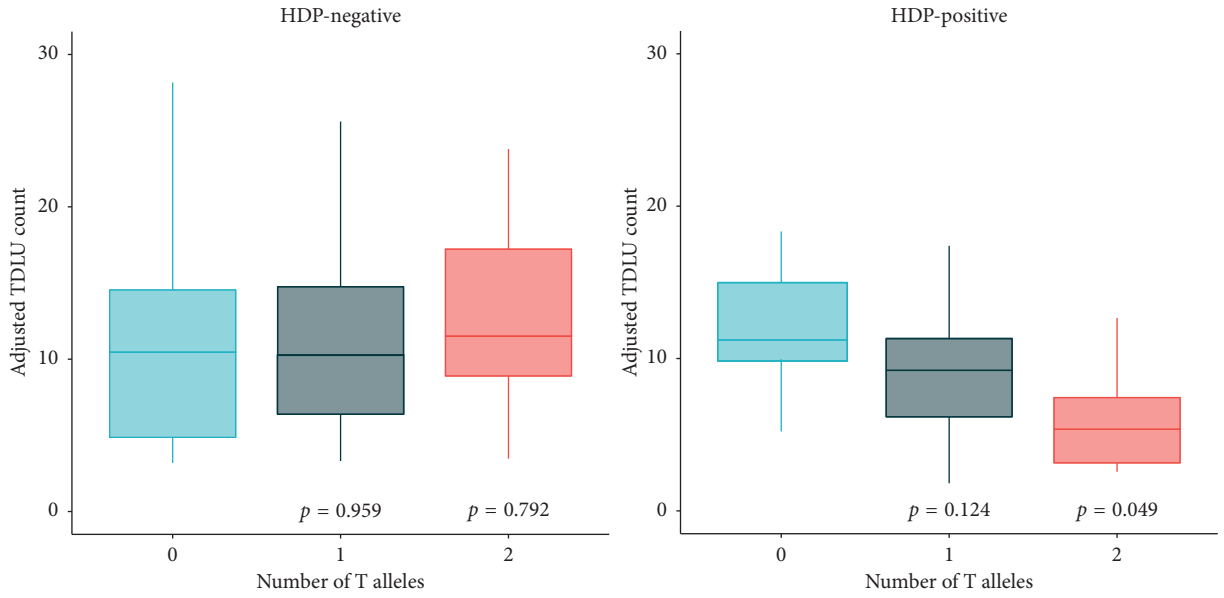

Figure 2: Box plots of adjusted TDLU counts by rs2016347 genotype stratified by HDP status.

Table 3: Summary table of the adjusted T allele CRs from the models stratified on HDP status.

	HDP-negative		HDP-positive	
	CR (95% CI)	p value	CR (95% CI)	p value
Factor model				
T alleles = 0	1 (ref.)		1 (ref.)	
T alleles = 1	1.014 (0.608, 1.689)	0.959	0.606 (0.320, 1.148)	0.124
T alleles = 2	1.083 (0.600, 1.955)	0.792	0.468 (0.219, 0.997)	0.049
Linear trend model				
Δ T alleles	1.042 (0.775, 1.400)	0.787	0.684 (0.468, 1.000)	0.050

These results are adjusted for family history, age at biopsy, parity, age at menarche, age at first birth, and BMI. Full model covariates can be found in the supplemental material (Tables S3 and S4).

3.5. Adjusted Stratified Model and Trend Analysis by HDP Status and rs2016347 Genotype. Covariate adjusted models stratified by HDP status are shown in Table 3 and include factor models which look at the impact of 1 and 2 rs2016347 T alleles separately and a trend model which treats the T alleles linearly. In HDP− women, there is no effect of genotype on TDLU counts in either model. Among HDP+ participants, those carrying 2 T alleles showed a significant ($p = 0.049$) decrease in TDLU counts of 53.2% when compared to those with 0 T alleles (GG genotype). Trend analysis in the HDP+ group also demonstrated a significant ($p = 0.050$) linear trend with a multiplicative decrease in TDLU counts of 31.6% per T allele.

4. Discussion

In the current study, we were able to demonstrate a statistically significant decrease in TDLU counts, signifying increased breast epithelial involution, in women who have experienced HDP and inherited the TT genotype of IGF1R SNP rs2016347, while there was no evidence of an association for women who experienced either the TT genotype or HDP. This association with increased breast involution is very consistent with our prior findings in the California Teachers Study (CTS) where breast cancer incidence was similarly reduced in women with preeclampsia if they also inherited the TT genotype of rs2016347 but not when preeclampsia alone was considered [19]. In both studies, carrying one T allele produced an intermediate effect; furthermore, in the current study, the impact on breast involution increased according to T allele copy number consistent with the progressive reduction in IGF1R mRNA expression observed in breast and other normal tissues with increasing rs2016347 T allele number [22].

In our formal test for an HDP-genotype interaction, we observed that the CR comparing HDP+ to HDP− exposure groups carrying 2 T alleles of rs2016347 was 52.3% ($p = 0.124$) lower than the CR comparing HDP+ to HDP− exposure groups carrying 0 T alleles of rs2016347, suggesting that the association of HDP with TDLU count is modified by rs2016347 genotype. Failing to achieve significant statistical interaction likely reflected our small number of HDP+ × 2T allele samples (21 of 191 total samples) and the extent of variance among sample TDLU counts. Nonetheless, the consistent pattern of association observed between this KTB analysis of normal breast

TDLUs and our prior CTS analysis of breast cancer incidence rates strongly suggests that a history of HDP in concert with inheritance of a functionally blunted IGF1R rs2016347 variant manifests as both enhanced mammary gland involution and reduced later-life breast cancer risk, both outcomes impacted by decades of significantly reduced mammary gland IGF axis stimulation.

The IGF axis, stimulated primarily by soluble IGF-1 growth factor binding to and activating cell membrane-bound IGF1R growth factor receptor, plays a key role in breast development throughout life. Around the time of menarche, ovaries begin producing estrogen and progesterone resulting in expansion of the mammary ductal system with its stem and progenitor cell-enriched TDLUs. The IGF axis impacts this developmental process by the increase in circulating IGF-1 levels that accompany early menarche [33–35]. During pregnancy and with the onset of HDP, circulating IGF-1 levels are substantially reduced while IGFBP3 levels are increased (further reducing free IGF-1 levels), and as these reciprocal changes are sustained beyond parturition, they can attenuate IGF axis effects on the mammary gland and accelerate later-life breast involution [11–13, 20, 21].

Biologically, IGF-1 and IGFBP3 levels appear to drive only TDLU counts and do not otherwise impact other TDLU measures such as span or acini counts per TDLU [7, 8], consistent with our inability to detect either span or acini score associations with HDP and/or rs2016347 genotypes (results not provided). Across epidemiologic studies, HDP by itself only marginally reduces later-life breast cancer risk; but, as seen here and in two prior studies [19–21], inheritance of the functionally blunted rs2016347 TT genotype appears to combine with the biological impact of HDP to reduce mammary gland TDLUs, mammographic density, and later-life breast cancer incidence. By itself, higher expression of IGF1R in TDLUs can increase later-life risk of developing breast cancer by nearly 16-fold [36]. In contrast, among those women who ultimately develop breast cancer, inheriting the IGF1R expression blunting effect of the rs2016347 T allele confers a greater clinical response rate to neoadjuvant chemotherapy and a better overall survival outcome [37, 38].

Many well-established breast cancer risk factors can also independently impact TDLU counts, as shown in Figure 1, necessitating our multivariate model analyses (Tables 2 and 3) that adjusted for potentially confounding risk factors such as age at first birth, age at time of biopsy, age at menarche, breast cancer family history in a first-degree relative, BMI, and parity. We observed that age at biopsy was inversely associated with TDLU counts in a pattern similar to that reported by others, showing a declining slope with aging that does not change much after menopause [29]. TDLUs varied weakly and inversely with BMI; while this only trended toward significance ($p = 0.055$), our findings are similar to what has previously been reported in other KTB cohorts [3, 39]. As with those other studies, we found that both parity and family history of breast cancer were associated with increased TDLU counts, while little consistent association was observed with regard to age at menarche or age at first birth. Likewise, Gail 5-year risk scores did not correlate with TDLU counts, consistent with findings from the Mayo Benign Breast Disease Cohort [40].

The use of specimens from the KTB provided a number of significant strengths to this study. First and foremost, it enabled assessment of entirely normal breast tissue donated by women without any history of breast cancer or other known breast disorders. Other "normal" breast studies commonly use resected tissue adjacent to breast tumors, biopsies taken for mammographically suspected breast lesions, or reduction mammoplasty samples. Furthermore, asking our participants if they had hypertension prior to pregnancy resulted in the exclusion of women with chronic hypertension, a cause of misclassification in many other HDP studies. In addition, the KTB has extensive data on reproductive history and other breast cancer risk factors, allowing us to account for many potentially confounding variables. Due to the relatively low number of women enrolled in the KTB at the time this study was initiated, we were limited in our ability to observe statistical significance for a moderate effect size, likely explaining the lack of statistical significance when formally testing for interaction between HDP history and rs2016347 genotype. We recognize that participants in the KTB are not completely representative of the general public, potentially limiting the generalizability of our findings. As such, it might be expected that women who volunteer for the KTB are more likely to have a positive family history of breast cancer, and this was noted for 26.7% of our study population, although women with BRCA1/2 positivity were excluded from our study cohort. Inclusion of only white non-Hispanic parous women was dictated by the low number of women of color enrolled by the KTB in its earlier stages.

5. Conclusions

Normal breast biopsy samples along with peripheral blood rs2016347 genotyping of 191 healthy parous female donors confirmed our mechanistic hypothesis that the pronounced breast cancer protective interaction between pregnancy hypertension (HDP) and inheritance of a functionally blunted IGF1R SNP (rs2016347) TT genotype likely results from enhanced breast glandular involution, as determined by fewer terminal duct lobular units (TDLUs).

Data Availability

The case and covariate data for this study were obtained from the Komen Tissue Bank (KTB). Generated data consisting of Gail scores, rs2016347 genotyping, and pathologic review of breast tissue samples with determination of TDLU parameters has been deposited in the KTB. All data for this analysis can be accessed on their virtual tissue bank at https://virtualtissuebank.iu.edu/.

Conflicts of Interest

The authors declare that there are no conflicts of interest regarding the publication of this paper.

Acknowledgments

This work was supported in part by a grant from the National Institutes of Health and National Cancer Institute (#U24CA210990). Additional support was received from the Elizabeth MA Stevens Donor Funds provided to the Buck Institute for Research on Aging.

Supplementary Materials

Supplementary Table S1: goodness-of-fit model comparisons considered for this analysis. Supplementary Table S2: fully adjusted negative binomial model with interaction terms for HDP status and rs2016347 genotype, including covariates age at biopsy, age at first birth, family history of breast cancer in first degree relative, BMI, parity, and age at menarche. Supplementary Table S3: fully adjusted negative binomial models stratified for HDP status including covariates age at biopsy, age at first birth, family history of breast cancer in first degree relative, BMI, parity, and age at menarche. Supplementary Table S4: fully adjusted negative binomial model with alleles treated linearly for trend in both HDP-positive and HDP-negative participants including covariates age at biopsy, age at first birth, family history of breast cancer in first degree relative, BMI, parity, and age at menarche. (*Supplementary Materials*)

References

[1] J. Russo and I. H. Russo, "Development of the human breast," *Maturitas*, vol. 49, no. 1, pp. 2–15, 2004.

[2] H. J. Baer, L. C. Collins, J. L. Connolly, G. A. Colditz, S. J. Schnitt, and R. M. Tamimi, "Lobule type and subsequent breast cancer risk: results from the nurses' health studies," *Cancer*, vol. 115, no. 7, pp. 1404–1411, 2009.

[3] J. D. Figueroa, R. M. Pfeiffer, L. A. Brinton et al., "Standardized measures of lobular involution and subsequent breast cancer risk among women with benign breast disease: a nested case-control study," *Breast Cancer Research and Treatment*, vol. 159, no. 1, pp. 163–172, 2016.

[4] T. R. Milanese, L. C. Hartmann, T. A. Sellers et al., "Age-related lobular involution and risk of breast cancer," *JNCI: Journal of the National Cancer Institute*, vol. 98, no. 22, pp. 1600–1607, 2006.

[5] D. C. Radisky, D. W. Visscher, R. D. Frank et al., "Natural history of age-related lobular involution and impact on breast cancer risk," *Breast Cancer Research and Treatment*, vol. 155, no. 3, pp. 423–430, 2016.

[6] M. S. Rice, R. M. Tamimi, J. L. Connolly et al., "Insulin-like growth factor-1, insulin-like growth factor binding protein-3 and lobule type in the nurses' health study II," *Breast Cancer Research*, vol. 14, no. 2, p. R44, 2012.

[7] H. N. Horne, M. E. Sherman, R. M. Pfeiffer et al., "Circulating insulin-like growth factor-I, insulin-like growth factor binding protein-3 and terminal duct lobular unit involution of the breast: a cross-sectional study of women with benign breast disease," *Breast Cancer Research*, vol. 18, no. 1, p. 24, 2016.

[8] H. Oh, R. M. Pfeiffer, R. T. Falk et al., "Serum insulin-like growth factor (IGF)-I and IGF binding protein-3 in relation to terminal duct lobular unit involution of the normal breast in Caucasian and African American women: the Susan G. Komen Tissue Bank," *International Journal of Cancer*, vol. 143, no. 3, pp. 496–507, 2018.

[9] J. V. Ilekis, E. Tsilou, S. Fisher et al., "Placental origins of adverse pregnancy outcomes: potential molecular targets: an executive workshop summary of the Eunice Kennedy Shriver National Institute of Child Health and Human Development," *American Journal of Obstetrics and Gynecology*, vol. 215, no. 1, pp. S1–S46, 2016.

[10] J. M. Roberts and C. Escudero, "The placenta in preeclampsia," *Pregnancy Hypertension: An International Journal of Women's Cardiovascular Health*, vol. 2, no. 2, pp. 72–83, 2012.

[11] S. Liao, M. H. Vickers, R. S. Taylor et al., "Maternal serum IGF-1, IGFBP-1 and 3, and placental growth hormone at 20 weeks' gestation in pregnancies complicated by pre-eclampsia," *Pregnancy Hypertension*, vol. 10, pp. 149–154, 2017.

[12] S. Kharb, P. Panjeta, V. S. Ghalaut, J. Bala, and S. Nanda, "Biomarkers in preeclamptic women with normoglycemia and hyperglycemia," *Current Hypertension Reviews*, vol. 12, no. 3, pp. 228–233, 2016.

[13] E. A. Dubova, K. A. Pavlov, V. M. Lyapin, G. V. Kulikova, A. I. Shchyogolev, and G. T. Sukhikh, "Expression of insulin-like growth factors in the placenta in preeclampsia," *Bulletin of Experimental Biology and Medicine*, vol. 157, no. 1, pp. 103–107, 2014.

[14] J. M. Faupel-Badger, Y. Wang, A. C. Staff et al., "Maternal and cord steroid sex hormones, angiogenic factors, and insulin-like growth factor axis in African-American preeclamptic and uncomplicated pregnancies," *Cancer Causes & Control*, vol. 23, no. 5, pp. 779–784, 2012.

[15] A. Halhali, A. R. Tovar, N. Torres, H. Bourges, M. Garabedian, and F. Larrea, "Preeclampsia is associated with low circulating levels of insulin-like growth factor I and 1, 25-dihydroxyvitamin D in maternal and umbilical cord compartments," *Journal of Clinical Endocrinology & Metabolism*, vol. 85, no. 5, pp. 1828–1833, 2000.

[16] S. Opdahl, P. R. Romundstad, M. D. K. Alsaker, and L. J. Vatten, "Hypertensive diseases in pregnancy and breast cancer risk," *British Journal of Cancer*, vol. 107, no. 1, pp. 176–182, 2012.

[17] N. L. P. Pacheco, A.-M. N. Andersen, and M. Kamper-Jørgensen, "Preeclampsia and breast cancer: the influence of birth characteristics," *The Breast*, vol. 24, no. 5, pp. 613–617, 2015.

[18] L. J. Vatten, P. R. Romundstad, D. Trichopoulos, and R. Skjærven, "Pre-eclampsia in pregnancy and subsequent risk for breast cancer," *British Journal of Cancer*, vol. 87, no. 9, pp. 971–973, 2002.

[19] M. J. Powell, J. Von Behren, S. Neuhausen, P. Reynolds, and C. C. Benz, "Functional IGF1R variant predicts breast cancer risk in women with preeclampsia in California Teachers Study," *Cancer Causes & Control*, vol. 28, no. 10, pp. 1027–1032, 2017.

[20] L. A. Prebil, R. R. Ereman, M. J. Powell et al., "First pregnancy events and future breast density: modification by age at first pregnancy and specific VEGF and IGF1R gene variants," *Cancer Causes & Control*, vol. 25, no. 7, pp. 859–868, 2014.

[21] M. Powell, L. A. Prebil, S. Rose, F. Jamshidian, C. Benz, and R. Ereman, "Abstract P3-07-03: insulin-like growth factor-1 receptor variant associated with decreased breast cancer risk in women with pregnancy-induced hypertension," in *Proceedings of the Thirty-Sixth Annual CTRC-AACR San Antonio*

Breast Cancer Symposium, San Antonio, TX, USA, December 2013.

[22] The Broad Institute of MIT and Harvard, *GTExPORTAL*, The Broad Institute of MIT and Harvard, Cambridge, MA, USA, 2019, https://gtexportal.org/home/.

[23] W. Ruan and D. L. Kleinberg, "Insulin-like growth factor I is essential for terminal end bud formation and ductal morphogenesis during mammary development," *Endocrinology*, vol. 140, no. 11, pp. 5075–5081, 1999.

[24] P. F. Christopoulos, P. Msaouel, and M. Koutsilieris, "The role of the insulin-like growth factor-1 system in breast cancer," *Molecular Cancer*, vol. 14, no. 1, p. 43, 2015.

[25] The Komen Tissue Bank at the IU Simon Cancer Center, *Standard Operating Procedures*, The Komen Tissue Bank at the IU Simon Cancer Center, Indianapolis, IN, USA, 2019, https://komentissuebank.iu.edu/researchers/sop/.

[26] R Core Team, *R: A Language and Environment for Statistical Computing*, R Foundation for Statistical Computing, Vienna, Austria, 2018, https://www.R-project.org/.

[27] W. N. Venables and B. D. Ripley, *Modern Applied Statistics with S*, ISBN 0-387-95457-0, Springer, New York, NY, USA, 4th edition, 2018.

[28] S. Jackman, *PSCL: Classes and Methods for R Developed in the Political Science Computational Laboratory*, United States Studies Centre, University of Sydney, Sydney, Australia, 2017, https://github.com/atahk/pscl/.

[29] A. Zeileis, C. Kleiber, and S. Jackman, "Regression models for count data in R," *Journal of Statistical Software*, vol. 27, no. 8, 2008.

[30] W. Hadley, *Ggplot2: Elegant Graphics for Data Analysis*, Springer-Verlag, New York, NY, USA, 2016.

[31] F. A. English, L. C. Kenny, and F. P. McCarthy, "Risk factors and effective management of preeclampsia," *Integrated Blood Pressure Control*, vol. 8, pp. 7–12, 2015.

[32] P. Lopez-Jaramillo, J. Barajas, S. M. Rueda-Quijano, C. Lopez-Lopez, and C. Felix, "Obesity and preeclampsia: common Pathophysiological mechanisms," *Frontiers in Physiology*, vol. 9, p. 1838, 2018.

[33] J. D. Veldhuis, J. N. Roemmich, E. J. Richmond, and C. Y. Bowers, "Somatotropic and gonadotropic axes linkages in infancy, childhood, and the puberty-adult transition," *Endocrine Reviews*, vol. 27, no. 2, pp. 101–140, 2006.

[34] C. S. Tam, F. de Zegher, S. P. Garnett, L. A. Baur, and C. T. Cowell, "Opposing influences of prenatal and postnatal growth on the timing of menarche," *The Journal of Clinical Endocrinology & Metabolism*, vol. 91, no. 11, pp. 4369–4373, 2006.

[35] K. Sorensen, L. Aksglaede, J. H. Petersen, A.-M. Andersson, and A. Juul, "Serum IGF1 and insulin levels in girls with normal and precocious puberty," *European Journal of Endocrinology*, vol. 166, no. 5, pp. 903–910, 2012.

[36] R. M. Tamimi, G. A. Colditz, Y. Wang et al., "Expression of IGF1R in normal breast tissue and subsequent risk of breast cancer," *Breast Cancer Research and Treatment*, vol. 128, no. 1, pp. 243–250, 2011.

[37] T. Winder, G. Giamas, P. M. Wilson et al., "Insulin-like growth factor receptor polymorphism defines clinical outcome in estrogen receptor-positive breast cancer patients treated with tamoxifen," *The Pharmacogenomics Journal*, vol. 14, no. 1, pp. 28–34, 2014.

[38] S. de Groot, A. Charehbili, H. W. M. van Laarhoven et al., "Insulin-like growth factor 1 receptor expression and IGF1R 3129G > T polymorphism are associated with response to neoadjuvant chemotherapy in breast cancer patients: results from the NEOZOTAC trial (BOOG 2010-01)," *Breast Cancer Research*, vol. 18, no. 1, 2016.

[39] J. D. Figueroa, R. M. Pfeiffer, D. A. Patel et al., "Terminal duct lobular unit involution of the normal breast: implications for breast cancer etiology," *JNCI: Journal of the National Cancer Institute*, vol. 106, no. 10, p. dju286, 2014.

[40] K. P. McKian, C. A. Reynolds, D. W. Visscher et al., "Novel breast tissue feature strongly associated with risk of breast cancer," *Journal of Clinical Oncology*, vol. 27, no. 35, pp. 5893–5898, 2009.

Hindawi
Journal of Oncology
Volume 2019, Article ID 1947215, 5 pages
https://doi.org/10.1155/2019/1947215

Research Article

Association of *ESR1* Mutations and Visceral Metastasis in Patients with Estrogen Receptor-Positive Advanced Breast Cancer from Brazil

Tomás Reinert,[1,2,3] **Guilherme Portela Coelho**,[4] **Jovana Mandelli**,[4] **Edinéia Zimermann**,[4] **Facundo Zaffaroni**,[5] **José Bines**,[6,7] **Carlos Henrique Barrios**,[3] **and Marcia Silveira Graudenz**[1]

[1]*PPG Ciências Médicas, Universidade Federal do Rio Grande do Sul (UFRGS), Porto Alegre, Brazil*
[2]*Centro de Pesquisa da Serra Gaúcha (CEPESG), Caxias do Sul, Brazil*
[3]*Latin American Cooperative Oncology Group (LACOG), Porto Alegre, Brazil*
[4]*Grupo Diagnose Patologia, Genética e Biologia Molecular, Caxias do Sul, Brazil*
[5]*FARO STAT Solutions, Porto Alegre, Brazil*
[6]*Instituto Nacional do Câncer (INCA), Rio de Janeiro, Brazil*
[7]*Clínica São Vicente, Rio de Janeiro, Brazil*

Correspondence should be addressed to Tomás Reinert; tomasreinert@hotmail.com

Received 15 April 2019; Accepted 2 June 2019; Published 14 August 2019

Guest Editor: Chia-Jung Li

Mutations in the *ESR1* gene (*ESR1m*) are important mechanisms of resistance to endocrine therapy in estrogen receptor-positive advanced breast cancer and have been recognized as a prognostic and predictive biomarker as well as a potential therapeutic target. However, the prevalence of *ESR1m* in real-world patients has not been adequately described. Therefore, we sought to evaluate the prevalence of *ESR1m* in metastatic samples from Brazilian patients with estrogen receptor-positive (ER+) advanced breast cancer previously treated with endocrine therapy. The presence of *ESR1m* was evaluated in formalin-fixed paraffin-embedded (FFPE) breast cancer tissue using real-time quantitative polymerase chain reaction (RT-qPCR). Mutations in codons 380, 537, and 538 of the *ESR1* gene were analyzed. Out of 77 breast cancer samples, 11 (14.3%) showed mutations in the *ESR1* gene. *ESR1m* were detected in a variety of organs, and the D538G substitution was the most common mutation. In visceral metastasis, *ESR1m* were detected in 25% (8/32) of the samples, whereas in nonvisceral metastasis, *ESR1m* were detected in 6.7% (3/45) of the samples. The odds of a sample with visceral metastasis having an *ESR1* mutation is 4.66 times the odds of a sample of nonvisceral metastasis having an *ESR1* mutation (95% CI: 1.13–19.27; p value = 0.0333). Our study indicates that the prevalence of *ESR1m* in samples from Brazilian patients with metastatic ER+ breast cancer is similar to that described in patients included in clinical trials. We observed an association of *ESR1m* with visceral metastasis.

1. Introduction

Estrogen receptor-positive breast cancer is the most common breast cancer subtype. Endocrine therapy (ET), a targeted treatment to the estrogen receptor (ER) pathway, is the fundamental initial therapeutic approach in all stages of the disease [1]. Nonetheless, clinical resistance associated with progression of disease remains a significant therapeutic challenge [2, 3]. Mutations of the *ESR1* gene, which encodes the ER protein, have been increasingly identified as a mechanism of endocrine resistance [4].

The potential clinical implications of *ESR1* mutations (*ESR1m*) remained underappreciated for more than a decade after its discovery since initial studies focused on primary tumors, where the prevalence of *ESR1m* is very low [5]. Subsequently, it was demonstrated that breast tumors undergo genomic evolution and *ESR1m* have been described in 9–40% of patients with advanced ER+ breast

cancer resistance to aromatase inhibitors [3, 4, 6–8]. *ESR1* mutation is a biomarker of worse prognosis and is being evaluated as a predictive biomarker as well as a potential therapeutic target [9].

Despite recent advances in the field, several questions remain unanswered about *ESR1m* such as the prediction of which tumor will develop this mechanism of resistance. At the same time, the majority of data are derived from patients included in clinical trials, more frequently in developed countries, and little is known about mechanisms of ET resistant in real-world patients, especially in the population from low- to middle-income countries. We aimed here to evaluate the prevalence of *ESR1m* in metastatic tumor tissues from breast cancer patients from Brazil.

2. Methods

From the archive of the Pathology Department at a single academic center, we collected formalin-fixed paraffin-embedded (FFPE) tissue specimens from consecutive patients enrolled between 2014 and 2017 with recurrent or metastatic breast cancer previously treated with endocrine therapy. Only tumors of ER-positive HER2-negative metachronous metastasis were selected. All hematoxylin and eosin (H&E) and immuno-histochemistry (IHQ) slides from tumor samples were reexamined by a pathologist who confirmed the diagnosis of metastatic carcinoma and quality (amount of reminiscent neoplastic tissue on paraffin-embedded archived tissue) of each specimen. Additionally, all the lesions were diagnosed as breast metastases by IHQ using one or more of the following markers: GATA3, GCDFP-15, and/or mammaglobin.

In each sample, the tumor area was marked by the pathologist and a cut of approximately 35 mg was performed, followed by the extraction of the genetic material (DNA) with the Wizard© Genomic DNA purification kit (Promega). DNA was quantified using Qubit fluorometric quantitation (Thermo Fischer Scientific), and 20 ng/μl was the threshold for the analysis of the mutation. The reactions were performed with the equipment 7500 fast real-time PCR system using TaqMan Genotyping master mix, primers, and TaqMan© probes, from Applied Biosystems (Foster City, CA) following all recommendations of the manufacturer. The analyzed mutations were Y537N, Y537C, Y537S, E380Q, and D538G. To detect the presence of the mutation, a Taqman© reference probe was used, followed by the analysis in the 7500 Software v2.06 (Thermo Fischer Scientific).

A sample size of 81 patients was calculated with an estimated prevalence of 30%, a desired precision of estimate of 0.1 and a confidence level of 0.95. The primary endpoint was the prevalence of *ESR1m*. The secondary endpoint was the association of *ESR1m* and site of metastasis (visceral versus nonvisceral). Data were analyzed using descriptive statistics. Logistic regression was applied in order to estimate the OR (odds ratio) and 95% confidence interval (95% CI). A p value less or equal to 0.05 was deemed to be significant. This project was reviewed and approved at the IRB institutional review board (Ethical Committee).

3. Results

Seventy-seven samples were included in the analysis. Of the initial 81 selected samples, 4 were removed from the analysis due to an insufficient amount of extracted DNA (all from bone metastasis). The prevalence of ESR mutation was 14.3% (11 samples). *ESR1m* were detected in metastatic tissues from different organs such as pleura ($n = 3$), liver ($n = 2$), lung ($n = 2$), ovary, lymph node, bone, and chest wall. The most frequently detected mutation was the D538G substitution ($n = 5$), followed by mutations in codon 537 (3 Y537N substitutions, 2 Y537C, and 1 Y537S). No mutations in codon 380 were detected. For more information on the molecular biology analysis, see Supplementary Material (available here).

The probability of having an *ESR1* mutation was modeled considering the information regarding local of metastasis (Table 1). In visceral metastasis, *ESR1m* were detected in 25% (8/32) of the samples, whereas in nonvisceral metastasis, an *ESR1m* were detected in 6.7% (3/45) of the samples. Despite the low number of cases with mutation (reflected in the wide CI), the logistic regression showed that the odds of a sample with visceral metastasis having an *ESR1* mutation is 4.66 times the odds of a sample of nonvisceral metastasis having an *ESR1* mutation (95% CI: 1.13–19.27; p value = 0.0333).

4. Discussion

Estrogen receptor-positive (ER+) tumors are the most frequent form of breast cancer and responsible for most of the deaths caused by this disease [10]. ET is the mainstay of ER+ breast cancer therapy in all stages of the disease. In the metastatic disease setting, the use of ET agents is associated with clinical benefit in the majority of patients. Nonetheless, disease progression associated with a complexity of mechanisms of resistance remains a significant challenge [10].

ER, a protein encoded by the *ESR1* gene, is expressed in the majority of breast cancers. ER expression is one of the defining features in classifying tumor subtype and assigning therapeutic strategies in breast cancer. Translational and clinical research has established the fundamental role of ER and its hormonal ligands in normal mammary gland development and in the etiology and progression of breast cancer [11].

Estrogen hormones have genome-wide transcriptional activities that regulate the expression of a network of molecular pathways that are important in various physiological and pathological processes [12]. Functionally, the ER consists of two transcriptional activation domains: the *N*-terminal, ligand-independent activation function domain (AF-1), and the *C*-terminal, ligand-dependent AF-2 domain. The ligand-binding domain (LBD) resides in the *C*-terminal region, while the DNA-binding and hinge domains are positioned in the central core of the protein [2]. Estrogen binding triggers a number of events resulting in activation of ER and induces conformational changes in the LBD, allowing the estrogen-ER complex to bind to specific DNA sequences while interacting with corepressor and coactivator

Table 1: Association of *ESR1m* with the site of metastasis (*n* (%)).

	Visceral Metastasis	Nonvisceral metastasis	Total
ESR1 mutation	8 (25.0%)	3 (6.7%)	11 (14.3%)
ESR1 without mutation	24 (75.0%)	42 (93.3%)	66 (85.7%)
Total	32 (41.6%)	45 (58.4%)	77 (100.0%)

proteins to regulate the transcription of estrogen-responsive genes. Breast tumors undergo genomic evolution during therapy, with the development of new alterations that confer resistance to therapy. *ESR1* is known to undergo LBD mutations, gene amplification, or translocations that are potential mechanisms of resistance to ET [13–15].

Physiologically, estrogens promote a balanced activation of liganded and unliganded transcriptional functions of the ER. When ligand-dependent ER signaling is suppressed by either estrogen deficiency or dysfunction of the receptor, there is a strong upregulation of unliganded ER activation and subsequent resistance to endocrine therapies [16]. The absence of estrogen results in a compensatory increase in the activity of the AF-1 domain accompanied by a significant increase in the expression levels of both coding and non-coding RNA transcripts [17].

Despite the relatively high frequency of elevated *ESR1* copy numbers in breast tumors [18], the clinical relevance of *ESR1* gene amplification as a prognostic or predictive biomarker is not clear and requires further study [15]. However, mutations in the *ESR1* gene have been consistently recognized as an important mechanism of resistance to aromatase inhibitors (AIs), with a prevalence that ranges from 9 to 40%, usually described from liquid biopsies collected from patients mostly included in randomized clinical trials in developed countries [9, 19, 20].

ESR1m are most commonly missense mutations clustered in codons 537 and 538 of the LBD. Remarkably, the majority of *ESR1m* localize to just a few amino acids within or near the critical helix 12 region of the ER LBD, where they are likely to be single-allele mutations, as pictured in Figure 1 [3]. The most prevalent *ESR1* point mutations are Y537S and D538G, while several others have been identified at significantly lower frequencies. *ESR1m* have been consistently associated with inferior outcomes and is being evaluated as predictive biomarkers to help guide therapeutic decisions [21]. At the same time, the development of specific targeted therapies directed to *ESR1*-mutant clones is an appealing concept with interesting preclinical data already published and promising clinical work in progress [22, 23].

Our study reports that the prevalence of *ESR1m* in real-world patients with breast cancer in Brazil is similar to that described in the literature. This finding has implications related to the development of a line of research of mechanisms of ET resistance in the neoadjuvant setting as well as to the design and conduct the clinical trials evaluating new generation selective ER degraders (SERDs) in an *ESR1m*-enriched cohort of patients. Despite the low number of cases with mutation, our data show a significant association of visceral site of metastasis and *ESR1m*. Early studies reported *ESR1m* in tumor samples obtained from different sites,

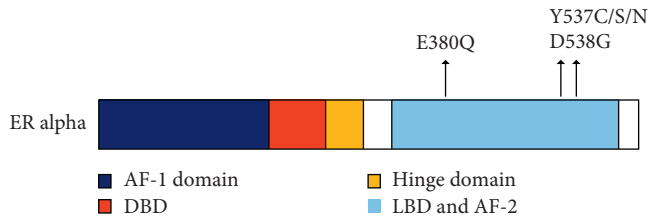

Figure 1: *ESR1* gene and most common mutations (reprinted with permission from Ma et al. [3]). A schematic diagram of *ESR1m* and their frequencies in ER+ advanced breast cancer after endocrine therapy. The structural domains of ER*α* are shown, including the transcription activation function 1 (AF-1) domain, the DNA-binding domain (DBD), the receptor dimerization and nuclear localization (hinge) domain, and the ligand-binding domain (LBD) and AF-2 domain.

including visceral and nonvisceral metastasis, suggesting that these mutations do not display specific organotropism [24, 25]. Contrastingly, multivariable analyses based on liquid biopsies of patients from the PALOMA3 and SOFEA trials reported that the detection of *ESR1m* is associated with bone and visceral disease, suggesting that *ESR1m* are infrequently detected in locoregional recurrences [26, 27]. In our study, *ESR1* mutation was identified in locoregional and distant metastasis in a variety of visceral (lung, liver, pleura, and ovary) and nonvisceral sites (bone, chest wall, and lymph nodes) indicating that these mutations do not have organotropism and suggesting that this mechanism of ET resistance could be associated with more aggressive disease phenotypes that usually present with hepatic and pleuropulmonary metastasis.

The generation of real-world data is an issue with practical implications for global breast cancer research, and it remains a challenge, especially in low- to middle-income countries (LMIC). Translating clinical research achievements into global clinical practice is the clear objective. Clinical trials are designed and conducted in a controlled fashion with specific inclusion and exclusion criteria. Nonetheless, the confirmation of patients' characteristics and outcomes in a more general population remains an integral part of the process. Observational studies have demonstrated significant clinical and epidemiological differences among breast cancer patients compared to patients from developed countries, with a higher proportion of patients with locally-advanced tumors and young patients, especially among the population treated in the public health system [28].

Nevertheless, the potential differences in the molecular epidemiology of breast tumors in real-world patients from LMIC have not been adequately studied. The prevalence of

biomarkers in breast cancer may vary in different regions of the world. A retrospective observational study with more than five thousand breast cancer patients demonstrated that the distribution of molecular subtypes of breast tumors differed according to geographic regions within Brazil and suggested that a variety of characteristics including socioeconomic and nutritional status as well as the proportion of African ancestry have to be considered to explain this heterogeneity [29]. It is important to understand the molecular characteristics of breast cancer in the Brazilian population in order to develop adequate public health programs and policies as well as to the development of therapeutic strategies and clinical trials. As an example, recently presented real-world data indicate a lower prevalence of PDL-1 expression in non-small-cell lung cancer patients in Brazil. The authors suggested that possible explanations for this discrepancy are inadequate sample handling, preanalytical issues, or epidemiology of the biomarker, all of which may have impacted the results of biomarkers outside clinical trials [30]. The unquestionable impact of breast cancer and the ongoing culture of globalization should be seen as opportunities to tackle critical global cancer research priorities, such as the development of research in LMIC, the encouragement of independent academic research, the improvement of access to clinical trials, and the development of international collaborations.

Our study has several limitations including its retrospective nature, relatively low sample size and the low number of *ERS1m* identified. Additionally, DNA extraction was unsuccessful in four samples of bone metastases, even though successful DNA extraction was achieved in the majority of bone samples (10 out of 14). We recognize that the detected prevalence of *ESR1m* can be underestimated given the fact that a PCR-based methodology was used and only specific mutations in the most commonly mutated codons were analyzed; therefore, cases with mutations in different codons of the *ESR1* gene potentially detectable with next-generation sequencing technologies were not identified [31, 32]. Another potentially important fact that might decrease the prevalence is that many patients in this cohort were treated with AIs in the adjuvant setting, whereas recent data suggest that *ESR1m* are probably more commonly associated with resistance to the AIs used in the metastatic disease setting [8].

This study is one of the first steps in a project of developing a comprehensive line of translational research in breast cancer through a collaboration of independent academic centers in Brazil. The publication of data of molecular biomarkers in real-world patients that are consistent with data from researches with patients treated in clinical trials is essential to allow validation of our methodology and to provide information for the development of translational and clinical research projects.

5. Conclusion

The prevalence of *ESR1m* in samples from Brazilian patients with metastatic ER+ breast cancer is similar to that described in patients included in clinical trials. A significant association between *ESR1m* and visceral site of metastasis was detected. *ESR1m* have potential clinical applications in breast cancer as a biomarker and a therapeutic target.

Data Availability

The results reported in the article are publicly available and are included in an online file in Supplemental Materials.

Conflicts of Interest

Tomas Reinert and Carlos Barrios received research funding from AstraZeneca. Tomas Reinert received speaker honoraria from AstraZeneca, Novartis, Pfizer, and Pierre Fabre. Carlos Barrios received speaker honoraria and plays an advisory role at Novartis, Roche, Pfizer, GSK, Boehringer Ingelhein, Eisai, AstraZeneca, BMS, MSD, and Libbs. All other authors declare no conflicts of interest.

Acknowledgments

This work was supported by AstraZeneca, Brazil, through an investigator-initiated grant (ESR 17-12682).

Supplementary Materials

Molecular biology analysis results. Each line represents a tumor sample, and the columns summarize information such as metastatic site, DNA quantification, the presence or absence of *ESR1m*, the mutant codon, and PCR cycle quantification value for each sample. (*Supplementary Materials*)

References

[1] F. Cardoso, E. Senkus, A. Costa et al., "4th ESO-ESMO international consensus guidelines for advanced breast cancer (ABC 4)," *Annals of Oncology*, vol. 29, no. 8, pp. 1634–1657, 2018.

[2] C. K. Osborne and R. Schiff, "Mechanisms of endocrine resistance in breast cancer," *Annual Review of Medicine*, vol. 62, no. 1, pp. 233–247, 2011.

[3] C. X. Ma, T. Reinert, I. Chmielewska, and M. J. Ellis, "Mechanisms of aromatase inhibitor resistance," *Nature Reviews Cancer*, vol. 15, no. 5, pp. 261–275, 2015.

[4] R. Jeselsohn, R. Yelensky, G. Buchwalter et al., "Emergence of constitutively active estrogen receptor- mutations in pretreated advanced estrogen receptor-positive breast cancer," *Clinical Cancer Research*, vol. 20, no. 7, pp. 1757–1767, 2014.

[5] C. M. Perou, T. Sørlie, M. B. Eisen et al., "Molecular portraits of human breast tumours," *Nature*, vol. 406, no. 6797, pp. 747–752, 2000.

[6] S. Kumar, D. Lindsay, Q. B. Chen et al., "Tracking plasma DNA mutation dynamics in estrogen receptor positive metastatic breast cancer with dPCR-SEQ," *NPJ Breast Cancer*, vol. 4, no. 1, p. 39, 2018.

[7] D. Chu, C. Paoletti, C. Gersch et al., "*ESR1* mutations in circulating plasma tumor DNA from metastatic breast cancer patients," *Clinical Cancer Research*, vol. 22, no. 4, pp. 993–999, 2016.

[8] G. Schiavon, S. Hrebien, I. Garcia-Murillas et al., "Analysis of *ESR1* mutation in circulating tumor DNA demonstrates

evolution during therapy for metastatic breast cancer," *Science Translational Medicine*, vol. 7, no. 313, Article ID 313ra182, 2015.

[9] R. Jeselsohn, G. Buchwalter, C. De Angelis, M. Brown, and R. Schiff, "*ESR1* mutations-a mechanism for acquired endocrine resistance in breast cancer," *Nature Reviews Clinical Oncology*, vol. 12, no. 10, pp. 573–583, 2015.

[10] K. Tryfonidis, D. Zardavas, B. S. Katzenellenbogen, and M. Piccart, "Endocrine treatment in breast cancer: cure, resistance and beyond," *Cancer Treatment Reviews*, vol. 50, pp. 68–81, 2016.

[11] T. Reinert, R. Goncalves, and J. Bines, "Implications of *ESR1* mutations in hormone receptor-positive breast cancer," *Current Treatment Options in Oncology*, vol. 19, no. 5, p. 24, 2018.

[12] A. Maggi, "Liganded and unliganded activation of estrogen receptor and hormone replacement therapies," *Biochimica et Biophysica Acta (BBA)—Molecular Basis of Disease*, vol. 1812, no. 8, pp. 1054–1060, 2011.

[13] S. Li, D. Shen, J. Shao et al., "Endocrine-therapy-resistant *ESR1* variants revealed by genomic characterization of breast-cancer-derived xenografts," *Cell Reports*, vol. 4, no. 6, pp. 1116–1130, 2013.

[14] S. W. Fanning, C. G. Mayne, V. Dharmarajan et al., "Estrogen receptor alpha somatic mutations Y537S and D538G confer breast cancer endocrine resistance by stabilizing the activating function-2 binding conformation," *elife*, vol 5, Article ID e12792, 2016.

[15] F. Holst, "Estrogen receptor alpha gene amplification in breast cancer: 25 years of debate," *World Journal of Clinical Oncology*, vol. 7, no. 2, pp. 160–173, 2016.

[16] Z. Suba, "Amplified crosstalk between estrogen binding and GFR signaling mediated pathways of ER activation drives responses in tumors treated with endocrine disruptors," *Recent Patents on Anti-Cancer Drug Discovery*, vol. 13, no. 4, pp. 428–444, 2018.

[17] L. Caizzi, G. Ferrero, S. Cutrupi et al., "Genome-wide activity of unliganded estrogen receptor-α in breast cancer cells," *Proceedings of the National Academy of Sciences*, vol. 111, no. 13, pp. 4892–4897, 2014.

[18] F. Holst, P. R. Stahl, C. Ruiz et al., "Estrogen receptor alpha (*ESR1*) gene amplification is frequent in breast cancer," *Nature Genetics*, vol. 39, no. 5, pp. 655–660, 2007.

[19] C. Fribbens, I. G. Murillas, M. Beaney et al., "Tracking evolution of aromatase inhibitor resistance with circulating tumour DNA analysis in metastatic breast cancer," *Annals of Oncology*, vol. 29, no. 1, pp. 145–153, 2018.

[20] W. Toy, Y. Shen, H. Won et al., "*ESR1* ligand-binding domain mutations in hormone-resistant breast cancer," *Nature Genetics*, vol. 45, no. 12, pp. 1439–1445, 2013.

[21] R. Jeselsohn, C. De Angelis, M. Brown, and R. Schiff, "The evolving role of the estrogen receptor mutations in endocrine therapy-resistant breast cancer," *Current Oncology Reports*, vol. 19, no. 5, p. 35, 2017.

[22] H. M. Weir, R. H. Bradbury, M. Lawson et al., "AZD9496: an oral estrogen receptor inhibitor that blocks the growth of ER-positive and *ESR1*-mutant breast tumors in preclinical models," *Cancer Research*, vol. 76, no. 11, pp. 3307–3318, 2016.

[23] S. W. Fanning, R. Jeselsohn, V. Dharmarajan et al., "The SERM/SERD bazedoxifene disrupts *ESR1* helix 12 to overcome acquired hormone resistance in breast cancer cells," *eLife*, vol. 7, 2018.

[24] Y. Kuang, B. Siddiqui, J. Hu et al., "Unraveling the clinicopathological features driving the emergence of *ESR1* mutations in metastatic breast cancer," *NPJ Breast Cancer*, vol. 4, no. 1, p. 22, 2018.

[25] D. R. Robinson, Y.-M. Wu, P. Vats et al., "Activating *ESR1* mutations in hormone-resistant metastatic breast cancer," *Nature Genetics*, vol. 45, no. 12, pp. 1446–1451, 2013.

[26] N. C. Turner, J. Ro, F. André et al., "Palbociclib in hormone-receptor-positive advanced breast cancer," *New England Journal of Medicine*, vol. 373, no. 3, pp. 209–219, 2015.

[27] C. Fribbens, B. O'Leary, L. Kilburn et al., "Plasma *ESR1* mutations and the treatment of estrogen receptor-positive advanced breast cancer," *Journal of Clinical Oncology*, vol. 34, no. 25, pp. 2961–2968, 2016.

[28] S. D. Simon, J. Bines, G. Werutsky et al., "Characteristics and prognosis of stage I–III breast cancer subtypes in Brazil: the AMAZONA retrospective cohort study," *The Breast*, vol. 44, pp. 113–119, 2019.

[29] F. M. Carvalho, L. M. Bacchi, K. M. Pincerato, M. Van de Rijn, and C. E. Bacchi, "Geographic differences in the distribution of molecular subtypes of breast cancer in Brazil," *BMC Women's Health*, vol. 14, no. 1, p. 102, 2014.

[30] A. C. Gelatti, F. Moura, A. M. F. Gaiger et al., "Lower prevalence of PD-L1 expression in advanced non-small lung cancer in Brazil," *Journal of Clinical Oncology*, vol. 36, no. 15, Article ID e21140, 2018.

[31] J. A. Shaw, D. S. Guttery, A. Hills et al., "Mutation analysis of cell-free DNA and single circulating tumor cells in metastatic breast cancer patients with high circulating tumor cell counts," *Clinical Cancer Research*, vol. 23, no. 1, pp. 88–96, 2017.

[32] R. Jeselsohn, "Are we ready to use *ESR1* mutations in clinical practice?," *Breast Care*, vol. 12, no. 5, pp. 309–313, 2017.

Hindawi
Journal of Oncology
Volume 2019, Article ID 8393769, 11 pages
https://doi.org/10.1155/2019/8393769

Research Article

Identification of Cell-Free Circulating MicroRNAs for the Detection of Early Breast Cancer and Molecular Subtyping

Karen C. B. Souza,[1] Adriane F. Evangelista,[1] Letícia F. Leal,[1] Cristiano P. Souza,[2] René A. Vieira,[3] Rhafaela L. Causin,[1] A. C. Neuber,[4] Daniele P. Pessoa,[1] Geraldo A. S. Passos,[5] Rui M. V. Reis,[1,6,7] and Marcia M. C. Marques[1,4,8]

[1]*Molecular Oncology Research Center, Barretos Cancer Hospital, Barretos, Brazil*
[2]*Department of Clinical Oncology, Barretos Cancer Hospital, Barretos, São Paulo, Brazil*
[3]*Department of Mastology and Breast Reconstruction, Barretos Cancer Hospital, Barretos, Brazil*
[4]*Tumor Biobank, Barretos Cancer Hospital, Barretos, São Paulo, Brazil*
[5]*Department of Basic and Oral Biology, School of Dentistry of Ribeirão Preto, University of São Paulo, Brazil*
[6]*Life and Health Sciences Research Institute (ICVS), Health Sciences School, University of Minho, Braga, Portugal*
[7]*ICVS/3B's-PT Government Associate Laboratory, Braga/Guimarães, Portugal*
[8]*Barretos School of Health Sciences, FACISB, Barretos, São Paulo, Brazil*

Correspondence should be addressed to Marcia M. C. Marques; mmcmsilveira@gmail.com

Received 14 February 2019; Revised 15 April 2019; Accepted 19 June 2019; Published 8 August 2019

Guest Editor: Chia-Jung Li

Early detection is crucial for achieving a reduction in breast cancer mortality. Analysis of circulating cell-free microRNAs present in the serum of cancer patients has emerged as a promising new noninvasive biomarker for early detection of tumors and for predicting their molecular classifications. The rationale for this study was to identify subtype-specific molecular profiles of cell-free microRNAs for early detection of breast cancer in serum. Fifty-four early-stage breast cancers with 27 age-matched controls were selected for circulating microRNAs evaluation in the serum. The 54 cases were molecularly classified (luminal A, luminal B, luminal B Her2 positive, Her-2, triple negative). NanoString platform was used for digital detection and quantitation of 800 tagged microRNA probes and comparing the overall differences in serum microRNA expression from breast cancer cases with controls. We identified the 42 most significant ($P \leq 0.05$, 1.5-fold) differentially expressed circulating microRNAs in each molecular subtype for further study. Of these microRNAs, 19 were significantly differentially expressed in patients presenting with luminal A, eight in the luminal B, ten in luminal B HER 2 positive, and four in the HER2 enriched subtype. AUC is high with suitable sensitivity and specificity. For the triple negative subtype miR-25-3p had the best accuracy. Predictive analysis of the mRNA targets suggests they encode proteins involved in molecular pathways such as cell adhesion, migration, and proliferation. This study identified subtype-specific molecular profiles of cell-free microRNAs suitable for early detection of breast cancer selected by comparison to the microRNA profile in serum for female controls without apparent risk of breast cancer. This molecular profile should be validated using larger cohort studies to confirm the potential of these miRNA for future use as early detection biomarkers that could avoid unnecessary biopsy in patients with a suspicion of breast cancer.

1. Introduction

Breast cancer is the most common female cancer in the world with an estimated 1.67 million new cases diagnosed worldwide in 2012 [1]. Both clinically and biologically breast cancer is a highly heterogeneous and guidelines provided by AJCC 7th Edition Staging for Breast suggest using a classification based on five molecular subtypes: luminal A, luminal B, luminal B HER2 positive, HER2-enriched, and triple negative [2]. The extent of disease at diagnosis is strongly associated with prognosis, so that efficient and non-invasive methods for early detection of initial stage disease are key for successful treatment and improving survival [3].

Mammography is currently the best method for early detection of breast cancer, but it has some limitations due to the high number false positives and the unnecessary stress that these diagnostic errors can cause [4, 5]. Biopsy represents the gold-standard procedure for definitive diagnosis, although this procedure is invasive and may also be painful. New multigene profiling panels for breast cancer are now available, such as Oncotype DX (Genomic Healthy, USA) MammaPrint (Agendia, Netherlands) and Prosigna/PAM50 (NanoString, USA); however, these assays are designed for evaluating the risk of tumor recurrence and not suited for early cancer detection [6]. In fact, there is a critical shortage of noninvasive methods based on diagnostically sensitive and specific breast cancer biomarkers suitable for both early detection and subtype classification of tumors [7].

Liquid biopsies, such as blood samples, are less invasive and easier to obtain compared to a tissue-based biopsy. For a number of human tumors, including breast cancer, biomarker analysis of circulating microRNAs (miRNA) from serum is one of the most effective noninvasive for diagnoses and evaluation of prognosis in different diseases [8]. The extensive stability of miRNAs in peripheral blood and other body fluids together with the relative ease of detection and evaluation makes circulating miRNA ideal biomarkers to be used as liquid biopsies [9]. Moreover, there is increasing evidence that malignant mammary epithelial cells can release miRNAs into peripheral blood so that the molecular profiling of these miRNAs is an opportunity to develop new liquid biopsies for early breast cancer detection and evaluation [10, 11]. Recently our group identified two circulating miRNAs as potential tumor suppressors in invasive breast cancer [12].

In breast cancer, several miRNAs have already been reported as potential biomarkers of metastasis, recurrence, prognosis, or response to therapy [13, 14]. Examples include miR-155 that is upregulated in breast cancer [15]. Another study showed that circulating levels of miR-195 were elevated in women with breast cancer (stage I-IV) in comparison to healthy women [16]. However, at the present time, few studies have found significantly altered miRNAs biomarkers that are suitable for use in early diagnosis and detection of breast cancer.

In this study, we applied multiplexed gene expression analysis using nCounter® Technology (NanoString Technologies, Seattle, WA, EUA) to identify miRNAs in liquid biopsy samples from early-stage breast cancer patients. We present analyses of 42 clinically relevant circulating, differentially expressed miRNAs in the serum of 54 Brazilian breast cancer patients. From these miRNAs, we selected a subset of new biomarkers capable of distinguishing female breast cancer patients from matched control of healthy women without risk of this type of cancer.

2. Materials and Methods

2.1. Study Design and Patients. This is case-control study with retrospective collection of biological samples and clinical data. The early-stage (CS I and II) cases (n=54) were selected from a bigger series of breast cancer patients diagnosed at Barretos Cancer Hospital (BCH), having the following features: age range 40-69 years old; no breast cancer recurrence; absence of family history/MIRIAD >10%; confirmation of tumor stage and molecular subtype; and availability of serum prior to chemotherapy or hormone therapy. Breast cancer cases included were classified by molecular subtype according to St. Gallen International Expert Consensus on the Primary Therapy of Early Breast Cancer 2011.

The selected cases were matched to 27 controls by age (± 3 years). These controls were healthy women that underwent mammography on the Prevention Department of BCH, whose Gail Risk model was less than 1.66, mammography result was BIRADS 1 or 2 and had blood collected.

All biological samples were retrieved from Barretos Cancer Hospital Tumor Biobank. This study was approved by the Ethics Committee of Barretos Cancer Hospital (Protocol n°1212/2016), in accordance with the Declaration of Helsinki.

2.2. RNA Isolation from Serum Samples. Total RNA isolation was recovered from 400uL of serum obtained from cases and controls by miRNeasy Serum/Plasma Kit, including RNase-Free DNase steps (Qiagen, Gaithersburg, MD, USA). RNA quantification was performed using the NanoDrop N-100 spectrophotometer (NannoDrop Products, Wilmington, DE).

2.3. NanoString nCounter® System Assays. The miRNA expression analysis was performed using the nCounter® Human v3 miRNA Expression panel employing the nCounter® Analysis System (NanoString Technologies, Seattle, USA). Briefly, around 100 ng total RNA was preprocessed Tags ligation followed by hybridization with the Reporter CodeSet and Capture ProbeSet (nCounter® Human v3 miRNA Expression Assay). Samples were processed using the NanoString PrepStation and immobilized into the nCounter cartridge, which was placed into the nCounter® Digital Analyzer for image capture (280 fields of view) and data acquisition. Normalization was performed using standard procedures established by Markowitz et al., using the Aromalight package (Bioconductor) in R environment.

2.4. miRNA Target Prediction. Target prediction was performed by miRDIP (microRNA Data Integration Portal: http://ophid.utoronto.ca/mirDIP/). The target genes were independently selected by five algorithms (DIANA, RNA22, TargetScan, microrna.org, and RNAHybrid), using some selection criteria of presence in at least four algorithms. We only considered the top 1% of target genes, including those that had already been identified by the Cancer Gene Index data (NCI) as being involved in breast cancer. To further determine how the selected genes were associated with breast cancer and the molecular pathways that were related to these genes, we used the plugin ReactomeFI on Cytoscape (Version 3.6.0, Seattle, WA, USA). Molecular pathways were selected considering p value lower than 0.01 and pathways that included at least three genes. The interaction network was performed by Cytoscape [13].

2.5. Statistical Analysis. Statistical analyses were performed considering the normal distribution of samples. Student's

Table 1: Clinicopathological characteristics of the cases.

Characteristics	Value (n,%)
Age, years	
Median	54.6
Range	41-69
Molecular subtype	
Luminal A	12 (22.2%)
Luminal B	12 (22.2%)
Luminal B HER2 positive	12 (22.2%)
Triple negative	12 (22.2%)
HER 2+	6 (11.1%)
Stage, n	
Stage I	21 (38.9%)
Stage II	33 (61.1%)
Tumor size (TNM)	
T1	30 (55.6%)
T2	20 (37%)
T3	4 (7.4%)
Lymph node status (TNM)	
N0	33 (61.1%)
N1	21 (38.9%)
Histological type	
Ductal	44 (81.5%)
Others	10 (18.5%)

TNM classification of malignant tumors: T describes the tumor size of primary tumor; N describes regional lymph nodes that are involved; M describes distant metastasis.

t-test was performed, using the Bioconductor multtest package. Fold-change estimation, area under (AUC) the Operating Characteristic Curve (ROC), sensitivity and specificity analysis were performed to determine the accuracy of differentially expressed miRNAs. The ROC curve analysis was performed using the ROCR package (Bioconductor) in R program. All images resulting from this analysis were generated from the ggplot2 and ComplexHeatmaps packages (Bioconductor).

3. Results

3.1. Study Population. The clinicopathological features of the 54 patients with early-stage breast cancer (cases) are summarized in Table 1. The median age of early-stage breast cancer cases was 54.6 years old (range 41-69 years). The control group (n=27) was matched with the early-stage breast cancer cases by age (± 3 years) and the median age was 54.3 years old (range 42-67 years).

3.2. Identification of Differentially Expressed miRNAs in Breast Cancer Cases. All cases were stratified according clinical stage I and II and by molecular subtypes (luminal A, luminal B, luminal B Her2 positive, Her-2, and triple negative). This stratification was employed for specifically distinguishing miRNAs biomarkers from the cases and controls for early detection of breast cancer.

Of the 800 miRNAs determined by NanoString Technology, 21 had significant differential expression ($P \leq 0.05$, 1.5-fold) in the luminal A subtype comprising 11 miRNAs that were downregulated and 10 miRNA that were upregulated in serum of breast cancer cases in comparison with serum from the matched healthy controls (Figure 1).

For luminal B subtype, 11 miRNAs had significant differential expression ($P \leq 0.05$, 1.5-fold), including 6 miRNAs that were downregulated and 5 miRNAs that were upregulated in serum of cases with breast cancer in comparison with the matched healthy controls (Figure 2).

For luminal B HER2 positive subtype, 12 miRNAs had significant differential expression ($P \leq 0.05$, 1.5-fold), including 8 miRNAs that were downregulated and 4 miRNAs that were upregulated in serum of cases with breast cancer in comparison with matched healthy controls (Figure 3).

For HER 2-enriched subtype, 4 miRNAs had significant differential expression ($P \leq 0.05$, 1.5-fold), including 3 miRNAs that were downregulated and one miRNA that was upregulated in serum of breast cancer cases compared with matched healthy controls (Figure 4).

For triple negative subtype, only miR-25-3p was upregulated ($P \leq 0.05$, 1.5-fold) in serum of the cases with breast cancer in comparison with matched healthy controls (Figure 5).

3.3. Evaluation of Circulating miRNAs as Biomarkers for Breast Cancer Subtypes. To evaluate the accuracy of the miRNAs as biomarkers for detection of breast cancer in serum, we determined the Receiver Operating Characteristic (ROC) curves, sensitivity and specificity of each miRNA. We considered an area under the ROC curve (AUC) ≥ 0.8 as a cutoff for further investigation and we identified 36 out of 42 differentially miRNAs as suitable biomarkers in the subtypes luminal A, luminal B, luminal B HER-2 positive and HER2-enriched (Table 2). For triple negative, miR-25-3p showed a slightly low AUC of 0.74.

Among these 36 miRNAs, 21 were downregulated and 16 were upregulated with miR-615-3p being upregulated in luminal B HER 2 positive cases, but also being downregulated in HER2-enriched tumors (Figures 6 and 7). The subtype specificity of the 42 circulating miRNAs (Table 2) showed that 19 miRNAs were significantly differentially expressed in patients presenting with luminal A molecular subtype, 8 miRNAs in patients presenting with luminal B subtype, 10 miRNAs in patients presenting with luminal B HER 2 positive subtype, 4 miRNAs in patients presenting with the subtype in HER2-enriched, and only one miRNA in the triple negative subtype.

3.4. Functional In Silico Analysis. In order to identify the potential target mRNAs of the differentially expressed miRNAs, we identified the top increased (miR-25-3p, Fold change 3,56) and top decreased (miR-378d, Fold change: -2,65) miRNAs in each of the five molecular subtypes of breast cancer (Figure 8).

We identified the target genes for miR-378d and miR-25-3p using the online prediction tool miRDIP. We were unable

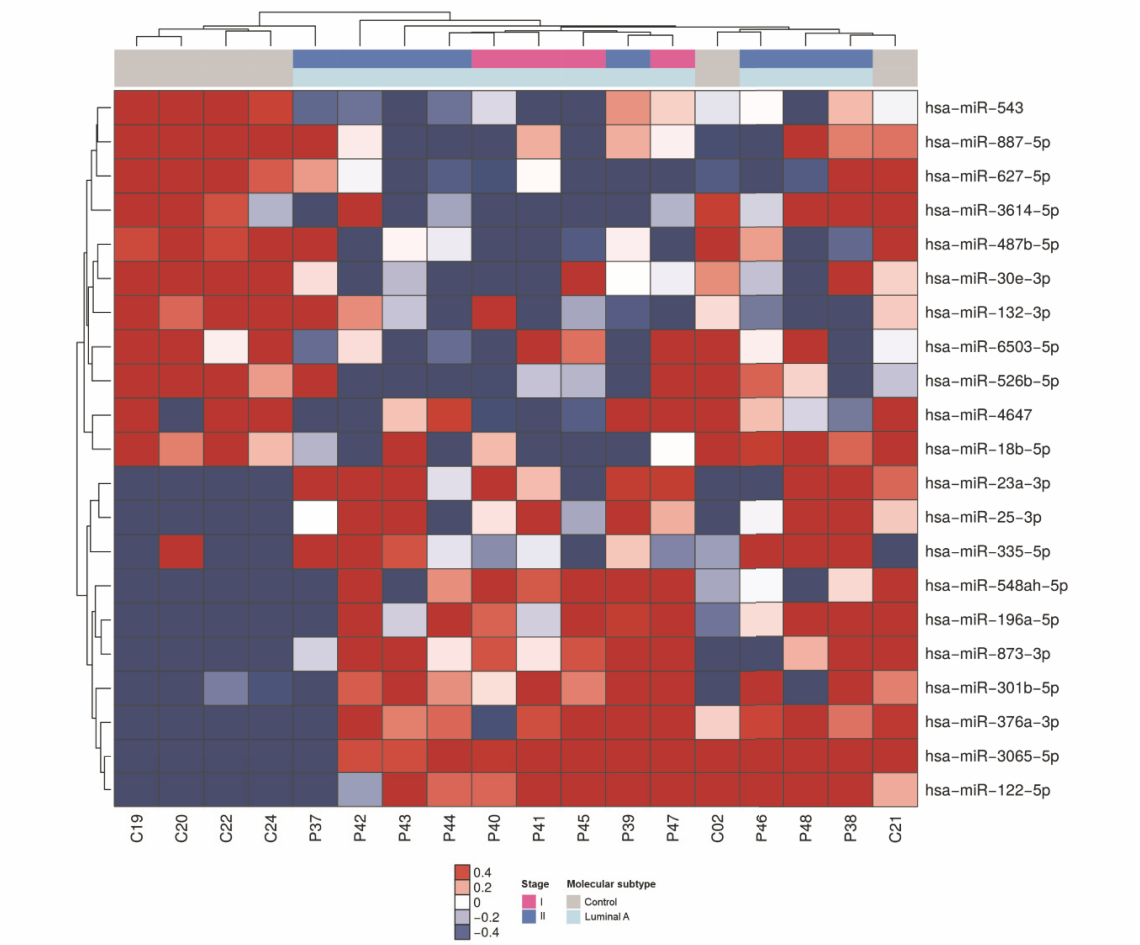

Figure 1: miRNAs differentially expressed in serum samples of patients with luminal A breast cancer. Heatmap demonstrating the differentially expressed miRNAs found in the serum of luminal A breast cancer patients compared with healthy women.

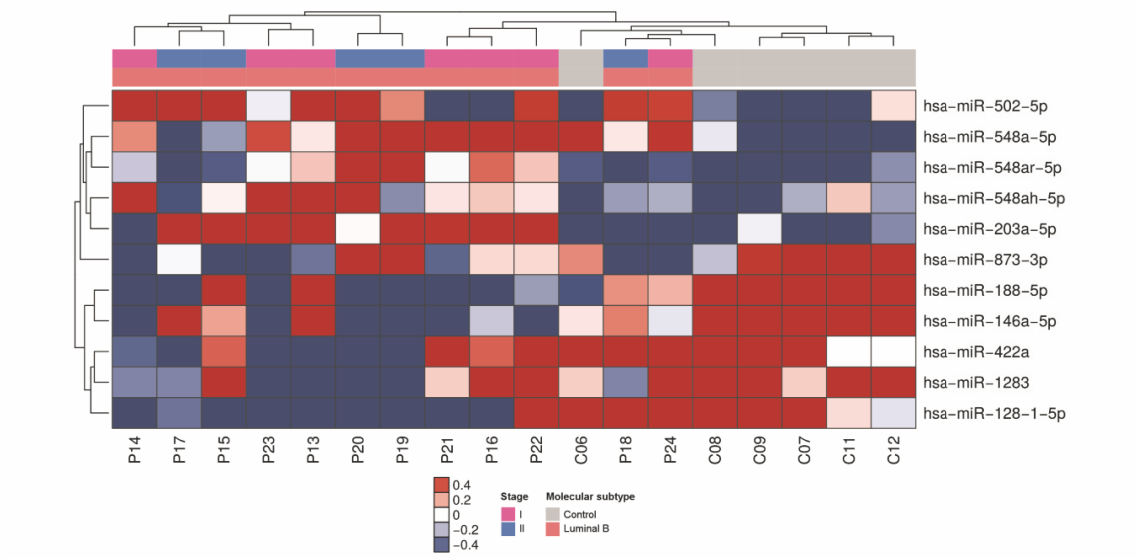

Figure 2: miRNAs differentially expressed in serum samples of patients with luminal B breast cancer. Heatmap demonstrating the differentially expressed miRNAs found in the serum of luminal B breast cancer patients compared with healthy women.

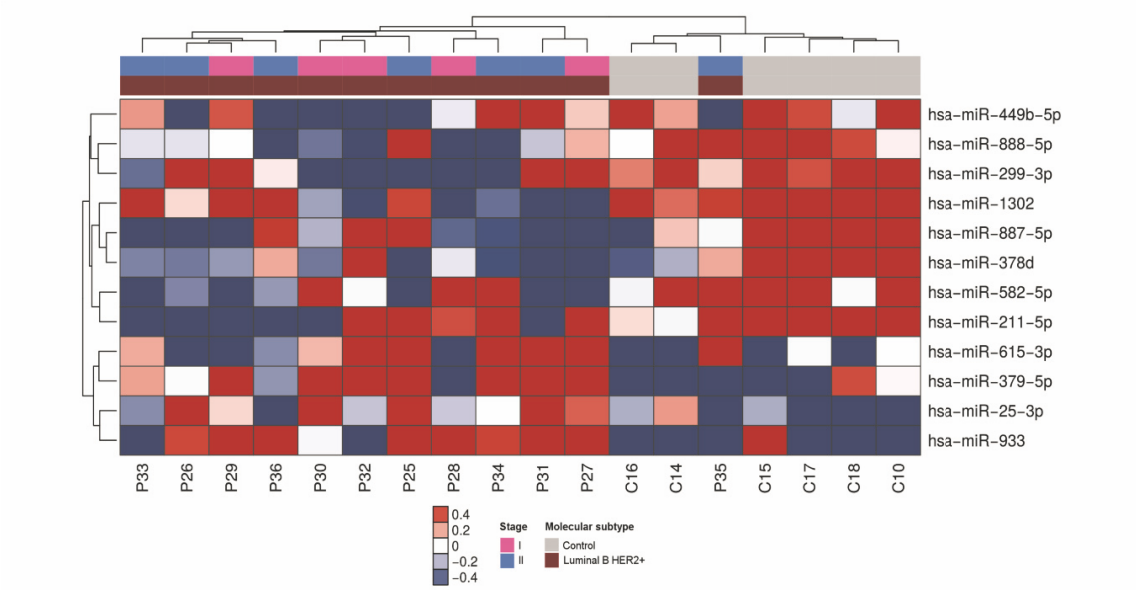

Figure 3: miRNAs differentially expressed in serum samples of patients with luminal B HER2 positive breast cancer. Heatmap demonstrating the differentially expressed miRNAs found in the serum of luminal B HER 2 positive breast cancer patients compared with healthy women.

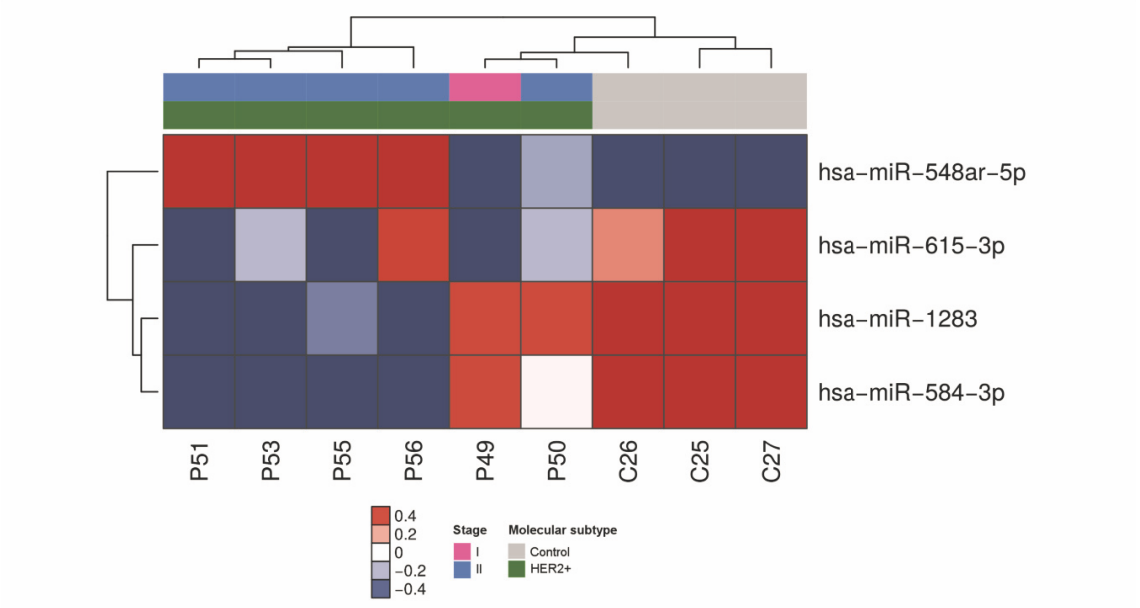

Figure 4: miRNAs differentially expressed in serum samples of patients with HER2-enriched breast cancer. Heatmap demonstrating the differentially expressed miRNAs found in the serum of HER2-enriched breast cancer patients compared with healthy women.

to identify target genes predicted for miR-378d, but there were 14 target genes predicted for miR-25-3p.

Among these miR-25-3p predicted target genes, we found four molecular pathways (Integrin signalling pathway, EPHB forward signalling, FoxO signalling pathway and Ras signalling pathway) that had statistical significance for the regulation of cell adhesion, migration, and proliferation. These molecular pathways also overlap with the target gene NRAS see Figure S1 in the Supplementary Material for comprehensive image analysis).

4. Discussion

Mammographic screening is the gold-standard tool for the detection of early breast cancer lesions, yet it has several limitations such as false positive results and it is not very well accepted by all women since it is a very uncomfortable approach [17, 18]. In addition, breast cancer is classified in different histological and molecular subtypes, which present distinctive degrees of aggressiveness [17, 18]. Currently, only tissue samples obtained from conventional biopsy procedure

Table 2: ROC curve of deregulated miRNAs by molecular subtype.

Molecular Subtype	miRNAs	Fc	Sensitivity	Specificity	Th	AUC
Luminal A	hsa-miR-18b-5p	-1.58	67%	83%	2.54	0.82
	hsa-miR-23a-3p	1.91	67%	100%	4.12	0.89
	hsa-miR-25-3p	3.56	92%	83%	3.08	0.92
	hsa-miR-487b-5p	-2.27	100%	92%	3.32	0.94
	hsa-miR-30e-3p	-2.05	100%	83%	2.85	0.92
	hsa-miR-122-5p	3.03	83%	83%	5.39	0.86
	hsa-miR-132-3p	-2.29	100%	75%	2.57	0.86
	hsa-miR-196a-5p	2.24	92%	83%	3.17	0.83
	hsa-miR-301b-5p	1.54	83%	83%	3.13	0.83
	hsa-miR-335-5p	1.69	75%	83%	2.75	0.85
	hsa-miR-376a-3p	2.20	83%	83%	3.53	0.83
	hsa-miR-526b-5p	-1.60	67%	83%	3.04	0.83
	hsa-miR-543	-1.84	67%	92%	3.64	0.89
	hsa-miR-548ah-5p	1.69	75%	83%	3.34	0.84
	hsa-miR-627-5p	-2.24	83%	92%	4.12	0.89
	hsa-miR-873-3p	2.11	100%	83%	3.13	0.90
	hsa-miR-887-5p	-1.75	83%	83%	3.21	0.87
	hsa-miR-3614-5p	-1.58	83%	75%	3.41	0.81
	hsa-miR-6503-5p	-1.76	67%	92%	3.33	0.83
Luminal B	hsa-miR-146a-5p	-1.67	83%	84%	3.20	0.83
	hsa-miR-188-5p	-1.60	83%	83%	3.79	0.83
	hsa-miR-203a-5p	1.87	75%	100%	2.64	0.80
	hsa-miR-502-5p	1.69	75%	100%	2.91	0.83
	hsa-miR-548ar-5p	1.90	67%	100%	5.05	0.81
	hsa-miR-548a-5p	1.85	83%	83%	2.71	0.85
	hsa-miR-548ah-5p	1.75	67%	83%	3.69	0.81
	hsa-miR-128-1-5p	-1.53	100%	75%	2.64	0.80
Luminal B HER2+	hsa-miR-25-3p	2.73	75%	83%	3.32	0.82
	hsa-miR-378d	-2.65	67%	92%	4.31	0.83
	hsa-miR-379-5p	1.87	67%	83%	3.13	0.85
	hsa-miR-449b-5p	-1.65	67%	83%	3.10	0.83
	hsa-miR-582-5p	-2.05	67%	75%	3.84	0.80
	hsa-miR-615-3p	1.78	67%	100%	2.96	0.83
	hsa-miR-887-5p	-1.74	67%	92%	3.71	0.82
	hsa-miR-888-5p	-1.62	83%	75%	3.38	0.86
	hsa-miR-933	1.53	83%	83%	2.47	0.89
	hsa-miR-1302	-1.54	83%	75%	3.27	0.80
HER2+	hsa-miR-548ar-5p	3.07	100%	77%	5.24	0.97
	hsa-miR-584-3p	-1.53	100%	100%	4.45	1.00
	hsa-miR-615-3p	-1.62	100%	84%	4.20	0.94
	hsa-miR-1283	-2.24	100%	100%	6.09	1.00

Accuracy of deregulated miRNAs with ROC curve ≥ 0.8. Fc: fold-change; Th: threshold; AUC: area under the curve.

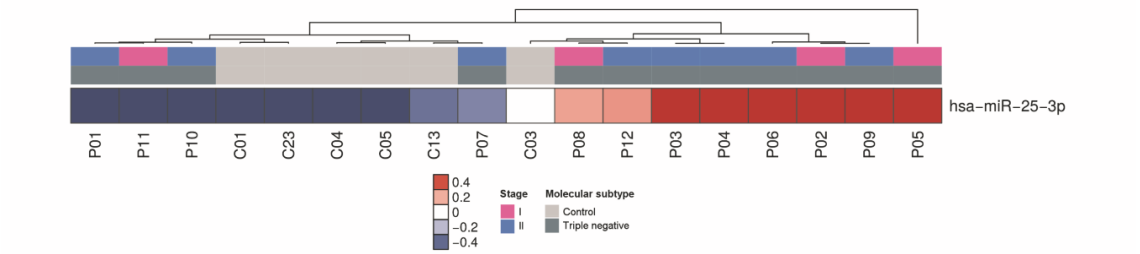

Figure 5: miRNAs differentially expressed in serum samples of patients with triple negative breast cancer. Heatmap demonstrating the differentially expressed miRNAs found in the serum of triple negative breast cancer patients compared with healthy women.

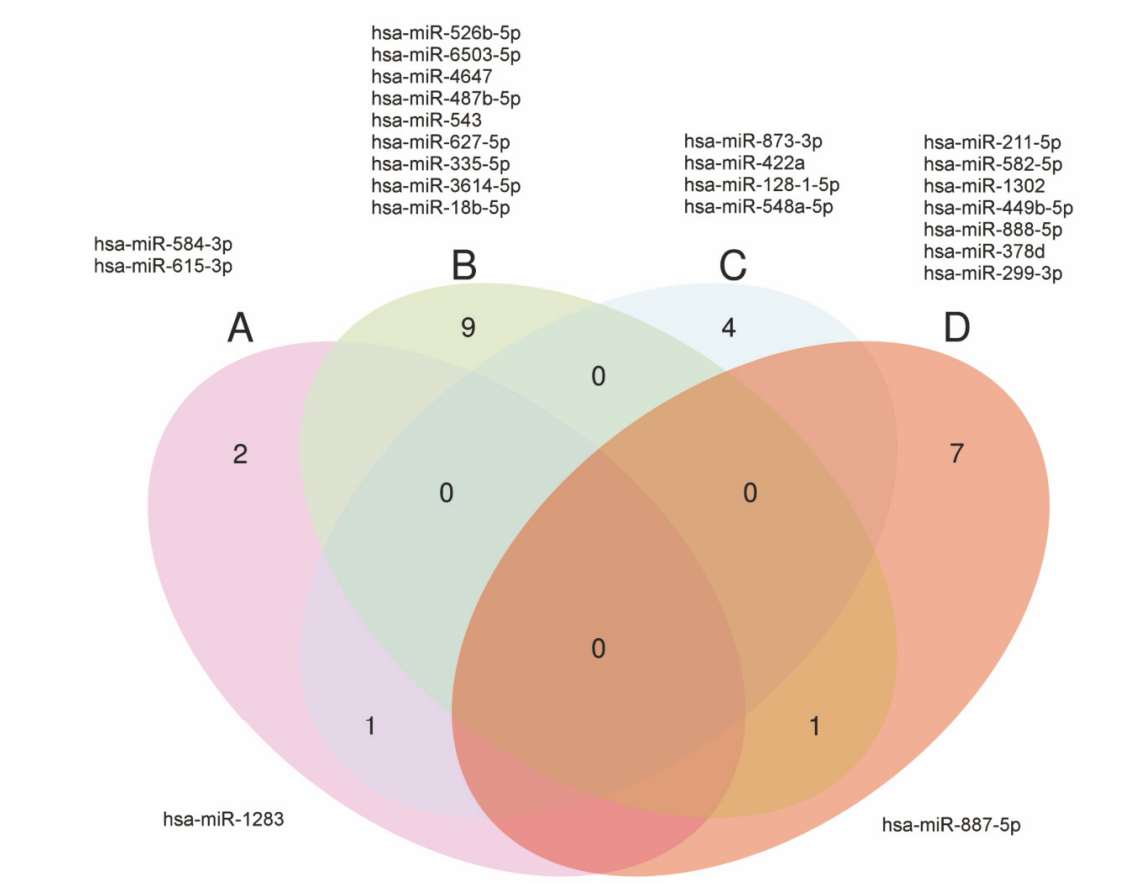

Figure 6: Venn diagram of downregulated miRNAs in serum of breast cancer patients. Venn diagram demonstrating 21 downregulated miRNAs, including miR-887-5p common between luminal A and luminal B HER2 positive. (a) HER 2; (b) luminal A; (c) luminal B; (d) luminal B HER2 positive.

can be useful for histological and molecular classification of this type of tumor. Thus, the liquid biopsy approach for breast cancer screening could improve the mammography sensitivity and could also be helpful for molecular classification [19, 20].

The miRNAs have attracted a great deal of attention as cancer biomarkers in the last few years due to the possibility of their detection from plasma or blood serum using conventional methods that could be adapted to clinical-laboratory routine [21, 22]. In addition, these circulating miRNAs have already been associated with the presence of various types of cancer [23, 24]. We therefore hypothesized that the identification of tumor-specific circulating miRNAs could be used for early detection of breast cancer as well as molecular biomarkers for identification of the different subtypes of breast cancer.

Most of minimally invasive biomarkers already described for breast cancer present low accuracy. A good example of minimally invasive biomarker for breast cancer is the CA 125, a serum biomarker that demonstrates 69% specificity and

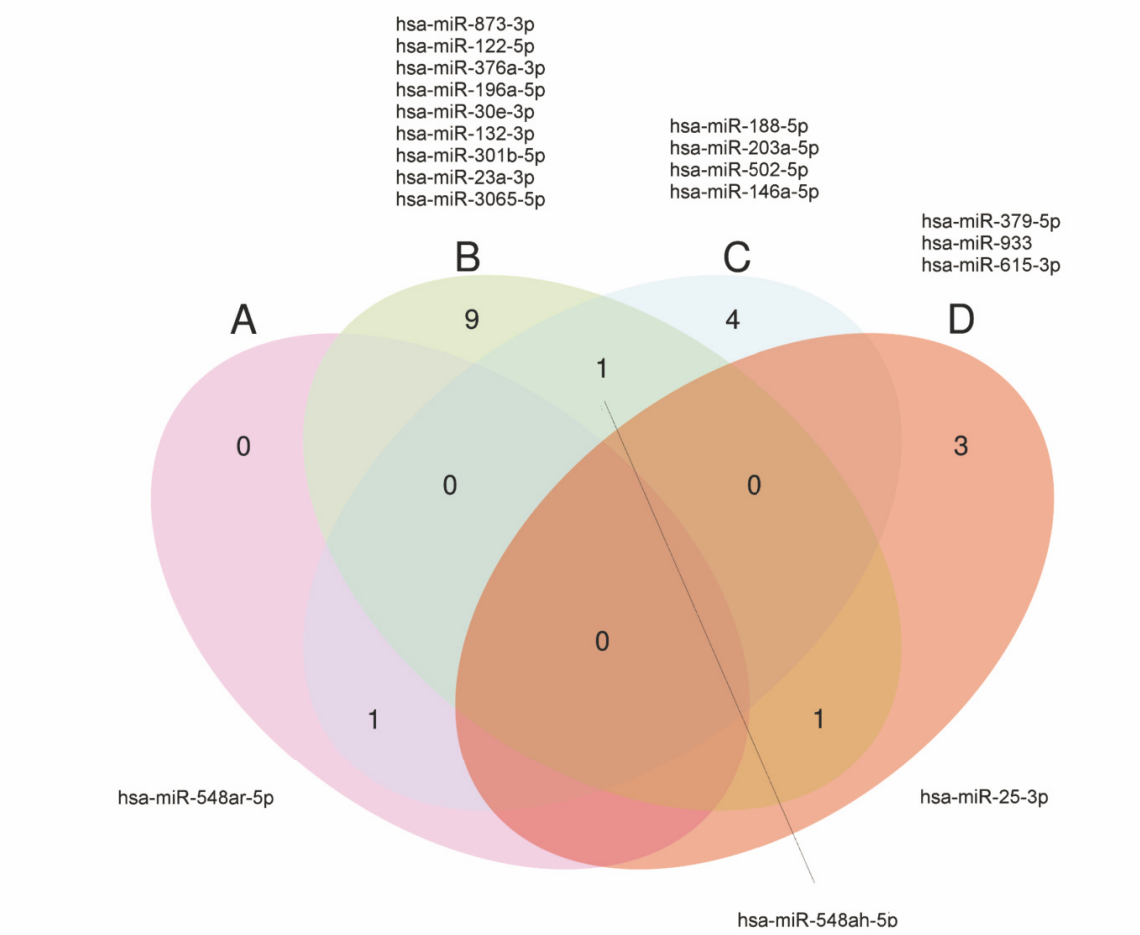

Figure 7: Venn diagram of upregulated miRNAs in serum of breast cancer patients. Venn diagram demonstrating 16 upregulated miRNAs, including miR-548ah-5p common between luminal A and luminal B, miR-548ar-5p common between HER2 and luminal B, and miR25-3p common between luminal A and luminal B HER 2 positive. (a) HER 2; (b) luminal A; (c) luminal B; (d) luminal B HER2 positive.

only 23% sensitivity [25]. Other serum biomarkers such as CEA and CA 15-3 are only reported to be effective in less than 15% of breast cancer patients [26].

An important finding of our study was that miR-25-3p could distinguish patients with triple negative breast cancer (the most aggressive subtype) from healthy controls. MiR-25-3p was also found to be upregulated in triple negative breast cancer tissue and cell lines [27]. Our prediction analyses showed that BTG2 is a putative target of miR-25-3p, so it seems possible that this miRNA may promote proliferation by targeting BTG2 in triple negative breast cancer. We found that miRNAs are important biomarkers for prognosis in triple negative breast cancer. For example, downregulated miR-221-3p is associated with poor prognostic biomarker for triple negative breast cancer [28]. However, few studies have been performed for early diagnosis using triple negative breast cancer because most cases of this aggressive molecular subtype are detected at an advanced stage.

In our study, it is possible that experimental variables due to sampling influenced the comparison between the 12 triple negative cases and the healthy controls. Also, the clinical and biological behavior of the triple negative molecular subtype is known to be more heterogeneous in comparison to the hormone receptor groups (luminal A, luminal B, luminal B HER 2 positive and HER2-enriched), which we were able to distinguish based on miRNA expression. Although the accuracy of the circulating miRNAs identified in HER2-enriched molecular subtype in our study was excellent, we believe it is necessary to validate these miRNAs using a larger cohort to increase the statistical power since only six patients were available for our analysis.

Considering that this study is retrospective, we have few serum breast cancer samples without any treatment available and small control group that Gail's Risk is determined. Thus, larger prospective studies are required to define the most robust circulating miRNA signature for improved clinical management of breast cancer using minimally invasive methods that avoid unnecessary biopsies. More extensive studies are needed to discover whether miR-25-3p could be a specific early detection biomarker for triple negative breast cancer.

5. Conclusions

Thus, in this case-control study we identified a molecular signature miRNAs as noninvasive biomarkers for each

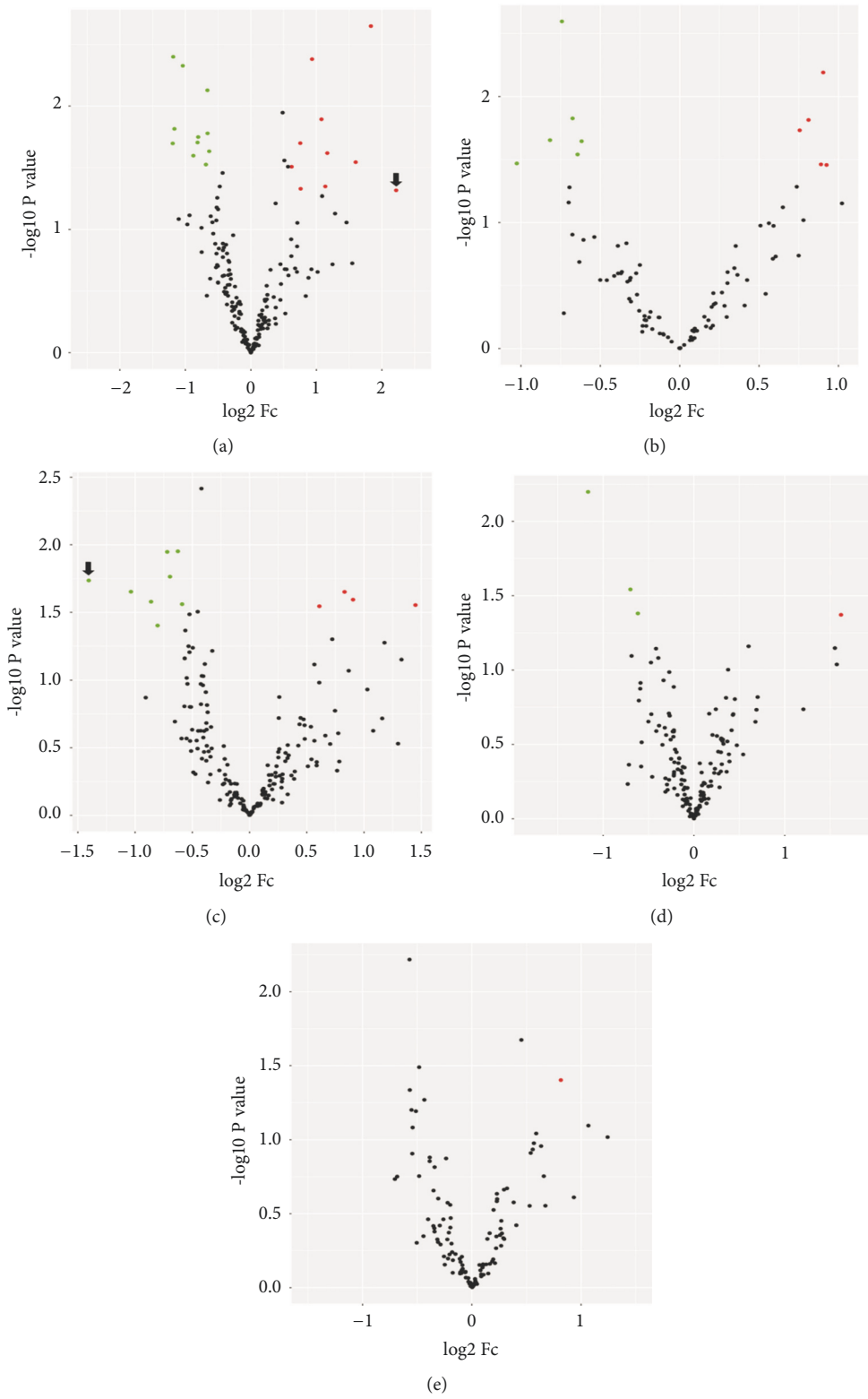

Figure 8: Differentially expressed miRNAs by molecular subtype breast cancer. Volcano plot demonstrating the profile of the differentially expressed miRNAs in different molecular subtypes of breast cancer. This plot demonstrates the fold change (x-axis) and the – log 10 P value (y-axis). The green circles represent the miRNAs downregulated and the red circles represent the miRNAs upregulated. The black circles indicate miRNAs that were not significantly expressed. Significance was determined with a P value cutoff of 0.05 and a 1.5-fold change. Molecular subtypes in breast cancer analyzed: (a) luminal A – arrow indicates the top upregulated miRNA (miR-25-3p); (b) luminal B; (c) luminal B HER 2 positive – arrow indicates the top downregulated miRNA (miR-378d); (d) HER2-enriched; (e) triple negative.

molecular subtype (luminal A, luminal B, luminal B HER2 positive and HER2-enriched breast) with increased precision. Future studies will be required to validate the clinical utility of these miRNAs using larger cohorts. Collectively our findings show that independently miRNAs can be detected in serum from patients with early breast cancer and their differential expression may be associated with specific molecular subtypes. Thus, the liquid biopsy approach using molecular biomarkers can be employed in the routine of breast cancer screening with potential to decrease the unnecessary invasive procedure.

Data Availability

The functional analyses and differentially expressed miRNAs data used to support the findings of this study are available from the corresponding author upon request.

Conflicts of Interest

The authors declare that there are no conflicts of interest regarding the publication of this paper.

Acknowledgments

We thank Barretos Cancer Hospital Biobank for the technical support in management of biological samples from patients. The authors would like to thank Dr. Jeremy Squire for carefully proofreading the English and for providing constructive criticism of the manuscript. This work was supported by grants from the Foundation for Research Support of the State of São Paulo (FAPESP process 2015/21082-0) and Public Ministry of Labor Campinas (Research, Prevention, and Education of Occupational Cancer).

Supplementary Materials

Table S1: miR-25-3p target genes predicted and molecular pathways determined by Reactome. *(Supplementary Materials)*

References

[1] "Fact Sheets by Cancer," 2018, http://globocan.iarc.fr/Pages/fact_sheets_cancer.aspx.

[2] "AJCC - American Joint Committee on Cancer," 2017, https://cancerstaging.org/Pages/default.aspx.

[3] "American Society of Clinical Oncology 2007 Update of Recommendations for the Use of Tumor Markers in Breast Cancer," *Journal of Oncology Practice*, vol. 3, no. 6, pp. 336–339, 2007.

[4] N. T. Brewer, T. Salz, and S. E. Lillie, "Systematic review: the long-term effects of false-positive mammograms," *Annals of Internal Medicine*, vol. 146, no. 7, pp. 502–510, 2007.

[5] P. C. Sharp, R. Michielutte, R. Freimanis, L. Cunningham, J. Spangler, and V. Burnette, "Reported pain following mammography screening," *JAMA Internal Medicine*, vol. 163, no. 7, pp. 833–836, 2003.

[6] M. Duffy, N. Harbeck, M. Nap et al., "Clinical use of biomarkers in breast cancer: Updated guidelines from the European Group on Tumor Markers (EGTM)," *European Journal of Cancer*, vol. 75, pp. 284–298, 2017.

[7] G. Siravegna, S. Marsoni, S. Siena, and A. Bardelli, "Integrating liquid biopsies into the management of cancer," *Nature Reviews Clinical Oncology*, vol. 14, no. 9, pp. 531–548, 2017.

[8] V. Y. Shin, J. M. Siu, I. Cheuk, E. K. Ng, and A. Kwong, "Circulating cell-free miRNAs as biomarker for triple-negative breast cancer," *British Journal of Cancer*, vol. 112, no. 11, pp. 1751–1759, 2015.

[9] J. Wittmann and H.-M. Jäck, "Serum microRNAs as powerful cancer biomarkers," *Biochimica et Biophysica Acta (BBA) - Reviews on Cancer*, vol. 1806, no. 2, pp. 200–207, 2010.

[10] C. Roth, B. Rack, V. Müller, W. Janni, K. Pantel, and H. Schwarzenbach, "Circulating microRNAs as blood-based markers for patients with primary and metastatic breast cancer," *Breast Cancer Research*, vol. 12, no. 6, Article ID R90, 2010.

[11] M. Chan, C. S. Liaw, S. M. Ji et al., "Identification of circulating microrna signatures for breast cancer detection," *Clinical Cancer Research*, vol. 19, no. 16, pp. 4477–4487, 2013.

[12] M. Marques, A. Evangelista, T. Macedo et al., "Expression of tumor suppressors miR-195 and let-7a as potential biomarkers of invasive breast cancer," *Clinics*, vol. 73, Article ID e184, 2018.

[13] D. Huo, W. M. Clayton, T. F. Yoshimatsu, J. Chen, and O. I. Olopade, "Identification of a circulating MicroRNA signature to distinguish recurrence in breast cancer patients," *Oncotarget*, vol. 7, pp. 55231–55248, 2016.

[14] I. Stückrath, B. Rack, W. Janni, B. Jäger, K. Pantel, and H. Schwarzenbach, "Aberrant plasma levels of circulating miR-16, miR-107, miR-130a and miR-146a are associated with lymph node metastasis and receptor status of breast cancer patients," *Oncotarget*, vol. 6, no. 15, pp. 13387–13401, 2015.

[15] F. Wang, Z. Zheng, J. Guo, and X. Ding, "Correlation and quantitation of microRNA aberrant expression in tissues and sera from patients with breast tumor," *Gynecologic Oncology*, vol. 119, no. 3, pp. 586–593, 2010.

[16] H. M. Heneghan, N. Miller, A. J. Lowery, K. J. Sweeney, J. Newell, and M. J. Kerin, "Circulating microRNAs as novel minimally invasive biomarkers for breast cancer," *Annals of Surgery*, vol. 251, no. 3, pp. 499–505, 2010.

[17] W. F. Anderson, P. S. Rosenberg, A. Prat, C. M. Perou, and M. E. Sherman, "How many etiological subtypes of breast cancer: two, three, four, or more?" *JNCI Journal of the National Cancer Institute*, vol. 106, no. 8, p. dju165, 2014.

[18] Z. I. Hu and H. L. McArthur, "Immunotherapy in breast cancer: the new frontier," *Current breast cancer reports*, vol. 10, no. 2, pp. 35–40, 2018.

[19] F. Zhang, Y. Deng, and R. Drabier, "Multiple biomarker panels for early detection of breast cancer in peripheral blood," *BioMed Research International*, vol. 2013, Article ID 781618, 7 pages, 2013.

[20] M. Zeeshan, B. Salam, Q. S. Khalid, S. Alam, and R. Sayani, "Diagnostic accuracy of digital mammography in the detection of breast cancer," *Cureus*, vol. 10, Article ID e2448, 2018.

[21] H. Li, J. Liu, J. Chen et al., "A serum microRNA signature predicts trastuzumab benefit in HER2-positive metastatic breast cancer patients," *Nature Communications*, vol. 9, no. 1, article no. 1614, 2018.

[22] I. Block, M. Burton, K. P. Sørensen et al., "Association of miR-548c-5p, miR-7-5p, miR-210-3p, miR-128-3p with recurrence in systemically untreated breast cancer," *Oncotarget*, vol. 9, no. 10, pp. 9030–9042, 2018.

[23] J. Hayes, P. P. Peruzzi, and S. Lawler, "MicroRNAs in cancer: biomarkers, functions and therapy," *Trends in Molecular Medicine*, vol. 20, no. 8, pp. 460–469, 2014.

[24] L. Tutar, E. Tutar, and Y. Tutar, "MicroRNAs and cancer; an overview," *Current Pharmaceutical Biotechnology*, vol. 15, no. 5, pp. 430–437, 2014.

[25] P. D. Wagner, M. Verma, and S. Srivastava, "Challenges for biomarkers in cancer detection," *Annals of the New York Academy of Sciences*, vol. 1022, no. 1, pp. 9–16, 2004.

[26] Y. Shao, X. Sun, Y. He, C. Liu, and H. Liu, "Elevated levels of serum tumor markers CEA and CA15-3 are prognostic parameters for different molecular subtypes of breast cancer," *PLoS ONE*, vol. 10, no. 7, Article ID e0133830, 2015.

[27] H. Chen, H. Pan, Y. Qian, W. Zhou, and X. Liu, "MiR-25-3p promotes the proliferation of triple negative breast cancer by targeting BTG2," *Molecular Cancer*, vol. 17, no. 1, 2018.

[28] L. Deng, Q. Lei, Y. Wang et al., "Downregulation of miR-221-3p and upregulation of its target gene PARP1 are prognostic biomarkers for triple negative breast cancer patients and associated with poor prognosis," *Oncotarget*, vol. 8, no. 65, pp. 108712–108725, 2017.

Hindawi
Journal of Oncology
Volume 2019, Article ID 6425708, 8 pages
https://doi.org/10.1155/2019/6425708

Research Article

Role of Four ABC Transporter Genes in Pharmacogenetic Susceptibility to Breast Cancer in Jordanian Patients

Laith N. AL-Eitan,[1,2] **Doaa M. Rababa'h**,[1] **Mansour A. Alghamdi**,[3] **and Rame H. Khasawneh**[4]

[1]*Department of Applied Biological Sciences, Jordan University of Science and Technology, Irbid 22110, Jordan*
[2]*Department of Biotechnology and Genetic Engineering, Jordan University of Science and Technology, Irbid 22110, Jordan*
[3]*College of Medicine, King Khalid University, Abha, Saudi Arabia*
[4]*Department of Hematopathology, King Hussein Medical Center (KHMC), Jordanian Royal Medical Services (RMS), Amman 11118, Jordan*

Correspondence should be addressed to Laith N. AL-Eitan; lneitan@just.edu.jo

Received 1 March 2019; Accepted 2 July 2019; Published 17 July 2019

Guest Editor: Chia-Jung Li

Breast cancer pharmacogenetics is increasingly being explored due to chemotherapy resistance among certain classes of patients. The ATP binding cassette (ABC) transporter genes have been previously implicated in breast cancer progression and drug response. In the present study, single nucleotide polymorphisms (SNPs) from the *ABCC1*, *ABCC2*, *ABCB1*, and *ABCG2* genes were screened in breast cancer patients and healthy volunteers from the Jordanian-Arab population. Only the *ABCB1* SNPs showed a significant association with BC in Jordanian-Arab patients, and the *ABCB1* SNP rs2032582 exhibited a strong genotypic association with BC. With regard to the clinical characteristics of BC, the *ABCC2* SNPs rs2273697 and rs717620 were found to be significantly associated with age at breast cancer diagnosis and breastfeeding status, while the *ABCB1* SNP rs1045642 was significantly associated with age at breast cancer diagnosis. In terms of pathological characteristics, the *ABCC1* SNP rs35628 and the *ABCB1* SNP rs2032582 were significantly associated with tumor size, the *ABCC2* SNP rs2273697 was significantly associated with estrogen receptor status, and the *ABCG2* SNP rs2231142 was significantly associated with axillary lymph node status. In this current study, we assume that significant genetic variants within the ABC superfamily may increase the risk of breast cancer among Jordanian women. Furthermore, these variants might be responsible for worse BC prognosis.

1. Introduction

Breast cancer (BC) is the most common female malignancy in the majority of countries [1]. Arab populations suffer from lower but steadily rising BC incidence rates compared to their American and European counterparts, and the clinical characteristics of the disease also differ between the aforementioned populations [2]. Such population-level differences in BC predisposition have been attributed to genetics and have been widely investigated, with different mutations having different levels of association with BC [3]. Compounding this issue is the fact that Arab BC genetics are not well researched, and much less is known about the genes involved in BC progression and drug response in Arab patients [4].

The ATP binding cassette (ABC) transporters comprise seven subfamilies of membrane proteins that facilitate the transport and modulate the effects of a wide range of drugs and their metabolites [5, 6]. Remarkably, an overexpression of certain ABC transporters in cancer cell lines resulted in multidrug resistance (MDR) and a potential failure of chemotherapy [7, 8]. For example, the *ABCC1* gene, also known as multidrug resistance-associated protein 1 (*MRP1*), is associated with worsened prognoses in a wide range of tumors, while the *ABCC2* gene was found to contribute to drug resistance [9, 10]. Likewise, the *ABCB1* gene is highly

Table 1: Minor allele frequencies among breast cancer patients and healthy controls and the HWEc p value of ABC gene polymorphisms.

Gene	SNP ID	SNP position [a]	Cases (n = 222)			Controls (n = 218)		
			MA[b]	MAF[c]	HWE[d] p-value	MA[b]	MAF[c]	HWE[d] p-value
ABCC1	rs35626	16076758	T	0.38	0.3	T	0.41	0.12
	rs35628	16077249	G	0.1	0.049	G	0.11	0.27
	rs4148351	16076711	T	0.16	0.037	T	0.2	N/A
ABCC2	rs2273697	99804058	A	0.25	N/A	A	0.24	0.089
	rs3740065	99845936	G	0.23	N/A	G	0.21	0.066
	rs717620	99782821	T	0.12	0.75	T	0.13	0.38
ABCB1	rs1045642	87509329	T	0.35	0.025	T	0.43	0.026
	rs1128503	87550285	A	0.36	0.039	A	0.44	0.074
	rs2032582	87531302	T	0.03	0.4591	T	0.01	0.615
ABCG2	rs2231142	88131171	T	0.04	0.552	T	0.04	0.572

[a]Chromosome positions are based on NCBI Human Genome Assembly Build. [b]MA: minor allele. [c]MAF: minor allele frequency. [d]HWE: Hardy–Weinberg equilibrium. N/A: not applicable.

polymorphic and induces chemoresistance by preventing drug accumulation in cancer cells [7]. In addition, the *ABCG2* gene, also known as the breast cancer resistance protein (*BCRP*), is responsible for the transport of many conventional chemotherapeutics and causes MDR in various cancer cells [11].

In the present study, four SNPs of ABC transporter genes, namely *ABCC1*, *ABCC2*, *ABCB1*, and *ABCG2*, were screened in Jordanian Arabs with and without breast cancer. Previous reports have indicated that these genes play a critical role in increasing tumor risk, especially in breast cancer [9, 11]. The aim of this study is to determine whether the aforementioned genes play a significant role in Jordanian breast cancer patients.

2. Materials and Methods

2.1. Ethical Approval and Conduct. The present study was given ethical approval by the Institutional Review Board (IRB) at Jordan University of Science and Technology. Written informed consent was obtained from all participants in this study before blood sample withdrawal.

2.2. Study Population and Design. The study cohort consisted of 222 women diagnosed with breast cancer as well as 218 healthy matched volunteers. All participants were recruited from the Jordanian population and were of Arab descent. 5 ml of blood were withdrawn from each participant into EDTA tubes and refrigerated until DNA extraction.

2.3. Genomic Extraction and Genotyping. Genomic DNA was extracted from a total of 440 blood samples using the Wizard® Genomic DNA Purification Kit (Promega, USA). Extracted DNA was evaluated in terms of concentration (ng/μl) and purity (A260/280) quantity using the Nano-Drop ND-1000 UV-Vis Spectrophotometer (BioDrop, UK). DNA samples were then loaded onto an agarose gel to confirm product quality. Samples that met our requirements were diluted using nuclease-free water for a final concentration of 20 ng/μl and a final volume of 30 μl. Genotyping was carried out by the Melbourne node of the Australian Genome Research Facility (AGRF) using the Sequenom MassARRAY® system (iPLEX GOLD) (Sequenom, San Diego, CA, USA).

2.4. Denomination of Genotypic-Phenotypic Correlation. In this study, several clinical and pathological features of BC were investigated in correlation with the studied variants. Clinical and pathological information for patients was collected from their medical records. P values were selected to estimate the association between SNPs and risk of BC. The analyses were done per genotype.

2.5. Statistical Analysis. Case-control analyses were carried out using different statistical software. Allelic and genotypic frequencies were calculated using the Hardy-Weinberg equilibrium (HWE) equation (Court lab - HW calculator) (http://www.oege.org/software/hwe-mr-calc.html). The Statistical Package for the Social Sciences (SPSS), version 25.0 (SPSS, Inc., Chicago, IL) was used to calculate the p values that allowed discrimination between cases and controls in association with the genotype. It also facilitated the analysis of the different genotype models. On the other hand, genotype-phenotype assessment was performed using the Chi-Square test and ANOVA tests [12]. P value denoted statistical significance if they were less than 0.05.

3. Results

3.1. ABC Transporter Variants and Their Minor Allele Frequencies (MAF). Table 1 displays the SNPs of the *ABCC1*, *ABCC2*, *ABCB1*, and *ABCG2* candidate genes. All of the polymorphic SNPs were tested for minor allele frequencies (MAF) and HWE p values in both the cases and controls (Table 1).

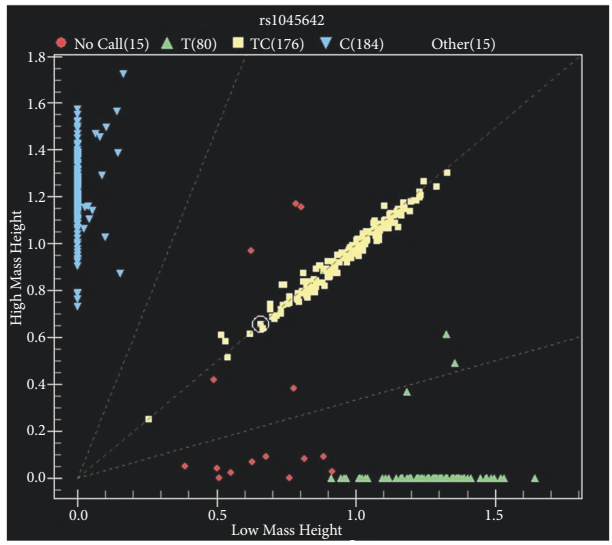

Figure 1: Scatter plot for rs1045642 within *ABCB1* gene. Each Dot represents a sample while different genotypes are indicated with different colors.

3.2. Association between ABC Transporter SNPs and Breast Cancer (BC). The allelic and genotypic frequencies of the ABC transporter SNPs were determined for both cases and controls (Table 2). All three *ABCB1* SNPs were found to be significantly associated with BC in Jordanian patients, with rs1045642, rs1128503, and rs2032582 having p values of 0.01164587, 0.01610842, and 0.03565022, respectively. Figure 1 shows a representative scatter pattern for rs1045642 of *ABCB1*. In contrast, only the rs2032582 SNP of *ABCB1* showed a strong genotypic association with BC (p value = $1e^{-8,}$ OR =6.72, 95% CI = 4.27 to 10.57). rs2032582 is a triallelic polymorphism comprising the A, C, and T (minor) alleles (the homozygous TT variant was not estimated in the current study population). None of the other investigated SNPs showed any significant correlation with BC, as all the allelic and genotypic frequencies were greater than 0.05 (Table 2).

Further genetic analyses were carried out to test for the association of different genetic models with BC. Table 3 summarizes three different genetic models and the chi-squared value for each. The *ABCG2* gene was excluded from the analysis because it expressed only two genotypes. For the *ABCC1* SNP rs4148351, Het (CT) versus Common Hz (CC) was found to be associated with BC in Jordanian Arabs ($\chi 2$ = 5.33; p value <0.05). Similarly, for the *ABCB1* SNP rs1128503, the Rare Hz (AA) versus Common Hz (GG) model was related to BC in Jordanian Arabs ($\chi 2$ =4.52; p value <0.05). No such association was found for any of the *ABCC2* SNPs (Table 3).

3.3. Association between ABC Transporter SNPs and Major Prognostic Factors of Breast Cancer (BC). Certain clinical and pathological characteristics of BC serve as major prognostic factors for the disease that are exploited in the process of treatment selection. None of the *ABCC1* SNPs showed any significant association with the clinical characteristics of BC, but the *ABCC2* SNPs rs2273697 and rs717620 were found to be significantly associated with age at breast cancer diagnosis (p value = 0.042) and breastfeeding status (p value = 0.05), respectively (Table 4). Meanwhile, the *ABCC1* SNP rs35628 was associated with the pathological characteristic of tumor size (p value = 0.014), while the *ABCC2* SNP rs2273697 was significantly associated with estrogen receptor status (p value = 0.013) (Table 4).

Likewise, rs1045642 was the only *ABCB1* SNP to be significantly associated with a clinical characteristic of BC, namely, age at breast cancer diagnosis (p value = 0.029) (Table 5). In contrast, rs2032582 was the only *ABCB1* SNP to show significant association with a pathological characteristic of BC, namely, tumor size (p value = 0.03) (Table 5). The *ABCG2* SNP rs2231142 was found to be significantly associated with axillary lymph node status (p value = 0.001) but not with any clinical characteristic (Table 5).

3.4. Association between ABC Transporter SNPs and Immunohistochemistry (IHC) Profiles of Breast Cancer (BC). Different combinations of the progesterone receptor, estrogen receptor, and Her2/neu expression molecular markers gives rise to three different immunohistochemistry profiles: Luminal A, Luminal B, and Triple Negative. These profiles and their correlation with the investigated SNPs are displayed in Tables 4 and 5. Only the *ABCC1* SNP rs35626 was found to be significantly correlated with the different IHC profiles (p value = 0.013).

4. Discussion

In the present study, four ABC transporter genes were screened in female BC patients and healthy volunteers from Jordan. Three SNPs from each of the *ABCC1, ABCC2,* and *ABCB1* genes and one SNP from the *ABCG2* gene were

Table 2: Association of the investigated ABCC1, ABCC2, ABCB1, and ABCG2 SNPs and breast cancer (BC).

Gene	SNP ID	Allele/Genotype	Allelic and Genotypic Frequencies in Cases and Controls		P-value*	Chi-square
			Cases (n = 222)	Controls (n = 218)		
ABCC1	rs35626	G	283(0.65)	256 (0.59)	0.073	3.214
		T	155 (0.35)	180 (0.41)		
		GG	95 (0.43)	81(0.37)	0.216	3.063
		GT	93 (0.42)	94(0.43)		
		TT	31 (0.14)	43 (0.2)		
	rs35628	A	394 (0.9)	388 (0.89)	0.788	0.072
		G	44 (0.1)	46 (0.11)		
		AA	180(0.82)	175(0.81)	0.820	0.395
		AG	34(0.16)	38(0.18)		
		GG	5(0.02)	4(0.02)		
	rs4148351	C	369(0.84)	346(0.8)	0.082	3.021
		T	69 (0.16)	88 (0.2)		
		CC	160 (0.73)	138 (0.64)	0.068	5.374
		CT	49 (0.22)	70(0.32)		
		TT	10 (0.05)	9(0.04)		
ABCC2	rs2273697	G	332(0.75)	331(0.76)	0.778	0.079
		A	108 (0.25)	103 (0.24)		
		AA	13 (0.06)	17(0.08)	0.412	1.773
		GA	82 (0.37)	69(0.32)		
		GG	125 (0.57)	131(0.6)		
	rs3740065	A	341(0.77)	345(0.79)	0.478	0.503
		G	101(0.23)	91(0.21)		
		AA	131(0.59)	141(0.65)	0.285	2.51
		AG	79(0.36)	63(0.29)		
		GG	11(0.05	14(0.06)		
	s717620	C	387(0.88)	377(0.87)	0.285	2.51
		T	55(0.12)	57 (0.13)		
		CC	170(0.77)	165(0.76)	0.928	0.149
		CT	47(0.21)	47(0.22)		
		TT	4(0.02)	5(0.02)		
ABCB1	rs1045642	C	288(0.65)	248(0.57)	0.012	6.364
		T	152(0.35)	186(0.43)		
		CC	102(0.46)	79(0.36)	0.063	5.499
		CT	84(0.38)	90(0.41)		
		TT	34(0.15)	48(0.22)		
	rs1128503	A	278(0.64)	242(0.56)	*0.016*	5.791
		G	158(0.36)	192(0.44)		
		AA	36(0.17)	49(0.23)	0.074	5.189
		GA	86(0.39)	94(0.43)		
		GG	96(0.44)	74(0.34)		
	rs2032582	A	144(0.33)	174(0.43)	*0.035*	6.668
		C	284(0.65)	252(0.58)		
		T	12(0.03)	6(0.01)		
		AA	29(0.13)	41(0.19)	*1e-8*	44.386
		CA	82(0.37)	90(0.42)		
		CC	97(0.44)	79(0.37)		
		TA	49(0.02)	2(0.0093)		
		TC	8(0.04)	4(0.02)		
ABCG2	rs2231142	T	17(0.04)	16(0.04)	0.902	0.015
		G	425 (0.96)	418 (0.96)		
		GG	204(0.92)	201(0.93)	0.899	0.016
		GT	17(0.08)	16(0.07)		

P value <0.05 was considered as significant.

Table 3: Genetic association analysis for the ABCC1, ABCC2, ABCB1, and ABCG2 SNPs using different genetic models.

Gene	SNP ID	Category Test	Odds Ratio	95% CI	Chi square∗
ABCC1	rs35626	Het (GT) vs. Common Hz (GG)	0.84	0.56-1.27	0.65
		Rare Hz (TT) vs. Het (GT)	0.73	0.42-1.25	1.31
		Rare Hz (TT) vs. Common Hz (GG)	0.61	0.36-1.06	3.04
	rs35628	Het (AG) vs. Common Hz (AA)	0.87	0.52-1.44	0.29
		Rare Hz (GG) vs. Het (AG)	1.4	0.35-5.63	0.22
		Rare Hz (GG) vs. Common Hz (AA)	1.22	0.32-4.6	0.08
	rs4148351	Het (CT) vs. Common Hz (CC)	0.6	0.39-0.93	5.33
		Rare Hz (TT) vs. Het (AG)	1.58	0.6-4.19	0.88
		Rare Hz (TT) vs. Common Hz (CC)	0.96	0.38-2.43	0.01
ABCC2	rs2273697	Het (GA) vs. Common Hz (GG)	1.55	0.71-3.42	1.21
		Rare Hz (AA) vs. Het (GA)	0.8	0.54-1.2	1.14
		Rare Hz (AA) vs. Common Hz (GG)	1.25	0.58-2.68	0.32
	rs3740065	Het (GA) vs. Common Hz (AA)	1.35	0.9-2.03	2.08
		Rare Hz (GG) vs. Het (GA)	0.63	0.27-1.48	1.16
		Rare Hz (GG) vs. Common Hz (AA)	0.85	0.37-1.93	0.16
	rs717620	Het (CT) vs. Common Hz (CC)	0.97	0.61-1.53	0.02
		Rare Hz (TT) vs. Het (CT)	0.8	0.2-3.17	0.1
		Rare Hz (TT) vs. Common Hz (CC)	0.78	0.2-2.94	0.14
ABCB1	rs1045642	Het (CT) vs. Common Hz (CC)	0.72	0.48-1.1	2.32
		Rare Hz (TT) vs. Het (CT)	0.85	0.5-1.43	0.39
		Rare Hz (TT) vs. Common Hz (CC)	0.61	0.37-1.03	3.46
	rs1128503	Het (GA) vs. Common Hz (AA)	1.25	0.74-2.1	0.68
		Rare Hz (GG) vs. Het (GA)	1.42	0.93-2.16	2.65
		Rare Hz (GG) vs. Common Hz (AA)	1.77	1.04-2.99	4.52

∗ For significant association $\chi 2$ should be >3.84 with P<0.025.
CI indicates confidence interval.

investigated for their association with BC in patients of Jordanian-Arab descent.

The *ABCC1 (MRP1)* gene has been previously reported as being a predictor of hematological toxicity in BC patients undergoing certain chemotherapy regimens [13]. It has also been found to be involved in MDR development in cases of neuroblastoma [14]. Moreover, *ABCC1* expression was found to be increased in children with acute lymphoblastic leukemia, and *ABCC1* gene induction resulted in worsened disease-free and overall survival rates [15, 16]. Our results show that none of the three investigated *ABCC1* SNPs showed any significant association with the clinical and pathological characteristics of BC. However, we found that the *ABCC1* SNP rs35626 was significantly associated with different immunohistochemistry (IHC) profiles in Jordanian-Arab patients.

Similar to *ABCC1*, the *ABCC2* gene is involved in decreased recurrence-free survival in BC patients receiving tamoxifen [17]. Nuclear expression of *ABCC2* in BC cells was also found to be associated with worsened clinical outcome [18]. Our findings showed that the *ABCC2* SNP rs2273697 was significantly associated with age at breast cancer diagnosis. Furthermore, rs2273697 was in correlation with estrogen receptor status for genotype association, patients were categorized according to the expression of estrogen receptor (positive versus negative) and tested with regard to their genotypes. However, in this study only gender was matched for the analysis. In addition, rs717620 was associated with breastfeeding status.

Three *ABCB1* SNPs rs1045642, rs1128503, and rs2032582 have been suggested to play a role in altered doxorubicin pharmacokinetics in Asian BC patients [19]. In the present study, all three aforementioned *ABCB1* SNPs were significantly associated with BC in Jordanian Arabs. Moreover, the *ABCB1* SNPs rs1045642 and rs2032582 were significantly associated with age at breast cancer diagnosis and tumor size, respectively.

Overexpression of the *ABCG2* gene was implicated in developing flavopiridol resistance in BC cells [20]. The homozygous genotype (CC) of the *ABCG2* SNP rs2231142 of the *ABCG2* gene resulted in significantly reduced intestinal transport activity compared to the wildtype (AA) [21]. In Kurdish BC patients, the A allele of the rs2231142 SNP may be a risk factor for BC progression, while the C allele was associated with poorer responses to anthracyclines and paclitaxel [22]. In contrast, the homozygous (CC) genotype of the *ABCG2* SNP rs2231142 was significantly associated with longer progression-free survival in Han Chinese BC patients [23]. In the present study, the *ABCG2* SNP rs2231142 was found to be significantly associated with axillary lymph node status in Jordanian BC patients.

Conclusively, screening certain ABC transporter genes in BC patients and healthy volunteers from the Jordanian-Arab

Table 4: Association between different ABCC1 and ABCC2 SNP genotypes and the clinicopathological characteristics of breast cancer (BC).

Clinical characteristics	*ABCC1*			*ABCC2*		
	rs35626 GG vs GT vs TT	rs35628 AA vs AG vs GG	rs4148351 CC vs CT vs TT	rs2273697 AA vs AG vs GG	rs3740065 AA vs AG vs GG	rs717620 CC vs CT vs TT
Body mass index ∗∗	0.535	0.116	0.068	0.813	0.461	0.084
Age at first pregnancy ∗∗	0.990	0.624	0.358	0.381	0.921	0.458
Age at BC diagnosis ∗∗	0.311	0.352	0.198	0.042	0.194	0.104
Allergy ∗	0.808	0.824	0.867	0.501	0.324	0.065
Age at menarche ∗∗	0.219	0.824	0.373	0.820	0.747	0.611
Breastfeeding status ∗	0.284	0.117	0.761	0.439	0.340	0.005
Age at menopause ∗∗	0.437	0.665	0.373	0.115	0.155	0.251
Family history ∗	0.669	0.605	0.762	0.472	0.891	0.415
Comorbidity ∗	0.764	0.967	0.976	0.130	0.741	0.140
Smoking ∗	0.237	0.287	0.163	0.320	0.406	0.362
Pathological characteristics						
Progesterone receptor status ∗	0.292	0.516	0.244	0.610	0.823	0.423
Estrogen receptor status ∗	0.730	0.550	0.562	0.013	0.839	0.125
HER2 ∗	0.146	0.500	0.330	0.441	0.226	0.842
IHC profile∗	0.013	0.838	0.260	0.381	0.775	0.270
Tumor differentiation ∗	0.754	0.940	0.963	0.768	0.718	0.431
Axillary lymph nodes ∗	0.113	0.184	0.817	0.138	0.989	0.213
Tumor stage ∗	0.491	0.751	0.665	0.748	0.999	0.357
Histology classification ∗	0.963	0.502	0.348	0.301	0.294	0.661
Tumor size ∗∗	0.888	0.014	0.968	0.720	0.576	0.922
Lymph node involvement ∗	0.694	0.944	0.794	0.165	0.339	0.528

∗ Pearson's chi-squared test was used to determine genotype-phenotype association.
∗∗ Analysis of variance (ANOVA) test was used to determine genotype-phenotype association.
P value <0.05 was considered as significant.

population revealed a number of interesting observations. Perhaps the most important finding was that the *ABCB1* SNPs were the only variants to be significantly associated with BC in Jordanian Arabs.

Data Availability

The datasets generated and/or analysed over the course of the study are not publicly available but are available from the corresponding author upon reasonable request.

Ethical Approval

This study was carried out in accordance with the recommendations of 'the Institutional Review Board (IRB) at Jordan University of Science and Technology (JUST) with ethical code number (14/78/2014).

Consent

Written informed consent was obtained from all individual participants included in the study. All subjects gave written informed consent in accordance with the Declaration of Helsinki. The protocol was approved by the JUST 'Human Ethics Committee'.

Conflicts of Interest

The authors declare that they have no conflicts of interest.

Table 5: Association between different ABCB1 and ABCG2 SNP genotypes and the clinicopathological characteristics of breast cancer (BC).

Clinical characteristics	*ABCB1*			*ABCG2*
	rs2032582 A vs C vs T	rs1128503 AA vs AG vs GG	rs1045642 CC vs CT vs TT	rs2231142 GG vs GT
Body mass index ∗∗	0.298	0.383	0.180	0.164
Age at first pregnancy ∗∗	0.212	0.326	0.815	0.490
Age at BC diagnosis ∗∗	0.931	0.924	*0.029*	0.592
Allergy ∗	0.310∗	0.331	0.169	0.511
Age at menarche ∗∗	0.508	0.525	0.115	0.947
Breastfeeding status ∗	0.708	0.291	0.665	0.553
Age at menopause ∗∗	0.746	0.258	0.676	0.563
Family history ∗	0.585	0.626	0.469	0.481
Comorbidity ∗	0.350	0.347	0.751	0.341
Smoking ∗	0.462	0.365	.303	0.429
Pathological characteristics				
Progesterone receptor status ∗	0.375	0.555	0.268	0.244
Estrogen receptor status ∗	0.470	0.480	0.299	0.312
HER2 ∗	0.712	0.886	0.835	0.560
IHC profile∗	0.186	0.645	0.160	0.606
Tumor differentiation ∗	0.429	0.632	0.595	0.926
Axillary lymph nodes ∗	0..373	0.718	0.847	0.001
Tumor stage ∗	0.700	0.705	0.723	0.722
Histology classification ∗	0.488	0.498	0.602	0.648
Tumor size ∗∗	0.030	0.032	0.556	0.249
Lymph node involvement ∗	0.021	0..056	0.417	0.381

∗ Pearson's chi-squared test was used to determine genotype-phenotype association.
∗∗ Analysis of variance (ANOVA) test was used to determine genotype-phenotype association.
P value <0.05 was considered as significant.

Acknowledgments

The authors thank the Jordanian Royal Medical Services (JRMS), Amman, Jordan, for approving this study in the first instance and making the clinical data and samples available for the study. This study was funded by the Deanship of Research (RN: 20140204), Jordan University of Science and Technology.

References

[1] L. A. Torre, F. Islami, R. L. Siegel, E. M. Ward, and A. Jemal, "Global cancer in women: burden and trends," *Cancer Epidemiology, Biomarkers & Prevention*, vol. 26, no. 4, pp. 444–457, 2017.

[2] L. Chouchane, H. Boussen, and K. S. R. Sastry, "Breast cancer in arab populations: molecular characteristics and disease management implications," *The Lancet Oncology*, vol. 14, no. 10, pp. e417–e424, 2013.

[3] A. Sheikh, S. A. Hussain, Q. Ghori et al., "The Spectrum of Genetic Mutations in Breast Cancer," *Asian Pacific Journal of Cancer Prevention*, vol. 16, no. 6, pp. 2177–2185, 2015.

[4] W. M. Sweileh, S. H. Zyoud, S. W. Al-Jabi, and A. F. Sawalha, "Contribution of Arab countries to breast cancer research: comparison with non-Arab Middle Eastern countries," *BMC Women's Health*, vol. 15, no. 1, 2015.

[5] H. Glavinas, P. Krajcsi, J. Cserepes, and B. Sarkadi, "The role of ABC transporters in drug resistance, metabolism and toxicity.," *Current Drug Delivery*, vol. 1, no. 1, pp. 27–42, 2004.

[6] M. Dean, A. Rzhetsky, and R. Allikmets, "The human ATP-binding cassette (ABC) transporter superfamily," *Genome Research*, vol. 11, no. 7, pp. 1156–1166, 2001.

[7] R. Vaclavikova, S. H. Nordgard, G. I. Alnaes et al., "Single nucleotide polymorphisms in the multidrug resistance gene 1 (ABCB1): effects on its expression and clinicopathological characteristics in breast cancer patients," *Pharmacogenetics and Genomics*, vol. 18, no. 3, pp. 263–273, 2008.

[8] F. J. Sharom, "ABC multidrug transporters: structure, function and role in chemoresistance," *Pharmacogenomics*, vol. 9, no. 1, pp. 105–127, 2008.

[9] V. Andersen, L. K. Vogel, T. I. Kopp et al., "High ABCC2 and Low ABCG2 Gene Expression Are Early Events in the Colorectal Adenoma-Carcinoma Sequence," *PLoS ONE*, vol. 10, no. 3, p. e0119255, 2015.

[10] E. Teodori, S. Dei, C. Martelli, S. Scapecchi, and F. Gualtieri, "The Functions and Structure of ABC Transporters: Implications for the Design of New Inhibitors of Pgp and MRP1 to Control Multidrug Resistance (MDR)," *Current Drug Targets*, vol. 7, no. 7, pp. 893–909, 2006.

[11] T. Nakanishi and D. D. Ross, "Breast cancer resistance protein (BCRP/ABCG2): its role in multidrug resistance and regulation of its gene expression," *Chinese Journal of Cancer*, vol. 31, no. 2, pp. 73–99, 2012.

[12] K. J. Preacher, *Calculation for the chi-square test: An interactive calculation tool for chi-square tests of goodness of fit and independence*, 2001, http://quantpsy.org/chisq/chisq.htm, [Accessed 19 Oct 2018].

[13] C. Vulsteke, D. Lambrechts, A. Dieudonné et al., "Genetic variability in the multidrug resistance associated protein-1 (ABCC1/MRP1) predicts hematological toxicity in breast cancer patients receiving (neo-)adjuvant chemotherapy with 5-fluorouracil, epirubicin and cyclophosphamide (FEC)," *Annals of Oncology*, vol. 24, no. 6, pp. 1513–1525, 2013.

[14] M. Munoz, M. Henderson, M. Haber, and M. Norris, "Role of the MRP1/ABCC1 Multidrug Transporter Protein in Cancer," *IUBMB Life*, vol. 59, no. 12, pp. 752–757, 2007.

[15] M. Kourti, N. Vavatsi, N. Gombakis et al., "Expression of Multidrug Resistance 1 (MDR1), Multidrug Resistance-Related Protein 1 (MRP1), Lung Resistance Protein (LRP), and Breast Cancer Resistance Protein (BCRP) Genes and Clinical Outcome in Childhood Acute Lymphoblastic Leukemia," *International Journal of Hematology*, vol. 86, no. 2, pp. 166–173, 2007.

[16] C. Atalay, A. Demirkazik, and U. Gunduz, "Role of ABCB1 and ABCC1 Gene Induction on Survival in Locally Advanced Breast Cancer," *Journal of Chemotherapy*, vol. 20, no. 6, pp. 734–739, 2013.

[17] K. Kiyotani, T. Mushiroda, C. K. Imamura et al., " Significant Effect of Polymorphisms in *CYP2D6* and *ABCC2* on Clinical Outcomes of Adjuvant Tamoxifen Therapy for Breast Cancer Patients ," *Journal of Clinical Oncology*, vol. 28, no. 8, pp. 1287–1293, 2010.

[18] A. MacIejczyk, E. Jagoda, T. Wysocka et al., "ABCC2 (MRP2, cMOAT) localized in the nuclear envelope of breast carcinoma cells correlates with poor clinical outcome," *Pathology & Oncology Research*, vol. 18, no. 2, pp. 331–342, 2012.

[19] S. Lal, Z. W. Wong, E. Sandanaraj et al., "Influence of ABCB1 and ABCG2 polymorphisms on doxorubicin disposition in Asian breast cancer patients," *Cancer Science*, vol. 99, no. 4, pp. 816–823, 2008.

[20] R. W. Robey, W. Y. Medina-Peèrez, K. Nishiyama et al., "Overexpression of the ATP-binding cassette half-transporter, ABCG2 (MXR/BCRP/ABCP1), in flavopiridol-resistant human breast cancer cells," *Clinical Cancer Research*, vol. 7, no. 1, pp. 145–152, 2001.

[21] Y. Tanaka, Y. Kitamura, K. Maeda, and Y. Sugiyama, "Quantitative Analysis of the ABCG2 c.421C>A Polymorphism Effect on in Vivo Transport Activity of Breast Cancer Resistance Protein (BCRP) Using an Intestinal Absorption Model," *Journal of Pharmaceutical Sciences*, vol. 104, no. 9, pp. 3039–3048, 2015.

[22] H. Ghafouri, B. Ghaderi, S. Amini, B. Nikkhoo, M. Abdi, and A. Hoseini, "Association of ABCB1 and ABCG2 single nucleotide polymorphisms with clinical findings and response to chemotherapy treatments in Kurdish patients with breast cancer," *Tumor Biology*, vol. 37, no. 6, pp. 7901–7906, 2016.

[23] W. Li, D. Zhang, F. Du et al., "ABCB1 3435TT and ABCG2 421CC genotypes were significantly associated with longer progression-free survival in Chinese breast cancer patients," *Oncotarget* , vol. 8, no. 67, pp. 111041–111052, 2017.

Hindawi
Journal of Oncology
Volume 2019, Article ID 8707053, 15 pages
https://doi.org/10.1155/2019/8707053

Review Article

Notch Signaling Activation as a Hallmark for Triple-Negative Breast Cancer Subtype

M. V. Giuli,[1] **E. Giuliani**,[1] **I. Screpanti**,[1] **D. Bellavia**,[1] **and S. Checquolo**[2]

[1]*Department of Molecular Medicine, "Sapienza" University of Rome, Rome, Italy*
[2]*Department of Medico-Surgical Sciences and Biotechnology, Sapienza University, Latina, Italy*

Correspondence should be addressed to D. Bellavia; diana.bellavia@uniroma1.it and S. Checquolo; saula.checquolo@uniroma1.it

Received 26 April 2019; Accepted 19 June 2019; Published 11 July 2019

Guest Editor: Chia-Jung Li

Triple-negative breast cancer (TNBC) is a subgroup of 15%-20% of diagnosed breast cancer patients. It is generally considered to be the most difficult breast cancer subtype to deal with, due to the lack of estrogen receptor (ER), progesterone receptor (PR), and human epidermal growth factor receptor 2 (HER2), which usually direct targeted therapies. In this scenario, the current treatments of TNBC-affected patients rely on tumor excision and conventional chemotherapy. As a result, the prognosis is overall poor. Thus, the identification and characterization of targets for novel therapies are urgently required. The Notch signaling pathway has emerged to act in the pathogenesis and tumor progression of TNBCs. Firstly, Notch receptors are associated with the regulation of tumor-initiating cells (TICs) behavior, as well as with the aetiology of TNBCs. Secondly, there is a strong evidence that Notch pathway is a relevant player in mammary cancer stem cells maintenance and expansion. Finally, Notch receptors expression and activation strongly correlate with the aggressive clinicopathological and biological phenotypes of breast cancer (e.g., invasiveness and chemoresistance), which are relevant characteristics of TNBC subtype. The purpose of this up-to-date review is to provide a detailed overview of the specific role of all four Notch receptors (Notch1, Notch2, Notch3, and Notch4) in TNBCs, thus identifying the Notch signaling pathway deregulation/activation as a pathognomonic feature of this breast cancer subtype. Furthermore, this review will also discuss recent information associated with different therapeutic options related to the four Notch receptors, which may be useful to evaluate prognostic or predictive indicators as well as to develop new therapies aimed at improving the clinical outcome of TNBC patients.

1. Introduction

Breast cancer is the most commonly diagnosed cancer in women worldwide [1, 2]. The presence or absence of estrogen receptors (ERs), progesterone receptors (PRs), and the human epidermal growth factor receptor 2 (HER2/neu) classifies breast cancer in different subtypes [3]. Hormone receptor positive breast cancers represent 60% of all breast cancers [4], while the lack of expression of ER, PR, and HER2 characterizes TNBC subtype [5, 6], which accounts for 15-20% of breast cancer cases.

TNBCs predominantly affect younger patients (< 40 years) and are more frequent in African-American women, where they are associated with BRCA gene mutations [7, 8]. They are heterogeneous tumors with aggressive phenotype and higher relapse rate. Moreover, compared to other BC subtypes, TNBCs are less differentiated [8, 9] and prone to metastasize within 5 years of diagnosis [8]. Furthermore, TNBC-bearing patients have a shorter overall survival when compared to other BC subtypes [7, 10]. The intertumoral and intratumoral heterogeneity represent one of the major challenges for the efficacy of the treatment of this cancer. Lehmann and colleagues classified TNBC into six different subtypes by analyzing their gene expression profiles: the basal-like (BL1 and BL2), mesenchymal (M), mesenchymal stem-like (MSL), immunomodulatory (IM), and luminal androgen receptor (LAR)-enriched tumors [9]. Since TNBCs patients are characterized by this molecular heterogeneity, chemotherapy (anthracycline and taxane-based treatments also with platinum agents addiction) represents the primary systemic treatment. Moreover, although combination therapies have ameliorated the response rates, this improvement

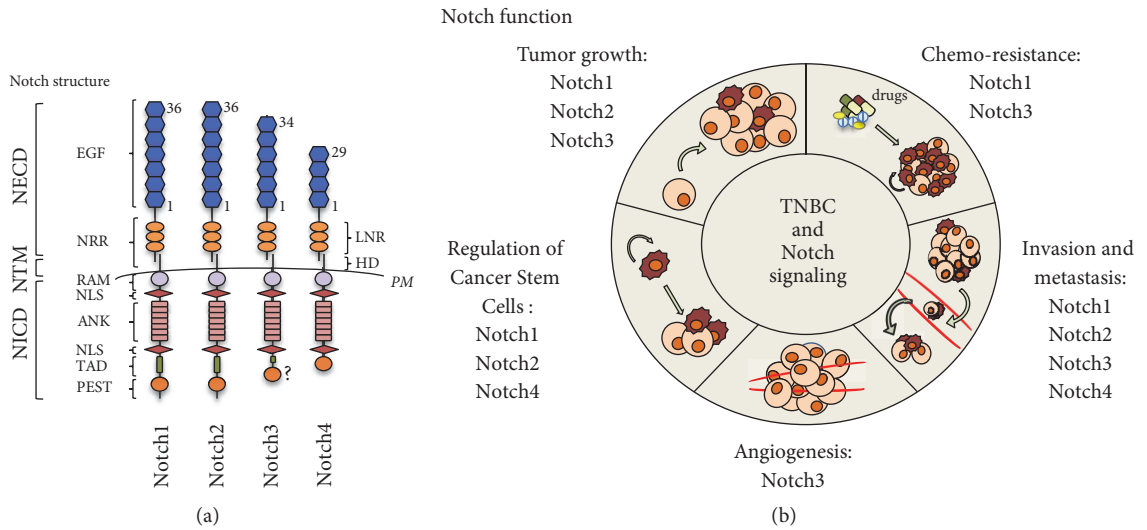

Figure 1: *Role of Notch signaling in TNBC.* (a) Schematic representation of the Notch receptors structure. Abbreviations. NECD: Notch extracellular domain; NTM: Notch transmembrane; NICD: Notch intracellular domain; EGF: epidermal growth factor-like repeats; NRR: negative regulatory region; LNR: Lin12/Notch repeats; HD: heterodimerization domain; *PM*: plasmatic membrane; RAM: RBP-j associated molecule; NLS: nuclear localization signal; ANK: ankyrin repeats; PEST: proline (P), glutamic acid (E), serine (S), and threonine (T). (b) The cartoon schematically depicts the involvement of each Notch receptor on TNBC initiation and progression.

leads to increased toxicity and multidrug resistance. On the basis of the stratification of TNBCs into subtypes, many preclinical and clinical trials are allowing the development of new targeted therapies to treat the 60–70% of patients who do not respond to chemotherapy [11]. These alternative approaches include the use of PARP and tyrosine kinase receptor inhibitors, the targeting of Wnt/β-catenin or PI3K/AKT/mTOR pathway, the emerging immunotherapy, and the use of epigenetic drugs and androgen receptor (AR) antagonists [12], as described below in more detail.

In this scenario, since it has been demonstrated that Notch signaling plays an important role in breast cancer cell growth, migration, invasion, and metastasis, and its aberrant activation is associated with a poor prognosis, resistance to treatments, and relapse [13], here we discuss the therapeutic potential of targeting Notch signaling in breast cancer treatment, focusing on the TNBC field. Until now, a lot of effort has been made to find the optimal pharmacological Notch inhibition, as the typical approach to target Notch pathway is mainly based on γ-secretase inhibitors (GSIs) use [14], which however represents a pan-Notch inhibitor drug strongly associated with severe gastrointestinal toxicity [15]. Inhibition of a specific receptor alone may reduce or avoid toxicity, thus showing a clear advantage over pan-Notch inhibitors. Although the Notch signaling pathway has been widely studied, the specific role of the individual Notch receptor in cancer is still unclear.

In this review we summarize (and discuss) the current knowledge of the role of each individual Notch receptor in TNBC (Figure 1), in order to suggest the identification of drugs targeting specific Notch(s) with an effective anticancer potential and low toxicity, trying to direct future directions in this challenging field (Table 1).

2. Notch Signaling Overview in TNBC

2.1. Notch Structure and Function. Juxtacrine signaling is pivotal in several developmental processes and relies on communication between one cell and a neighboring cell through the interaction of transmembrane receptors and ligands [16]. The Notch signaling pathway is an example of this short-range cell-cell communication and plays an essential role in metazoan development [17]. The Notch receptor is a single-pass transmembrane protein expressed on the plasmatic membrane as a processed heterodimer after the cleavage by furin-like protein convertase in the Golgi compartment [18]. It was discovered in Drosophila melanogaster. The fly genome encodes only one Notch protein while two receptors, which have redundant roles, were identified in Caenorhabditis elegans [19]. In contrast, mammals have four Notch paralogs that only partly share the same functions [20] and this is due to their variable structural homology [21].

Regarding the structural organization of the Notch receptors (Figure 1(a)), they share a three-domain structure: an extracellular domain (NECD), a transmembrane region (NTM), and an intracellular domain (NICD) which translocates to the nucleus after two sequential proteolytic cleavages triggered by ADAM metalloproteases and a γ-secretase complex, respectively. According to the canonical Notch signaling model, these events are due to the interaction between the receptors and their ligands [21], expressed on neighboring cells.

The NECD contains 29 to 36 epidermal growth factor-like (EGF-like) repeats which are responsible for the ligands binding [22], the negative regulatory region (NRR), consisting of three cysteine-rich LNR Notch repeats, and the heterodimerization domain (HD), which prevents receptor activation in the absence of ligands [23]. The NTM region contains

Table 1: Summary of notch receptors-related processes and treatments in TNBC.

Notch receptor	Process	Refs	Treatment	Studies	Refs
Notch1	Tumor growth	[59–61]			
	Mitochondrial metabolism	[60, 80]	mAbs	Preclinical	[156]
	Regulation of cancer stem cells	[64, 65, 68]	mAbs (+chemotherapeutic agents)	Preclinical	[64, 66, 156, 159]
	Drug resistance	[67–70, 73, 75]	GSI + chemotherapeutic agents	Preclinical and clinical	[74, 151–153]
	Invasion and metastasis	[59, 71, 73]			
Notch2	Tumor growth	[87, 88]			
	Regulation of cancer stem cells	[84, 85]	mAbs	Preclinical	[157]
	Invasion and metastasis	[84, 85]			
Notch3	Tumor growth	[92, 93]			
	Angiogenesis	[97, 98]	mAbs	Preclinical and clinical	[93, 157, 161]
	Drug resistance	[110, 111]			
	Invasion and metastasis	[103, 104, 107]			
Notch4	Regulation of cancer stem cells	[125–128]	mAbs	Preclinical	[126]
	Invasion and metastasis	[117, 118]	GSI	Preclinical	[118]

Abbreviations. mAbs: monoclonal antibodies; GSI: γ-secretase inhibitor.

a γ-secretase cleavage site which is critical for signal activation [24]. The NICD consists of a RAM (RBP-j-Associated Molecule) domain, ankyrin (ANK) repeats flanked by two nuclear localization signals (NLS), a transcriptional activation domain (TAD), and a C-terminal Pro-Glu-Ser-Thr (PEST) domain which is the substrate of ubiquitin ligases that target the NICD for proteasomal degradation [25]. Both RAM ad ANK domains are necessary to recruit transcriptional coactivators within the nucleus [26] (Figure 1(a)).

In mammals, the five Notch ligands, Dll1, Dll3, and Dll4 (members of the Delta family of ligands) and Jagged1 and Jagged2 (members of the Serrate family of ligands), are single-pass transmembrane proteins [27]. Dll3 gene encodes a decoy receptor and, as a result, it is not able to activate Notch receptors in-trans [28].

Notch signaling has pleiotropic effects during development and in adult tissues, in spite of the simplicity of the core pathway [29]. As a matter of fact, Notch activity affects both proliferation and cell death and drives differentiation and acquisition of specific cell fates. Furthermore, it is involved in the maintenance of stem cells [30].

Since the Notch receptors is central for these processes, its deregulation has been implicated in the development of congenital diseases [31] or cancer, as either oncogenes or tumor suppressors [32, 33].

Specifically, Notch signaling pathway is involved in mammary development and homeostasis as well as in the promotion of breast cancer when dysregulated [34]. Indeed, accumulating evidence sustains the importance of Notch pathway in mammary stem cells (MaSCs) generation and maintenance during mammary gland development [35]. This process normally takes place over a period of rapid growth during puberty and, subsequently, it undergoes cycles of expansion and regression with each estrous cycle, pregnancy, lactation, and involution until menopause [36]. In this scenario, it has been demonstrated that Notch pathway plays a fundamental role in regulating both self-renewal [37] and differentiation of MaSCs [38, 39], thus allowing mammary gland homeostasis. Thus, the aberrant activation of Notch signaling has been shown to be an early event in breast cancer development [37]. A TCGA breast cancer data was analyzed for mutations in Notch receptors genes [40]. Among the 956 breast tumor samples analyzed, there were 42 mutations in Notch genes: 25 of them are clustered in the HD or lead to a PEST domain disruption, finally leading to NICD overexpression [40, 41]. In addition, compared to normal tissues, a lower expression of known Notch negative regulators in breast cancer was frequently found [42, 43]. In particular, FBXW7 mutations were significantly more frequent in TNBC compared to other breast tumor subtypes [44] and these determine an increased NICD stability, thus correlating with poorer prognosis of breast cancer-bearing patients [45]. Moreover, a novel molecular mechanism that correlates low NUMB expression with high Notch activity in the regulation of breast tumor EMT, especially in TNBCs, was found [46].

In keeping with these findings, the role of Notch signaling in breast cancer initiation and progression has been extensively studied and most of the reported data highlights its oncogenic role in breast cancer [47].

2.2. Role of Notch Paralogs in TNBC

2.2.1. Notch1. The first demonstration that Notch receptors are oncogenes also in regard to breast cancer derives from studies on murine models. In particular, the Notch1 gene was identified as a novel target for mouse mammary tumor virus (MMTV) insertional activation, thus leading to the overexpression of Notch1 mutated forms, finally involved in mammary tumor formation [48]. Compared with normal tissues, Notch1 is fairly expressed in human breast cancer and its elevated expression represents an early event during carcinogenesis, as it has been demonstrated that the enforced expression of ectopic N1ICD contributes to the incidence and development of breast cancer [49], being predictive of poorest

overall patient survival [50–52]. Several studies have related Notch1 signaling to TNBCs [53]. In particular, the basal-like 1 (BL1) and mesenchymal stem-like (MSL) subtypes are characterized by the high expression of this receptor [54, 55], strongly correlated with ominous outcomes of tumor [56].

Notch pathway is aberrantly activated via multiple mutational mechanisms and it is liable of TNBC tumor development. Although PEST domain mutations in Notch1 protein mainly regard oncogenic events in T-ALL [57], around 13% of TNBC exhibits in-frame deletions of Notch1 exons 21-27, which disrupt the NRR and HD domains, thus leading to upregulation of its pathway caused by either ligand-independent receptor activation or N1ICD half-life extension [40]. As a consequence, Notch1-mutated-TNBCs show a strong overexpression of Notch1 target genes, like NOTCH3, HES1, HEY2, MYC, CCND1, HES4, NRARP, and NOTCH1 itself, in comparison with Notch1 wild-type tumors, thus resulting in oncogenic phenotype of TNBCs [40]. In addition, a correlation has been found between the expression of Notch1 protein and known prognostic factors in breast cancer, analyzed by IHC assay in 115 breast cancer tissues [58]. The presence of Notch1 in tumor tissue was significantly associated with TNBC subtype (P=0.041), high metastasis rate (P=0.035), tumor-node-metastasis (TNM) stages, and ALDH1 *status*, a known marker of cancer stem cells (CSCs).

Furthermore, a significant positive correlation was observed between Notch1 protein and both AKT and NF-κB proteins activation in preclinical models, thus finally promoting TNBC cell growth, migration, and invasion [59]. Interestingly, more recently Hossain and colleagues described in detail noncanonical mechanisms downstream of Jagged-1-mediated Notch1 activation that trigger AKT phosphorylation, NF-κB activation, and mitochondrial metabolism, thus leading to the transcription of survival genes in TNBC cells [60]. In agreement with these data, it has been demonstrated that *Genistein*, a phytochemical originally isolated from soybean, by inhibiting Notch1, affected MDA-MB-231 TNBC growth through modulating NF-κB activity [61].

It is well demonstrated that CSCs are involved in initiation, progression, and chemotherapy resistance of cancers [62, 63].

Notch1 appears to be in part responsible for maintaining CSC stemness in TNBCs, and the specific inhibition of its signaling has a remarkable inhibitory effect on this cancer subtype, thus increasing the sensitivity of TNBC to chemotherapeutic reagents [64]. It is reported that in HCC70, SUM149, and MDA-MB-231 TNBC cell lines, the c-Jun N-terminal kinase (JNK) protein promotes CSC self-renewal and maintenance via transcription of Notch1, whose activation affects migration and invasion of tumor cells [65]. In accordance with these findings, both JNK and Notch1 knockdown significantly reduced mammosphere formation in TNBC cells [65]. Moreover, Mittal and colleagues, by using a novel monoclonal antibody to inhibit Notch1 (MAb602.101), observed a significant reduction in tumor growth and in the number and sizes of mammospheres compared to controls, thus resulting in the depletion of the putative cancer stem-like cell subpopulation [66]. Furthermore, Bhola and colleagues demonstrated that resistance to TORC1/2 inhibition in TNBC is driven by Notch1 activation whose expression is increased in response to treatment. In consequence, genetic and pharmacological blockade of Notch1 is able to revert the increase in CSC markers expression, mammosphere formation, and tumor-initiating ability, all induced during TORC1/2 inhibition treatment [67]. All these studies sustained an important correlation between Notch1 inhibition and the restoration of the sensitivity to drug treatments, thus showing interesting findings which would improve the efficacy of conventional therapies by directly targeting the CSC niche [64, 68]. In addition, significant upregulated Notch-1 protein levels are found in Doxorubicin resistant MCF-7 cells compared to parental sensitive MCF-7 cells [69]. In keeping with these data, Notch1 inhibition enhanced the antitumor effects of Paclitaxel, the first-line chemotherapeutic drug for clinical treatment of TNBC, in both MDA-MB-231 and MCF-7 chemoresistant cells [70].

Emerging evidence demonstrated the involvement of Notch1 also in the invasion and migration steps which characterize the epithelial-to-mesenchymal transition (EMT) process in TNBC [71]. The authors observed that Notch1 is negatively regulated by miR-3178, which is significantly lower in TNBCs when compared to the other subtypes: the lower levels of miR-3178 lead to increased Notch1 activity followed by increased Snail1 expression, which finally contributes to EMT regulation [71]. Indeed, the inhibition of Slug/Notch1 signaling axis, by regulating EMT process, seems to be sufficient to decrease tumor-initiating cells (TICs) number, tumor induction, and metastasis [72]. In keeping with these data, Notch1 expression is higher in Cisplatin-resistant MDA-MB-231 TNBC cells, compared to the parental cells, and this helped to induce chemoresistance via activating AKT pathway and promoting EMT [73]. Furthermore, it has been demonstrated that the combined treatment with Doxorubicin plus GSIs of the same resistant cells, besides downregulating Notch-1, is also able to decrease both Cyclin D1 and antiapoptotic protein Bcl-2 while upregulating PTEN and proapoptotic proteins, finally leading to synergistic antitumor effects *in vitro* and *in vivo* TNBC xenografts models [74].

More recently, Lee and colleagues demonstrated that Notch1 inactivation, obtained as a consequence of the knockdown of Tribbles Homolog 3 (TRIB3) protein in MDA-MB-231 and AS-B244 radio-resistant TNBC cells, correlated with a cell resensitization toward radiation therapy [75]. Interestingly, some studies showed a Notch1 involvement in metabolic alterations of cancer cells. Abnormal mitochondrial fission is implicated in the development and progression of many human cancers [76] and Notch signaling has been reported to be closely related to mitochondrial network and function in different cellular contexts [77–79]. Dynamin related protein (Drp1) is involved in mitochondrial fission while Mitofusin-1 (Mfn1) is a mitochondrial membrane protein that participates in mitochondrial fusion, thus contributing to the maintenance of the mitochondrial network. Perumalsamy and colleagues identified the N1ICD-Akt-Mfn signaling cascade as a novel pathway regulating cell survival, in a way independent of the canonical functions associated with N1ICD activity, thus demonstrating the Notch1

involvement in mitochondrial network and apoptotic resistance in HeLa cells [79]. More recently, it was demonstrated that the Notch1/Mfn2 pathway was able to favor the protective effect of melatonin on myocardial infarction, by using both *in vitro* and *in vivo* models [78]. In TNBC context, Chen and colleagues demonstrated that the observed increase in the mitochondrial fission, characterized by the combined upregulation of Drp1 and downregulation of Mfn1, was due to a positive feedback loop closely dependent on Notch1 protein: mitochondrial fission contributes to activation of Notch1, which in turn promotes and amplifies the mitochondrial fission through the maintenance of both Drp1 and Mfn1 altered expression. This process strongly correlated with TNBC progression and a poorer overall survival of TNBC-bearing patients [80].

All these studies suggest that activation of the Notch1 pathway is a key event in TNBC etiology and it contributes to the development and progression of malignant phenotype of TNBC subtype.

2.2.2. Notch2. The role of Notch2 in breast cancer is less well characterized with respect to Notch1. Previous studies reported that Notch2 increases tumorigenicity in thymic lymphoma [81] and in embryonal brain tumor cell lines [82]. Conversely, Notch2 signaling causes cells growth arrest in small cell lung cancer [83]. Therefore, the cellular context is important for tumorigenic outcome of Notch2 signaling. Notch2 can play a different role in TNBCs, thus acting as an oncogene or tumor suppressor. Evidence for its oncogenic role came from studies on cultured breast cancer cells where knockdown of Notch2 leads to the inhibition of cell migration and cancer stem cell survival [84, 85]. In particular, Kim and colleagues revealed that treatment of MCF-7, MDA-MB-231, and SUM159 human breast cancer cells with Benzyl isothiocyanate (BITC), a constituent of cruciferous vegetables, increases levels of the active form of Notch1, Notch2, and Notch4 in both cultured and xenografted cells. In this scenario, only Notch2 activation is able to impede inhibitory effect of treatment on cell migration [85]. In keeping with these data, the proapoptotic effect of Zerumbone (ZER), a sesquiterpene isolated from subtropical ginger, on TNBC cells was counteracted by Notch2 activation and significantly increased upon its knockdown [86].

Analysis of Notch2 expression in normal mammary tissue and breast tumors, in association with clinical data, also sustained a tumor suppressor function for this receptor. The most convincing evidence for this Notch2 capability is provided by O'Neill and colleagues [87]. They reported that overexpression of N2ICD in MDA-MB-231 cells is potently able to suppress tumor growth both *in vitro* and *in vivo* in xenografts. Therefore, Notch2 plays a role in the inhibition of mammary adenocarcinoma growth, mostly in comparison with Notch4 ICD in the same context. Another study revealed that the *in vivo* growth of MDA-MB-231 and SUM159 xenografted cells is enhanced by stable knockdown of Notch2 [88]. Notably, this increased *in vivo* tumor growth is determined by the increase in cytokines secretion and Notch1 activation, thus suggesting a compensatory response of cancer cell [88]. More interestingly, numerous studies suggested that Notch2 overexpression is related to a greater chance of survival of breast cancer patients [89]. Parr and colleagues analyzed Notch-1 and Notch-2 mRNA and protein expression levels in normal and breast cancer tissues also in association whit clinicopathological parameters [89]. The results showed that high level of either Notch1 mRNA or protein is associated with a poorer outcome for patients while a high expression of Notch2 is correlated with a better prognosis. In addition, the authors demonstrated an opposite expression of Notch1 and Notch2 proteins during tumor development, related to its differentiation state. Regarding Notch2 gene mutational pattern in TNBC samples, many focal amplifications were also found in its PEST or HD domain: in particular, the PEST domain showed six mutations, three of them leading to a gain of function, while the HD domain exhibited two missense mutations, finally leading to Notch2 overexpression [40].

All these data suggest that Notch-2 role remains ambiguous in TNBC. However, to date there is much more evidence to support the view that it should have a tumor suppressive role rather than an oncogenic role.

2.2.3. Notch3. As we have previously described, TNBCs are genetically unstable and they are usually characterized by a complex pattern of genetic aberrations such as focal amplifications. On the basis of the evidence that Notch3 is highly expressed in TNBCs [51], Turner and colleagues subjected a wide subset of TNBCs to high resolution microarray-based comparative genomic hybridization and to genome-wide gene expression analysis in order to model mutational signatures of Notch3 gene. The obtained results highlighted that Notch3 gene amplification is quite recurrent and it is significantly overexpressed when amplified [90]. Furthermore, a broad spectrum of activating mutations that disrupt both HD and PEST domains, thus favoring N3ICD expression, were discovered in Notch3 gene [40].

In keeping with these findings, the presence of activating mutations, coincident with gene amplification and overexpression, lends genetic weight to the idea that there is a selective pressure to increase Notch3 activity for TNBCs initiation and progression. Indeed, the correlation between Notch3 signaling and TNBCs is corroborated by several studies.

First of all, it is already ascertained that Notch3 has transforming potentials *in vivo*, since transgenic mice overexpressing the intracellular domain of Notch3 (N3ICD) developed breast cancer [91]. In addition, Notch3 pivotal role in the proliferation of ErbB2-negative breast cancer cell lines has been demonstrated [92].

More recently, it was shown that Notch3 altered expression activates an oncogenic program in a panel of TNBCs. Selective Notch3 inhibition impairs tumor growth, whereas Notch3 agonism correlates with a malignant phenotype and increased proliferation. Indeed, transcriptomic analyses showed a Notch signature that includes overexpression of the c-Myc oncogene [93].

As occurred for cancers in general, TNBC malignancy correlates with tumor angiogenesis [94–96]. Reedijk and

colleagues pointed out that Jagged1 and Notch3 are overexpressed in blood vessels of primary breast cancer [97], but little is done to understand whether Jagged1 and Notch3 are closely related to angiogenesis in TNBCs. Recently, Xue and colleagues speculated on the possible crosstalk between VEGF and Notch signaling in TNBCs [98] but further studies are needed. In addition, they showed that Jagged1 and Notch3 are detected in TNBCs at significantly higher levels than in no-TNBCs and their expression leads to more aggressive clinicopathological characteristics and poorer prognosis, confirming previous studies [56]. Moreover, RNAi-mediated depletion of Jagged1 and Jagged2 proteins in ErbB2-negative breast cancer cell lines inhibited proliferation and induced apoptosis *in vitro*, thus demonstrating an important autocrine/juxtacrine loop between Jagged1/Jagged2 ligands and Notch3 in TNBC context [99], which was then also observed in other tumor contexts [100].

In general, in about 50% of breast cancer patients bone is recognized as the first site of metastasis and TGFβ plays a central role in this process [101]. Increasing evidence suggested that cancer cells interact with the bone microenvironment in order to promote the initiation and progression of bone metastasis [102]. Zhang and colleagues focused their attention on Notch3 and bone metastasis potential relationship in TNBCs: they observed that both osteoblasts and their secretion of TGFβ increased Notch3 expression in TNBC cells that reside in the bone marrow niche. Notably, the inhibition of Notch3 expression is able to reduce osteolytic bone metastasis in xenograft animal models of TNBCs [103].

All these data supported the hypothesis of Notch3 involvement in promoting TNBC invasiveness and cancer cell seeding to secondary organs, thus being able to influence the acquirement of the metastatic phenotype and to complete the invasion-metastasis cascade. In this view, Leontovich and colleagues demonstrated that the MDA-MB-231 LM cells, isolated from experimental lung metastasis (LM), showed higher self-renewal capacity with respect to parental cells thanks to the upregulation of Notch3 reprogramming network. *In vitro* inhibition of Notch3 impaired the invasive capacity of MDA-MB-231 LM cells and interfered with late stages of the invasion-metastasis cascade. Interestingly, the pivotal role of Notch3 in determining an invasive phenotype and worst outcome was corroborated in unique TNBC cells resulting from a patient-derived brain metastasis [104].

Recently, some studies reported different molecular mechanism by which Notch3 seems to inhibit EMT in breast cancer [105, 106], including TNBCs [107], but overall high transcript levels of Notch3 were associated with less distant metastasis and better prognosis only in ER+ breast cancer [105, 106, 108].

Currently, several groups focus on the understanding of how the tumor microenvironment dictates treatment response. For instance, stromal cells sustain cancer cell survival after genotoxic and targeted therapy through paracrine and juxtacrine signaling [109]. In particular, it was demonstrated that stromal cells expressing Jagged1 on their surface were able to activate Notch3 on TNBC cells, thus promoting the expansion of cells resistant to chemotherapy and reinitiating tumor growth [110]. Therefore, these data supported the Notch3 role in chemoresistance of TNBCs.

Furthermore, Notch3 seems to be also involved in the resistance to targeted treatments, such as tyrosine kinase inhibitors (TKIs) against EGFR [111]. Targeting EGFR may be a promising approach to treat TNBCs since it is commonly overexpressed in this breast cancer subtype [112], but several clinical trials failed due to intrinsic and acquired resistance. In this scenario, the authors demonstrated a novel role of Notch3 in promoting resistance to TKI-gefitinib through regulating EGFR localization, thus rendering it targetable by TKI-gefitinib [111].

Overall, these studies suggested that Notch3 is strictly associated with pathogenesis of TNBCs and it is responsible for their aggressive phenotype.

2.2.4. Notch4. The first evidence that Notch4 could function as a protooncogene was associated with mouse mammary tumors which showed integration of the mouse mammary tumors virus (MMTV) into the Notch4 locus [113]. The major consequence of this integration is the production of a truncated protein which is constitutively activated. Therefore, aberrant expression of Notch4 leads to mammary epithelial dysplasia and impaired differentiation, finally resulting in mammary tumorigenesis in mice [114].

Several studies documented a correlation between TNBCs and high expression of Notch4. Speiser and colleagues analyzed 29 TNBC-bearing patients and Notch4 was widely expressed in 73% of the cases [53], in agreement with a previous study [115]. Moreover, Wang and colleagues analyzed a wider panel of breast cancers (98 samples) in which TNBCs exhibited the highest Notch4 expression [116], thus suggesting a pivotal role of Notch4 receptor in this subtype. This was further confirmed from genome-wide analysis of TNBC human samples in which Notch4 was found commonly mutated in patients with progression free survival (PFS) less than 3 months [41]. Notch4 seems to be associated with metastatic TNBCs: Lawson and colleagues, by analyzing the transcriptomic signature of TBNC patient-derived xenografts, detected high levels of Notch4 in metastatic cells [117]. In accordance with these findings, the expression of Notch4 correlated with overall poor prognosis and experimental evidence indicates that Notch4 contributed to tumor invasion and metastasis by sustaining EMT at the invasive front of primary tumors [118]. Castro and colleagues performed *in vivo* experiments on mice that established spontaneous lung metastasis from JygMC(A) cells. The authors state that Notch4 promoted tumor growth and metastasis through the finding of Notch4 nuclear localization in both primary tumors and lung metastasis. The treatment with an orally active GSI inhibitor (RO4929097) reverted the phenotype, thus inhibiting primary tumor growth, reducing the number of metastatic lung nodules, and finally confirming the contribution of Notch4 during mammary tumor progression [118]. More recently, Castro and colleagues tested Sulforaphane (SFN) in both human and murine TNBC cells and they observed that the same JygMC(A) cells were more resistant to SFN. Molecularly,

the authors demonstrated that SNF is able to reduce the promoter activity of Cripto1, a known positive regulator of Notch receptor maturation and signaling [119], thus linking the Cripto-mediated Notch4 signaling impairment with the observed inhibition of the proliferation of breast CSCs [120]. As previously mentioned, CSCs are associated with high-grade breast cancer and distant metastasis [121, 122] and contribute to intratumor heterogeneity [123]. Therefore, the understanding of signaling networks that regulate CSCs is urgently required. Since stem cells and cancer stem cells are usually characterized by the activation of the same pathways and Notch4 has been implicated in mammary stem cells [124], during the last decade several studies demonstrated that Notch4 activity strongly correlated with self-renewal and chemoresistance of breast cancer stem cells (BCSCs). Harrison and colleagues isolated BCSCs from breast cancer cell lines and primary breast cancer samples. They compared the activation of Notch1 and Notch4 in BCSC-enriched population to differentiated cells and they found that Notch1 and Notch4 are differentially expressed: Notch1 promotes the proliferation of progenitor cells and sustains their differentiation whereas Notch4 plays a role in the commitment of BCSCs to progenitor cells. Interestingly, decreased levels of Notch4 (but not of Notch1), obtained by both RNA interference or pharmacological treatment, significantly reduced mammosphere formation *in vitro* and reduced tumor formation *in vivo*, thus suggesting a specific role of Notch4 in regulating this subpopulation [125]. These results were consistent with a previous study in which Notch4-neutralizing antibody is able to inhibit cancer stem cell activity *in vitro* [126].

In keeping with these data, Rustighi and colleagues found that Notch1/4 is involved in the maintenance of breast stem cell self-renewal. The authors pinpointed the role of the prolyl-isomerase Pin1 in sustaining high levels and transcriptional activity of Notch1/4 through preventing their E3-ligase FBXW7-dependent proteasomal degradation [127, 128]. More interestingly, the authors demonstrated that the Notch1/4 suppression, Pin1-dependent, correlated with a sensitization of BCSCs to chemotherapy *in vitro* and *in vivo* [128].

All together these results suggest that high Notch4 levels are crucial to promote mesenchymal signature and to keep pro-stemness signaling constant during tumor progression of TNBC.

3. Notch-Targeting Approaches and Clinical Perspectives in TNBC

Chemotherapy is the current primary therapy for TNBCs in the neoadjuvant, adjuvant, and metastatic settings [129]. Although there is a small subgroup of patients with TNBC for whom chemotherapy may be effective, the heterogeneity of these tumors requires the development of most promising new targets and associated therapies that may improve the outcome of TNBC-bearing patients. The deregulation of various signaling pathways has been confirmed in patients suffering from TNBC and has recently come under development as a novel treatment option [130]. Among them, ADP ribose polymerase (PARP) inhibitors named PARPi (olaparib, veliparib, rucaparib, niraparib, talazoparib, and CEP-9722) have been evaluated on TNBC patients as mono- or combination therapies. Interestingly, BRCA mutated tumor cells are more sensitive to PARPi for combined loss of PARP and homolog recombination repair [131]. Tyrosine kinase receptors targeted by therapy include epidermal growth factor receptor (EGFR), fibroblast growth factor receptor (FGFR), and vascular endothelial growth factor receptor (VEGFR) [90]. Expression of EGFR has been reported in up to 89% of TNBC patients, particularly for BL2-subtype tumors [132], which depend on EGFR for proliferation and represent the major candidates for anti-EGFR therapies [133]. Unfortunately, only limited benefit has been reported in clinical trials using anti-EGFR agents, such as monoclonal antibodies (Cetuximab or Panitumumab), in combination with chemotherapy [134, 135]. Defect of Wnt/β-catenin pathway has been identified as an alternative therapeutic approach [136] and PI3K/AKT/mTOR pathway is also emerging as a promising target. It has been reported that inhibition of the PI3K pathway enhanced sensitivity to PARPi in TNBC cell lines [137]. Moreover, Yunokawa et al. reported positive effects of Everolimus, an mTOR inhibitor [138]. For years, TNBC was not considered sensitive to immunotherapy, but now this option is emerging as an exciting treatment [139], because of the immunogenic nature of TNBC compared with other breast cancer subtypes [140]. However, these strategies are effective in less than 20% of cancer patients or are useful only for certain TN cancer subgroups [141]. Therefore, further therapeutic strategies are urgently needed.

In this scenario, targeted therapy focused on modulating aberrant Notch signaling is emerging as a possible treatment approach for patients with TNBC (Table 1). Novel opportunities arise from the discovery of Notch crosstalk with many oncogenic signaling which suggested that Notch pathway may be considered such a multitarget drugs' candidate [13, 142–144]. To date, several clinical studies involved targeting of Notch pathway with either γ-secretase inhibitors (GSIs) or monoclonal antibodies (mAbs) against Notch receptors [145], which represent the major therapeutic targets of Notch signaling pathway.

3.1. γ-Secretase Inhibitors (GSIs) in TNBC. GSIs act by preventing the cleavage of the active form of all Notch receptors, thus inhibiting their transcriptional activity [146, 147]. It is demonstrated that GSIs interfere with cell cycle, lead to apoptosis in both luminal and TNBC cell lines [14], and, in particular, reduce the growth and dissemination of MDA-MB-231 TNBC xenografts [148]. It is shown that GSI treatment upregulates the proapoptotic protein Phorbol-12-myristate-13-acetate-induced protein 1 (NOXA), reduces CSC colony formation, and results in apoptosis of human TNBC cell lines [149]. In another study, it is demonstrated that 13% of TNBCs with PEST domain mutations in NOTCH1, NOTCH2, and NOTCH3 receptors and patient-derived xenografts are highly sensitive to the PF-03084014 GSI [40]. These mutations provoke a truncation in the C-terminus of Notch protein,

removing the PEST domain while retaining the γ-secretase cleavage site. These findings suggest that GSI might be promising in treatments of TNBC subset with specific Notch sequence alterations.

Unfortunately, the gastrointestinal negative effects impede the clinical use of GSIs [150], suggesting that much more work is required for having favorable effects after GSI treatments. In this scenario, novel therapeutic strategies will likely come from combinations of GSIs with conventional chemotherapy, in order to reduce the single dose of both treatments, thus limiting either toxicity. Zhi-Lu Li and colleagues demonstrated the feasibility of the combined use of GSIs and Doxorubicin on MDA-MB-231 cells, resulting in encouraging new therapeutic approach in TNBC treatment [74]. Actually, RO-4929097 and MK0752 GSIs are investigated in phase I/II clinical trials and, recently, the combination of RO-4929097 and chemotherapics like Paclitaxel and Carboplatin is in a phase I clinical trial for TNBCs [151]. Moreover, since preclinical studies prompted evaluation of combination of PF-03084014 GSI with docetaxel for the treatment of patients with TNBC [152, 153], Locatelli and colleagues designed a phase I study in order to evaluate safety, tolerability, pharmacokinetics, and antitumor activity of this combination. Preliminary results demonstrated feasibility of the combined GSI-chemotherapy approach, thus promoting further studies in order to use Notch signaling inhibitors in combination with conventional chemotherapy in the treatment of TNBC-bearing patients [154].

3.2. Monoclonal Antibodies (mAbs) in TNBC. Despite these encouraging results on GSI treatment, there is an increasing number of studies based on the use of monoclonal antibodies against Notch members in order to achieve higher specificity. The use of specific monoclonal antibodies is based on their capacity to bind the extracellular regulatory region of the receptor, to mask the cleavage domain of metalloproteinase ADAM, and to induce a conformational change of the receptor into its inactive form [155]. Recently, it has been shown that an antibody against the negative regulatory region (NRR) of Notch1 resulted in reduced proliferation, restricted expression of its targets HES1, HES5, and HEY-L, reduced colony forming ability, and lessened cancer stem-like population in MDA-MB-231 cell lines [156]. As previously mentioned, the inhibition of Notch1 with the novel monoclonal antibody MAb602.101 reduced TNBC cell lines tumor growth and sphere-forming potential, thus directly affecting CSCs niche [66]. In accordance with these results, TNBC patients which display high level of Notch1 expression are characterized by poorer survival, thus suggesting that hyperactivation of Notch1 receptor may be used as a predictive marker for TNBCs [66] and finally pointing out the Notch1 inhibition as a potential novel approach to achieve the outcome of TNBC-bearing patients. Interestingly, it has been also demonstrated that the antibody use can amplify chemotherapy treatments: in a TNBC patient-derived xenograft model, Notch1 monoclonal antibodies exhibited synthetically antitumor efficacy combined with docetaxel via inhibition of CSCs generation and maintenance [64].

Moreover, a Notch2/3 blocking monoclonal antibody named tarextumab (OMP-59R5) was developed: it was successfully tested on patient-derived epithelial tumor xenograft models, including breast, thus showing significant antitumor activity [157]. Recently, Choy and colleagues used a novel monoclonal antibody that selectively targets the Notch3 NRR (anti-N3.A4) [158] to make a comparison between Notch3-specific versus pan-Notch effects for treatment of TNBCs. They documented that both treatments significantly inhibited colony formation *in vitro* and modestly reduced tumor growth *in vivo* to similar extent [93]. Therefore, the authors strongly suggested that the therapeutic targeting of Notch3 could provide therapeutic benefit without the known toxicities associated with pan-Notch inhibition, as GSIs fail to distinguish the particular Notch receptor driving growth [93]. Similar results have been obtained by Farnie and colleagues who demonstrated that Notch4-neutralizing antibody inhibited cancer stem cell activity *in vitro* [126].

Notch ligands targeting could be also a promising strategy to reduce Notch activation. Hoey and colleagues used monoclonal antibody against DLL4 ligand to block its binding to Notch1, thus observing antitumor effects in a wide range of human tumor xenografts from various tumor types, including breast cancer. Specifically, the inhibition of DLL4-Notch1 axis decreased CSC frequency [159]. More recently, a monoclonal antibody against Jagged1 ligand has been developed to be used for the treatment of established bone metastasis that is refractory to chemotherapy [160]. The authors observed that chemotherapy agents were able to induce Jagged1 expression at the cell membrane of osteoblasts and mesenchymal stem cells of bone marrow, which in turn activated Notch signaling, finally promoting chemoresistance [160].

Interestingly, more recently it has been demonstrated that the overexpression of Notch receptors or their ligands at the cell membrane of cancer cells might be also turned to our advantage in order to effectively deliver cytotoxic agents to the tumor sites. In this view, a novel anti-Notch3 antibody-drug conjugate currently named PF-066580808 is now under clinical investigation (phase I) for the treatment of breast cancer, including TNBCs [161]. Besides above described approaches, several natural compounds and their derivatives are showing Notch inhibition and antiproliferative activities in different *in vitro* cancer models, thus suggesting their potential application as additional therapeutic option in Notch-related cancers [68, 162].

Further studies into mechanisms of action of individual Notch receptor in TNBC development and behavior should be addressed in order to ameliorate the understanding of the complexity and mechanisms that underlie TNBCs. In this view, the aforementioned results suggest that the potential targeting of the Notch signaling pathway with different molecules should be studied in more detail to further improve the treatment options for TNBC-bearing patients.

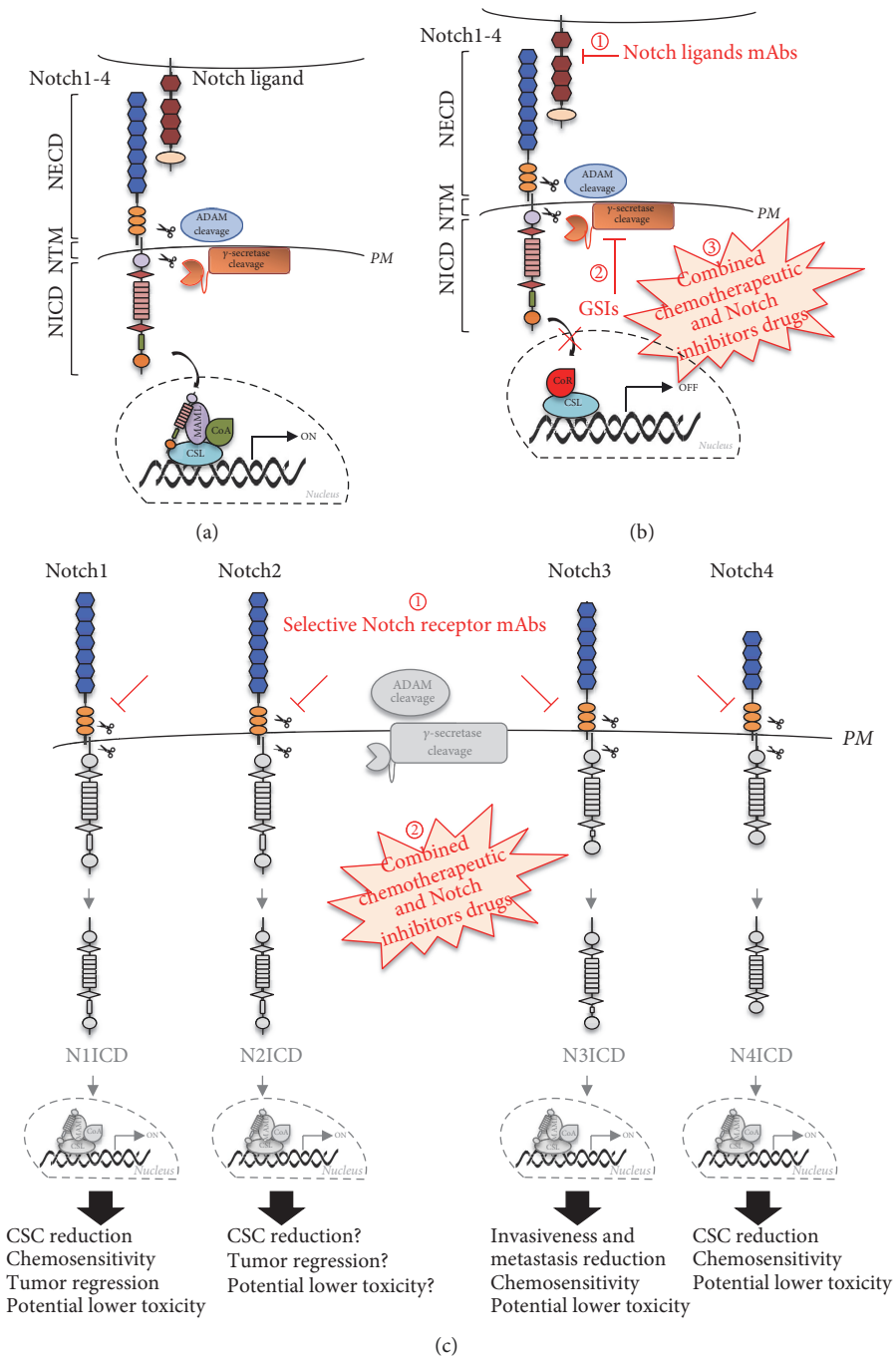

Figure 2: *Notch-targeting therapeutic approaches in TNBCs.* (a) The canonical Notch signaling pathway: ligand binding promotes sequential cleavages of the Notch receptors (Notch1-4) by ADAM enzyme and γ-secretase complex, resulting in the release of NICD, which translocates in the nucleus, interacts with transcriptional regulators to transcriptionally activate the canonical Notch target genes (ON), thus leading to the regulation of TNBC growth and progression. (b) Notch inhibitors with lower or absent selectivity, respectively, include mAbs targeting the Notch ligands and GSIs. (1) mAbs against Notch ligands prevent ligand-receptor interaction and the subsequent Notch cleavages, preventing Notch signaling triggering. Little is known about the specific Notch-ligand relationship in TNBC; thus further studies are needed to consider ligand blocking as a potential alternative selective approach in TNBC treatment. (2) GSIs act as pan-Notch inhibitors since they prevent the cleavage of all Notch receptors, thus avoiding the release of any NICD. This unselective mechanism of action is strongly correlated with a high intestinal toxicity in patients, which significantly impairs their clinical use. (3) Lower doses of GSIs used in combination with chemotherapeutic drugs result in improved clinical outcome and less toxicity, which however must be overcome. (c) A higher selectivity can be obtained by using monoclonal antibodies directed against the extracellular domain of a specific Notch receptor (1): mAbs mask the cleavage domain of ADAM, thus preventing the binding of this enzyme and the subsequent γ-secretase cleavage. The final effect will depend on the specific block of the single Notch receptor, also used in combination with chemotherapeutic drugs (2). Several studies detailed in the text have suggested that a greater selectivity in the Notch inhibition approach for TNBCs treatment is strongly correlated with a higher probability of success in favoring tumor regression, associated with less toxicity and therefore with a potential better prognosis of TNBC-bearing patients. Abbreviations. ADAM: a disintegrin and metalloproteinase; CSL: CBF1/Su(H)/Lag-1; CoA: coactivator; CoR: corepressor; GSIs: γ-secretase inhibitors; mAb: monoclonal antibody; MAML1: mastermind-like 1; NECD: Notch extracellular domain; NICD: Notch intracellular domain; NTM: Notch transmembrane; *PM*: plasmatic membrane.

4. Conclusion

TNBC is an aggressive subgroup of human breast cancer, characterized by high rates of relapse and frequent metastasis. Since unresponsiveness to current treatment is often observed, the development of novel strategies to treat also this form of breast cancer is urgently required.

Several pathways are involved in the pathogenesis of TNBC. Among them, Notch signaling plays a key role in tumor initiation and mainly in tumor progression. Indeed, several experimental studies documented the role of Notch signaling in promoting EMT for cancer cell seeding to secondary organs and in sustaining the maintenance of CSCs which are responsible for chemoresistance. Therefore, inhibition of Notch signaling has been considered as an attractive strategy for the treatment of TNBC. Several pan-Notch inhibitors are currently under clinical trials in combination with chemotherapy [163] but they fail to distinguish individual Notch receptors and cause intestinal toxicity. In addition, since individual Notch receptors can have opposite role in the same cancer, their simultaneous inhibition may have pleiotropic effects possibly resulting in tumor stimulation.

This review covers the roles of individual Notch receptors in TNBC development and progression, thus showing that they only partly share the same functions in TNBC context. As a result, determining the Notch receptor which is specifically involved in different TNBC subtypes might be useful to identify patients who are most likely able to respond to different targeted therapy, paving the way for avoidance or likely reduction of the therapeutic complications associated with nonselective Notch inhibitors. In conclusion, this review will aid further research in identifying a suitable treatment for TNBC, as the specific inhibition of a single Notch receptor or ligand might promote new clinical trials aiming to evaluate more selective and less toxic alternatives for Notch inhibition in the treatment of TNBC-bearing patients (Figure 2).

Conflicts of Interest

The authors declare that they have no conflicts of interest.

Authors' Contributions

M. V. Giuli and E. Giuliani contributed equally to this work.

References

[1] R. L. Siegel, K. D. Miller, S. A. Fedewa et al., "Colorectal cancer statistics," *CA: A Cancer Journal for Clinicians*, vol. 67, no. 3, pp. 177–193, 2017.

[2] L. A. Torre, R. L. Siegel, E. M. Ward, and A. Jemal, "Global cancer incidence and mortality rates and trends–an update," *Cancer Epidemiology, Biomarkers & Prevention*, vol. 25, no. 1, pp. 16–27, 2016.

[3] R. W. Carlson, D. C. Allred, B. O. Anderson, H. J. Burstein, W. B. Carter, S. B. Edge et al., "Breast cancer. Clinical practice guidelines in oncology," *Journal of the National Comprehensive Cancer Network*, vol. 7, no. 2, pp. 122–192, 2009.

[4] A. U. Buzdar, "Role of biologic therapy and chemotherapy in hormone receptor- and HER2-positive breast cancer," *Annals of Oncology*, vol. 20, no. 6, pp. 993–999, 2009.

[5] V. G. Abramson, B. D. Lehmann, T. J. Ballinger, and J. A. Pietenpol, "Subtyping of triple-negative breast cancer: implications for therapy," *Cancer*, vol. 121, no. 1, pp. 8–16, 2015.

[6] B. D. Lehmann and J. A. Pietenpol, "Identification and use of biomarkers in treatment strategies for triple-negative breast cancer subtypes," *The Journal of Pathology*, vol. 232, no. 2, pp. 142–150, 2014.

[7] L. A. Carey, C. M. Perou, C. A. Livasy et al., "Race, breast cancer subtypes, and survival in the carolina breast cancer study," *The Journal of the American Medical Association*, vol. 295, no. 21, pp. 2492–2502, 2006.

[8] R. Dent, M. Trudeau, K. I. Pritchard et al., "Triple-negative breast cancer: clinical features and patterns of recurrence," *Clinical Cancer Research*, vol. 13, no. 15 Pt1, pp. 4429–4434, 2007.

[9] B. D. Lehmann, J. A. Bauer, X. Chen et al., "Identification of human triple-negative breast cancer subtypes and preclinical models for selection of targeted therapies," *The Journal of Clinical Investigation*, vol. 121, no. 7, pp. 2750–2767, 2011.

[10] J. D. Prescott, S. Factor, M. Pill, and G. W. Levi, "Descriptive analysis of the direct medical costs of multiple sclerosis in 2004 using administrative claims in a large nationwide database," *Journal of Managed Care Pharmacy*, vol. 13, no. 1, pp. 44–52, 2007.

[11] G. Bianchini, J. M. Balko, I. A. Mayer, M. E. Sanders, and L. Gianni, "Triple-negative breast cancer: challenges and opportunities of a heterogeneous disease," *Nature Reviews Clinical Oncology*, vol. 13, no. 11, pp. 674–690, 2016.

[12] A. Lee and M. B. Djamgoz, "Triple negative breast cancer: Emerging therapeutic modalities and novel combination therapies," *Cancer Treatment Reviews*, vol. 62, pp. 110–122, 2018.

[13] S. Guo, M. Liu, and R. R. Gonzalez-Perez, "Role of Notch and its oncogenic signaling crosstalk in breast cancer," *Biochimica et Biophysica Acta (BBA) - Reviews on Cancer*, vol. 1815, no. 2, pp. 197–213, 2011.

[14] S. Rasul, R. Balasubramanian, A. Filipović, M. J. Slade, E. Yagüe, and R. C. Coombes, "Inhibition of γ-secretase induces G2/M arrest and triggers apoptosis in breast cancer cells," *British Journal of Cancer*, vol. 100, no. 12, pp. 1879–1888, 2009.

[15] J. H. van Es, M. E. van Gijn, O. Riccio et al., "Notch/γ-secretase inhibition turns proliferative cells in intestinal crypts and adenomas into goblet cells," *Nature*, vol. 435, no. 7044, pp. 959–963, 2005.

[16] T. Yaron, Y. Cordova, and D. Sprinzak, "Juxtacrine signaling is inherently noisy," *Biophysical Journal*, vol. 107, no. 10, pp. 2417–2424, 2014.

[17] S. Artavanis-Tsakonas, M. D. Rand, and R. J. Lake, "Notch signaling: cell fate control and signal integration in development," *Science*, vol. 284, no. 5415, pp. 770–776, 1999.

[18] C. M. Blaumueller, H. Qi, P. Zagouras, and S. Artavanis-Tsakonas, "Intracellular cleavage of notch leads to a heterodimeric receptor on the plasma membrane," *Cell*, vol. 90, no. 2, pp. 281–291, 1997.

[19] K. Fitzgerald, H. A. Wilkinson, and I. Greenwald, "glp-1 can substitute for lin-12 in specifying cell fate decisions in Caenorhabditis elegans," *Development*, vol. 119, no. 4, pp. 1019–1027, 1993.

[20] J. Wu and E. H. Bresnick, "Bare rudiments of notch signaling: how receptor levels are regulated," *Trends in Biochemical Sciences*, vol. 32, no. 10, pp. 477–485, 2007.

[21] D. Bellavia, S. Checquolo, A. F. Campese, M. P. Felli, A. Gulino, and I. Screpanti, "Notch3: from subtle structural differences to functional diversity," *Oncogene*, vol. 27, no. 38, pp. 5092–5098, 2008.

[22] N. A. Rana and R. S. Haltiwanger, "Fringe benefits: functional and structural impacts of O-glycosylation on the extracellular domain of Notch receptors," *Current Opinion in Structural Biology*, vol. 21, no. 5, pp. 583–589, 2011.

[23] C. Sanchez-Irizarry, A. C. Carpenter, A. P. Weng, W. S. Pear, J. C. Aster, and S. C. Blacklow, "Notch subunit heterodimerization and prevention of ligand-independent proteolytic activation depend, respectively, on a novel domain and the LNR repeats," *Molecular and Cellular Biology*, vol. 24, no. 21, pp. 9265–9273, 2004.

[24] S. J. Bray, "Notch signalling: a simple pathway becomes complex," *Nature Reviews Molecular Cell Biology*, vol. 7, no. 9, pp. 678–689, 2006.

[25] R. Kopan and M. X. G. Ilagan, "The canonical notch signaling pathway: unfolding the activation mechanism," *Cell*, vol. 137, no. 2, pp. 216–233, 2009.

[26] K. Hori, A. Sen, and S. Artavanis-Tsakonas, "Notch signaling at a glance," *Journal of Cell Science*, vol. 126(Pt 10), pp. 2135–2140, 2013.

[27] B. D'Souza, A. Miyamoto, and G. Weinmaster, "The many facets of Notch ligands," *Oncogene*, vol. 27, no. 38, pp. 5148–5167, 2008.

[28] E. Ladi, J. T. Nichols, W. Ge et al., "The divergent DSL ligand Dll3 does not activate Notch signaling but cell autonomously attenuates signaling induced by other DSL ligands," *The Journal of Cell Biology*, vol. 170, no. 6, pp. 983–992, 2005.

[29] R. Palermo, S. Checquolo, D. Bellavia, C. Talora, and I. Screpanti, "The molecular basis of notch signaling regulation: a complex simplicity," *Current Molecular Medicine*, vol. 14, no. 1, pp. 34–44, 2014.

[30] A. Louvi and S. Artavanis-Tsakonas, "Notch and disease: a growing field," *Seminars in Cell & Developmental Biology*, vol. 23, no. 4, pp. 473–480, 2012.

[31] J. Masek and E. R. Andersson, "The developmental biology of genetic Notch disorders," *Development*, vol. 144, no. 10, pp. 1743–1763, 2017.

[32] J. C. Aster, W. S. Pear, and S. C. Blacklow, "The varied roles of notch in cancer," *Annual Review of Pathology*, vol. 24, no. 12, pp. 245–275, 2017.

[33] S. Cialfi, R. Palermo, S. Manca et al., "Loss of Notch1-dependent p21(Waf1/Cip1) expression influences the Notch1 outcome in tumorigenesis," *Cell Cycle*, vol. 13, no. 13, pp. 2046–2245, 2014.

[34] E. Braune, A. Seshire, and U. Lendahl, "Notch and wnt dysregulation and its relevance for breast cancer and tumor initiation," *Biomedicines*, vol. 6, no. 4, p. 101, 2018.

[35] A. Santoro, T. Vlachou, M. Carminati, P. G. Pelicci, and M. Mapelli, "Molecular mechanisms of asymmetric divisions in mammary stem cells," *EMBO Reports*, vol. 17, no. 12, pp. 1700–1720, 2016.

[36] R. C. Hovey and J. F. Trott, "Morphogenesis of mammary gland development," *Advances in Experimental Medicine and Biology*, vol. 554, Article ID 15384579, pp. 219–228, 2004.

[37] G. Farnie and R. B. Clarke, "Mammary stem cells and breast cancer—role of Notch signalling," *Stem Cell Reviews and Reports*, vol. 3, no. 2, pp. 169–175, 2007.

[38] M. Wicha, G. Dontu, M. Al-Hajj, and M. Clarke, "Stem cells in normal breast development and breast cancer," *Cell Proliferation*, vol. 5, no. S1, pp. 59–72, 2003.

[39] S. R. Oakes, D. Gallego-Ortega, and C. J. Ormandy, "The mammary cellular hierarchy and breast cancer," *Cellular and Molecular Life Sciences*, vol. 71, no. 22, pp. 4301–4324, 2014.

[40] K. Wang, Q. Zhang, D. Li et al., "PEST domain mutations in Notch receptors comprise an oncogenic driver segment in triple-negative breast cancer sensitive to a gamma-secretase inhibitor," *Clinical Cancer Research*, vol. 21, no. 6, pp. 1487–1496, 2015.

[41] Z. Hu, N. Xie, C. Tian et al., "Identifying circulating tumor DNA mutation profiles in metastatic breast cancer patients with multiline resistance," *EBioMedicine*, vol. 32, pp. 111–118, 2018.

[42] S. Akhoondi, D. Sun, N. von der Lehr et al., "FBXW7/hCDC4 is a general tumor suppressor in human cancer," *Cancer Research*, vol. 67, no. 19, pp. 9006–9012, 2007.

[43] S. Pece, M. Serresi, E. Santolini et al., "Loss of negative regulation by Numb over Notch is relevant to human breast carcinogenesis," *The Journal of Cell Biology*, vol. 167, no. 2, pp. 215–221, 2004.

[44] L. Santarpia, Y. Qi, K. Stemke-Hale et al., "Mutation profiling identifies numerous rare drug targets and distinct mutation patterns in different clinical subtypes of breast cancers," *Breast Cancer Research and Treatment*, vol. 134, no. 1, pp. 333–343, 2012.

[45] M. Ibusuki, Y. Yamamoto, S. Shinriki, Y. Ando, and H. Iwase, "Reduced expression of ubiquitin ligase FBXW7 mRNA is associated with poor prognosis in breast cancer patients," *Cancer Science*, vol. 102, no. 2, pp. 439–445, 2011.

[46] J. Zhang, X. Shao, H. Sun et al., "NUMB negatively regulates the epithelial-mesenchymal transition of triple-negative breast cancer by antagonizing Notch signaling," *Oncotarget*, vol. 7, no. 38, pp. 61036–61053, 2016.

[47] S. Stylianou, G. Collu, R. Clarke, and K. Brennan, "Aberrant activation of Notch signalling in human breast cancer," *Breast Cancer Research*, vol. 66, no. 3, pp. 1517–1525, 2006.

[48] A. Dievart, N. Beaulieu, and P. Jolicoeur, "Involvement of Notch1 in the development of mouse mammary tumors," *Oncogene*, vol. 18, no. 44, pp. 5973–5981, 1999.

[49] H. Kiaris, K. Politi, L. M. Grimm et al., "Modulation of notch signaling elicits signature tumors and inhibits Hras1-induced oncogenesis in the mouse mammary epithelium," *The American Journal of Pathology*, vol. 165, no. 2, pp. 695–705, 2004.

[50] B. C. Dickson, A. M. Mulligan, H. Zhang et al., "High-level JAG1 mRNA and protein predict poor outcome in breast cancer," *Modern Pathology*, vol. 20, no. 6, pp. 685–693, 2007.

[51] M. Reedijk, S. Odorcic, L. Chang et al., "High-level coexpression of JAG1 and NOTCH1 is observed in human breast cancer and is associated with poor overall survival," *Cancer Research*, vol. 65, no. 18, pp. 8530–8537, 2005.

[52] M. Reedijk, D. Pinnaduwage, B. C. Dickson et al., "JAG1 expression is associated with a basal phenotype and recurrence in lymph node-negative breast cancer," *Breast Cancer Research and Treatment*, vol. 111, no. 3, pp. 439–448, 2008.

[53] J. Speiser, K. Foreman, E. Drinka et al., "Notch-1 and notch-4 biomarker expression in triple-negative breast cancer," *International Journal of Surgical Pathology*, vol. 20, no. 2, pp. 139–145, 2012.

[54] C. W. Lee, K. Simin, Q. Liu et al., "A functional Notch–survivin gene signature in basal breast cancer," *Breast Cancer Research*, vol. 10, no. 6, p. R97, 2008.

[55] S. Zhang, W. Chung, G. Wu, S. E. Egan, L. Miele, and K. Xu, "Manic fringe promotes a claudin-low breast cancer phenotype through notch-mediated PIK3CG induction," *Cancer Research*, vol. 75, no. 10, pp. 1936–1943, 2015.

[56] B. Cohen, M. Shimizu, J. Izrailit et al., "Cyclin D1 is a direct target of JAG1-mediated Notch signaling in breast cancer," *Breast Cancer Research and Treatment*, vol. 123, no. 1, pp. 113–124, 2010.

[57] A. P. Weng, A. A. Ferrando, and W. Lee, "Activating mutations of NOTCH1 in human T cell acute lymphoblastic leukemia," *Science*, vol. 306, no. 5694, pp. 269–271, 2004.

[58] Y. Zhong, S. Shen, Y. Zhou et al., "NOTCH1 is a poor prognostic factor for breast cancer and is associated with breast cancer stem cells," *OncoTargets and Therapy*, vol. 9, pp. 6865–6871, 2016.

[59] H. Zhu, F. Bhaijee, N. Ishaq, D. J. Pepper, K. Backus, A. S. Brown et al., "Correlation of Notch1, pAKT and nuclear NF-kappaB expression in triple negative breast cancer," *American Journal of Cancer Research*, vol. 3, no. 2, pp. 230–239, 2013.

[60] F. Hossain, C. Sorrentino, D. A. Ucar et al., "Notch signaling regulates mitochondrial metabolism and NF-κB Activity in triple-negative breast cancer cells via IKKα-dependent non-canonical pathways," *Frontiers in Oncology*, vol. 8, no. 575, 2018.

[61] H. Pan, W. Zhou, W. He et al., "Genistein inhibits MDA-MB-231 triple-negative breast cancer cell growth by inhibiting NF-κB activity via the Notch-1 pathway," *International Journal of Molecular Medicine*, vol. 30, no. 2, pp. 337–343, 2012.

[62] W. H. Matsui, "Cancer stem cell signaling pathways," *Medicine*, vol. 1, S1, pp. S8–S19, 2016.

[63] D. R. Pattabiraman and R. A. Weinberg, "Tackling the cancer stem cells-what challenges do they pose?" *Nature Reviews Drug Discovery*, vol. 13, no. 7, pp. 497–512, 2014.

[64] M. Qiu, Q. Peng, I. Jiang et al., "Specific inhibition of Notch1 signaling enhances the antitumor efficacy of chemotherapy in triple negative breast cancer through reduction of cancer stem cells," *Cancer Letters*, vol. 328, no. 2, pp. 261–270, 2013.

[65] X. Xie, T. S. Kaoud, R. Edupuganti et al., "c-Jun N-terminal kinase promotes stem cell phenotype in triple-negative breast cancer through upregulation of Notch1 via activation of c-Jun," *Oncogene*, vol. 36, no. 18, pp. 2599–2608, 2017.

[66] S. Mittal, A. Sharma, S. A. Balaji et al., "Coordinate hyperactivation of Notch1 and Ras/MAPK pathways correlates with poor patient survival: novel therapeutic strategy for aggressive breast cancers," *Molecular Cancer Therapeutics*, vol. 13, no. 12, pp. 3198–3209, 2014.

[67] N. E. Bhola, V. M. Jansen, J. P. Koch et al., "Treatment of triple-negative breast cancer with TORC1/2 inhibitors sustains a drug-resistant and notch-dependent cancer stem cell population," *Cancer Research*, vol. 76, no. 2, pp. 440–452, 2016.

[68] R. Palermo, F. Ghirga, M. G. Piccioni et al., "Natural products inspired modulators of cancer stem cells-specific signaling pathways Notch and hedgehog," *Current Pharmaceutical Design*, vol. 24, no. 36, pp. 4251–4269, 2019.

[69] X. Li, M. Ji, S. Zhong et al., "MicroRNA-34a modulates chemosensitivity of breast cancer cells to adriamycin by targeting Notch1," *Archives of Medical Research*, vol. 43, no. 7, pp. 514–521, 2012.

[70] Y. Zhou, Q. Sun, Y. Zhang et al., "Targeted inhibition of Notch1 gene enhances the killing effects of paclitaxel on triple negative breast cancer cells," *Asian Pacific Journal of Tropical Medicine*, vol. 10, no. 2, pp. 179–183, 2017.

[71] P. Kong, L. Chen, M. Yu, J. Tao, J. Liu, and Y. Wang, "miR-3178 inhibits cell proliferation and metastasis by targeting Notch1 in triple-negative breast cancer," *Cell Death & Disease*, vol. 9, no. 11, p. 1059, 2018.

[72] W. Huang, E. E. Martin, B. Burman, M. E. Gonzalez, and C. G. Kleer, "The matricellular protein CCN6 (WISP3) decreases Notch1 and suppresses breast cancer initiating cells," *Oncotarget*, vol. 7, no. 18, pp. 25180–25193, 2016.

[73] Y. Xiao, D. Zeng, Y. Liang et al., "Major vault protein is a direct target of Notch1 signaling and contributes to chemoresistance in triple-negative breast cancer cells," *Cancer Letters*, vol. 440-441, pp. 156–167, 2019.

[74] Li. ZL, C. Chen, Y. Yang, C. Wang, T. Yang, X. Yang et al., "Gamma secretase inhibitor enhances sensitivity to doxorubicin in MDA-MB-231 cells," *International Journal of Clinical and Experimental Pathology*, vol. 8, no. 5, pp. 4378–4387, 2015.

[75] Y. Lee, W. Wang, W. Chang et al., "Tribbles homolog 3 involved in radiation response of triple negative breast cancer cells by regulating Notch1 activation," *Cancers*, vol. 11, no. 2, p. 127, 2019.

[76] S. L. Archer, "Mitochondrial fission and fusion in human diseases," *The New England Journal of Medicine*, vol. 370, no. 11, Article ID 24620884, p. 1074, 2014.

[77] K. Mitra, R. Rikhy, M. Lilly, and J. Lippincott-Schwartz, " DRP1-dependent mitochondrial fission initiates follicle cell differentiation during *Drosophila* oogenesis ," *The Journal of Cell Biology*, vol. 197, no. 4, pp. 487–497, 2012.

[78] H. Pei, J. Du, X. Song, L. He, Y. Zhang, and X. Li, "Melatonin prevents adverse myocardial infarction remodeling via Notch1/Mfn2 pathway," *Free Radical Biology & Medicine*, vol. 97, pp. 408–417, 2016.

[79] L. R. Perumalsamy, M. Nagala, and A. Sarin, "Notch-activated signaling cascade interacts with mitochondrial remodeling proteins to regulate cell survival," *Proceedings of the National Acadamy of Sciences of the United States of America*, vol. 107, no. 15, pp. 6882–6887, 2010.

[80] L. Chen, J. Zhang, Z. Lyu, Y. Chen, X. Ji, and H. Cao, "Positive feedback loop between mitochondrial fission and Notch signaling promotes survivin-mediated survival of TNBC cells," *Cell Death & Disease*, vol. 9, no. 11, p. 1050, 2018.

[81] J. L. Rohn, A. S. Lauring, M. L. Linenberger, and J. Overbaugh, "Transduction of Notch2 in feline leukemia virus-induced thymic lymphoma," *Journal of Virology*, vol. 70, no. 11, pp. 8071–8080, 1996.

[82] X. Fan, I. Mikolaenko, I. Elhassan et al., "Notch1 and Notch2 have opposite effects on embryonal brain tumor growth," *Cancer Research*, vol. 64, no. 21, pp. 7787–7793, 2004.

[83] V. Sriuranpong, M. W. Borges, R. K. Ravi, D. R. Arnold, B. D. Nelkin, S. B. Baylin et al., "Notch signaling induces cell cycle arrest in small cell lung cancer cells," *Cancer Research*, vol. 61, no. 7, pp. 3200–3205, 2001.

[84] C.-H. Chao, C.-C. Chang, M.-J. Wu et al., "MicroRNA-205 signaling regulates mammary stem cell fate and tumorigenesis," *The Journal of Clinical Investigation*, vol. 124, no. 7, pp. 3093–3106, 2014.

[85] S. Kim, A. Sehrawat, and S. V. Singh, "Notch2 activation by benzyl isothiocyanate impedes its inhibitory effect on breast cancer cell migration," *Breast Cancer Research and Treatment*, vol. 134, no. 3, pp. 1067–1079, 2012.

[86] A. Sehrawat, K. Sakao, and S. V. Singh, "Notch2 activation is protective against anticancer effects of zerumbone in human breast cancer cells," *Breast Cancer Research and Treatment*, vol. 146, no. 3, pp. 543–555, 2014.

[87] C. F. O'Neill, S. Urs, C. Cinelli et al., "Notch2 signaling induces apoptosis and inhibits human MDA-MB-231 xenograft growth," *The American Journal of Pathology*, vol. 171, no. 3, pp. 1023–1036, 2007.

[88] S. Kim, E. Hahm, J. A. Arlotti et al., "Withaferin A inhibits in vivo growth of breast cancer cells accelerated by Notch2 knockdown," *Breast Cancer Research and Treatment*, vol. 157, no. 1, pp. 41–54, 2016.

[89] C. Parr, G. Watkins, and W. Jiang, "The possible correlation of Notch-1 and Notch-2 with clinical outcome and tumour clinicopathological parameters in human breast cancer," *International Journal of Molecular Medicine*, vol. 14, no. 5, pp. 779–786, 2004.

[90] N. Turner, M. B. Lambros, H. M. Horlings et al., "Integrative molecular profiling of triple negative breast cancers identifies amplicon drivers and potential therapeutic targets," *Oncogene*, vol. 29, no. 14, pp. 2013–2023, 2010.

[91] C. Hu, A. Diévart, M. Lupien, E. Calvo, G. Tremblay, and P. Jolicoeur, "Overexpression of activated murine Notch1 and Notch3 in transgenic mice blocks mammary gland development and induces mammary tumors," *The American Journal of Pathology*, vol. 168, no. 3, pp. 973–990, 2006.

[92] H. Hirose, H. Ishii, K. Mimori et al., "Notch pathway as candidate therapeutic target in Her2/Neu/ErbB2 receptor-negative breast tumors," *Oncology Reports*, vol. 23, no. 1, pp. 35–43, 2010.

[93] L. Choy, T. Hagenbeek, M. Solon et al., "Constitutive NOTCH3 signaling promotes the growth of basal breast cancers," *Cancer Research*, vol. 77, no. 6, pp. 1439–1452, 2017.

[94] F. Andre, B. Job, P. Dessen et al., "Molecular characterization of breast cancer with high-resolution oligonucleotide comparative genomic hybridization array," *Clinical Cancer Research*, vol. 15, no. 2, pp. 441–451, 2009.

[95] B. K. Linderholm, H. Hellborg, U. Johansson et al., "Significantly higher levels of vascular endothelial growth factor (VEGF) and shorter survival times for patients with primary operable triple-negative breast cancer," *Annals of Oncology*, vol. 20, no. 10, pp. 1639–1646, 2009.

[96] R. A. Mohammed, I. O. Ellis, A. M. Mahmmod et al., "Lymphatic and blood vessels in basal and triple-negative breast cancers: characteristics and prognostic significance," *Modern Pathology*, vol. 24, no. 6, pp. 774–785, 2011.

[97] M. Reedijk, "Notch signaling and breast cancer," *Advances in Experimental Medicine and Biology*, vol. 727, pp. 241–257, 2012.

[98] S. Xue, L. He, X. Zhang, J. Zhou, F. Li, and X. Wang, "Expression of Jagged1/Notch3 signaling pathway and their relationship with the tumor angiogenesis in TNBC," *Archives of Medical Research*, vol. 48, no. 2, pp. 169–179, 2017.

[99] N. Yamaguchi, T. Oyama, E. Ito et al., "NOTCH3 signaling pathway plays crucial roles in the proliferation of ErbB2-negative human breast cancer cells," *Cancer Research*, vol. 68, no. 6, pp. 1881–1888, 2008.

[100] M. Pelullo, R. Quaranta, C. Talora et al., "Notch3/Jagged1 circuitry reinforces notch signaling and sustains T-ALL," *Neoplasia*, vol. 16, no. 12, pp. 1007–1017, 2014.

[101] W. Kozlow and T. A. Guise, "Breast cancer metastasis to bone: mechanisms of osteolysis and implications for therapy," *Journal of Mammary Gland Biology and Neoplasia*, vol. 10, no. 2, pp. 169–180, 2005.

[102] Y. Nefedova, P. Cheng, M. Alsina et al., "Involvement of Notch-1 signaling in bone marrow stroma-mediated de novo drug resistance of myeloma and other malignant lymphoid cell lines," *Blood*, vol. 103, no. 9, pp. 3503–3510, 2004.

[103] Z. Zhang, H. Wang, S. Ikeda et al., "Notch3 in human breast cancer cell lines regulates osteoblast-cancer cell interactions and osteolytic bone metastasis," *The American Journal of Pathology*, vol. 177, no. 3, pp. 1459–1469, 2010.

[104] A. A. Leontovich, M. Jalalirad, J. L. Salisbury et al., "NOTCH3 expression is linked to breast cancer seeding and distant metastasis," *Breast Cancer Research*, vol. 20, no. 1, p. 105, 2018.

[105] H. Lin, Y. Liang, X. Dou et al., "Notch3 inhibits epithelial–mesenchymal transition in breast cancer via a novel mechanism, upregulation of GATA-3 expression," *Oncogenesis*, vol. 7, no. 8, p. 59, 2018.

[106] X. Wen, M. Chen, Y. Wu et al., "Inhibitor of DNA binding 2 inhibits epithelial-mesenchymal transition via up-regulation of Notch3 in breast cancer," *Translational Oncology*, vol. 11, no. 5, pp. 1259–1270, 2018.

[107] X. Zhang, X. Liu, J. Luo et al., "Notch3 inhibits epithelial–mesenchymal transition by activating Kibra-mediated Hippo/YAP signaling in breast cancer epithelial cells," *Oncogenesis*, vol. 5, no. 11, pp. e269–e269, 2016.

[108] J. Xu, F. Song, T. Jin et al., "Prognostic values of Notch receptors in breast cancer," *Tumor Biology*, vol. 37, no. 2, pp. 1871–1877, 2016.

[109] D. W. McMillin, J. M. Negri, and C. S. Mitsiades, "The role of tumour–stromal interactions in modifying drug response: challenges and opportunities," *Nature Reviews Drug Discovery*, vol. 12, no. 3, pp. 217–228, 2013.

[110] M. C. Boelens, T. J. Wu, B. Y. Nabet et al., "Exosome transfer from stromal to breast cancer cells regulates therapy resistance pathways," *Cell*, vol. 159, no. 3, pp. 499–513, 2014.

[111] G. Diluvio, F. Del Gaudio, M. V. Giuli et al., "NOTCH3 inactivation increases triple negative breast cancer sensitivity to gefitinib by promoting EGFR tyrosine dephosphorylation and its intracellular arrest," *Oncogenesis*, vol. 7, no. 5, p. 42, 2018.

[112] K. A. Hoadley, V. J. Weigman, C. Fan et al., "EGFR associated expression profiles vary with breast tumor subtype," *BMC Genomics*, vol. 8, no. 1, p. 258, 2007.

[113] D. Gallahan, C. Kozak, and R. Callahan, "A new common integration region (int-3) for mouse mammary tumor virus on mouse chromosome 17," *Journal of Virology*, vol. 61, no. 1, pp. 218-20, 1987.

[114] D. Gallahan, C. Jhappan, G. Robinson, L. Hennighausen, R. Sharp, and E. Kordon, "Expression of a truncated Int3 gene in developing secretory mammary epithelium specifically retards lobular differentiation resulting in tumorigenesis," *Cancer Research*, vol. 56, no. 8, pp. 1775–1785, 1996.

[115] K. Yao, P. Rizzo, P. Rajan et al., "Notch-1 and Notch-4 receptors as prognostic markers in breast cancer," *International Journal of Surgical Pathology*, vol. 19, no. 5, pp. 607–613, 2011.

[116] J. Wang, X. Wei, X. Dou, W. Huang, C. Du, and G. Zhang, "The association between Notch4 expression, and clinicopathological characteristics and clinical outcomes in patients with breast cancer," *Oncology Letters*, vol. 15, no. 6, pp. 8749–8755, 2018.

[117] D. A. Lawson, N. R. Bhakta, K. Kessenbrock et al., "Single-cell analysis reveals a stem-cell program in human metastatic breast cancer cells," *Nature*, vol. 526, no. 7571, pp. 131–135, 2015.

[118] N. P. Castro, N. D. Fedorova-Abrams, A. S. Merchant et al., "Cripto-1 as a novel therapeutic target for triple negative breast cancer," *Oncotarget*, vol. 6, no. 14, pp. 11910–11929, 2015.

[119] K. Watanabe, T. Nagaoka, J. M. Lee et al., "Enhancement of Notch receptor maturation and signaling sensitivity by Cripto-1," *The Journal of Cell Biology*, vol. 187, no. 3, pp. 343–353, 2009.

[120] N. P. Castro, M. C. Rangel, A. S. Merchant et al., "Sulforaphane suppresses the growth of triple-negative breast cancer stem-like cells in vitro and in vivo," *Cancer Prevention Research*, vol. 12, no. 3, pp. 147–158, 2019.

[121] M. Balic, H. Lin, L. Young et al., "Most early disseminated cancer cells detected in bone marrow of breast cancer patients have a putative breast cancer stem cell phenotype," *Clinical Cancer Research*, vol. 12, no. 19, pp. 5615–5621, 2006.

[122] S. Pece, D. Tosoni, S. Confalonieri et al., "Biological and molecular heterogeneity of breast cancers correlates with their cancer stem cell content," *Cell*, vol. 140, no. 1, pp. 62–73, 2010.

[123] J. Stingl and C. Caldas, "Molecular heterogeneity of breast carcinomas and the cancer stem cell hypothesis," *Nature Reviews Cancer*, vol. 7, no. 10, pp. 791–799, 2007.

[124] A. Raouf, Y. Zhao, K. To et al., "Transcriptome analysis of the normal human mammary cell commitment and differentiation process," *Cell Stem Cell*, vol. 3, no. 1, pp. 109–118, 2008.

[125] H. Harrison, G. Farnie, S. J. Howell et al., "Regulation of breast cancer stem cell activity by signaling through the Notch4 receptor," *Cancer Research*, vol. 70, no. 2, pp. 709–718, 2010.

[126] G. Farnie, R. B. Clarke, K. Spence et al., "Novel cell culture technique for primary ductal carcinoma in situ: role of Notch and epidermal growth factor receptor signaling pathways," *Journal of the National Cancer Institute*, vol. 99, no. 8, pp. 616–627, 2007.

[127] A. Rustighi, L. Tiberi, A. Soldano et al., "The prolyl-isomerase Pin1 is a Notch1 target that enhances Notch1 activation in cancer," *Nature Cell Biology*, vol. 11, no. 2, pp. 133–142, 2009.

[128] A. Rustighi, A. Zannini, L. Tiberi et al., "Prolyl-isomerase Pin1 controls normal and cancer stem cells of the breast," *EMBO Molecular Medicine*, vol. 6, no. 1, pp. 99–119, 2014.

[129] S. A. O'Toole, J. M. Beith, E. K. Millar et al., "Therapeutic targets in triple negative breast cancer," *Journal of Clinical Pathology*, vol. 66, no. 6, pp. 530–542, 2013.

[130] V. S. Jamdade, N. Sethi, N. A. Mundhe, P. Kumar, M. Lahkar, and N. Sinha, "Therapeutic targets of triple-negative breast cancer: a review," *British Journal of Pharmacology*, vol. 172, no. 17, pp. 4228–4237, 2015.

[131] H. E. Bryant, N. Schultz, H. D. Thomas et al., "Specific killing of BRCA2-deficient tumours with inhibitors of poly(ADP-ribose) polymerase," *Nature*, vol. 434, no. 7035, pp. 913–917, 2005.

[132] N. A. Makretsov, D. G. Huntsman, T. O. Nielsen et al., "Hierarchical clustering analysis of tissue microarray immunostaining data identifies prognostically significant groups of breast carcinoma," *Clinical Cancer Research*, vol. 10, no. 18 Pt 1, pp. 6143–6151, 2004.

[133] K. Nakai, M. C. Hung, and H. Yamaguchi, "A perspective on anti-EGFR therapies targeting triple-negative breast cancer," *American Journal of Cancer Research*, vol. 6, no. 8, pp. 1609–1623, 2016.

[134] L. A. Carey, H. S. Rugo, P. K. Marcom et al., "TBCRC 001: randomized phase II study of cetuximab in combination with carboplatin in stage IV triple-negative breast cancer," *Journal of Clinical Oncology*, vol. 30, no. 21, pp. 2615–2623, 2012.

[135] J. O'Shaughnessy, "A decade of letrozole: FACE," *Breast Cancer Research and Treatment*, vol. 105, no. S1, pp. 67–74, 2007.

[136] J. Xu, J. R. Prosperi, N. Choudhury, O. I. Olopade, and K. H. Goss, "Beta-catenin is required for the tumorigenic behavior of triple-negative breast cancer cells," *PloS One*, vol. 10, no. 2, Article ID 4319896, p. e0117097, 2015.

[137] H. Zhao, Q. Yang, Y. Hu, and J. Zhang, "Antitumor effects and mechanisms of olaparib in combination with carboplatin and BKM120 on human triple negative breast cancer cells," *Oncology Reports*, vol. 40, no. 6, pp. 3223–3234, 2018.

[138] M. Yunokawa, F. Koizumi, Y. Kitamura et al., "Efficacy of everolimus, a novel mTOR inhibitor, against basal-like triple-negative breast cancer cells," *Cancer Science*, vol. 103, no. 9, pp. 1665–1671, 2012.

[139] D. Amara, D. M. Wolf, L. van 't Veer, L. Esserman, M. Campbell, and C. Yau, "Co-expression modules identified from published immune signatures reveal five distinct immune subtypes in breast cancer," *Breast Cancer Research and Treatment*, vol. 161, no. 1, pp. 41–50, 2017.

[140] Z. Liu, M. Li, Z. Jiang, and X. Wang, "A comprehensive immunologic portrait of triple-negative breast cancer," *Translational Oncology*, vol. 11, no. 2, pp. 311–329, 2018.

[141] E. Andreopoulou, S. J. Schweber, J. A. Sparano, and H. M. Mcdaid, "Therapies for triple negative breast cancer," *Expert Opinion on Pharmacotherapy*, vol. 16, no. 7, pp. 983–998, 2015.

[142] S. Checquolo, R. Palermo, S. Cialfi et al., "Differential subcellular localization regulates c-Cbl E3 ligase activity upon Notch3 protein in T-cell leukemia," *Oncogene*, vol. 29, no. 10, pp. 1463–1474, 2010.

[143] S. Cialfi, R. Palermo, S. Manca et al., "Glucocorticoid sensitivity of T-cell lymphoblastic leukemia/lymphoma is associated with glucocorticoid receptor-mediated inhibition of Notch1 expression," *Leukemia*, vol. 27, no. 2, pp. 485–488, 2013.

[144] G. Franciosa, G. Diluvio, F. D. Gaudio et al., "Prolyl-isomerase Pin1 controls Notch3 protein expression and regulates T-ALL progression," *Oncogene*, vol. 35, no. 36, pp. 4741–4751, 2016.

[145] N. Takebe, D. Nguyen, and S. X. Yang, "Targeting notch signaling pathway in cancer: clinical development advances and challenges," *Pharmacology & Therapeutics*, vol. 141, no. 2, pp. 140–149, 2014.

[146] I. Krop, T. Demuth, T. Guthrie et al., "Phase I pharmacologic and pharmacodynamic study of the gamma secretase (Notch) inhibitor MK-0752 in adult patients with advanced solid tumors," *Journal of Clinical Oncology*, vol. 30, no. 19, pp. 2307–2313, 2012.

[147] L. Luistro, W. He, M. Smith et al., "Preclinical profile of a potent-secretase inhibitor targeting notch signaling with in vivo efficacy and pharmacodynamic properties," *Cancer Research*, vol. 69, no. 19, pp. 7672–7680, 2009.

[148] C. C. Zhang, A. Pavlicek, Q. Zhang et al., "Biomarker and pharmacologic evaluation of the gamma-secretase inhibitor PF-03084014 in breast cancer models," *Clinical Cancer Research*, vol. 18, no. 18, pp. 5008–5019, 2012.

[149] C. Séveno, D. Loussouarn, S. Bréchet, M. Campone, P. Juin, and S. Barillé-Nion, "γ-Secretase inhibition promotes cell death, Noxa upregulation, and sensitization to BH3 mimetic ABT-737 in human breast cancer cells," *Breast Cancer Research*, vol. 14, no. 3, p. R96, 2012.

[150] M. Fouladi, C. F. Stewart, J. Olson et al., "Phase I trial of MK-0752 in children with refractory CNS malignancies: a pediatric brain tumor consortium study," *Journal of Clinical Oncology*, vol. 29, no. 26, pp. 3529–3534, 2011.

[151] R. Olsauskas-Kuprys, A. Zlobin, and C. Osipo, "Gamma secretase inhibitors of Notch signaling," *OncoTargets and Therapy*, vol. 6, pp. 943–955, 2013.

[152] A. F. Schott, M. D. Landis, G. Dontu et al., "Preclinical and clinical studies of gamma secretase inhibitors with docetaxel on human breast tumors," *Clinical Cancer Research*, vol. 19, no. 6, pp. 1512–1524, 2013.

[153] C. C. Zhang, Z. Yan, Q. Zong et al., "Synergistic effect of the γ-secretase inhibitor pf-03084014 and docetaxel in breast cancer

models," *Stem Cells Translational Medicine*, vol. 2, no. 3, pp. 233–242, 2013.

[154] M. A. Locatelli, P. Aftimos, E. C. Dees et al., "Phase I study of the gamma secretase inhibitor PF-03084014 in combination with docetaxel in patients with advanced triple-negative breast cancer," *Oncotarget*, vol. 8, no. 2, pp. 2320–2328, 2017.

[155] Y. Wu, C. Cain-Hom, L. Choy et al., "Therapeutic antibody targeting of individual Notch receptors," *Nature*, vol. 464, no. 7291, pp. 1052–1057, 2010.

[156] A. Sharma, A. N. Paranjape, A. Rangarajan, and R. R. Dighe, "A monoclonal antibody against human Notch1 ligand-binding domain depletes subpopulation of putative breast cancer stem-like cells," *Molecular Cancer Therapeutics*, vol. 11, no. 1, pp. 77–86, 2012.

[157] W.-C. Yen, M. M. Fischer, F. Axelrod et al., "Targeting notch signaling with a Notch2/Notch3 antagonist (tarextumab) inhibits tumor growth and decreases tumor-initiating cell frequency," *Clinical Cancer Research*, vol. 21, no. 9, pp. 2084–2095, 2015.

[158] K. Li, Y. Li, W. Wu et al., "Modulation of notch signaling by antibodies specific for the extracellular negative regulatory region of NOTCH3," *The Journal of Biological Chemistry*, vol. 283, no. 12, pp. 8046–8054, 2008.

[159] T. Hoey, W. Yen, F. Axelrod et al., "DLL4 blockade inhibits tumor growth and reduces tumor-initiating cell frequency," *Cell Stem Cell*, vol. 5, no. 2, pp. 168–177, 2009.

[160] H. Zheng, Y. Bae, S. Kasimir-Bauer, R. Tang, J. Chen, and G. Ren, "Therapeutic antibody targeting tumor- and osteoblastic niche-derived jagged1 sensitizes bone metastasis to chemotherapy," *Cancer Cell*, vol. 32, no. 6, pp. 731–747, 2017.

[161] L. S. Rosen, R. Wesolowski, R. Baffa et al., "A phase I, dose-escalation study of PF-06650808, an anti-Notch3 antibody–drug conjugate, in patients with breast cancer and other advanced solid tumors," *Investigational New Drugs*, 2019.

[162] M. Mori, L. Tottone, D. Quaglio et al., "Identification of a novel chalcone derivative that inhibits Notch signaling in T-cell acute lymphoblastic leukemia," *Scientific Reports*, vol. 7, no. 1, p. 2213, 2017.

[163] D. Bellavia, R. Palermo, M. P. Felli, I. Screpanti, and S. Checquolo, "Notch signaling as a therapeutic target for acute lymphoblastic leukemia," *Expert Opinion on Therapeutic Targets*, vol. 22, no. 4, pp. 331–342, 2018.

Hindawi
Journal of Oncology
Volume 2019, Article ID 4382606, 10 pages
https://doi.org/10.1155/2019/4382606

Review Article

A Review of the Hereditary Component of Triple Negative Breast Cancer: High- and Moderate-Penetrance Breast Cancer Genes, Low-Penetrance Loci, and the Role of Nontraditional Genetic Elements

Darrell L. Ellsworth,[1] Clesson E. Turner,[2] and Rachel E. Ellsworth [2,3]

[1]*E-Squared Genomic Solutions, Johnstown, PA, USA*
[2]*Murtha Cancer Center/Research Program, Uniformed Services University and Walter Reed National Military Medical Center, Bethesda, MD, USA*
[3]*Henry M Jackson Foundation for the Advancement of Military Medicine, Bethesda, MD, USA*

Correspondence should be addressed to Rachel E. Ellsworth; rellsworth@murthacancercenter.org

Received 8 April 2019; Accepted 23 June 2019; Published 9 July 2019

Guest Editor: Chia-Jung Li

Triple negative breast cancer (TNBC), representing 10-15% of breast tumors diagnosed each year, is a clinically defined subtype of breast cancer associated with poor prognosis. The higher incidence of TNBC in certain populations such as young women and/or women of African ancestry and a unique pathological phenotype shared between TNBC and BRCA1-deficient tumors suggest that TNBC may be inherited through germline mutations. In this article, we describe genes and genetic elements, beyond *BRCA1* and *BRCA2*, which have been associated with increased risk of TNBC. Multigene panel testing has identified high- and moderate-penetrance cancer predisposition genes associated with increased risk for TNBC. Development of large-scale genome-wide SNP assays coupled with genome-wide association studies (GWAS) has led to the discovery of low-penetrance TNBC-associated loci. Next-generation sequencing has identified variants in noncoding RNAs, viral integration sites, and genes in underexplored regions of the human genome that may contribute to the genetic underpinnings of TNBC. Advances in our understanding of the genetics of TNBC are driving improvements in risk assessment and patient management.

1. Introduction

Breast cancer is a complex disease characterized by clinical, pathological, and molecular heterogeneity, which may influence risk assessment, diagnosis, treatment, and clinical outcomes [1]. Pathological characterization of breast disease includes a number of variables such as histological architecture, degree of cellular differentiation, tumor size, presence of local or distant metastasis, and hormone receptor and human epidermal growth factor receptor 2 (HER2) status.

Triple negative breast cancers (TNBC), which do not express the estrogen (ER) or progesterone receptors (PR) and have little or no HER2 protein expression, account for 10-15% of breast cancers diagnosed each year [2]. TNBC represents an aggressive form of disease, often diagnosed at a later stage, characterized by high-tumor grade, larger size, poorly differentiated histology, more frequent lymph node metastases, and younger age at diagnosis [3]. TNBC is more likely to present as an interval cancer, appearing between screening mammograms, possibly due to higher proliferation rates than other tumor types [4]. Risk of distant metastasis and death are significantly higher in patients with TNBC within five years of diagnosis [3], and TNBC displays distinctive patterns of metastasis with a higher affinity for lung, brain, and distant lymph nodes compared to other subtypes.

Like all types of breast cancer, TNBC exhibits marked heterogeneity in terms of histology, patterns of metastatic dissemination, response to therapies, and patient outcomes.

While the majority of TNBC are invasive ductal carcinomas, other histologies may be triple negative as well, with five-year survival outcomes ranging from 100% in patients with medullary tumors to 56% in those with metaplastic TNBC [5]. Although there is significant overlap between TNBC and basal-like tumors, as defined by immunohistochemistry (IHC) and patterns of gene expression, 28% of TNBC are classified as luminal A, luminal B, HER2-enriched, or normal-like [6]. Evaluation of TNBC at the gene expression level has shown variability in levels of estrogen related genes, genes involved in oxidation reduction, and proliferation genes, suggesting that additional subclassification of TNBC is warranted [7]. Cluster analysis of 587 TNBC identified six subtypes including basal-like 1, basal-like 2, immunomodulatory, mesenchymal, mesenchymal stem-like, and luminal androgen receptor, each of which may be responsive to different targeted or chemotherapeutic agents [8].

A number of risk factors have been associated with TNBC that have not been linked to increased risk for other cancer subtypes. In contrast to luminal A tumors, TNBC/basal-like tends to be associated with younger age at diagnosis, African ancestry, younger age at menarche and at first full-term pregnancy, higher parity, lack of breastfeeding, and higher BMI and waist-to-hip circumference ratio [2, 9–11]. The frequency of TNBC in African Americans (29.8%) is intermediate between that in West African women (53.2%) and White American women (15.5%), suggesting a genetic component to TNBC [12]. Strong associations between TNBC and BRCA mutation status have been reported: 70-90% and 16-23% of breast tumors in *BRCA1* and *BRCA2* mutation carriers are TNBC [11]; however, germline mutations in *BRCA1* and *BRCA2* only account for 15.4% of patients with TNBC [13], and the prevalence of *BRCA1* and *BRCA2* mutations is lower in African American women (20.4%) with TNBC compared to European American women (33.3%) [14]. These data suggest that TNBC has a genetic component and genes other than *BRCA1* and *BRCA2* may play a role in disease etiology. In this review we examine current data regarding the contribution of germline mutations in high- and moderate-penetrance genes to TNBC. In addition, we evaluate the latest genome-wide association studies (GWAS) and candidate gene approaches to identify low-penetrance genes. Finally, we consider the role of nontraditional genetic variants including single nucleotide polymorphisms (SNPs) in microRNA (miRNA) binding sites, retroelements, and novel sequences not present in the current reference genome in the etiology of TNBC.

2. Methods

Relevant literature was identified by searching the PubMed database (https://www.ncbi.nlm.nih.gov/pubmed). Search terms included TRIPLE NEGATIVE BREAST CANCER, GENETICS, HEREDITARY CANCER, miRNA, and VIRUS INTEGRATION. Only articles written in English were included. To ensure data presented here were current, articles published within the last 12 months and/or meta-analyses are highlighted.

3. GENES

3.1. High-Penetrance Breast Cancer Genes

3.1.1. BRCA1 and BRCA2. *BRCA1* and *BRCA2* are known to be tumor suppressor genes that function in DNA repair pathways. Cells lacking functional BRCA1 or BRCA2 are deficient for double-stranded break repair, resulting in genomic instability that leads to cancer predisposition. Current clinical data suggest BRCA1- and BRCA2-deficient tumors may have heightened sensitivity to platinum agents or poly (ADP-ribose) polymerase I (PARP) inhibitors [25]. In a large collection of families with hereditary breast cancer (n=237), 52% of families had disease that was likely attributable to mutations in *BRCA1* while 32% had disease linked to *BRCA2* [26]. Rebbeck et al. investigated whether the location or type of *BRCA1/BRCA2* mutations is associated with variation in breast and ovarian cancer risk. Patients carrying mutations in exon 11 of *BRCA1* appeared to have different disease phenotypes than patients carrying other *BRCA1* mutations. Similarly, mutations in exon 11 of *BRCA2* were associated with variability in breast and ovarian cancer risk [27]. Mutations in both genes have been associated with increased risk of TNBC albeit at different frequencies and within different age groups.

The first breast cancer susceptibility gene, *BRCA1*, was identified in 1994 [28]. *BRCA1* is located on chromosome 17q21 and is comprised of 24 exons, 22 of which encode an 1863 amino acid protein. The BRCA1 protein has multiple sequence motifs including RING, DNA-binding, and BRCA1 C-terminus (BCTR) domains that allow BRCA1 to interact with other proteins and assist in subcellular localization. *BRCA1* is a tumor suppressor gene that contributes to repair of damaged replication forks and double-strand breaks, transcriptional regulation in response to DNA damage, chromatin remodeling, and regulation of cell division, apoptosis, and transcription [29]. *BRCA2* is a tumor suppressor gene located on chromosome 13q12 that was identified in 1995 [30]. *BRCA2* has 27 exons and the BRCA2 protein interacts with RAD51 through the BRC motif. BRCA2 is also a transcriptional coregulator involved in DNA repair through homologous recombination.

As early as 1998, histological characterization revealed that in comparison with sporadic tumors, tumors in *BRCA1* mutation carriers exhibited a distinct phenotype that includes high mitotic counts, pushing margins, and lymphocytic infiltration [31]. Histologic characteristics of TNBC also include high-grade with high mitotic indices, regions of central necrosis, conspicuous lymphocytic infiltrate, and pushing borders [32]. In fact, TNBC represents the predominant tumor type in patients with *BRCA1* mutations, accounting for 71% (range 42-100%) of tumors, while TNBC has been diagnosed in only 25% of patients with germline *BRCA2* mutations [33]. In contrast, the frequency of *BRCA1* or *BRCA2* mutations in women with TNBC is generally lower, with an average of 35% (range 9-100%) and 8% (2-12%) of women with TNBC harboring germline BRCA1 and BRCA2 mutations, respectively. In addition to differences in mutation frequency, age distribution differs between *BRCA1* and *BRCA2* positive patients with TNBC, with an average age

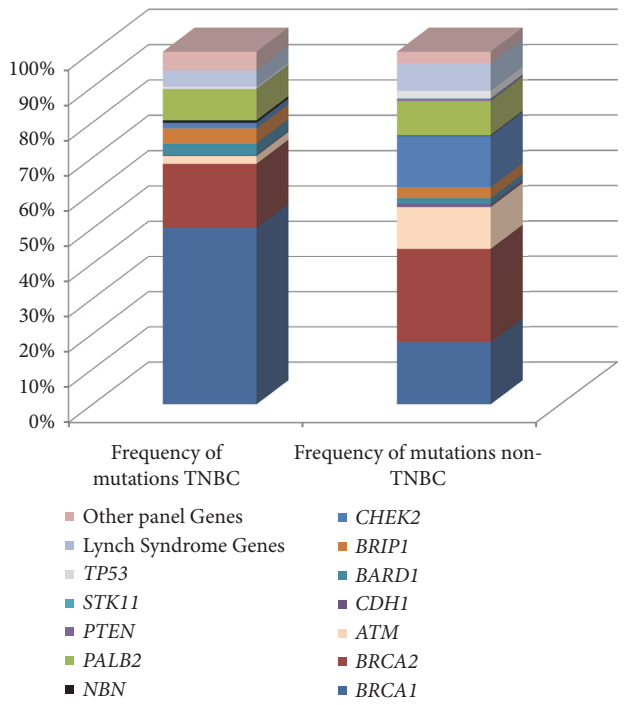

Figure 1: Frequency of mutations by gene within women carrying pathogenic germline mutations with TNBC (n=692) or non-TNBC subtypes (n=2,696). Adapted from Buys et al. 2017.

at diagnosis of 47.2 years and 58.8 years in those with *BRCA1* and *BRCA2* mutations, respectively [34]. In a recent study that included over 10,000 patients with TNBC, germline mutations were associated with odds ratios of 16.27-26.90 for *BRCA1* and 5.42-6.33 for *BRCA2* [35].

3.1.2. PALB2. The BRCA2 binding protein known as partner and localizer of BRCA2 (*PALB2*) stabilizes and regulates BRCA2 through localization and stabilization within important nuclear structures such as chromatin and the nuclear matrix and by promotion of recombination repair and checkpoint functions [36]. *PALB2* was recently classified as a high-risk breast cancer gene with an odds ratio (OR) of 7.46 [95% confidence interval (CI)=5.12-11.19] [37]. Mutations in *PALB2* are associated with aggressive disease. Over half (54.5%) of the familial and sporadic breast cancer patients from Finland who carried the 1592delT *PALB2* mutation presented with TNBC compared to other familial (12.2%) or sporadic (9.4%) breast cancer patients [38]. Similarly, in a predominantly European-Caucasian cohort of women, 46% of tumors in women with *PALB2* mutations were TNBC [39]. When mutation profiles were determined in a cohort of 4,797 women diagnosed with TNBC, panel testing performed at Myriad Genetics, found that 1.3% of women had pathogenic variants in *PALB2* (Figure 1) [40]. In a similar cohort of 1,824 women with TNBC unselected for family history of cancer, deleterious mutations in *PALB2* were detected in 1.2% of patients [41]. In a group of 347 Australian women with TNBC the prevalence of deleterious *PALB2* germline mutations was ~1% [42]. A recent study of 10,901 women with TNBC (8,753 women with clinical test results and 2,148 tested in the research setting) found that germline mutations in *PALB2* were associated with high-risk of TNBC (OR=14.41; 95%CI=9.27-22.60) and were enriched in patients with TNBC compared to non-TNBC tumors (OR2.12; 95% CI=1.63-2.74) [35].

3.1.3. TP53. Tumor protein p53 (*TP53*), which encodes the p53 phosphoprotein, is a tumor suppressor gene that plays a critical role in each of the 10 Hallmarks of Cancer as defined by Hanahan and Weinberg [43]. As a result of this functional diversity, the p53 signaling pathway is at least partially disrupted in most human cancers and *TP53* mutations are the most frequent genetic changes seen in human cancers [44]. Although the frequency of somatic mutations in *TP53* is higher in basal-like tumors than any other subtype [45], germline mutations in *TP53* have not been associated with an increased risk of TNBC. The mutation rate for *TP53* in a cohort of 2,134 BRCA1/BRCA2 mutation negative women with familial breast cancer was 0.52% and *TP53* mutations carriers showed enrichment for HER2+ tumors [39]. In a large cohort of 35,409 women with a single diagnosis of breast cancer, mutations in *TP53* were detected in 0.7% of women with TNBC compared to 2.1% of those with non-TNBC subtypes [40]. In 133 women from Taiwan with early-onset and/or family history of breast cancer, only two women carried a pathogenic mutation in *TP53* and both had ER+/HER2+ tumors [46]. Similarly, only one of 1,824 women with TNBC evaluated by Couch et al. [41] carried a *TP53* mutation. These results suggest that germline mutations in *TP53* are not associated with increased risk of TNBC.

3.1.4. PTEN. Phosphatase and tensin homolog (*PTEN*) is a tumor suppressor gene involved in the regulation of the phosphoinositol-3-kinase and AKT signaling pathways and control of cellular proliferation and survival. *PTEN* is the second most frequently mutated gene in human cancers (after *TP53*) and germline mutations in *PTEN* are frequently observed in cancer susceptibility syndromes [47]. PTEN has recently been shown to protect the genome from instability by maintaining chromosomal integrity. While women with Cowden syndrome who carry germline mutations in *PTEN* have a lifetime risk of breast cancer of 50% [48], there is no consistent breast cancer phenotype associated with *PTEN* mutations. Most *PTEN*-associated tumors are more likely to be luminal than TNBC. Observations that (1) prevalence of pathogenic mutations in *PTEN* did not differ significantly in women with TNBC (n=692) compared to those with non-TNBC tumors (n=2,696) [40] and (2) only one deleterious mutation in 267 patients was observed [41] support the idea that mutations in *PTEN* are not associated with increased risk of TNBC.

3.1.5. STK11. The serine/threonine protein kinase 11 (*STK11*) gene is a highly penetrant breast cancer gene that regulates energy metabolism and cell polarity. Patients who carry mutation in *STK11* present with Peutz-Jeghers syndrome with high risk for various cancers, including breast (lifetime

risk 24-54%) and cervical cancers [49]. Currently, there is little evidence to support an association between germline mutations in *STK11* and TNBC as mutations in *STK11* were not observed in (1) a cohort of 2,134 BRCA1/BRCA2 mutation negative women with familial breast cancer, (2) 1,824 women of primarily white ethnicity with TNBC [39, 41], and (3) 4,797 women of mixed ethnicities with TNBC [40].

3.1.6. CDH1. The Cadherin 1 (*CDH1*) gene encodes an adhesion molecule involved in maintenance of epithelial cell morphology. Germline mutations in *CDH1* have been associated with increased risk of Hereditary Diffuse Gastric Cancer, a cancer predisposition syndrome associated with increased lifetime risk of breast cancer, particularly invasive lobular carcinoma (ILCA) [48]. Given that ILCAs are frequently ER+, an association between germline mutations in *CDH1* and TNBC is unlikely. Accordingly, germline mutations in *CDH1* were rare (0.0-0.3%) in women with TNBC [40, 41].

3.2. Moderate-Penetrance Breast Cancer Genes

3.2.1. RAD51D. The human RAD51, S Cerevisiae, homolog of D (*RAD51D*) gene plays an important role in maintaining genomic integrity through homologous recombination and repair of double-stranded breaks and inter-strand cross-links in DNA. Mutations in *RAD51D* are associated with a >3-fold increased risk of breast cancer. Mutation rates in patients with TNBC range from 0.20 to 0.95% and tend to be higher in women with TNBC (0.90%) compared to those with non-TNBC tumors (0.5%) [40, 41, 50, 51]. Recent data from Shimelis et al. [35] found that although the mutation frequency of *RAD51D* in 8,243 patients with TNBC was low (0.3%), risk of developing TNBC was high (OR 6.97; 95% CI =2.6-18.66). Together, these data suggest that although the frequency of mutations in *RAD51D* is low, mutation carriers are at increased risk for TNBC.

3.2.2. ATM. The ataxia telangiectasia mutated (*ATM*) gene encodes a phosphatidylinositol 3-kinase that phosphorylates key substrates involved in DNA repair and control of the cell cycle. In a large cohort of European women (42,671 cases and 42,164 controls) an association with overall breast cancer risk was observed with the c.7271 T>G mutation; however, as tumors were not stratified by subtype, a specific link to TNBC could not be determined [52]. In a group of Polish women with TNBC unselected for family history, one woman out of 158 with TNBC harbored a mutation in *ATM* whereas no *ATM* mutations were detected in 44 women with non-TNBC hereditary breast cancer [53]. Additional studies observed an enrichment of *ATM* mutations in patients with ER positive tumors [39, 46, 54] and a five-fold increase in *ATM* mutations in patients with non-TNBC compared to TNBC tumors [40].

3.2.3. CDKN2A. The cyclin-dependent kinase inhibitor 2A (*CDKN2A*) gene is a tumor suppressor gene involved in cell cycle regulation. [37]. The role of germline mutations in *CDKN2A* in hereditary breast cancers has been difficult to study due to the limited number of variants observed in case-control studies. A mutation frequency of 1.2% has been reported in 692 patients with TNBC compared to 0.9% in 2,696 patients with non-TNBC [40].

3.2.4. MSH2. The MutS, E. coli, homolog of 2 (*MSH2*) gene is involved in DNA mismatch repair and is associated with autosomal dominant Lynch Syndrome. Mutations in *MSH2* may contribute to genomic instability and an increased mutation rate in cancer cells. Evaluation of the G322D variant of *MSH2* in 70 Polish women with TNBC and age-matched controls revealed that the D allele was associated with decreased risk of TNBC (OR=0.11; 95 % CI=0.05-0.21) [55]. A relatively low mutation rate (0.7%) was observed in *MSH2* in women with TNBC compared to 1.2% in women with non-TNBC [40].

3.2.5. CHEK2. Checkpoint kinase 2 (*CHEK2*) encodes a serine threonine kinase involved in DNA repair that serves as a cell cycle checkpoint regulator and tumor suppressor gene. Mutations in *CHEK2* have been associated with various forms of cancer. A large study evaluating *CHEK2* mutations in breast cancer patients from Poland found that *CHEK2* carriers were significantly more likely to have ER+ (OR = 3.9; 95% CI = 2.7–5.4) than ER- (OR = 2.1; 95% CI = 1.3–3.3) tumors [56]. In a similar study, *CHEK2* mutations were enriched in Polish women with hereditary non-TNBC (11.3%) compared to those with TNBC (1.3%) [53]. In 35,409 women subjected to panel testing, the frequency of pathogenic *CHEK2* mutations was 1.6% in women with TNBC compared to 14.3% in those with other phenotypes [40].

3.2.6. BARD1. The BRCA1-associated RING domain 1 (*BARD1*) gene encodes a protein that interacts with BRCA1 to form a heterodimer, which functions in DNA repair. The heterodimer, essential for BRCA1 stability, may be disrupted by tumorigenic mutations in *BARD1* in patients with breast or ovarian cancer. Of 42 women with TNBC enrolled in the neoadjuvant Trial of Principle study, four harbored missense or nonsense mutations in *BARD1*, of which two (1347A>G and Arg658Cys) have been confirmed as pathogenic [57]. In a study of 105 women with TNBC from Spain, *BARD1* mutations were detected in two patients (1.9%) [50]. Likewise, nine (0.5%) of the 1,824 women in the Triple Negative Breast Cancer Consortium (TNBCC), had *BARD1* mutations [41]. Although not exclusive to TNBC, the mutation frequency in *BARD1* was 3.3% in women with TNBC compared to 1.7% in women with non-TNBC [40]. In a study of 4,032 Caucasian women with TNBC, the mutation rate of *BARD1* was 0.7% compared to 0.2% in women with non-TNBC and the OR for an association with TNBC compared to non-TNBC disease was 3.73 (95% CI=2.3-5.95) [35].

3.3. Low-Penetrance Breast Cancer Loci.

Mutations in high- and moderate-penetrance breast cancer genes account for ~14% of all TNBC cases [40, 41]. Genome-wide association studies (GWAS) over the last decade have identified SNPs that are associated with breast cancer risk in an additive fashion.

In an early study to identify susceptibility loci for breast cancer, ~266,000 SNPs across the genome were genotyped in 408 breast cancer cases with a strong family history and 400 controls from the United Kingdom. In the second phase of this study, ~12,000 SNPs that showed an association with breast cancer in phase I were genotyped in an additional 3,990 cases and 3,916 controls [58]. To determine whether any SNPs were reliably associated with breast cancer risk, the 30 most significant SNPs from phase II were further validated in an additional 21,860 cases and 22,578 controls. Six SNPs were associated with increased risk ($P \leq 10^{-5}$), including SNPs in or near the fibroblast growth factor receptor 2 (*FGFR2*; rs2981582) gene, lymphocyte-specific protein (*LSP1*; rs3817198), mitogen-activated protein kinase kinase kinase 1 (*MAP3K1*; rs889312), and tox high mobility group box family member 3 (*TOX3*; rs12443621 and rs8051542) and in the chromosome 8q24 region (rs13281615). These gene regions were further investigated by ER status in 23,039 cases and 26,273 controls from the Breast Cancer Association Consortium (BCAC) [59]. SNPs rs2981582 in *FGFR2* and rs13281615 (in 8q24) were more strongly associated with ER+ than ER- disease. Although rs3803662 showed the strongest association with ER- tumors, with women homozygous for the variant allele (AA) having an OR of 1.28 (95% CI=1.13-1.45), risk was higher for women with ER+ disease (OR=1.48, 95% CI=1.37-1.60). A 2011 study evaluated breast cancer risk associations with eight SNPs identified through GWAS and two in the candidate genes caspase 8, apoptosis-related cysteine protease (*CASP8*), and transforming growth factor, beta-1 (*TGFβ1*) by immunohistochemistry-defined subtypes [18]. Within the 885-1,644 TNBC cases available for study, five SNPs were significantly associated ($P \leq 0.02$) with TNBC including rs3803662 (*TOX3*; OR=1.21; 95% CI=1.11-1.30), rs889312 (*MAP3K1*, OR=1.11; 95% CI=1.02-1.20), rs3817198 (*LSP1*, OR=1.11; 95% CI=1.03-1.21), rs13387042 (chromosome 2q35, OR=1.12; 95% CI=1.05-1.21), and rs1982073 (*TGFβ1*, OR=1.11; 95% CI=1.01-1.23). In a meta-analysis of 4,754 ER- breast cancer cases and 31,663 controls from three GWAS, SNP rs2284378 on chromosome 20q11 was associated with ER- tumors ($P=1.1 \times 10^{-8}$) and showed a stronger association with TNBC (OR=1.16, $P=6.4 \times 10^{-3}$) than for ER-/HER2+ tumors (OR=1.07; P=0.41), although the differences did not reach statistical significance [60]. In a second meta-analysis of three GWAS including 4,193 ER- breast cancer cases and 35,194 controls, combined with 40 follow-up studies, variants at rs4245739 located in the 3′ region of the mouse double minute 4 homolog (*MDM4*) oncogene on chromosome 1q32.1 seemed to be specific to TNBC [16].

In addition to the loci summarized above, a GWAS approach identified the 19p13 chromosomal region as a modifier of breast cancer risk in *BRCA1* mutation positive individuals [23]. Five SNPs from 19p13 were genotyped in 2,301 women with TNBC and 3,949 controls to evaluate the association between the 19p13 locus and TNBC in the general population. Minor alleles for SNPs rs8170 (OR per A allele =1.28, 95% CI =1.16-1.41) and rs2363956 (OR per C allele=0.80, 95% CI 0.74-0.87) were associated with TNBC risk in women without *BRCA1* mutations. In the TNBCC, 22 known breast cancer susceptibility loci were studied in 2,980 Caucasian women and 4,978 controls to assess relationships with TNBC. Two SNPs from the 19p13.1 locus [rs8170 ($P=2.25 \times 10^{-8}$) and rs8100241 ($P=8.66 \times 10^{-7}$)] were associated with risk of TNBC, as were SNPs from the estrogen receptor (*ESR1*; rs2046210 and rs12662670), *RAD51L1* (rs999737), and *TOX3* (rs3803662) [21]. Subsequent studies in the BCAC using 48,869 breast cancer cases and 49,787 controls demonstrated that rs8170 was a TNBC-specific risk variant (OR=1.25; 95% CI=1.18-1.33) [24]. A haplotype analysis in this study that included both rs8170 and rs8100241 found that the C-G and T-G haplotypes were both associated with risk of TNBC (C-G OR=1.17; 95% CI=1.09–1.25 and T-G OR=1.35; 95% CI=1.25–1.46) compared with the C-A haplotype.

A GWAS that included women of both European ancestry (1,718 ER- cases, 3,670 controls) and African ancestry (1,004 ER- cases, 2,745 controls) identified a SNP on chromosome 5p15 (rs10069690) from the telomerase reverse transcriptase (*TERT*) – cleft lip and palate-associated transmembrane protein 1-like (*CLPTM1L*) gene region that was associated with TNBC. Combining genotype data from multiple studies for rs10069690 produced a per allele OR of 1.25 (95% CI=1.16-1.34, $P=1.1 \times 10^{-9}$) for risk of TNBC. For women with TNBC diagnosed at <50 years of age, the risk increased to 1.48 (95% CI=1.30-1.68, $P=1.9 \times 10^{-9}$) [61]. Lack of an association with ER+/HER2+ or ER+/HER2- disease suggests that, as observed for the chromosome 19p13 locus, the *TERT-CLPTM1L* locus is specific to TNBC. In a subsequent validation analysis using 15,252 *BRCA1* and 8,211 *BRCA2* mutation positive individuals to assess disease subtype-specific associations for 74 previously identified breast cancer susceptibility loci, several chromosomal regions discussed above, including 5p15.33 (*TERT*), 6q25.1 (*ESR1*), and 19p13.11, showed a significant association with increased risk of TNBC in *BRCA1* mutation positive individuals [20].

Pooled analysis of the Collaborative Oncological Gene-Environment Study (COGS) and TNBCC SNP data further refined the GWAS data [17]. Multiple data sets, consisting of 22 studies from 7 different countries were combined in a two-stage analysis. Evaluation of SNPs from 3,677 women with TNBC and 4,708 controls supported the association of 25 known breast cancer susceptibility loci, including 2q35, *LGR6*, *MDM4*, *TERT*, *ESR1*, *TOX3*, and 19p13.1 with TNBC. Newly identified associations with TNBC were observed for an additional 15 SNPs from 14 loci. Interestingly, SNPs in *CASP8*, *MAP3K1*, *LSP1*, and *FTO* were not found to be associated with risk of TNBC. More recently, Milne et al. performed GWAS in 21,468 patients with ER- disease and 18,908 BRCA1 mutation positive individuals combined with 100,594 controls [15]. When evaluating the subset of individuals with TNBC, associations with 10 previously reported loci were replicated and 10 new susceptibility loci were identified. To date, seven chromosomal loci have been associated with risk for TNBC in multiple studies (Table 1).

Table 1: Odds ratios for TNBC for loci identified in more than one study.

Location	Gene	SNP	Risk Allele	OR/HR	95% CI	P-value	Reference
1q32	*MDM4*	rs4245739	C	1.18	1.13-1.23	$4.3x10^{-15}$	[15]
			C	1.17	1.09-1.26	$3.1x10^{-5}$	[16]
			C	1.19	1.11-1.29	$4.0x10^{-6}$	[17]
2q35		rs13387042	G	0.93	0.87-1.00	0.049	[17]
			G	1.12	1.05-1.21	0.001	[18]
5p15	*TERT*	rs10069690	A	1.28	1.23-1.33	$2.4x10^{-33}$	[15]
			A	1.24	1.14-1.34	$1.4x10^{-7}$	[17]
			A	1.25	1.16-1.34	$1.1x10^{-9}$	[19]
			A	1.27	1.20-1.36	$5.2x10^{-14}$	[20]
		rs2736108	T	0.77	0.69-0.87	$8.3x10^{-6}$	[17]
6q25	*ESR1*	rs2046210	A	1.16	1.08-1.24	$5.3x10^{-5}$	[17]
			A	1.23	1.16-1.31	$5.5x10^{-12}$	[20]
			A	1.29	1.17-1.42	$4.4x10^{-7}$	[21]
		rs3757318	A	1.33	1.17-1.51	$9.3x10^{-6}$	[17]
		rs12662670	G	1.33	1.15-1.53	$1.1x10^{-4}$	[21]
14q24	*RAD51L1*	rs999737	T	0.86	0.80-0.93	$3.0x10^{-4}$	[21]
			T	0.89	0.80-0.98	0.02	[22]
		rs2588809	A	0.91	0.83-1.00	0.041	[17]
16q12	*TOX3*	rs3803662	A	1.09	1.01-1.17	0.022	[17]
			A	1.21	1.11-1.30	$3.1x10^{-6}$	[18]
			A	1.17	1.09-1.26	$3.7x10^{-5}$	[21]
19p13		rs8170	A	1.26	1.16-1.37	$1.3x10^{-7}$	[17]
			T	1.27	1.17-1.38	$2.3x10^{-8}$	[21]
			A	1.28	1.16-1.41	$1.2x10^{-6}$	[23]
			A	1.25	1.18-1.33	$3.3x10^{-13}$	[24]
		rs2363956	C	0.82	0.77-0.88	$2.3x10^{-8}$	[17]
			C	0.80	0.74-0.87	$1.1x10^{-7}$	[23]
		rs8100241	A	0.81	0.76-0.86	$2.4x10^{-13}$	[20]
			A	0.84	0.78-0.90	$8.7x10^{-7}$	[21]

4. Other Genetic Elements

Genetic elements other than susceptibility genes within the germline may also contribute to risk of TNBC. miRNAs represent a group of nonprotein coding RNAs that alter gene expression by binding to messenger RNA (mRNA) regions and reducing transcription or promoting mRNA degradation. Polymorphisms within the germline may eliminate or create miRNA binding sites or alter the function of miRNAs. For example, patients carrying the A allele for SNP rs743554, located within a predicted miRNA binding site of the integrin beta 4 (*ITGB4*) gene, were found to be at increased risk for ER- breast cancer (OR=2.09; 95% CI=1.19-3.67). Although HER2 status was not included in this study and thus associations with TNBC could not be determined, the A allele was also associated with decreased survival [hazard ration (HR)=2.21, 95% CI=1.21-3.68] [62]. A GWAS analysis of miRNA-associated SNPs performed in women of African ancestry found two SNPs that were associated with increased risk of ER- breast cancer: mir-4725 (rs73991220; OR=1.27, 95% CI=1.09-1.48) and *PAPD4* (rs146287903; OR=0.49, 95% CI=0.33-0.72) [63]. Given the increased risk of TNBC in women of African ancestry, future studies are needed to evaluate the potential role of these two SNPs in TNBC etiology. Similarly, the G allele of rs2910164, located within miR146a which may bind to the 3′ untranslated regions of the *BRCA1* and *BRCA2* genes and thus regulate their expression, has been associated with breast cancer risk (OR=1.77; 95% CI=1.40-2.23) [64]. Although risk for developing specific subtypes of breast cancer was not evaluated for this SNP, the link between *BRCA1* dysfunction and TNBC warrant further investigation.

Recent studies suggest that retroviral sequence elements from ancient retroviral infections may contribute to heritable TNBC. Some members of the human endogenous retrovirus HERV-K family are related to the endogenous mouse mammary tumor virus (MMTV) which can function as a mammary carcinogen in mice. While HML-2 proviruses have not been found at significantly higher frequencies in the genomes of patients with breast cancer compared to healthy controls and have not been associated with breast cancer histology [65, 66], the frequencies of detection for

HERV-K113 and HERV-K115 are significantly higher in individuals of African ancestry (21.8% and 34.1%, respectively) compared to individuals from the United Kingdom (4.2% and 1.0%) [67]. Given the enrichment of the TNBC subtype in women of African ancestry, the presence of these sequences should be evaluated in larger populations with available ER, PR, and HER2 status. More recently, Marchi et al. mined whole genome sequence data generated by next-generation sequencing and identified 17 sites of viral integration not present in the human reference sequence [68] that may contribute to breast cancer risk.

Sequences not present in the human reference genome may harbor additional genes and/or genetic elements that contribute to risk of TNBC. *De novo* assembly of whole genome sequences from Asian and African individuals revealed ~5 Mb of novel sequences from both individuals and populations [69]. The authors estimate that a complete human pan-genome would contain 19-40 Mb of novel sequence not present in the current reference genome. Sixty-nine genes, any of which may increase risk of TNBC, were located within unmapped regions of the African genome. Data from our own laboratory demonstrated that the insertion frequency of a 30 Kb region of chromosome 7p11 that harbors the promoter and first three of the four exons that compromise the phophoserine phosphatase-like (*PSPHL)* gene was 76% in African American women compared to only 21% in European American women [70]. While presence of an intact *PSPHL* gene was not associated with increased risk of breast cancer or TNBC, other uncharacterized genes from regions variably represented between populations may contribute to increased risk of TNBC

5. Conclusions

Identification of the *BRCA1* gene 25 years ago revolutionized the field of cancer risk assessment. Associations between germline *BRCA1* mutations and TNBC led the National Comprehensive Cancer Network to amend their *BRCA1/2* testing criteria in 2011 to include individuals diagnosed with TNBC [71]. Current guidelines allow testing for patients diagnosed with TNBC at ≤60 years of age with or without a significant family history of breast cancer [72]. *BRCA1* and *BRCA2* testing in 439 women with TNBC from the Australian Breast Cancer Tissue Bank supports TNBC pathology as a sufficient criterion for testing as 59% of women with pathogenic mutations did not have a family history of breast or ovarian cancer [34]. In a recent study of 10,901 TNBC patients, pathogenic variants were detected in TNBC risk-associated genes in 4.3% of patients not meeting NCCN testing criteria (diagnosed at >60 years of age without a family history) [35]. Because many of the mutations detected in this group were clinically actionable, the authors suggest that all patients with TNBC may benefit from genetic testing.

The importance of identifying the genetic etiology of TNBC extends beyond risk assessment. Surgical options are not dictated by tumor subtype; however, *BRCA1* and *BRCA2* mutation carriers are at increased risk for contralateral breast and ovarian cancer; thus the option of mastectomy with or without prophylactic removal of the contralateral breast and salpigo-oophorectomy should be considered. For carriers of mutations in other TNBC genes, such as *BARD1* and *PALB2*, evidence is not yet sufficient to recommend mastectomy or oophorectomy [72]. Because patients with TNBC do not respond to hormone- or HER2-targeted treatments, chemotherapy is the primary treatment option. Carcinomas from patients with TNBC from patients with pathogenic *BRCA1/BRCA2* mutations have demonstrated unique sensitivity to platinum agents in both the neoadjuvant and adjuvant settings [73]. More recently, PARP inhibitors, which exploit DNA repair deficiencies in cells with dysfunctional BRCA1 or BRCA2 proteins, leading to synthetic lethality, have shown promise with Olaparib approved by the FDA for the treatment of TNBC in patients with germline *BRCA1/BRCA2* mutations [74].

Despite recent achievements in identifying additional TNBC susceptibility genes and optimizing patient management for mutation carriers, future studies are needed. For example, what is the clinical utility of the low-penetrance genes/loci SNPs? In perhaps the largest GWAS to date, comprised of 94,075 cases and 75,017 controls of European ancestry that were derived from 69 different studies, 313 SNPs were assembled into a polygenic risk score (PRS) for both ER positive and ER negative tumors [75]. Preliminary studies evaluating the utility of the PRS are underway in Canada and Europe; however, given that the models were developed using cases and controls of European ancestry, the ability of this assay to accurately determine risk of TNBC in patients of other ancestries, especially African with its higher frequency of TNBC in young women, may be suboptimal. In conjunction, additional studies of nontraditional elements of the genome including retrotransposons and pseudogenes may reveal additional heritable risk factors for TNBC. Finally, for the ~4% of TNBC patients with germline mutations in genes other than *BRCA1* and *BRCA2* [35, 41], effective management strategies and novel therapeutics are urgently needed.

Disclosure

The contents of this publication are the sole responsibility of the author(s) and do not necessarily reflect the views, opinions, or policies of Uniformed Services University of the Health Sciences (USUHS), The Henry M. Jackson Foundation for the Advancement of Military Medicine, Inc., the Department of Defense (DoD), the Departments of the Army, Navy, or Air Force. Mention of trade names, commercial products, or organizations does not imply endorsement by the U.S. Government.

Conflicts of Interest

The authors declare no conflicts of interest.

Acknowledgments

This research was supported by a cooperative agreement from the Uniformed Services University of the Health Sciences

(HU0001-16-2-0004) through the Henry M. Jackson Foundation for the Advancement of Military Medicine, Inc.

References

[1] M. Gort, M. Broekhuis, R. Otter, and N. S. Klazinga, "Improvement of best practice in early breast cancer: actionable surgeon and hospital factors," *Breast Cancer Research and Treatment*, vol. 102, no. 2, pp. 219–226, 2007.

[2] K. R. Bauer, M. Brown, R. D. Cress et al., "Descriptive analysis of estrogen receptor (ER)-negative, progesterone receptor (PR)-negative, and HER2-negative invasive breast cancer, the so-called triple-negative phenotype," *Cancer*, vol. 109, no. 9, pp. 1721–1728, 2007.

[3] R. Dent, M. Trudeau, K. I. Pritchard et al., "Triple-negative breast cancer: clinical features and patterns of recurrence," *Clinical Cancer Research*, vol. 13, no. 15, pp. 4429–4434, 2007.

[4] K. Collett, I. M. Stefansson, and J. Eide, "A basal epithelial phenotype is more frequent in interval breast cancers compared with screen detected tumors," *Cancer Epidemiology Biomarkers & Prevention*, vol. 14, no. 5, pp. 1108–1112, 2005.

[5] E. Montagna, P. Maisonneuve, N. Rotmensz et al., "Heterogeneity of triple-negative breast cancer: histologic subtyping to inform the outcome," *Clinical Breast Cancer*, vol. 13, no. 1, pp. 31–39, 2013.

[6] A. Prat and C. M. Perou, "Deconstructing the molecular portraits of breast cancer," *Molecular Oncology*, vol. 5, no. 1, pp. 5–23, 2011.

[7] A. Prat, B. Adamo, M. C. U. Cheang, C. K. Anders, L. A. Carey, and C. M. Perou, "Molecular characterization of basal-like and non-basal-like triple-negative breast cancer," *The Oncologist*, vol. 18, no. 2, pp. 123–133, 2013.

[8] B. D. Lehmann, J. A. Bauer, X. Chen et al., "Identification of human triple-negative breast cancer subtypes and preclinical models for selection of targeted therapies," *The Journal of Clinical Investigation*, vol. 121, no. 7, pp. 2750–2767, 2011.

[9] M. J. Lund, K. F. Trivers, P. L. Porter et al., "Race and triple negative threats to breast cancer survival: a population-based study in Atlanta, GA," *Breast Cancer Research and Treatment*, vol. 113, no. 2, pp. 357–370, 2009.

[10] R. C. Millikan, B. Newman, C.-K. Tse et al., "Epidemiology of basal-like breast cancer," *Breast Cancer Research and Treatment*, vol. 109, no. 1, pp. 123–139, 2008.

[11] L. A. Newman, J. S. Reis-Filho, M. Morrow, L. A. Carey, and T. A. King, "The 2014 society of surgical oncology Susan G. komen for the cure symposium: triple-negative breast cancer," *Annals of Surgical Oncology*, vol. 22, no. 3, pp. 874–882, 2015.

[12] E. Jiagge, A. S. Jibril, D. Chitale et al., "Comparative analysis of breast cancer phenotypes in african american, white american, and west versus east african patients: correlation between african ancestry and triple-negative breast cancer," *Annals of Surgical Oncology*, vol. 23, no. 12, pp. 3843–3849, 2016.

[13] P. Sharma, J. R. Klemp, B. F. Kimler et al., "Germline BRCA mutation evaluation in a prospective triple-negative breast cancer registry: implications for hereditary breast and/or ovarian cancer syndrome testing," *Breast Cancer Research and Treatment*, vol. 145, no. 3, pp. 707–714, 2014.

[14] R. Greenup, A. Buchanan, W. Lorizio et al., "Prevalence of BRCA mutations among women with triple-negative breast cancer (TNBC) in a genetic counseling cohort," *Annals of Surgical Oncology*, vol. 20, no. 10, pp. 3254–3258, 2013.

[15] R. L. Milne, K. B. Kuchenbaecker, K. Michailidou et al., "Identification of ten variants associated with risk of estrogen-receptor-negative breast cancer," *Nature Genetics*, vol. 49, no. 12, pp. 1767–1778, 2017.

[16] M. Garcia-Closas, F. J. Couch, S. Lindstrom et al., "Genome-wide association studies identify four ER negative-specific breast cancer risk loci," *Nature Genetics*, vol. 45, no. 4, pp. 392–398, 2013.

[17] K. S. Purrington, S. Slager, D. Eccles et al., "Genome-wide association study identifies 25 known breast cancer susceptibility loci as risk factors for triple-negative breast cancer," *Carcinogenesis*, vol. 35, no. 5, pp. 1012–1019, 2014.

[18] A. Broeks, M. K. Schmidt, M. E. Sherman et al., "Low penetrance breast cancer susceptibility loci are associated with specific breast tumor subtypes: findings from the breast cancer association consortium," *Human Molecular Genetics*, vol. 20, no. 16, pp. 3289–3303, 2011.

[19] C. A. Haiman, G. K. Chen, C. M. Vachon et al., "A common variant at the TERT-CLPTM1L locus is associated with estrogen receptor-negative breast cancer," *Nature Genetics*, vol. 43, no. 12, pp. 1210–1214, 2013.

[20] K. B. Kuchenbaecker, S. L. Neuhausen, M. Robson et al., "Associations of common breast cancer susceptibility alleles with risk of breast cancer subtypes in BRCA1 and BRCA2 mutation carriers," *Breast Cancer Research*, vol. 16, no. 6, 2014.

[21] K. N. Stevens, C. M. Vachon, A. M. Lee et al., "Common breast cancer susceptibility loci are associated with triple-negative breast cancer," *Cancer Research*, vol. 71, no. 19, pp. 6240–6249, 2011.

[22] J. D. Figueroa, M. Garcia-Closas, M. Humphreys et al., "Associations of common variants at 1p11.2 and 14q24.1 (RAD51l1) with breast cancer risk and heterogeneity by tumor subtype: findings from the Breast Cancer Association Consortium," *Human Molecular Genetics*, vol. 20, no. 23, Article ID ddr368, pp. 4693–4706, 2011.

[23] A. C. Antoniou, X. Wang, Z. S. Fredericksen et al., "A locus on 19p13 modifies risk of breast cancer in BRCA1 mutation carriers and is associated with hormone receptor–negative breast cancer in the general population," *Nature Genetics*, vol. 42, no. 10, pp. 885–892, 2010.

[24] K. N. Stevens, Z. Fredericksen, C. M. Vachon et al., "19p13.1 is a triple-negative-specific breast cancer susceptibility locus," *Cancer Research*, vol. 72, no. 7, pp. 1795–1803, 2012.

[25] A. N. Tutt, C. J. Lord, N. McCabe et al., "Exploiting the DNA repair defect in BRCA mutant cells in the design of new therapeutic strategies for cancer," *Cold Spring Harbor Symposia on Quantitative Biology*, vol. 70, pp. 139–148, 2005.

[26] D. Ford, D. F. Easton, M. Stratton et al., "Genetic heterogeneity and penetrance analysis of the BRCA1 and BRCA2 genes in breast cancer families," *American Journal of Human Genetics*, vol. 62, no. 3, pp. 676–689, 1998.

[27] T. R. Rebbeck, N. Mitra, F. Wan et al., "Association of type and location of BRCA1 and BRCA2 mutations with risk of breast and ovarian cancer," *The Journal of the American Medical Association*, vol. 313, no. 13, pp. 1347–1361, 2015.

[28] Y. Miki, J. Swensen, and D. Shattuck-Eidens, "A strong candidate for the breast and ovarian cancer susceptibility gene BRCA1," *Science*, vol. 266, pp. 66–71, 1994.

[29] A. Paul and S. Paul, "The breast cancer susceptibility genes (BRCA) in breast and ovarian cancers," *Frontiers in Bioscience - Landmark*, vol. 19, no. 4, pp. 605–618, 2014.

[30] R. Wooster, G. Bignell, J. Lancaster et al., "Identification of the breast cancer susceptibility gene *BRCA2*," *Nature*, vol. 378, no. 6559, pp. 789–792, 1995.

[31] S. R. Lakhani, J. Jacquemier, J. P. Sloane et al., "Multifactorial analysis of differences between sporadic breast cancers and cancers involving BRCA1 and BRCA2 mutations," *Journal of the National Cancer Institute*, vol. 90, no. 15, pp. 1138–1145, 1998.

[32] N. C. Turner and J. S. Reis-Filho, "Basal-like breast cancer and the BRCA1 phenotype," *Oncogene*, vol. 25, no. 43, pp. 5846–5853, 2006.

[33] B. N. Peshkin, M. L. Alabek, and C. Isaacs, "BRCA1/2 mutations and triple negative breast cancers," *Breast Disease*, vol. 32, no. 1-2, pp. 25–33, 2010.

[34] M. W. Wong-Brown, C. J. Meldrum, J. E. Carpenter et al., "Prevalence of BRCA1 and BRCA2 germline mutations in patients with triple-negative breast cancer," *Breast Cancer Research and Treatment*, vol. 150, no. 1, pp. 71–80, 2015.

[35] H. Shimelis, H. LaDuca, C. Hu et al., "Triple-negative breast cancer risk genes identified by multigene hereditary cancer panel testing," *Journal of the National Cancer Institute*, vol. 110, no. 8, pp. 855–862, 2018.

[36] B. Xia, Q. Sheng, K. Nakanishi et al., "Control of BRCA2 cellular and clinical functions by a nuclear partner, PALB2," *Molecular Cell*, vol. 22, no. 6, pp. 719–729, 2006.

[37] F. J. Couch, H. Shimelis, C. Hu et al., "Associations between cancer predisposition testing panel genes and breast cancer," *JAMA Oncology*, vol. 3, no. 9, pp. 1190–1196, 2017.

[38] T. Heikkinen, H. Karkkainen, K. Aaltonen et al., "The breast cancer susceptibility mutation PALB2 1592delT is associated with an aggressive tumor phenotype," *Clinical Cancer Research*, vol. 15, no. 9, pp. 3214–3222, 2009.

[39] T. P. Slavin, K. N. Maxwell, J. Lilyquist et al., "The contribution of pathogenic variants in breast cancer susceptibility genes to familial breast cancer risk," *Npj Breast Cancer*, vol. 3, no. 1, 2017.

[40] S. S. Buys, J. F. Sandbach, A. Gammon et al., "A study of over 35,000 women with breast cancer tested with a 25-gene panel of hereditary cancer genes," *Cancer*, vol. 123, no. 10, pp. 1721–1730, 2017.

[41] F. J. Couch, S. N. Hart, P. Sharma et al., "Inherited Mutations in 17 Breast Cancer Susceptibility Genes Among a Large Triple-Negative Breast Cancer Cohort Unselected for Family History of Breast Cancer," *Journal of Clinical Oncology*, vol. 33, no. 4, pp. 304–311, 2015.

[42] M. W. Wong-Brown, K. A. Avery-Kiejda, N. A. Bowden, and R. J. Scott, " Low prevalence of germline *PALB2* mutations in Australian triple-negative breast cancer ," *International Journal of Cancer*, vol. 134, no. 2, pp. 301–305, 2014.

[43] D. Hanahan and R. A. Weinberg, "Hallmarks of cancer: the next generation," *Cell*, vol. 144, no. 5, pp. 646–674, 2011.

[44] P. Hainut, "TP53: Coordinator of the Processes That Underlie the Hallmarks of Cancer," in *p53 in the Clinics*, Springer, New York, NY, USA, 2013.

[45] A. Dumay, J. Feugeas, E. Wittmer et al., " Distinct *tumor protein p53* mutants in breast cancer subgroups ," *International Journal of Cancer*, vol. 132, no. 5, pp. 1227–1231, 2013.

[46] P. Lin, W. Kuo, A. Huang et al., "Multiple gene sequencing for risk assessment in patients with early-onset or familial breast cancer," *Oncotarget* , vol. 7, no. 7, 2016.

[47] Y. Yin and W. H. Shen, "PTEN: a new guardian of the genome," *Oncogene*, vol. 27, no. 41, pp. 5443–5453, 2008.

[48] A. C. Vargas, J. S. Reis-Filho, and S. R. Lakhani, "Phenotype-genotype correlation in familial breast cancer," *Journal of Mammary Gland Biology and Neoplasia*, vol. 16, no. 1, pp. 27–40, 2011.

[49] C. Rousset-Jablonski and A. Gompel, "Screening for familial cancer risk: focus on breast cancer," *Maturitas*, vol. 105, pp. 69–77, 2017.

[50] M. Gonzalez-Rivera, M. Lobo, S. Lopez-Tarruellaa et al., "Frequency of germline DNA genetic findings in an unselected prospective cohort of triple-negative breast cancer patients participating in a platinum-based neoadjuvant chemotherapy trial," *Breast Cancer Research and Treatment*, vol. 156, no. 3, pp. 507–515, 2016.

[51] C. Kraus, J. Hoyer, G. Vasileiou et al., "Gene panel sequencing in familial breast/ovarian cancer patients identifies multiple novel mutations also in genes others than BRCA1/2," *International Journal of Cancer*, vol. 140, no. 1, pp. 95–102, 2017.

[52] M. C. Southey, D. E. Goldgar, R. Winqvist et al., "*PALB2* , *CHEK2* and *ATM* rare variants and cancer risk: data from COGS ," *Journal of Medical Genetics*, vol. 53, no. 12, pp. 800–811, 2016.

[53] P. Domagala, A. Jakubowska, K. Jaworska-Bieniek et al., "Prevalence of germline mutations in genes engaged in dna damage repair by homologous recombination in patients with triple-negative and hereditary non-triple-negative breast cancers," *PLoS ONE*, vol. 10, no. 6, p. e0130393, 2015.

[54] B. Decker, J. Allen, C. Luccarini et al., " Rare, protein-truncating variants in *ATM* , *CHEK2* and *PALB2* , but not *XRCC2* , are associated with increased breast cancer risks ," *Journal of Medical Genetics*, vol. 54, no. 11, pp. 732–741, 2017.

[55] B. Smolarz, M. Makowska, D. Samulak et al., "Gly322Asp and Asn127Ser single nucleotide polymorphisms (SNPs) of hMSH2 mismatch repair gene and the risk of triple-negative breast cancer in Polish women," *Familial Cancer*, vol. 14, no. 1, pp. 81–88, 2015.

[56] C. Cybulski, T. Huzarski, T. Byrski et al., "Estrogen receptor status in CHEK2-positive breast cancers: implications for chemoprevention," *Clinical Genetics*, vol. 75, no. 1, pp. 72–78, 2009.

[57] S. De Brakeleer, J. De Greve, C. Desmedt et al., "Frequent incidence of BARD1-truncating mutations in germline DNA from triple-negative breast cancer patients," *Clinical Genetics*, vol. 89, no. 3, pp. 336–340, 2016.

[58] D. F. Easton, K. A. Pooley, and A. M. Dunning, "Genome-wide association study identifies novel breast cancer susceptibility loci," *Nature*, vol. 447, no. 7148, pp. 1087–1093, 2007.

[59] M. Garcia-Closas, P. Hall, H. Nevanlinna et al., "Heterogeneity of breast cancer associations with five susceptibility loci by clinical and pathological characteristics," *PLOS Genetics*, vol. 4, no. 4, 2008.

[60] A. Siddiq, F. J. Couch, G. K. Chen et al., "A meta-analysis of genome-wide association studies of breast cancer identifies two novel susceptibility loci at 6q14 and 20q11," *Human Molecular Genetics*, vol. 21, no. 24, pp. 5373–5384, 2012.

[61] C. A. Haiman, G. K. Chen, C. M. Vachon et al., "A common variant at the TERT-CLPTM1L locus is associated with estrogen receptor–negative breast cancer," *Nature Genetics*, vol. 43, no. 12, pp. 1210–1214, 2011.

[62] A. Brendle, H. Lei, A. Brandt et al., "Polymorphisms in predicted microRNA-binding sites in integrin genes and breast cancer: ITGB4 as prognostic marker," *Carcinogenesis*, vol. 29, no. 7, pp. 1394–1399, 2008.

[63] F. Qian, Y. Feng, Y. Zheng et al., "Genetic variants in microRNA and microRNA biogenesis pathway genes and breast cancer risk among women of African ancestry," *Human Genetics*, vol. 135, no. 10, pp. 1145–1159, 2016.

[64] A. Upadhyaya, R. A. Smith, and D. Chacon-Cortes, "Association of the microRNA-single nucleotide polymorphism rs2910164 in miR146a with sporadic breast cancer susceptibility: a case control study," *Gene*, vol. 576, no. 1, part 1, pp. 256–260, 2016.

[65] J. H. Wildschutte, D. R. Ram, V. L. Subramanian, Stevens., and J. M. Coffin, "The distribution of insertionally polymorphic endogenous retroviruses in breast cancer patients and cancer-free controls," *Retrovirology*, no. 11, article 62, 2014.

[66] T. Burmeister, A. D. Ebert, W. Pritze et al., "Insertional polymorphisms of endogenous HERV-K113 and HERV-K115 retroviruses in breast cancer patients and age-matched controls," *AIDS Research and Human Retroviruses*, vol. 20, no. 11, pp. 1223–1229, 2004.

[67] D. Moyes, A. Martin, S. Sawcer et al., "The distribution of the endogenous retroviruses HERV-K113 and HERV-K115 in health and disease," *Genomics*, vol. 86, no. 3, pp. 337–341, 2005.

[68] E. Marchi, A. Kanapin, G. Magiorkinis, and R. Belshaw, "Unfixed endogenous retroviral insertions in the human population," *Journal of Virology*, vol. 88, no. 17, pp. 9529–9537, 2014.

[69] R. Li, Y. Li, H. Zheng et al., "Building the sequence map of the human pan-genome," *Nature Biotechnology*, vol. 28, no. 1, pp. 57–63, 2010.

[70] S. Rummel, C. E. Penatzer, C. D. Shriver, and R. E. Ellsworth, "PSPHL and breast cancer in African American women: causative gene or population stratification?" *BMC Genetics*, vol. 15, no. 1, p. 38, 2014.

[71] National Comprehensive Cancer Network, *Genetic/Familial High-Risk Assessment: Breast And Ovarian*, National Comprehensive Cancer Network, Ed., 2011.

[72] National Comprehensive Cancer Network, *GenEtic/Familial High-Risk Assessment: Breast And Ovarian Cancer*, 2019.

[73] J. H. Park, J. Ahn, and S. Kim, "How shall we treat early triple-negative breast cancer (TNBC): from the current standard to upcoming immuno-molecular strategies," *ESMO Open*, vol. 3, 2018.

[74] A. S. Zimmer, M. Gillard, S. Lipkowitz, and J. Lee, "Update on PARP inhibitors in breast cancer," *Current Treatment Options in Oncology*, vol. 19, no. 5, 2018.

[75] N. Mavaddat, K. Michailidou, J. Dennis et al., "Polygenic Risk Scores for Prediction of Breast Cancer and Breast Cancer Subtypes," *American Journal of Human Genetics*, vol. 104, no. 1, pp. 21–34, 2019.

Hindawi
Journal of Oncology
Volume 2019, Article ID 3980273, 12 pages
https://doi.org/10.1155/2019/3980273

Research Article

A Novel Role for Cathepsin S as a Potential Biomarker in Triple Negative Breast Cancer

Richard D. A. Wilkinson,[1] **Roberta E. Burden**,[2] **Sara H. McDowell**,[1] **Darragh G. McArt**,[1] **Stephen McQuaid**,[3] **Victoria Bingham**,[3] **Rich Williams**,[1] **Órla T. Cox**,[4] **Rosemary O'Connor**,[4] **Nuala McCabe**,[1,5] **Richard D. Kennedy**,[1,5] **Niamh E. Buckley**,[2] **and Christopher J. Scott**[1]

[1]*Centre for Cancer Research and Cell Biology, Queen's University Belfast, BT9 7AE, UK*
[2]*School of Pharmacy, Queen's University Belfast, BT9 7BL, UK*
[3]*Northern Ireland Molecular Pathology Laboratory, Queen's University Belfast, BT9 7AE, UK*
[4]*School of Biochemistry and Cell Biology, University College Cork, Ireland*
[5]*ALMAC Diagnostics, ALMAC Group, BT63 5QD, UK*

Correspondence should be addressed to Christopher J. Scott; c.scott@qub.ac.uk

Received 18 April 2019; Accepted 4 June 2019; Published 27 June 2019

Guest Editor: Chia-Jung Li

Cathepsin S (CTSS) has previously been implicated in a number of cancer types, where it is associated with poor clinical features and outcome. To date, patient outcome in breast cancer has not been examined with respect to this protease. Here, we carried out immunohistochemical (IHC) staining of CTSS using a breast cancer tissue microarray in patients who received adjuvant therapy. We scored CTSS expression in the epithelial and stromal compartments and evaluated the association of CTSS expression with matched clinical outcome data. We observed differences in outcome based on CTSS expression, with stromal-derived CTSS expression correlating with a poor outcome and epithelial CTSS expression associated with an improved outcome. Further subtype characterisation revealed high epithelial CTSS expression in TNBC patients with improved outcome, which remained consistent across two independent TMA cohorts. Further *in silico* gene expression analysis, using both in-house and publicly available datasets, confirmed these observations and suggested high CTSS expression may also be beneficial to outcome in ER-/HER2+ cancer. Furthermore, high CTSS expression was associated with the BL1 Lehmann subgroup, which is characterised by defects in DNA damage repair pathways and correlates with improved outcome. Finally, analysis of matching IHC analysis reveals an increased M1 (tumour destructive) polarisation in macrophage in patients exhibiting high epithelial CTSS expression. In conclusion, our observations suggest epithelial CTSS expression may be prognostic of improved outcome in TNBC. Improved outcome observed with HER2+ at the gene expression level furthermore suggests CTSS may be prognostic of improved outcome in ER- cancers as a whole. Lastly, from the context of these patients receiving adjuvant therapy and as a result of its association with BL1 subgroup CTSS may be elevated in patients with defects in DNA damage repair pathways, indicating it may be predictive of tumour sensitivity to DNA damaging agents.

1. Introduction

Breast cancer is a highly heterogeneous disease and may be classified into different sub-types which affects treatment approach and patient prognosis [1]. Classification of breast cancer has been assigned via the presence/absence of the estrogen receptor (ER) or HER2 amplification, which allow use of targeted treatments such as tamoxifen and trastuzumab, respectively. Tumour cells lacking these receptors, in addition to the progesterone receptor (PR), are termed "triple negative" (TNBC) and have the poorest outcome due in part to the lack of targeted therapies available. TNBCs are therefore typically treated with a cocktail of chemotherapies such as FEC (5-*F*U, *E*pirubicin, and *C*yclophosphamide). Despite a high rate of response to chemotherapy, TNBC is associated with high rates of relapse and death [2]. This "triple

negative paradox" is underpinned by a high level of molecular heterogeneity [3]. In response to this, increased efforts have been made to identify markers which may improve patient outcome following diagnosis [4, 5], not only to allow better treatment stratification but also to identify new therapeutic targets.

The cysteine protease cathepsin S (CTSS) is one of a family of 11 cysteine cathepsin proteases, and has been found to be associated with a variety of pathologies, including cancer [6, 7]. In contrast to other members of the cysteine cathepsins, CTSS is normally constrained to macrophage and lymphoid tissues. However, presence of CTSS has been observed in a number of cancer types, including prostate [8, 9], gastric [10] and hepatocellular [11] carcinomas. Furthermore, increased CTSS expression has been shown to hold prognostic value in grade IV astrocytomas [12], colorectal carcinomas [13], and gastric cancer [14], where it is associated with a poor outcome. Collectively, these observations have attracted interest in its therapeutic potential in cancer [7].

The viability of targeting this protease in cancer has been evaluated using pancreatic and colorectal carcinoma gene depletion models [15–17], and treatment with a monoclonal antibody inhibitor FSN0503 [18] and a selective small molecule inhibitor compound [19]. Inhibition/depletion of CTSS produced reductions in tumour invasion, burden, proliferation and vascularisation, as well as increased apoptosis.

Recently, Sevenich and colleagues examined the role of CTSS in breast cancer progression, identifying a role for CTSS in breast-to-brain metastases via cleavage of JAM-B, a junctional adhesion molecule involved in blood-brain barrier transmigration [17]. However, the clinical utility of CTSS as a biomarker in breast cancer has not been investigated to date. In this study we therefore aimed to understand the specific expression of CTSS, not only within epithelial and stromal compartments in breast tumours, but also the known molecular subgroups. This expression data was correlated with clinical outcome to investigate the potential prognostic and/or predictive role of CTSS.

2. Materials and Methods

2.1. Tissue Microarray Patient Sample Selection and Immunohistochemical Staining. All tissue samples were located from the Belfast and the South Eastern Health and Social Care Trust (BSHSCT) were obtained under the auspices of the Northern Ireland Biobank (NIB) (www.nibiobank.org), which has ethical approval (ref: 11/NI/0013) to collect, store and distribute de-identified/anonymised samples to researchers. The present study has ethical approval from NIB approval (reference. NIB14-0125). Tissue microarray study design, patient selection and construction of the BR300 cohort has been described previously in Boyle et al. [20]. This study was designed as outlined in Supplementary Figure 1. Briefly, the patient cohort compiled 296 female patients with *de novo* breast cancer and included matching clinical, pathological and outcome parameters. All patients within the cohort were diagnosed and received treatment in Northern Ireland, with the vast majority of the tissue resection samples obtained, processed and reported from one of the two hospitals in the Belfast catchment area between September 1997 and May 2009. All tissue data presented here was obtained by surgical resection, comprising of total or partial mastectomies with axillary node clearance. All patients present within the cohort subsequently received anthracycline-based chemotherapy with or without radiotherapy. Patients exhibiting positive hormone receptor or HER2 status were administered hormone therapy or trastuzumab. None of the patients were treated neoadjuvantly. Patient exclusion criteria included male sex and past history of any cancer type. Unique TNBC cases were collated from two independent bespoke TNBC TMA cohorts available from the NIB and previously described in Humphries et al. [21] and Orr et al. [22]. Immunohistochemical staining of CTSS was carried out in the Northern Ireland Molecular Pathology Laboratory (QUB). Sections were cut from the TMA blocks to a diameter of 4 μm using a rotary microtome, dried at 37°C overnight, and then used for immunohistochemical staining with rabbit anti-human CTSS antibody (1:250) (HPA002988, Atlas Antibodies, UK) using an automated immuno-stainer (Leica Bond-Max, UK). All sections were visualised with DAB, counterstained with haematoxylin and mounted in DPX. To avoid bias, scoring was carried out by at least two independent assessors experienced in IHC analysis in breast TMAs. Preliminary analysis revealed that patients with a CTSS score of 0 and 1 behaved similarly in terms of survival, as were patients with CTSS scores of 2 and 3. Patients were therefore stratified based on low CTSS (score of 0 and 1) or high CTSS (score of 2 and 3) expression, and the effect of expression on overall survival observed.

2.2. Generation of Kaplan-Meier Curves for Analysis of TMA and Publicly Available Gene Datasets. Matching clinical data was obtained from the NIB upon completion of CTSS scoring. The expression data was matched with the clinical data according to the anonymous patient IDs using Microsoft Excel. Evaluation of CTSS expression on survival was completed using non-censored data, and was subsequently analysed using GraphPad Prism.

Comparative analysis of gene expression versus overall survival (2014; N=1117) and relapse free survival (N=3971) was carried out using online repository KM plotter (www.kmplot.com) [23]. Using the breast cancer dataset, survival dependent on CTSS gene expression was analysed based on intrinsic patient subtype, using a collation of previously published and publicly available Affymetrix microarray datasets, available through GEO, European Bioinformatics Institute and TCGA. Gene expression was evaluated using a median expression of CTSS probes 202901_x_at and 202902_s_at. Patient overall survival was split according to a median value cut-off point into high/low expression and all the data right-censored at 120 months (10 years). Data was obtained directly from www.kmplot.com and the figures generated using GraphPad Prism. Data was presented as percentage survival versus time in months.

Table 1: *Clinicopathological information for BR300 tissue microarray categorised according to compartmental CTSS scores.* CTSS scores of 0 and 1 behaved similarly in terms of survival, as were patients with CTSS scores of 2 and 3. Patients were therefore stratified based on low CTSS (score of 0 and 1) or high CTSS (score of 2 and 3) expression. Differences between clinical information was evaluated based on high and low CTSS scores in either the epithelial and stromal compartments. Statistical significance determined by Chi-Square test. Figure in brackets indicates percentage of total. LVI=lymphovascular invasion. N=number of patients.

BR300 Cohort		CTSS Epithelial				CTSS Stromal			
		N (%)	Low (%)	High (%)	*p*-value	N (%)	Low (%)	High (%)	*p*-value
Characteristic		267 (100)	221 (100)	46 (100)		262 (100)	79 (100)	183 (100)	
Age	N≤51	140 (52)	113 (51)	27 (59)		140 (53)	41 (52)	99 (54)	
Median = 51	N>51	127 (48)	108 (49)	19 (41)	0.42	122 (47)	38 (48)	84 (46)	0.79
Grade	1	4 (1)	4 (2)	0 (0)		4 (2)	3 (4)	1 (1)	
	2	106 (40)	99 (45)	7 (15)		103 (39)	45 (57)	58 (32)	
	3	157 (59)	118 (53)	39 (85)	0.0004***	155 (59)	31 (39)	124 (68)	< 0.0001***
Tumour	1	54 (20)	45 (20)	9 (20)		54 (21)	14 (18)	40 (22)	
	2	171 (64)	146 (66)	25 (54)		166 (63)	52 (66)	114 (62)	
	3	36 (13)	24 (11)	12 (26)		36 (14)	11 (14)	25 (14)	
	4/4b	6 (2)	6 (3)	0 (0)	0.035*	6 (2)	2 (3)	4 (2)	0.9
Node	0	114 (43)	86 (39)	28 (61)		113 (43)	33 (42)	80 (44)	
	1	93 (35)	83 (38)	14 (30)		91 (35)	26 (33)	64 (35)	
	2	34 (13)	31 (14)	3 (7)		33 (13)	13 (16)	20 (11)	
	3	26 (10)	25 (11)	1 (2)	0.020*	26 (10)	7 (9)	19 (10)	0.66
LVI	Yes	168 (63)	145 (66)	23 (50)		164 (63)	51 (65)	113 (62)	
	No	96 (36)	73 (33)	23 (50)		96 (37)	26 (33)	70 (38)	
	Unknown	3 (1)	3 (1)	0 (0)	0.076	3 (1)	2 (3)	1 (1)	0.3
Histology	Ductal	210 (79)	172 (78)	38 (83)		207 (79)	49 (62)	158 (86)	
	Lobular	27 (10)	24 (11)	3 (7)		26 (10)	16 (20)	10 (5)	
	Mixed	24 (9)	21 (10)	3 (7)		23 (9)	12 (15)	11 (6)	
	Other	6 (2)	4 (2)	2 (4)	0.52	6 (2)	2 (3)	4 (2)	< 0.0001***
Radiotherapy	Yes	220 (82)	182 (82)	38 (83)		215 (82)	70 (89)	145 (79)	
	No	47 (18)	39 (18)	8 (17)	1.00	47 (18)	9 (11)	38 (21)	0.080
Hormone	Yes	157 (59)	147 (67)	10 (22)		157 (60)	65 (82)	88 (48)	
Therapy	No	110 (41)	74 (33)	36 (78)	< 0.0001***	109 (42)	14 (18)	95 (52)	< 0.0001***

2.3. Analysis of CTSS and Macrophage Polarisation. BR300 CTSS epithelial scores were matched with CD68, CD14 and CD163 IHC, previously stained and described by Buckley et al. [24], and split according to no CTSS expression (score = 0) or CTSS expression (score = 1-3). Analysis of macrophage polarisation by gene signatures was carried out as previously described by Jezequel et al. and Denardo et al. [25, 26], using gene expression collected and described in Buckley et al. [24].

2.4. Statistical Analysis. The TMA IHC clinicopathological analysis and the macrophage IHC was analysed by Chi-Square test. Differences in overall survival within the CTSS BR300 and the TNBC bespoke IHC, as well as the publically available gene expression (overall survival and relapse free survival) were evaluated by Log-Rank test and hazard ratios with 95% confidence limits reported. Statistical evaluation of CTSS expression St. Gallen and Lehmann subtypes, as well as the macrophage polarisation gene expression signatures within the BR300 cohort, were analysed using one-way ANOVA. Significance is defined as $^{*}p < 0.05$, $^{**}p < 0.01$, and $^{***}p < 0.001$.

3. Results

3.1. Patho-Physiological Characterisation of CTSS Expression in the Patient Samples. To first investigate the role of CTSS expression in breast cancer, we applied IHC of CTSS on a tissue microarray (TMA) representing a cohort of 296 patients (hereafter referred to as BR300 cohort) [20]. Previously, several groups have indicated an importance for either tumour infiltrating lymphocyte- (TIL-) derived [27] or epithelial-derived CTSS expression [16] in tumour progression. Therefore, CTSS protein expression was evaluated for epithelial and stromal compartments separately. Based on initial assessment of staining patterns, expression was categorised as either; 0: no expression, 1: low expression, 2: moderate expression and 3: high expression, in both epithelial and stromal cells (Figure 1). When matched with the clinical data, a significant association between increased CTSS expression and tumour grade was observed in epithelial (p=0.0004) and stromal (p<0.0001) cells (Table 1). In addition, there was a significant association between high CTSS expression, and increased tumour stage (p=0.035) in the

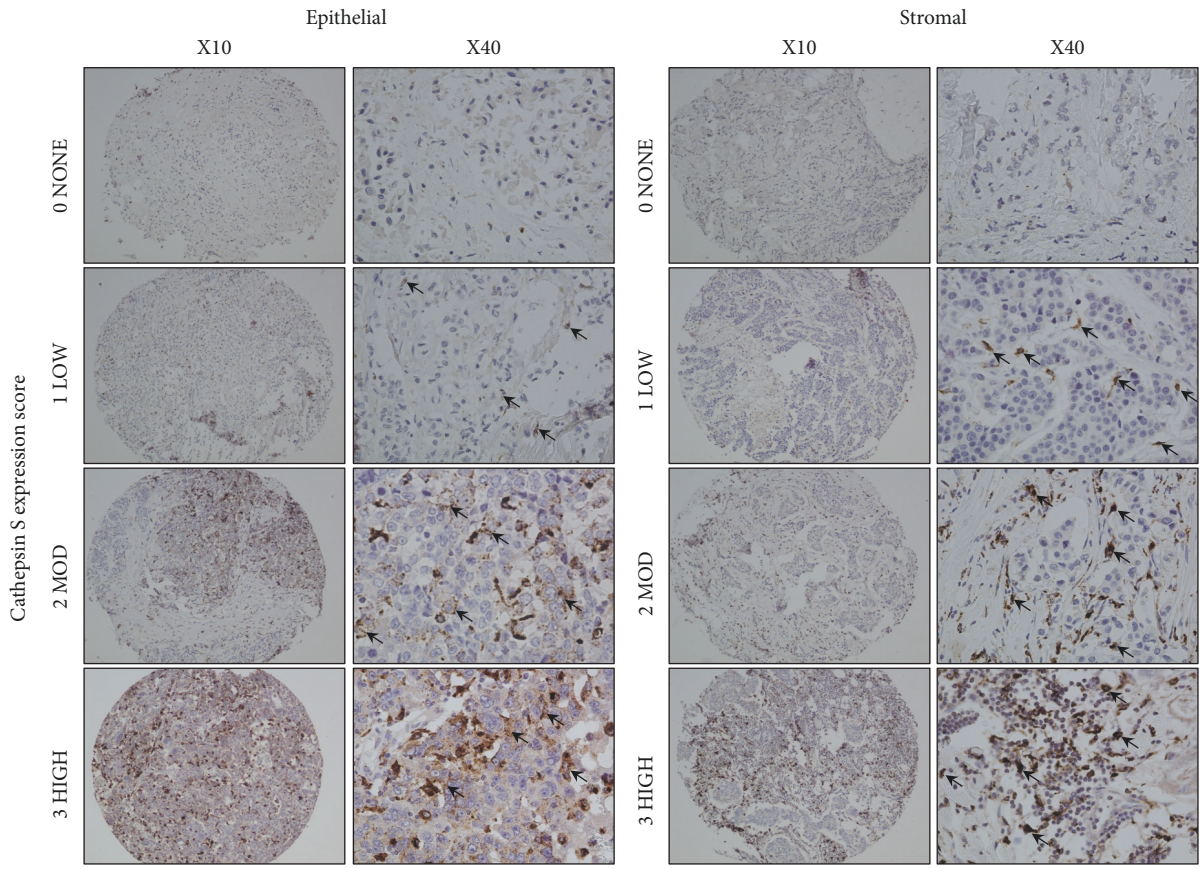

Figure 1: *Representative images of CTSS expression in patient samples.* CTSS-specific expression is indicated by brown staining versus blue nuclear counter staining. Samples represent either epithelial or stromal CTSS staining. Black arrows indicate areas of CTSS expression, which was separated according to high (3), moderate (2), low (1), or no expression (0).

epithelial cells. We also observed decreased node (p=0.020) as well as reduced lymphovascular invasion (LVI), which approached significance, in patients with high epithelial CTSS expression. Finally, increased expression of CTSS in the stromal cells revealed a significant association with ductal breast cancer (p<0.0001), though it is important to note that the study is underpowered to robustly assess any association with other histologies. No significant differences were observed between histology and epithelial cell CTSS expression, and no significant difference was observed in the age of patients comparing high or low CTSS expression in either epithelial or stromal cells. Interestingly, despite no significant differences with respect to radiotherapy with CTSS expression, a significantly larger number of patients with high epithelial and stromal CTSS expression did not receive hormone therapy, suggesting a negative association between CTSS expression and ER status (p<0.0001) (Table 1).

3.2. Increased CTSS Expression in Epithelial Cells Associated with Improved Outcome. Preliminary analysis revealed that patients with a CTSS score of 0 and 1 behaved similarly in terms of survival, as were patients with CTSS scores of 2 and 3. Patients were therefore stratified based on low CTSS (score of 0 and 1) or high CTSS (score of 2 and 3) expression, and the effect of expression on overall survival analysed. The resulting Kaplan-Meier plots revealed distinct patterns for epithelial and stromal cell CTSS expression with respect overall survival. Consistent with previous findings, high stromal CTSS expression was associated with poor outcome (HR=1.66 (CI=1.00-2.70) p=0.049) (Figure 2(a)). Intriguingly, the opposite was observed with respect to high epithelial CTSS expression, which was highly significantly associated with an improved outcome (HR=0.45 (CI=0.25-0.81) p=0.0082) (Figure 2(b)). This led us to further investigate if the expression of epithelial-derived CTSS was specific to certain sub-types of breast cancer.

3.3. Increased Epithelial Cell CTSS Expression Is Associated with Improved Outcome in Triple Negative Breast Cancer. Following evaluation of CTSS protein expression and the association with survival using the BR300 patient cohort, we next wished to observe differential CTSS expression within breast cancer subtypes. Patients were subdivided into their respective subtypes according to St. Gallen classification [28]. While high CTSS was associated with good outcome, there were very few cases, which prohibited further robust analysis (Supplementary Figures 2(a)-2(e)).

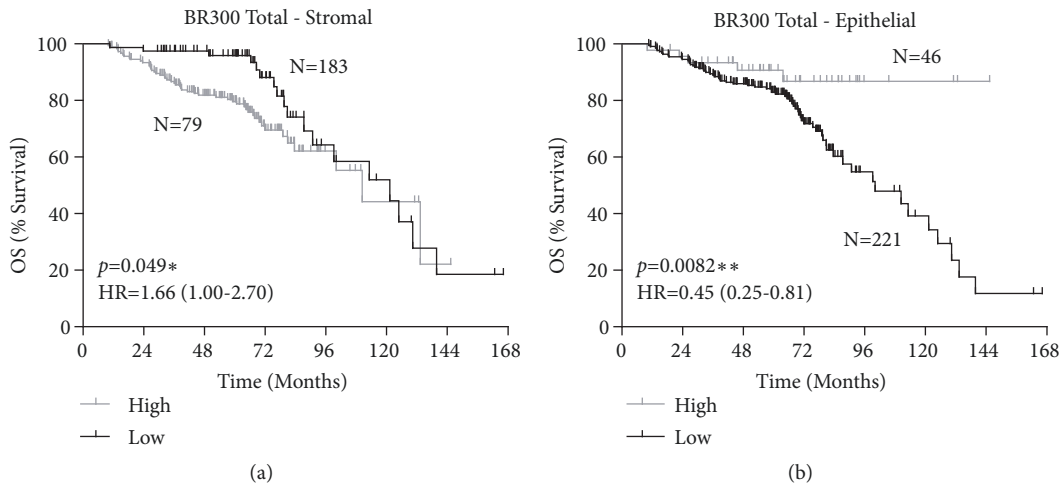

Figure 2: *CTSS expression is differentially associated with patient outcome based on cell compartment.* Kaplan-Meier curve stratified overall survival (OS) based on high or low CTSS expression in (a) stromal and (b) epithelial compartment. Log-Rank p-value and hazard ratio (HR) with 95% confidence intervals indicated. N=number of patients.

Interestingly, matching outcome data for the triple negative breast cancer patients (N=69) to the CTSS epithelial expression revealed an association of high CTSS expression with a significantly improved outcome (HR=0.37 (CI=0.14-1.00) p=0.049) (Figure 3(a)(i)). Analysis of stromal CTSS expression revealed a non-significant trend towards poor outcome which may be due to the low number of patients within the low CTSS expression arm (HR=1.68 (CI=0.36-7.82) p=0.51) (Figure 3(a)(ii)).

To supplement this observation, scoring of CTSS in a bespoke triple negative breast cancer cohort (N=84) was carried out [21, 22]. Analysis of the stromal CTSS expression revealed no significant difference to outcome, but reassuringly, a trend complementing the outcome in the BR300 cohort was observed, with high CTSS epithelial expression demonstrating improved outcome in triple negative breast cancer patients, however, given the relatively small size of this cohort, significance was not quite reached (p=0.073) (Figure 3(b)). To enhance statistical power, the two cohorts were combined and as a result demonstrated a clear and significant improvement for TNBC patients with epithelial derived CTSS expression (HR=0.41 (CI=0.22-0.75) p=0.0036) (Figure 3(c)(i)) in contrast to stromal CTSS expression which showed no significant difference to outcome (Figure 3(c)(ii)).

3.4. Increased CTSS Gene Expression Associated with Improved Outcome in Triple Negative Breast Cancer. Given the results from the TMA analysis, we investigated if CTSS gene expression could also predict outcome. This allowed us to interrogate the role of CTSS further using publicly available gene expression datasets. We first validated the TMA findings using a gene expression dataset matched to the BR300 cohort [29]. Consistent with the IHC analysis, we observed CTSS to be expressed highest in TNBC (Figure 4(a)). Lehman subtype analysis of the TNBC subgroup revealed CTSS expression varied significantly across all subgroups with the highest expression observed in the IM group and lowest expression in the LAR and M groups (Figure 4(b) and Supplementary Figure 3). Refinement of the Lehmann subtype study has since shown that the molecular signatures defining the IM and MSL groups were derived from infiltrating lymphocyte and stromal cells [30]. Therefore the high CTSS expression in the IM group is most likely associated with tumour associated immune cells. Analysis of CTSS across the four epithelial-derived subgroups displayed a significant variation in expression as a whole with expression in the BL1 subtype significantly higher than the LAR and M subtypes. Of note, the BL1 subgroup is also associated with improved outcome [30].

To supplement these observations made with our in-house patient dataset, evaluation of the relationship of gene expression and survival was carried out with publicly available datasets using KM Plotter [23]. The results indicated no significant differences between high and low *CTSS* gene expression on overall survival (OS) or relapse free survival (RFS) of breast cancer patients as a whole (Supplementary Table 1; Supplementary Figure 4). Further dissection of *CTSS* expression with respect to individual subtypes revealed no significant difference between high and low *CTSS* expression on either OS or RFS in luminal A, nor luminal B (Supplementary Table 1; Supplementary Figure 4). However, a striking significant correlation between CTSS and survival was observed in HER2+ (OS HR=0.38 (CI=0.20-0.71) p=0.0031, RFS HR=0.47 (0.32-0.70) p=0.0002) and TNBC patients (OS HR=0.43 (CI=0.27-0.71) p=0.0009, and RFS HR=0.46 (0.36-0.60) p<0.0001) (Figure 5) (Supplementary Table 1).

3.5. Expression of CTSS in TNBC Epithelial Cells Is Associated with the Enhanced Presence of M1 Macrophages. In order to understand some of the molecular pathology underpinning the observed association between CTSS and good outcome in TNBC patients, we interrogated the tumour microenvironment for possible clues. Given the association between CTSS expression with macrophages, we

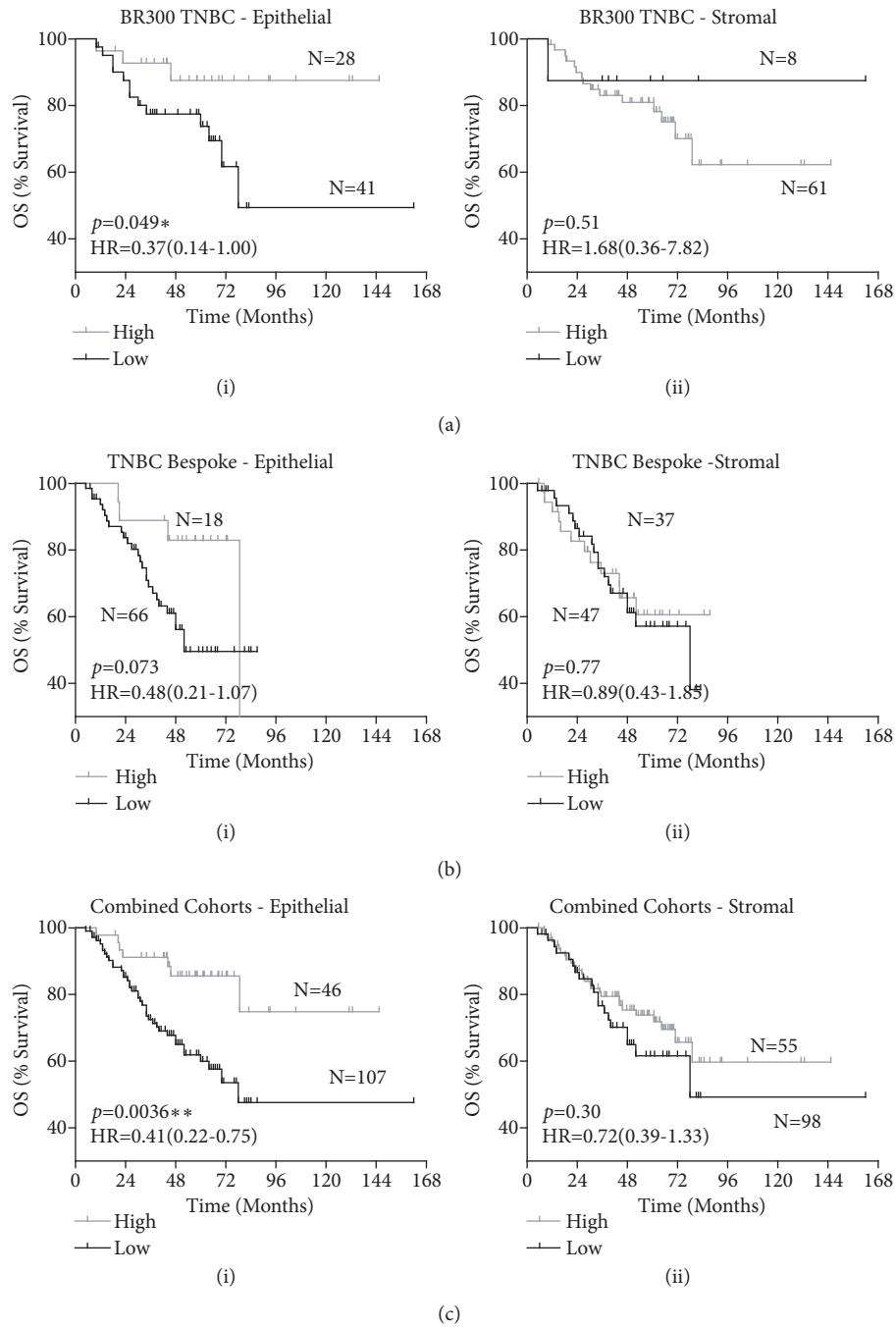

Figure 3: *Increased epithelial cell CTSS expression is associated with improved outcome in TNBC.* Kaplan-Meier curves stratifying overall survival (OS) of (a) the BR300 TNBC patients-alone, (b) the bespoke TNBC enriched cohort-alone, and (c) the combined BR300 and bespoke TNBC cohorts, based on high or low CTSS expression in the (i) epithelial and (ii) stromal compartment. Log-Rank p-value and hazard ratio (HR) with 95% confidence intervals indicated. N=number of patients.

decided to examine the expression of activated M1 (tumour destructive) or alternatively activated M2 (tumour protective) macrophage polarisation markers in the context of CTSS expression.

IHC scoring of CTSS in the TNBC epithelial cells correlated significantly with an increased expression of macrophage marker CD68 (p=0.0011), indicative of increased macrophage infiltration (Figure 6(a)). With this increased presence of macrophages, there was a significant increase in M1 marker CD14 (p=0.014) (Figure 6(b)), and no significant change in the expression of M2 marker CD163 (Figure 6(c)). Using two gene expression based algorithms [25, 26], previously utilised in our TNBC cohort [24], analysis revealed a significant enhancement in M1-like phenotype with presence

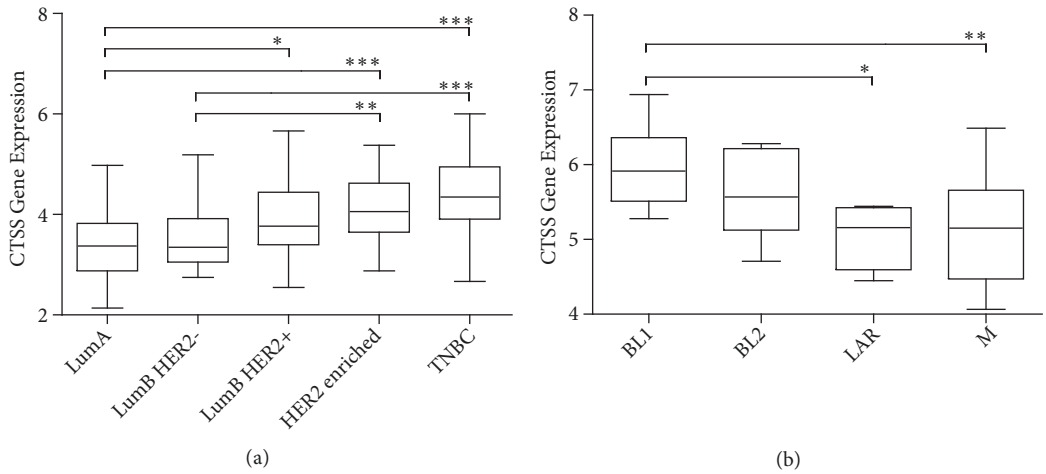

Figure 4: *CTSS gene expression is highest in BR300 TNBC subtype and associated with DNA damage/cell cycle pathways.* CTSS gene expression was evaluated using an in house dataset containing 300 breast cancer patients. Analysis revealed (a) CTSS expression to be highest in TNBC. (b) Lehman subgroups analysis of the TNBC patients revealed an association with the BL1 group which encompasses DNA damage and cell cycle pathways. Significance for both panels was determined by one-way ANOVA. $^{*}p < 0.05$, $^{**}p < 0.01$, and $^{***}p < 0.001$.

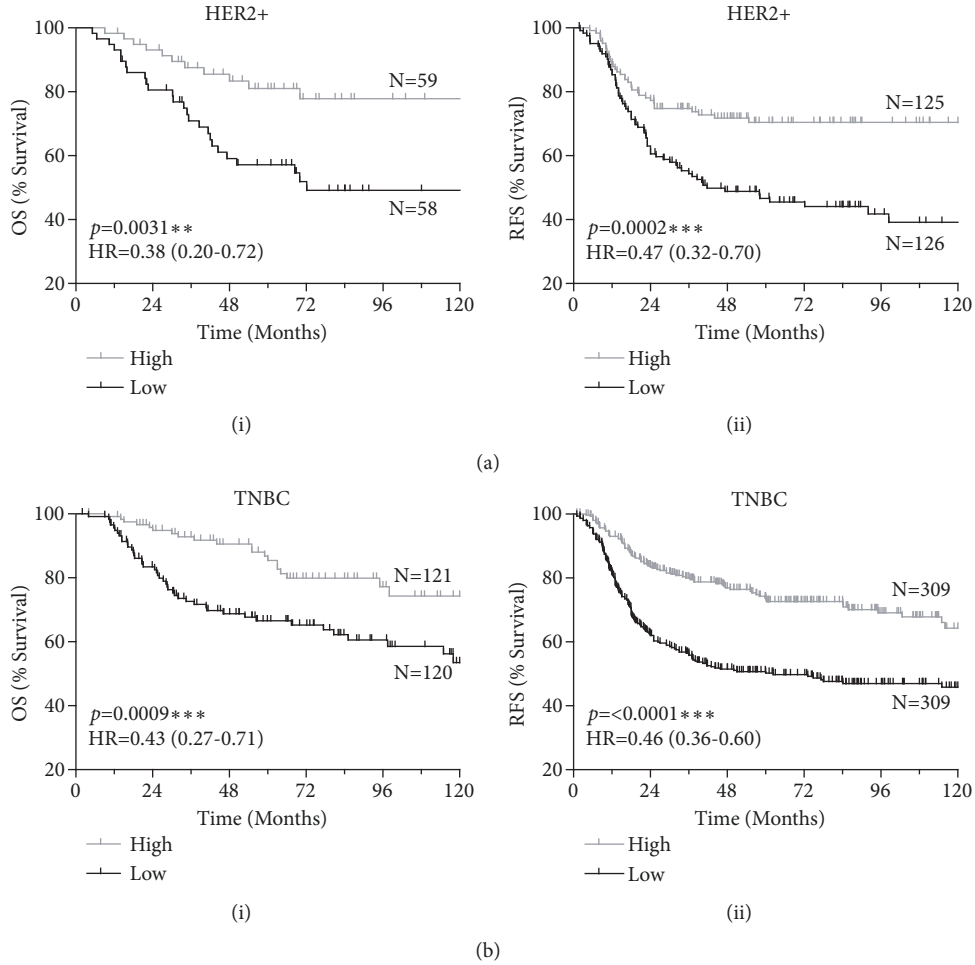

Figure 5: *Analysis of publicly available gene expression datasets reveal improved outcome with high CTSS expression in HER2+ and TNBC patients.* Kaplan-Meier curves stratifying (a) HER2+ and (b) TNBC patients based on high or low CTSS expression and evaluating (i) overall survival (OS) and (ii) relapse free survival (RFS). Log-Rank p-value and hazard ratio (HR) with 95% confidence intervals indicated. N=number of patients.

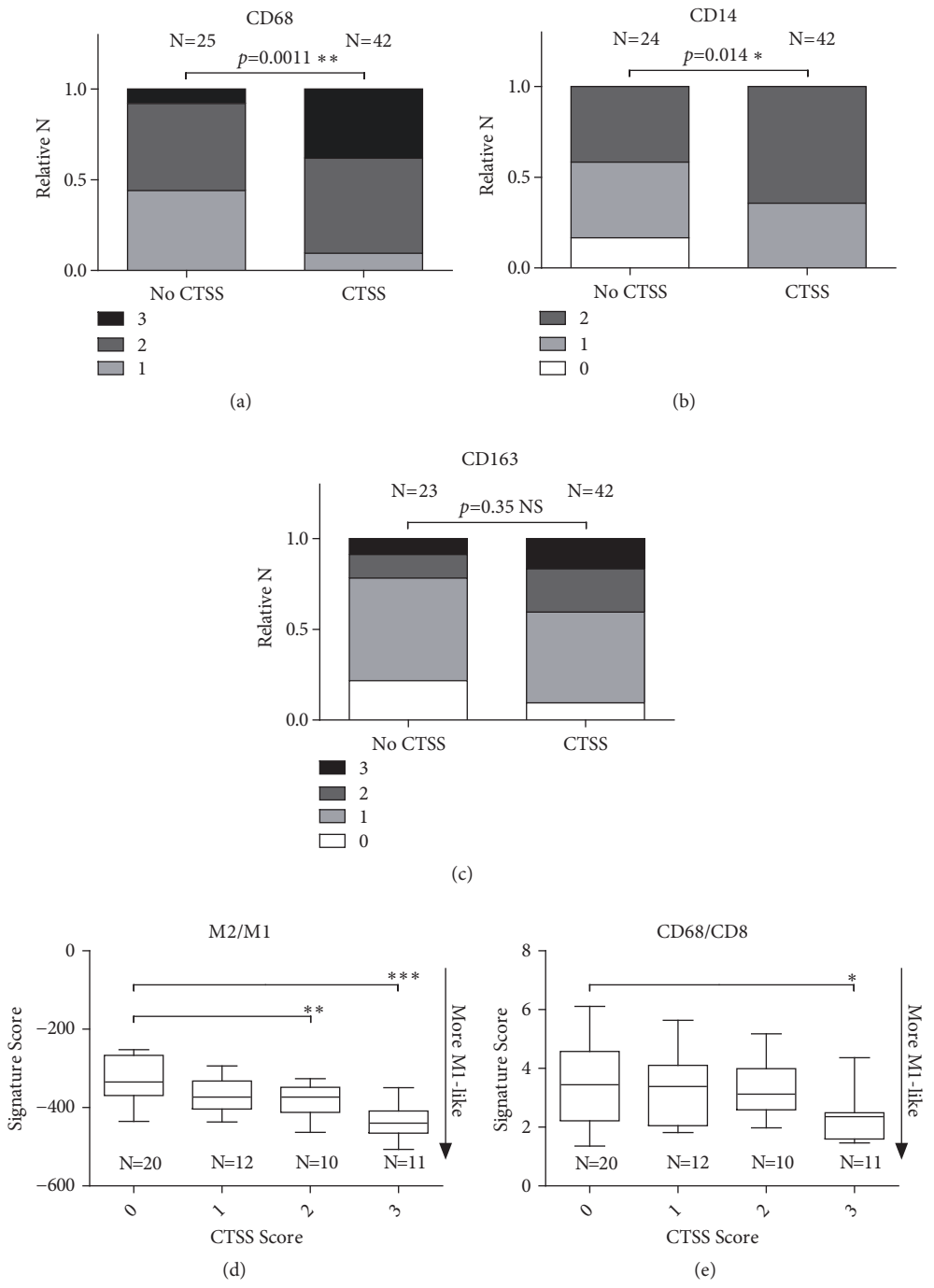

Figure 6: *Epithelial cell CTSS expression in TNBC patients is associated with an M1 macrophage phenotype.* Immunohistochemical epithelial CTSS scores were matched with (a) macrophage marker CD68, (b) M1 polarisation marker CD14 and (c) M2 polarisation marker CD163. Shading indicates proportion of IHC score for each marker. Statistical significance determined by Chi-Square analysis. Macrophage polarisation was analysed using gene expression algorithms and correlated with CTSS IHC expression generating (d) M2/M1 and (e) CD68/CD8 signature scores. Statistical significance determined by one-way ANOVA. N=number of patients. $^{*}p < 0.05$, $^{**}p < 0.01$, and $^{***}p < 0.001$.

of epithelial CTSS expression ($p<0.001$ and $p<0.05$) (Figures 6(d) and 6(e)).

Taken together, this suggests increased expression of CTSS in the epithelial cells associates with increased infiltration of M1 polarised macrophages thus resulting a more immunocompetent microenvironment, and rationalises the improved survival observed with epithelial CTSS expression in the TNBC sub-type.

4. Discussion

In this study we have demonstrated a multifaceted role for CTSS as a biomarker in TNBC. This investigation began by observing differences in patient outcome based on CTSS expression, with stromal-associated CTSS expression shown to be associated with a poor outcome, whereas high CTSS expression in epithelial cells is associated with an improved outcome. Interestingly, the observation of epithelial CTSS expression in TNBC patients revealed an association with improved outcome, which remained consistent in gene expression analysis. We furthermore observed increased M1 polarisation of macrophage in patients exhibiting high CTSS expression in the epithelial cells. Taken together, we found differential CTSS expression had compartmental and subtype effects on patient outcome, highlighting a potentially novel role for this protease in TNBC.

Due to their potent and promiscuous proteolytic function, cysteine cathepsins have previously been implicated in a number of pathological roles as a result of extracellular matrix remodelling including angiogenesis, invasion and metastases [7]. As such, increased CTSS expression has been shown be associated with poor clinical features in a number of cancer types [8–11], as well as holding prognostic value with expression associated with poor outcome in others [12, 13]. To the best of our knowledge, this is the first investigation of CTSS expression in breast cancer using clinical samples evaluating clinical outcome, and furthermore, accounting for outcome based on epithelial or stromal CTSS expression.

We observed clinicopathological patterns with respect CTSS expression and compartment type. When comparing high versus low CTSS scores, we observed an increase in the number of patients with grade 3 tumours with high CTSS expression in both epithelial (53.39% low versus 84.78% high) and stromal (39.24% low versus 67.76% in high) cells. Furthermore, patients with high epithelial CTSS expression also demonstrated decreased node scoring and LVI positivity, indicators of improved outcome. In the epithelial cells, a significant association with increased tumour stage was also observed with high CTSS expression. These are consistent with observations made elsewhere regarding CTSS expression in breast cancer [31]. Interestingly, high CTSS expression in infiltrating cells was associated with poor outcome. This is consistent with the increased aberrant expression of this protease in other carcinomas where as a result of protumorigenic role of this protease in cancer, increased CTSS has been associated with poor outcome reported as a result of tumour associated macrophages (TAMs) [15]. In contrast to this, CTSS expression in the epithelial cells displayed an opposite phenotype. Upon further analysis of subtypes, and within the context of this cohort, we found high CTSS expression to be associated with improved outcome with epithelial CTSS expression in TNBC patients. Taken altogether, this indicates a dual role for this protease in tumour development based on compartmental and subtype expression.

Further *in silico* analysis confirmed these clinical outcome findings, and also highlighted a potential association of CTSS and outcome in the HER2+ subgroup, suggesting a role for CTSS as a biomarker in ER- disease as a whole. This complements the increased number of patients with high epithelial CTSS who did not receive adjuvant hormone therapy (78%), suggesting these tumours exhibit an ER- background. Interestingly, Gautam and colleagues also observed an association between high epithelial CTSS expression and ER- subtype [31]. From a clinical perspective, patients with ER- breast cancers are significantly associated with poor outcome compared to ER+ breast cancer patients, as they lack the relevant targets for therapy [32–36]. Consequentially, there is a real need to stratify these patients further, to maximise improved outcome in patients. Based on our observations, there may be value in further characterising CTSS expression in a larger ER- patient comparative cohort, as this protease may hold utility as a prognostic biomarker in this setting.

An important feature of this study was the use of patient samples who all received adjuvant treatment prior to collection of tumour resections. Analysis of our in-house TNBC gene expression dataset using the Lehmann subgroups demonstrated an association of CTSS expression with the BL1 group, characterised by defects in DNA damage repair pathways. Interestingly, previous investigation using publicly available gene datasets representing 300 TNBC patients who received neo-adjuvant chemotherapeutic treatment, revealed the BL1 subgroup to display the greatest pathological complete response versus the BL2 and LAR patient subgroups [30]. This suggests that expression of CTSS in epithelial cells may be associated with tumours defective in DNA damage repair, and therefore, indicates CTSS expression may be predictive of sensitivity to DNA damaging chemotherapies. Whilst this study has focused on IHC analysis of resected tumours, others have demonstrated that CTSS levels can be detected in patient serum for a variety of diseases [7]. Considering the suggested link between CTSS expression from a prognostic and predictive perspective, it may be of interest to further investigate in liquid biopsies.

The relevance of the tumour immune microenvironment is becoming more important with the development of therapeutic strategies to target this compartment [37]. Consequentially, appreciation of underlying biological associations between tumour and immune cells may help better guide therapies in the future. Here we show a positive correlation between TNBC epithelial derived CTSS expression and a more favourable M1 microenvironment. The relationship between CTSS and TAMs has been widely reported using *in vivo* models [16, 17, 27, 38–40]. These studies have highlighted the relevance of macrophages as a source of CTSS at the tumour site. Furthermore, these studies have associated an M2-marcophage phenotype (tumour protective), and have implicated CTSS in a modulating role via an autophagy-mediated mechanism [40, 41]. Interestingly, the epithelial CTSS expression in TNBC patients demonstrated an enriched M1 polarisation phenotype, consistent with the observed improved outcome. We believe this underlines a more complex relationship between tumour epithelial and stromal cell compartments than has been demonstrated in pre-clinical models, and possibly between cancer types, highlighting a need for further in-depth analysis in patient samples.

5. Conclusion

In conclusion, we have characterised the expression profile of CTSS in breast cancer patient samples and have found that both compartmental and subtype expression of this protease can affect patient outcome. This study highlights a need for further investigation into this protease within breast cancer, to consolidate the potential predictive and prognostic utility of CTSS expression in different subtypes. Furthermore, a deeper appreciation of the biology underlying this disease will help guide treatment regimens and possible application of CTSS inhibitors in the future.

Abbreviations

BL1: Basal-like 1
BL2: Basal-like 2
BR300: Breast 300 cohort
CI: 95% Confidence interval
CTSS: Cathepsin S
ER: Estrogen receptor
HR: Hazard ratio
IHC: Immunohistochemistry
IM: Immunomodulatory
LAR: Luminal Androgen Receptor
LVI: Lymphovascular invasion
M: Mesenchymal
MSL: Mesenchymal stem cell-like
N: Number of patients
NIB: Northern Ireland Biobank
OS: Overall survival
RFS: Relapse free survival
TAM: Tumour associated macrophage
TMA: Tissue microarray
TNBC: Triple negative breast cancer.

Data Availability

All TMA samples are available upon application from the Northern Ireland Biobank (http://www.nibiobank.org).

Additional Points

The article by Lewis and colleagues should be cited in any published manuscripts which may arise from the use of these samples [42].

Conflicts of Interest

Roberta E. Burden and Christopher J. Scott own shares in Fusion Antibodies Ltd. Nuala McCabe and Richard D. Kennedy are employees of ALMAC group Ltd. The authors declare that there are no conflicts of interest regarding the publication of this article.

Authors' Contributions

Richard D. A. Wilkinson was responsible for public database analysis and macrophage marker analysis and wrote the manuscript. Niamh E. Buckley handled in-house gene expression analysis and Lehman subgroup analysis. Stephen McQuaid and Victoria Bingham made the preparation and CTSS IHC staining of breast TMA cohorts. Richard D. A. Wilkinson, Stephen McQuaid, Niamh E. Buckley, and Sara H. McDowell handled scoring of CTSS breast TMA cohorts. Niamh E. Buckley, Órla T. Cox, and Rosemary O'Connor did the scoring of CD14, CD68, and CD163 TMA slides. Richard D. A. Wilkinson and Darragh G. McArt did the patient outcome analysis of CTSS TMA and statistical analysis. Niamh E. Buckley, Nuala McCabe, and Richard D. Kennedy were responsible for gene expression signature data. Christopher J. Scott, Rich Williams, and Roberta E. Burden handled project conception, direction, and funding. All authors read and agreed to content of manuscript prior to submission.

Acknowledgments

This work was supported in part by MRC grant [G0901615] and MRC Confidence in Concept Funding. This work was supported by Breast Cancer Now (Scientific Fellowship NEB [2012MaySF122] and PhD Studentship [2017NovPhD1005]). The samples used in this research were received from the Northern Ireland Biobank which has received funds from HSC Research and Development Division of the Public Health Agency in Northern Ireland and the Friends of the Cancer Centre.

Supplementary Materials

Supplementary Figure 1: Flowchart describing study design. *Supplementary Figure 2:* Breakdown of CTSS scores across subtypes and associated Kaplan-Meier OS figures. (a) Percentage breakdown of patients with high and low CTSS in (i) epithelial and (ii) stromal compartments. Kaplan-Meier curve of (b) Luminal A, (c) Luminal B/HER2-, (d) Luminal B/HER2+, and (e) HER2+ breast cancer subtypes overall survival (OS) stratified based on high or low CTSS expression in (i) stromal and (ii) epithelial compartment. Log-Rank p-value indicated. N=number of patients. *Supplementary Figure 3:* Complete Lehman analysis figure of subtype CTSS gene expression. *Supplementary Figure 4:* No effect on OS or RFS in total, Luminal A, or Luminal B breast cancer subtypes stratified by gene expression. Kaplan-Meier curves stratifying (a) total breast cancer patient population, (b) luminal A patient population, and (c) luminal B patient population, based on high or low CTSS gene expression evaluating (i) overall survival (OS) and (ii) relapse free survival (RFS). Log-rank p-value and hazard ratio (HR) indicated. N=number of patients. *Supplementary Table 1:* Increased CTSS gene expression associated with improved survival in HER2+ and Triple Negative breast cancers. Analysis of publicly available gene expression data with matching clinical outcome from KM plotter revealed a significant association of increased CTSS expression with improved overall survival and relapse free survival. N=number of patients. HR= hazard ratio. CI=95% confidence intervals. *(Supplementary Materials)*

References

[1] X. Dai, T. Li, Z. Bai et al., "Breast cancer intrinsic subtype classification, clinical use and future trends," *American Journal of Cancer Research*, vol. 5, no. 10, pp. 2929–2943, 2015.

[2] C. Liedtke, C. Mazouni, K. R. Hess et al., "Response to neoadjuvant therapy and long-term survival in patients with triple-negative breast cancer," *Journal of Clinical Oncology*, vol. 26, no. 8, pp. 1275–1281, 2008.

[3] L. A. Carey, E. C. Dees, L. Sawyer et al., "The triple negative paradox: primary tumor chemosensitivity of breast cancer subtypes," *Clinical Cancer Research*, vol. 13, no. 8, pp. 2329–2334, 2007.

[4] B. S. Yadav, P. Chanana, and S. Jhamb, "Biomarkers in triple negative breast cancer: a review," *World Journal of Clinical Oncology*, vol. 6, no. 6, pp. 252–263, 2015.

[5] O. T. Cox, S. J. Edmunds, K. Simon-Keller et al., "PDLIM2 is a marker of adhesion and β-catenin activity in triple-negative breast cancer," *Cancer Research*, vol. 79, no. 10, pp. 2619–2633, 2019.

[6] D. M. Small, R. E. Burden, and C. J. Scott, "The emerging relevance of the cysteine protease cathepsin S in disease," *Clinical Reviews in Bone and Mineral Metabolism*, vol. 9, no. 2, pp. 122–132, 2011.

[7] R. D. Wilkinson, R. Williams, C. J. Scott, and R. E. Burden, "Cathepsin S: therapeutic, diagnostic, and prognostic potential," *Biological Chemistry*, vol. 396, no. 8, pp. 867–882, 2015.

[8] C. Lindahl, M. Simonsson, A. Bergh et al., "Increased levels of macrophage-secreted cathepsin S during prostate cancer progression in TRAMP mice and patients," *Cancer Genomics & Proteomics*, vol. 6, no. 3, pp. 149–160, 2009.

[9] P. L. Fernández, X. Farré, A. Nadal et al., "Expression of Cathepsins B and S in the progression of prostate carcinoma," *International Journal of Cancer*, vol. 95, no. 1, pp. 51–55, 2001.

[10] Y. Yang, L. S. Kiat, C. L. Yee et al., "Cathepsin S mediates gastric cancer cell migration and invasion via a putative network of metastasis-associated proteins," *Journal of Proteome Research*, vol. 9, no. 9, pp. 4767–4778, 2010.

[11] J. Xu, D. Li, Z. Ke, R. Liu, G. Maubach, and L. Zhuo, "Cathepsin S is aberrantly overexpressed in human hepatocellular carcinoma," *Molecular Medicine Reports*, vol. 2, no. 5, pp. 713–718, 2009.

[12] T. Flannery, S. McQuaid, C. McGoohan et al., "Cathepsin S expression: An independent prognostic factor in glioblastoma tumours - A pilot study," *International Journal of Cancer*, vol. 119, no. 4, pp. 854–860, 2006.

[13] J. A. Gormley, S. M. Hegarty, A. O'Grady et al., "The role of Cathepsin S as a marker of prognosis and predictor of chemotherapy benefit in adjuvant CRC: a pilot study," *British Journal of Cancer*, vol. 105, no. 10, pp. 1487–1494, 2011.

[14] W. Liu, D. Liu, K. Cheng et al., "Evaluating the diagnostic and prognostic value of circulating cathepsin S in gastric cancer," *Oncotarget*, vol. 7, no. 19, pp. 28124–28138, 2016.

[15] V. Gocheva, W. Zeng, D. Ke et al., "Distinct roles for cysteine cathepsin genes in multistage tumorigenesis," *Genes & Development*, vol. 20, no. 5, pp. 543–556, 2006.

[16] D. M. Small, R. E. Burden, J. Jaworski et al., "Cathepsin S from both tumor and tumor-associated cells promote cancer growth and neovascularization," *International Journal of Cancer*, vol. 133, no. 9, pp. 2102–2112, 2013.

[17] L. Sevenich, R. L. Bowman, S. D. Mason et al., "Analysis of tumour- and stroma-supplied proteolytic networks reveals a brain-metastasis-promoting role for cathepsin S," *Nature Cell Biology*, vol. 16, no. 9, pp. 876–888, 2014.

[18] R. E. Burden, J. A. Gormley, T. J. Jaquin et al., "Antibody-mediated inhibition of cathepsin S blocks colorectal tumor invasion and angiogenesis," *Clinical Cancer Research*, vol. 15, no. 19, pp. 6042–6051, 2009.

[19] R. D. Wilkinson, A. Young, R. E. Burden, R. Williams, and C. J. Scott, "A bioavailable cathepsin S nitrile inhibitor abrogates tumor development," *Molecular Cancer*, vol. 15, no. 1, article 29, 2016.

[20] D. P. Boyle, D. G. McArt, G. Irwin et al., "The prognostic significance of the aberrant extremes of p53 immunophenotypes in breast cancer," *Histopathology*, vol. 65, no. 3, pp. 340–352, 2014.

[21] M. P. Humphries, S. Hynes, V. Bingham et al., "Automated tumour recognition and digital pathology scoring unravels new role for PD-L1 in predicting good outcome in ER-/HER2+ breast cancer," *Journal of Oncology*, vol. 2018, Article ID 2937012, 14 pages, 2018.

[22] K. Orr, N. E. Buckley, P. Haddock et al., "Thromboxane A2 receptor (TBXA2R) is a potent survival factor for triple negative breast cancers (TNBCs)," *Oncotarget*, vol. 7, no. 34, pp. 55458–55472, 2016.

[23] B. Győrffy, P. Surowiak, J. Budczies, and A. Lánczky, "Online survival analysis software to assess the prognostic value of biomarkers using transcriptomic data in non-small-cell lung cancer," *PLoS ONE*, vol. 8, no. 12, article e82241, 2013.

[24] N. E. Buckley, P. Haddock, R. De Matos Simoes et al., "A BRCA1 deficient, NFkappaB driven immune signal predicts good outcome in triple negative breast cancer," *Oncotarget*, vol. 7, no. 15, pp. 19884–19896, 2016.

[25] P. Jézéquel, D. Loussouarn, C. Guérin-Charbonnel et al., "Gene-expression molecular subtyping of triple-negative breast cancer tumours: importance of immune response," *Breast Cancer Research*, vol. 17, article 43, 2015.

[26] D. G. DeNardo, D. J. Brennan, E. Rexhepaj et al., "Leukocyte complexity predicts breast cancer survival and functionally regulates response to chemotherapy," *Cancer Discovery*, vol. 1, no. 1, pp. 54–67, 2011.

[27] V. Gocheva, H.-W. Wang, B. B. Gadea et al., "IL-4 induces cathepsin protease activity in tumor-associated macrophages to promote cancer growth and invasion," *Genes & Development*, vol. 24, no. 3, pp. 241–255, 2010.

[28] I. Vasconcelos, A. Hussainzada, and S. Berger, "The St. Gallen surrogate classification for breast cancer subtypes successfully predicts tumor presenting features, nodal involvement, recurrence patterns and disease free survival," *The Breast*, vol. 29, pp. 181–185, 2016.

[29] J. M. Mulligan, L. A. Hill, S. Deharo et al., "Identification and validation of an anthracycline/cyclophosphamide-based chemotherapy response assay in breast cancer," *Journal of the National Cancer Institute*, vol. 106, no. 1, article djt335, 2014.

[30] B. D. Lehmann, B. Jovanović, X. Chen et al., "Refinement of triple-negative breast cancer molecular subtypes: implications for neoadjuvant chemotherapy selection," *PLoS ONE*, vol. 11, no. 6, article e0157368, 2016.

[31] J. Gautam, Y. K. Bae, and J.-A. Kim, "Up-regulation of cathepsin S expression by HSP90 and 5-HT7 receptor-dependent serotonin signaling correlates with triple negativity of human breast cancer," *Breast Cancer Research and Treatment*, vol. 161, no. 1, pp. 29–40, 2017.

[32] J. P. Crowe, N. H. Gordon, C. A. Hubay et al., "Estrogen receptor determination and long term survival of patients with

carcinoma of the breast," *Surgery, gynecology & obstetrics*, vol. 173, no. 4, pp. 273–278, 1991.

[33] P. T. Truong, V. Bernstein, E. Wai, B. Chua, C. Speers, and I. A. Olivotto, "Age-related variations in the use of axillary dissection: a survival analysis of 8038 women with T1-ST2 breast cancer," *International Journal of Radiation Oncology, Biology, Physics*, vol. 54, no. 3, pp. 794–803, 2002.

[34] L. A. Carey, C. M. Perou, C. A. Livasy et al., "Race, breast cancer subtypes, and survival in the carolina breast cancer study," *The Journal of the American Medical Association*, vol. 295, no. 21, pp. 2492–2502, 2006.

[35] K. Yu, J. Wu, Z. Shen, and Z. Shao, "Hazard of breast cancer-specific mortality among women with estrogen receptor-positive breast cancer after five years from diagnosis: implication for extended endocrine therapy," *The Journal of Clinical Endocrinology & Metabolism*, vol. 97, no. 12, pp. E2201–E2209, 2012.

[36] V. Sopik, P. Sun, and S. A. Narod, "The prognostic effect of estrogen receptor status differs for younger versus older breast cancer patients," *Breast Cancer Research and Treatment*, vol. 165, no. 2, pp. 391–402, 2017.

[37] A. R. Poh and M. Ernst, "Targeting macrophages in cancer: from bench to bedside," *Frontiers in Oncology*, vol. 8, article 49, 2018.

[38] M. Verdoes, L. Edgington, F. A. Scheeren et al., "A nonpeptidic cathepsin S activity-based probe for noninvasive optical imaging of tumor-associated macrophages," *Chemistry & Biology*, vol. 19, no. 5, pp. 619–628, 2012.

[39] T. Shree, O. C. Olson, B. T. Elie et al., "Macrophages and cathepsin proteases blunt chemotherapeutic response in breast cancer," *Genes & Development*, vol. 25, no. 23, pp. 2465–2479, 2011.

[40] M. Yang, J. Liu, J. Shao et al., "Cathepsin S-mediated autophagic flux in tumor-associated macrophages accelerate tumor development by promoting M2 polarization," *Molecular Cancer*, vol. 13, article 43, 2014.

[41] S. J. Salpeter, Y. Pozniak, E. Merquiol, Y. Ben-Nun, T. Geiger, and G. Blum, "A novel cysteine cathepsin inhibitor yields macrophage cell death and mammary tumor regression," *Oncogene*, vol. 34, no. 50, pp. 6066–6078, 2015.

[42] C. Lewis, S. McQuaid, P. Clark et al., "The Northern Ireland biobank: a cancer focused repository of science," *Open Journal of Bioresources*, vol. 5, no. 9, 2018.

Hindawi
Journal of Oncology
Volume 2019, Article ID 6201764, 10 pages
https://doi.org/10.1155/2019/6201764

Research Article

Overexpression of Kynurenine 3-Monooxygenase Correlates with Cancer Malignancy and Predicts Poor Prognosis in Canine Mammary Gland Tumors

Yi-Han Chiu,[1,2] Han-Jung Lei,[3] Kuo-Chin Huang,[4] Yi-Lin Chiang,[3] and Chen-Si Lin[3,5]

[1]*Department of Nursing, St. Mary's Junior College of Medicine, Nursing and Management, Yilan 26647, Taiwan*
[2]*Institute of Long-Term Care, Mackay Medical College, New Taipei City 25245, Taiwan*
[3]*Graduate Institute of Veterinary Clinical Science, School of Veterinary Medicine, National Taiwan University, Taipei 10617, Taiwan*
[4]*Holistic Education Center, Mackay Medical College, New Taipei City 25245, Taiwan*
[5]*Animal Cancer Center, College of Bioresources and Agriculture, National Taiwan University, No. 1, Sec. 4, Roosevelt Road, Taipei 10617, Taiwan*

Correspondence should be addressed to Chen-Si Lin; cslin100@ntu.edu.tw

Received 20 February 2019; Accepted 8 April 2019; Published 2 May 2019

Guest Editor: Chia-Jung Li

Tumor biomarkers are developed to indicate tumor status, clinical outcome, or prognosis. Since currently there are no effective biomarkers for canine mammary tumor (CMT), this study intended to verify whether kynurenine 3-monooxygenase (KMO), one of the key enzymes involved in tryptophan catabolism, is competent for predicting prognosis in patients with CMT. By investigating a series of 86 CMT clinical cases, we found that both gene and protein expression of KMO discriminated malignant from benign CMTs and was significantly higher in stage IV and V tumors than in lower-stage CMTs. About 73.7% of malignant CMTs showed strong expression of KMO which correlated with lower overall survival rates in patients. Further, downregulation of KMO activity significantly inhibited cell proliferation of CMT cells. Taken together, the findings indicated that KMO is a potential biomarker for tumor diagnosis, and this might open up new perspectives for clinical applications of CMT.

1. Introduction

Dogs are viewed as a desirable animal model for human cancer research, as they share a living environment closely related to humans, with similar development patterns of spontaneous tumors and cancer epidemiology [1]. In addition, the genes associated with cancer are much more closely related between dogs and humans than between mice and humans [2]. Recently, many studies have highlighted the similar risk factors are associated with breast cancer among dogs and humans. For example, the outbred nature of dogs compared with mice provides a similar level of genetic diversity among dogs as that found among humans [1]. The *BRCA* gene acts as the tumor suppressor and is significant for the development of canine mammary tumors (CMTs) and human breast cancer [3]. Studies demonstrated that BRCA 1/2 made approximately equal contributions to early-onset human breast cancer, and higher prevalence of BRCA gene mutation was found in breast cancer patients from China and England to show its relevance in the development of breast cancer [4, 5]. Moreover, inbreeding traits within particular breeds of dogs result in low genetic variation [6], which may also aid the identification of potential risk factors or biomarkers for both human and canine cancer malignancy.

Biomarkers are useful tools in cancer diagnosis, tumor monitoring, and prognosis. Most biomarkers are involved in tumor development and therefore can be applied in cancer therapies [7–10]. Estrogen receptor (ER), progesterone receptor (PR), and human epidermal growth factor receptor 2 (HER2) are biomarkers measured in routine examinations for human breast cancer. The progression of breast cancer

and canine mammary tumors is mainly stimulated by hormones. In human breast cancer, patients with tumors that are ER-positive and/or PR-positive have a better response to hormonal treatment and there is a lower risk of mortality after diagnosis as compared with patients with ER-negative and/or PR-negative tumors [11]. In canine mammary tumors, studies have demonstrated that the expression of ER-α or PR is related to the histological subtype of canine mammary tumors [12], the occurrence of metastases [13], and the survival rate [14–16], but some studies showed no correlations between these factors [17, 18]. HER-2 is a cell membrane surface-bound receptor tyrosine kinase that is involved in several signal transduction pathways and promotes cell growth. Protein overexpression or gene amplification of HER-2 in breast cancer often correlates with poorer clinical outcomes [19–22], and therefore HER-2 is used as an indicator for prognosis [20, 23–25]. The role of HER-2 overexpression in canine mammary tumors is still controversial. Some studies have demonstrated that a high level of HER-2 protein is related to poorer outcomes, such as a higher tumor grade or a greater mitotic count [26, 27], while other studies have demonstrated opposite results [28, 29]. Although other molecular markers have shown potential for diagnosis and prognosis, there is no sufficient evidence proving their efficacy for routine examination and treatment [30–32]. Therefore, it is important to discover new potential biomarkers for clinical application for canine mammary tumor therapy.

Kynurenine 3-monooxygenase (KMO) is a key enzyme in the kynurenine pathway. KMO catalyzes the hydrolysis of kynurenine (KYN) to form 3-hydroxy kynurenine (3-HK) and further generates the downstream metabolite quinolinic acid. Both 3-HK and quinolinic acid may lead to excitotoxicity in the CNS and act as important factors in neurodegenerative diseases [33–36]. As KMO is located at the critical branching point in the kynurenine pathway, elevation of KMO protein shifts the pathway towards the formation of 3-HK instead of kynurenine acid, which is an antagonist of NMDA receptors to protect neuronal cells from the excitotoxicity. KMO plays a role in balancing NMDA receptor agonists and antagonists; therefore, KMO inhibitors can be applied in therapy for neurodegenerative diseases [37]. Presently little is known about KMO for its significance on tumor development. Jin et al. found that high KMO expression is correlated with aggressive malignant phenotype of human hepatocellular carcinoma (HCC) cells and poor prognosis and thus concluded that KMO can be served as a promising biomarker of HCC prognosis [38]. A high level of KMO promotes the synthesis of downstream metabolites of the kynurenine pathway, such as 3-HK, 3-hydroxyanthranilic acid, and quinolinic acid, which participate in the regulation of the immune response and tumor tolerance [39, 40]. On the other hand, a high level of quinolinic acid might stimulate more NMDA receptors, which promotes tumor proliferation through the ERK pathway.

No other study has investigated the role of KMO in canine tumor development. In this study we disclose the association between KMO expression and the malignancy of canine mammary tumors. This study aimed to verify whether KMO is a potential biomarker for the diagnosis of CMT and whether KMO can be a useful molecule in prognostic prediction and therapeutic development for mammary tumors in the future.

2. Materials and Methods

2.1. Canine Tissue Specimens. Canine mammary tumor tissue specimens were collected in accordance with regulations of the Institutional Animal Care and Use Committee (IACUC) at National Taiwan University Veterinary Hospital and conformed to the guidelines of the protocol IACUC-NTU-101-EL-106. The patients were diagnosed and underwent surgery to remove tumors from 2012 to 2016. All of the patients underwent surgical removal of CMT without other therapy. The clinical histories of the patients were recorded in depth, and follow-up information was continually documented until May 2018. The histological classification and stage of CMT were determined according to the guidelines of the World Health Organization [41]. All tumor pathological diagnoses in this study were done before analyzing the role of KMO in CMT malignancy, but the blind tests were performed by our operators to investigate the KMO gene and protein expression of the tumor cases.

2.2. Real-Time RT-PCR. Total RNA was extracted from collected CMT specimens using TRIzol (Invitrogen) and treated with DNase I (Fermentas) to remove contaminated genomic DNA for real-time RT-PCR analysis. Reverse transcription was carried out using a Mastercycler Personal thermal cycler (Eppendorf) with SuperScript II RT (Invitrogen) to synthesize complementary DNA. Primers that specifically bind to canine indoleamine 2,3-dioxygenase (*IDO*) and *KMO* genes were designed using Primer Express software (Applied Biosystems). The housekeeping genes used were β-actin and hypoxanthine-phosphoribosyl transferase (*HPRT*), which represents one of the best reference genes for canine mammary gland [42] (Table 1). Real-time RT-PCR was performed on a Bio-Rad real-time PCR machine with the use of SYBR Green PCR Master Mix according to the procedure described previously [43]. Data were presented as fold change in gene expression level in the sample normalized to the housekeeping genes using $2^{-\Delta Ct}$ method.

2.3. Immunohistochemistry and Protein Scoring System. Sections (5-μm-thick) of formalin-fixed, paraffin-embedded tumor specimens were deparaffinized by submerging slides in two changes of xylene for 20 min each time. Fresh xylene was used for the second tank. The sections were then rehydrated in graded ethanol for 5 min each. After rehydration, the sections were rinsed with distilled water and antigen retrieval was performed with citrate buffer (10.2 mM Trisodium citrate dihydrate, 1.9 mM Citric acid hydrate, pH 6.0) in a decloaking chamber (BIOCARE MEDICAL) at 121°C for 3 min and then at 90°C for 30 s. Endogenous peroxidase activity was quenched using 3% hydrogen peroxide in PBS for 30 min at room temperature, and then the slides were rinsed with Tris-buffered saline (TBS, 24.7 mM Tris-base, 136.9 mM Sodium

Table 1: Primers for canine *IDO*, *KMO*, actin, and *HPRT*.

Gene	Forward	Reverse
IDO	CAGCTCACCGGGACTTTCTT	TCCATGGCATTAGTGCCTCC
KMO	ATGGAGTCATCAGACGTTCA	GTGACCCCATGGAGTTTGCA
Actin	CGACCTGACCGACTACCTCA	TTTGATGTCACGCACGATTT
HPRT	TGCTCGAGATGTGATGAAGG	TCCCCTGTTGACTGGTCATT

Table 2: Classification of KMO expression as determined by immunoreactive score (IRS).

Intensity of immunoreactivity	Score	Proportion reactive	Score
No staining	0	No staining	0
Weak cytoplasmic staining	1	< 10%	1
Moderate cytoplasmic staining	2	10%-50%	2
Strong cytoplasmic staining	3	> 50%	3

chloride, pH 7.6) and were blocked with 3% bovine serum albumin (BSA) in TBS for 1 h at room temperature. After blocking, the slides were incubated with rabbit anti-human KMO polyclonal antibody (Proteintech) at a 1:50 dilution in blocking buffer. The rabbit anti-human KMO polyclonal antibody was pretested on human and dog's kidneys as a positive control. Rabbit normal serum (Biogenex) replaced the primary antibody in the same protocol as a negative control. All of the slides were incubated with the primary antibodies overnight at 4°C. On the next day, the slides were rinsed with TBS buffer and the signals of proteins were detected by BioGenex Super Sensitive™ Detection Systems (BioGenex). Briefly, the slides were incubated with Super enhancer™ and Polymer-HRP (BioGenex) for 1 h each at room temperature. TBS buffer was used to wash the slides following each staining step. The slides were treated with Diaminobenzidine tetrahydrochloride (DAB) (BioGenex), which was used as a substrate to visualize protein signals for 1 min and then stained with Mayer's hematoxylin (Sigma-Aldrich) for 30 s. The sections were washed with distilled water for 10 min and then dried at room temperature. After dehydration, the slides were mounted by water-soluble glycerol gelation and examined under a bright-field microscope (Olympus).

All of the immunohistochemical slides were examined by a veterinary pathologist who did not have the patients' clinical information. A total of 5 random fields were chosen from tumor regions to evaluate the expression of each protein. The IHC staining of the samples was evaluated by a gynecological histopathologist using the immunoreactive scoring (IRS) system as described previously [44]; the system is used to rank the protein expressions and the value that equals the staining intensity multiplied by the percentage of positive cells [45]. Grading was performed in a blinded fashion. Samples were interpreted as COX-2-positive if the IRS was ≥4. The standard IRS scores are shown in Table 2. The level of KMO protein was examined under high-power microscopic fields (HPFs, 400×) and scored by the IRS system. The standard for staining intensity is shown in Figure 3.

2.4. Assays for Verifying KMO Biofunctions. Canine CMT cell lines CMT-1 and MPG were kindly provided by Dr. Lin CT of the School of Veterinary Medicine, National Taiwan University (Taipei, Taiwan). Both were cultured in Dulbecco's modified Eagle's Medium (DMEM, Gibco) supplemented with 10% fetal bovine serum (FBS, Caisson) and 1% penicillin/streptomycin (Caisson) at 37°C in a humidified atmosphere of 5% CO_2. To verify the role of KMO in cell growth, 3000 cells/well of CMT-1 or MPG cells were seeded in a 96-well plate and treated with KMO inhibitor, Ro 61-8048 (Sigma-Aldrich), at the indicated concentrations for 24, 48, and 72 h. After the treatment, quantification of cell proliferation was performed using WST-1 reagent according to the manufacturer's protocol (Roche). For *KMO* knockdown, small interfering RNAs (siRNAs), including control and *KMO*, were used, and the reagents were all purchased from Santa Cruz Biotech Inc. CMT-1 and MPG cells were transfected for 48 h with siRNAs against *KMO* (Forward 5′-CCAAGGUAUUCCCAUGAGATT-3′, reverse 5′-UCUCAUGGGAAUACCUUGGTT-3′; scramble siRNA duplex: forward: 5′-UUCUCCGAACGUGUCACGUTT-3′; reverse: 5′-ACGUGACACGUUCGGAGAATT-3′). The cell viability of the cells was quantified using WST-1 and cell extracts were analyzed by KMO immunoblotting.

2.5. Western Immunoblotting. The sample (30 μg of protein/lane) was subjected to SDS-PAGE and blotted from 12% (w/v) polyacrylamide gel to a hydrophobic polyvinylidene difluoride (PVDF) membrane for WB analysis. After blocking the PVDF membrane in PBS, 0.05% Tween 20 (PBST) plus 5% skim milk for 2h, the membrane was then sequentially incubated with the anti-human KMO polyclonal antibody (1:2000) (Proteintech) for 2h, and horseradish peroxidase conjugated anti-rabbit IgG (A9169, Sigma-Aldrich) for 1 h at room temperature. Finally, the membrane was washed extensively with PBST and developed with a chemiluminescent peroxidase substrate (Sigma-Aldrich).

2.6. Statistical Analysis. Comparisons of mean values were performed using independent two-sample *t* tests with SPSS 16.0 statistics software. The associations between the variables of the categorical factors, including clinical outcomes and the

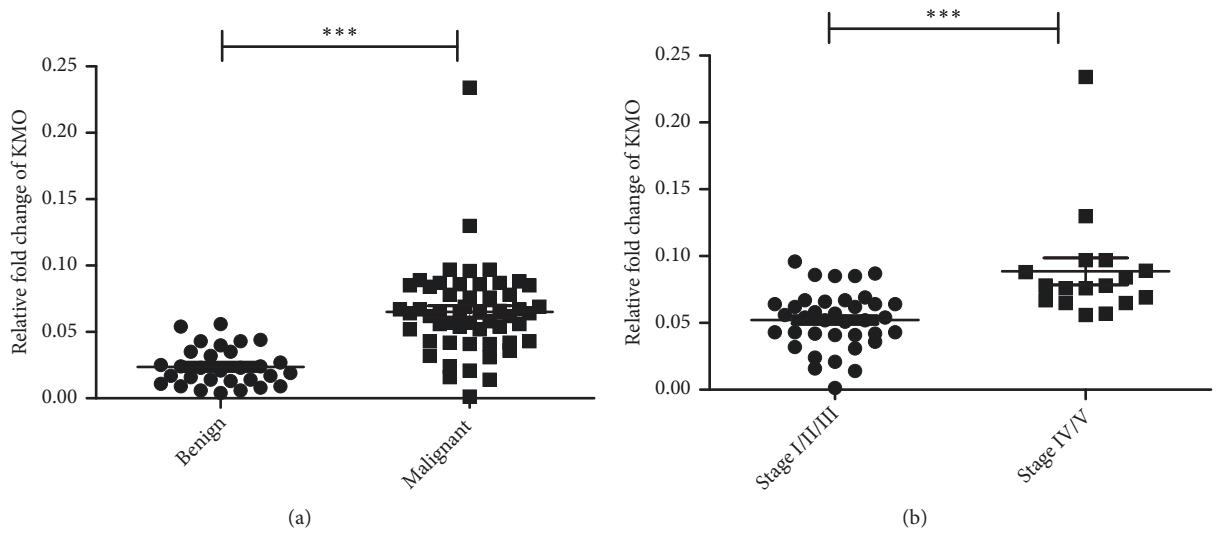

Figure 1: *Comparison of the KMO gene expression in CMTs.* (a) *KMO* gene expression in benign ($n = 30$) and malignant CMT tissues ($n = 54$). (b) *KMO* gene expression in canine malignant CMTs at stages I/II/III ($n = 37$) and stages IV/V ($n = 17$). ($***P < 0.0001$).

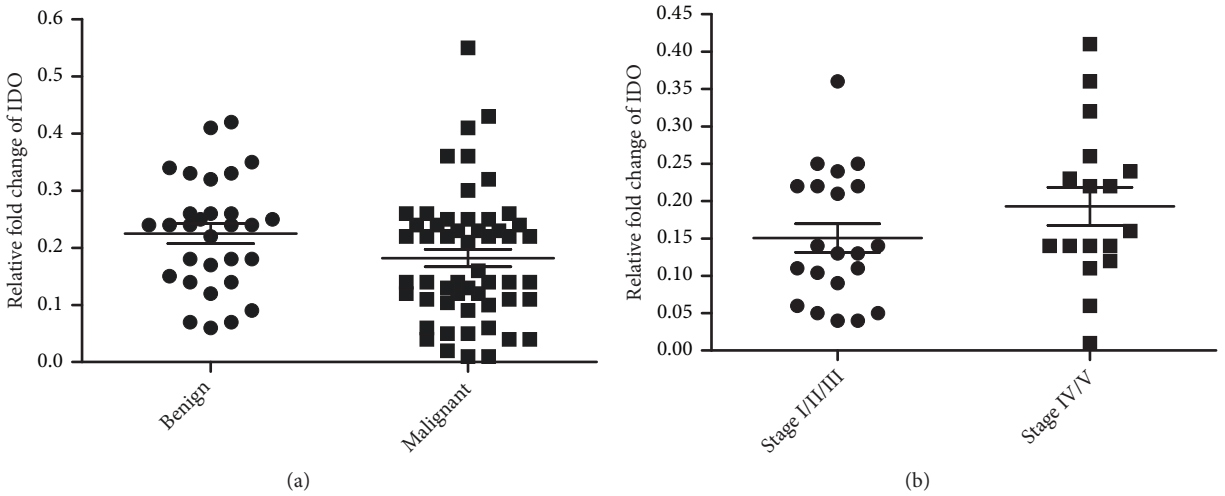

Figure 2: *Expression level of the IDO gene in CMTs.* (a) *IDO* gene expression in benign and malignant CMT tissues. (b) *IDO* gene expression in canine malignant CMTs at stages I/II/III and stages IV/V.

expression of proteins, were calculated by Spearman's correlation coefficient. The significance of the difference between the variables of the categorical factors was determined using a two-tailed χ^2 test. The Kaplan–Meier method was used to estimate the survival durations through the follow-up period.

3. Results

3.1. KMO Gene Expression and Tumor Malignancy. *KMO* gene expression in clinical CMT specimens was first identified in 84 cases using real-time PCR. Interestingly, significantly higher expressions of *KMO* ($p < 0.0001$) were observed in malignant CMTs than in benign CMTs (Figure 1(a)). In addition, the *KMO* gene ($p < 0.0001$) was overexpressed in stage VI/V CMTs (Figure 1(b)). The data showed that *KMO* gene expression discriminated dogs with malignant CMTs from dogs with benign CMTs and indicated that the expression level of the *KMO* gene may provide valuable information for the diagnosis of malignancy and metastasis in canine CMTs.

3.2. The Correlation between the Expressions of KMO and Indoleamine-2,3-Dioxygenase Genes in CMTs. Indoleamine-2,3-dioxygenase (IDO) is located upstream of KMO in the kynurenine pathway [46]. We therefore sought to clarify whether the overexpression of *KMO* was related to the *IDO* expression. The results showed that there was no significant difference in *IDO* expression between malignant and benign CMTs or between CMTs with or without metastasis (Figures 2(a) and 2(b)). These findings indicated that *KMO* overexpression was not *IDO*-dependent in CMTs.

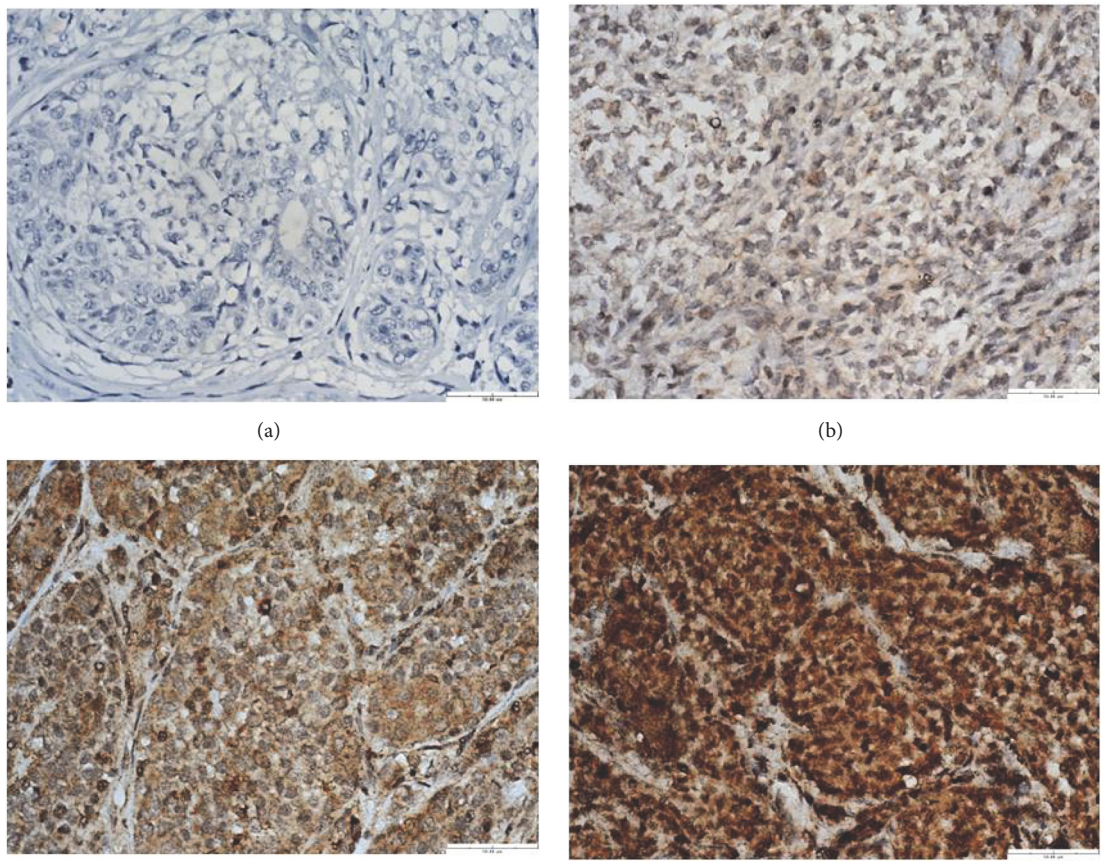

Figure 3: *Immunohistochemical analysis of KMO protein expression in CMTs.* (a) CMT stained without antibody against KMO as a negative control, which did not show immunoreactivity in the cytoplasm. (b) CMT with weak KMO cytoplasmic staining (1+). (c) CMT with moderate KMO cytoplasmic staining (2+). (d) CMT with strong KMO cytoplasmic staining (3+). Scale bar = 50.00 μm.

3.3. The Correlation between KMO Protein Expression and CMT Malignancy. To further determine the association between KMO and tumor progression, KMO expression in CMTs was analyzed by immunohistochemistry and scored by immunoreactive scoring (IRS) under the conditions listed in Table 1: Primers for canine *IDO*, *KMO*, actin, and *HPRT*.

Table 2 shows that the standards for scoring KMO protein are shown in Figure 3. According to the IRS, KMO expression could be classified into three groups. Thus, tumors were identified as KMO negative (IRS 0-3), weak (IRS 4-6), and strong (IRS 7-9). Further analysis showed that the level of KMO expression was significantly associated with ovariohysterectomy (OHE) status; 21/39 (53%) patients with a strong KMO expression had OHE prior to the surgery to remove tumors ($p < 0.05$). The level of KMO expression was also significantly associated with tumor malignancy, tumor size, and tumor recurrence. In total, of 39 CMTs with a strong KMO expression, 27/39 (69%) tumors were malignant ($p < 0.001$). The correlations between the level of KMO expression and the characteristics of the patients with CMTs are summarized in Table 3. Moreover, as shown in Figure 4, KMO IRS in malignant CMTs was significantly higher than that in benign CMTs ($p < 0.001$). These results suggested that

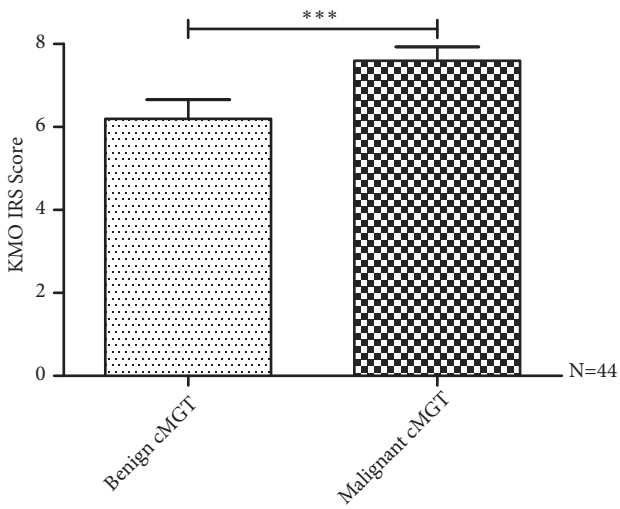

Figure 4: *Correlation between KMO IRS and pathologic malignancy in CMTs.* The expression of the KMO protein was analyzed by immunohistochemistry and scored by immunoreactive score (IRS). KMO IRS showed a statistically significant association with tumor malignancy ($P < 0.05$). KMO IRS in malignant CMTs was significantly higher than that in benign CMTs ($***P < 0.001$).

Table 3: Characteristics of the patients correlated with expression of KMO protein.

Characteristics	KMO			*P* value
	Negative 0-3	Weak 4-6	Strong 7-9	
All patients	6/ 86 (7%)	41/86 (48%)	39/86 (45%)	
Age				
<9 years	4/6 (67%)	12/41 (29%)	6/39 (15%)	
≥ 9 years	2/6 (33%)	29/41 (71%)	33/39 (85%)	0.271
Tumor size				
≤ 5 cm maximum diameter	4/6 (67%)	31/41 (76%)	25/39 (64%)	
> 5 cm maximum diameter	2/6 (33%)	10/41 (24%)	14/39 (36%)	*0.028*∗
Ovariohysterectomy status				
No	5/6 (100%)	37/41 (90%)	18/39 (47%)	*0.031*∗
Yes	1/6 (0%)	4/41 (10%)	21/39 (53%)	
Malignancy				
Benign	6/6 (100%)	31/41 (76%)	12/39 (31%)	
Malignant	0/6 (0%)	10/41 (24%)	27/39 (69%)	*0.0004*∗∗
Tumor stage (N=37)				
I, II and III	---	3/10 (30%)	11/27 (41%)	
IV and V	---	7/10 (70%)	16/27 (59%)	*0.046*∗
Lymph node metastasis				
No	---	7/10 (70%)	16/27 (59%)	0.208
Yes	---	3/10 (30%)	11/27 (41%)	
Distant metastasis				
No	---	8/10 (80%)	24/27 (89%)	0.951
Yes	---	2/10 (20%)	3/27 (11%)	
Recurrence				
No	6/6 (100%)	19/41 (46%)	9/27 (33%)	
Yes	0/6 (0%)	22/41 (54%)	18/27 (67%)	*0.025*∗

∗$P < 0.05$; ∗∗$P < 0.01$.

the KMO level can be used to discriminate malignant CMTs from benign tumors.

3.4. The Association between KMO Expression and the Survival Time in CMT Patients. Because tumor malignancy determines the survival outcome of cancer patients, we next evaluated the association between KMO expression and the overall survival rate of dogs with CMTs. The KMO expression could be classified into three groups according to the IRS. The Kaplan–Meier survival curves showed that patients with strong KMO-expressing tumors had a significantly shorter survival time and a remarkably lower survival rate than those with negative or weak KMO-expressing tumors ($p < 0.001$) (Figure 5). Taken together, the results shown here were similar to the profile of the *kmo* gene, demonstrating that KMO is a potential biomarker for predicting the prognosis of CMT dogs.

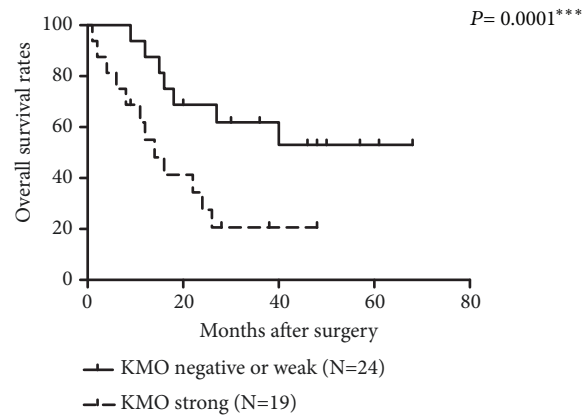

Figure 5: *Association between KMO expression and survival time of CMT patients.* Patients with KMO strong staining tumors had a significantly shorter survival time and a remarkably lower survival rate than those with KMO negative or weak tumors (∗∗∗$P < 0.001$).

3.5. The Role of KMO in the Proliferation of CMT Cells. High KMO expression was proved to be associated with the malignancy of CMT and indicated a poor outcome of the patients. The role of KMO in CMT development was next verified. We first examined the KMO expression in CMT cell lines (CMT-1 and MPG cells) and found that both had identifiable KMO protein amounts (Figure 6(a)). Incubation of CMT-1 and MPG cells with a KMO inhibitor (Ro 61-8048) for 1~3 days significantly inhibited cell proliferation (Figure 6(b)), and similar results were also observed when

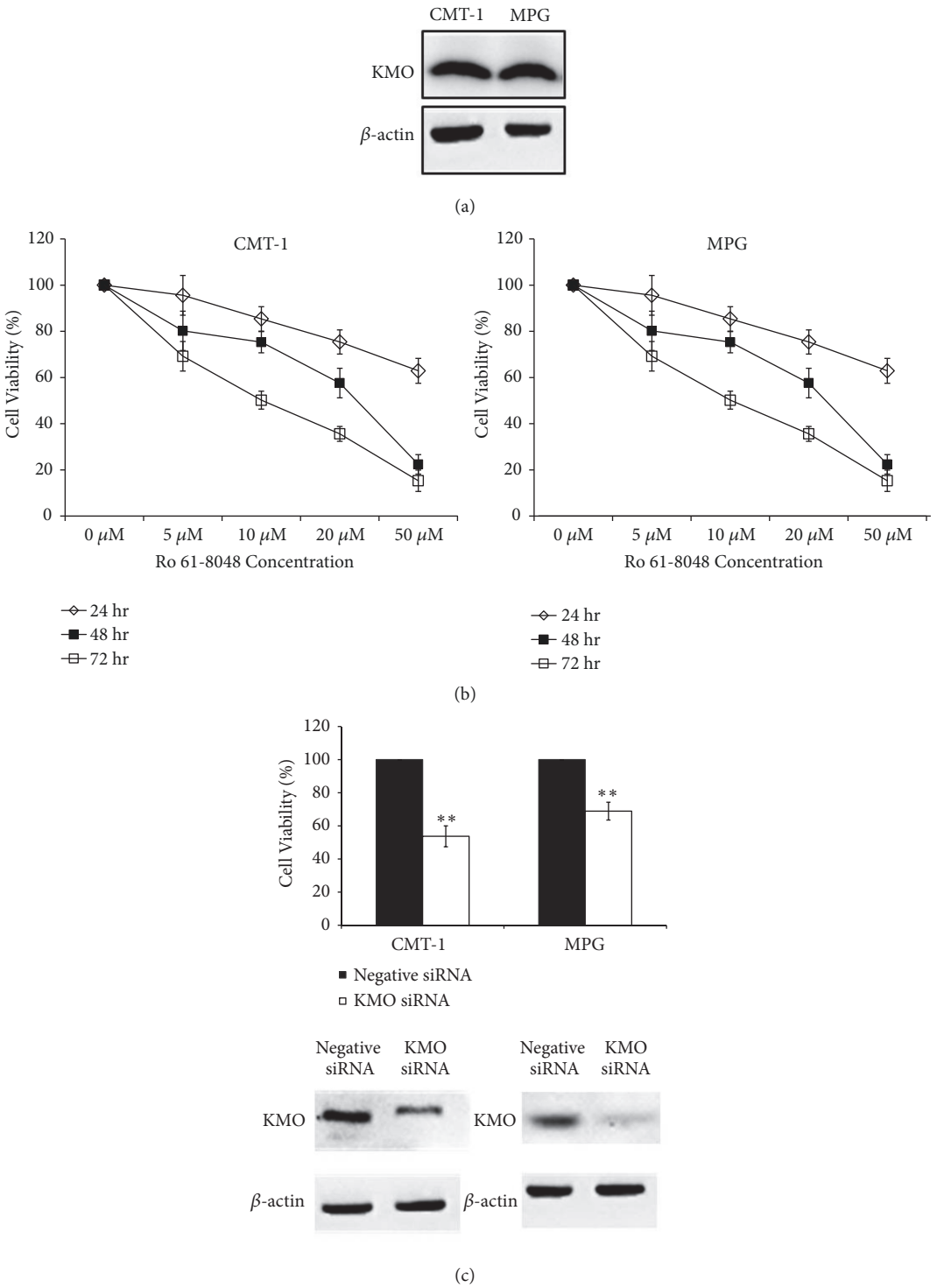

Figure 6: *Downregulated KMO activities with KMO inhibitor or siRNA inhibited cell proliferation in CMT cells.* (a) KMO expression in CMT-1 and MPG cells. (b) Cells treated with Ro 61-8048 for 24, 48, and 72 hrs were found to exhibit significantly suppressed cell proliferation of CMT-1 and MPG cells. (c) Knockdown of *KMO* with siRNA reduced cell proliferation in comparison to cells with control siRNA treatment. *Columns*, mean; *bars*, SD ($n = 3$). $**P < 0.01$.

silencing KMO expression with specific siRNAs against *KMO* (Figure 6(c)). The data suggested that KMO might play an important role in CMT cell growth.

4. Discussion

CMT is the most frequently diagnosed type of cancer in female dogs [47, 48], and approximately half of CMTs are malignant [49]. Surgical excision is the most effective treatment for CMT, but dogs with CMT have around a 30-58% recurrence or metastasis rate within 2 years following surgical removal [49, 50], and about 40-60% die from cancer-related diseases within the first 2 years [51]. The low survival rate of patients implies a low rate of specific diagnoses and ineffective therapies in CMT treatment. Challenges of CMT treatment include complex histological classification as well as unpredictable tumor behavior and prognosis [52]. Therefore, it is necessary to improve the accuracy of diagnosis to facilitate the determination of appropriate therapies.

Herein, we identified KMO as a novel and potential biomarker in CMT, which can help to improve diagnosis and predict the prognosis of CMTs. Our results showed that 31.8% of the total CMTs and 73.7% of the malignant CMTs had strong expressions of KMO protein (Table 3). This indicated that the expression of KMO protein issignificantly associated with tumor malignancy and demonstrated the potential of KMO in discriminating malignant tumors from benign ones. Furthermore, the survival rate of patients with a strong KMO protein expression was lower than that of those with weak or negative KMO expression. This result suggested that KMO could be a promising biomarker not only for tumor malignancy but also for predicting the prognosis of CMT patients.

KMO is involved in the metabolism of tryptophan and catalyzes the conversion of kynurenine into 3-HK and 3-hydroxyanthranilic acid, which are further converted into quinolinic acid, generating NAD^+ for essential cell survival [53]. The kynurenine pathway involves physiological and pathological processes in the nervous and immune systems. KMO is notable because it has been proven to be a potential therapeutic target for stroke, seizures, and Huntington's disease [54]. IDO is located upstream of KMO in the kynurenine pathway [43]. The potential association between IDO expression and cancer has been intensively studied [55]; however, their relationship is still ambiguous and sometimes controversial. Reports have shown that IDO overexpression in human tumors is related to tumor growth, but other reports have suggested that IDO expression in tumor cells and antigen-presenting cells inhibits tumor proliferation [55]. In our results, *KMO* overexpression was independent of *IDO* expression in CMTs, suggesting that KMO might induce tumor malignancy via a novel mechanism not involving IDO.

We also demonstrated that knockdown of KMO expression or blocking of its activity could suppress proliferation of CMT cells. Herein, we found that though CMT-1 and MPG are both cell lines of canine mammary gland tumors, CMT-1 is developed from canine mammary carcinoma (epithelial cell origin) while MPG is derived from the canine mixed mammary gland tumor. The different cell origins of CMT-1 and MPG may have relied on differently growth signal pathways and therefore have different sensitivities to KMO knockdown. KMO has been reported to play a role as an agonist for the N-methyl-D-aspartic acid (NMDA) receptor [56]. NMDA receptors are known to initiate gene activation and cell proliferation and promote cell survival via the extracellular signal-regulated kinase (ERK1/2) pathways [57]. Recently, a report showed that NMDA receptors were overexpressed in human breast cancer cell lines [58]. Another metabolite of kynurenine produced by the action of KMO, 3-hydroxyanthranilic acid, causes apoptosis of Th1 cells by activating caspase-8 [59] and induces apoptosis of T-cells through the inhibition of NF-κB [60]. Taken together, although the detailed mechanisms still need to be fully elucidated, our results have offered significant evidences of involvement of KMO in CMT progression and provided precious advice for further study on human breast cancer therapy.

5. Conclusions

A significant parallel increase of KMO mRNA and protein expression in malignant CMT was revealed and correlated with shorter survival time in CMT patients. Our results also showed that KMO plays a role in controlling cell growth and malignancy in canine mammary tumors. These findings indicate the potential applications of KMO in cancer prognosis and therapeutic developments.

Data Availability

The data used to support the findings of this study are available from the corresponding author upon request.

Disclosure

The results shown here have been patented in the United States with the Patent no. US204110275081 A1.

Conflicts of Interest

The authors declare that they have no conflicts of interest.

Acknowledgments

This study was supported by the National Science Council of Taiwan (NSC 102-2313-B-002-031-MY3).

References

[1] M. Paoloni and C. Khanna, "Translation of new cancer treatments from pet dogs to humans," *Nature Reviews Cancer*, vol. 8, no. 2, pp. 147–156, 2008.

[2] M. M. Hoffman and E. Birney, "Estimating the neutral rate of nucleotide substitution using introns," *Molecular Biology and Evolution*, vol. 24, no. 2, pp. 522–531, 2007.

[3] P. J. Rivera, M. Melin, T. Biagi et al., "Mammary tumor development in dogs is associated with BRCA1 and BRCA2," *Cancer Research*, vol. 69, no. 22, pp. 8770–8774, 2009.

[4] J. Peto, N. Collins, R. Barfoot et al., "Prevalence of BRCA1 and BRCA2 gene mutations in patients with early-onset breast cancer," *Journal of the National Cancer Institute*, vol. 91, no. 11, pp. 943–949, 1999.

[5] L. Sun, J. Liu, S. Wang, Y. Chen, and Z. Li, "Prevalence of BRCA1 gene mutation in breast cancer patients in Guangxi, China," *International Journal of Clinical and Experimental Pathology*, vol. 7, no. 9, pp. 6262–6269, 2014.

[6] F. C. F. Calboli, J. Sampson, N. Fretwell, and D. J. Balding, "Population structure and inbreeding from pedigree analysis of purebred dogs," *Genetics*, vol. 179, no. 1, pp. 593–601, 2008.

[7] R. Klopfleisch, H. von Euler, G. Sarli, S. S. Pinho, F. Gärtner, and A. D. Gruber, "Molecular carcinogenesis of canine mammary tumors: news from an old disease," *Veterinary Pathology*, vol. 48, no. 1, pp. 98–116, 2011.

[8] D. Kanojia, M. Garg, S. Gupta, A. Gupta, and A. Suri, "Sperm-associated antigen 9, a novel biomarker for early detection of breast cancer," *Cancer Epidemiology, Biomarkers & Prevention*, vol. 18, no. 2, pp. 630–639, 2009.

[9] J. S. Ross, E. A. Slodkowska, W. F. Symmans, L. Pusztai, P. M. Ravdin, and G. N. Hortobagyi, "The HER-2 receptor and breast cancer: Ten years of targeted anti-HER-2 therapy and personalized medicine," *The Oncologist*, vol. 14, no. 4, pp. 320–368, 2009.

[10] P. Prihantono, M. Hatta, C. Binekada et al., "Ki-67 expression by immunohistochemistry and quantitative real-time polymerase chain reaction as predictor of clinical response to neoadjuvant chemotherapy in locally advanced breast cancer," *Journal of Oncology*, vol. 2017, Article ID 6209849, 8 pages, 2017.

[11] L. K. Dunnwald, M. A. Rossing, and C. I. Li, "Hormone receptor status, tumor characteristics, and prognosis: a prospective cohort of breast cancer patients," *Breast Cancer Research*, vol. 9, no. 1, article R6, 2007.

[12] J. Martín De Las Mulas, Y. Millán, and R. Dios, "A prospective analysis of immunohistochemically determined estrogen receptor α and progesterone receptor expression and host and tumor factors as predictors of disease-free period in mammary tumors of the dog," *Veterinary Pathology*, vol. 42, no. 2, pp. 200–212, 2005.

[13] A. Nieto, L. Peña, M. D. Pérez-Alenza, M. A. Sánchez, J. M. Flores, and M. Castaño, "Immunohistologic detection of estrogen receptor alpha in canine mammary tumors: clinical and pathologic associations and prognostic significance," *Veterinary Pathology*, vol. 37, no. 3, pp. 239–247, 2000.

[14] C.-C. Chang, M.-H. Tsai, J.-W. Liao, J. P.-W. Chan, M.-L. Wong, and S.-C. Chang, "Evaluation of hormone receptor expression for use in predicting survival of female dogs with malignant mammary gland tumors," *Journal of the American Veterinary Medical Association*, vol. 235, no. 4, pp. 391–396, 2009.

[15] E. A. Sartin, S. Barnes, R. P. Kwapien, and L. G. Wolfe, "Estrogen and progesterone receptor status of mammary carcinomas and correlation with clinical outcome in dogs," *American Journal of Veterinary Research*, vol. 53, no. 11, pp. 2196–2200, 1992.

[16] A. Bergamaschi, E. Tagliabue, T. Sørlie et al., "Extracellular matrix signature identifies breast cancer subgroups with different clinical outcome," *The Journal of Pathology*, vol. 214, no. 3, pp. 357–367, 2008.

[17] W. Toniti, S. Buranasinsup, A. Kongcharoen, P. Charoonrut, P. Puchadapirom, and C. Kasorndorkbua, "Immunohistochemical determination of estrogen and progesterone receptors in canine mammary tumors," *Asian Pacific Journal of Cancer Prevention*, vol. 10, no. 5, pp. 907–912, 2009.

[18] F. Sassi, C. Benazzi, G. Castellani, and G. Sarli, "Molecular-based tumour subtypes of canine mammary carcinomas assessed by immunohistochemistry," *BMC Veterinary Research*, vol. 6, p. 5, 2010.

[19] R. Simon, A. Nocito, T. Hübscher et al., "Patterns of HER-2/neu amplification and overexpression in primary and metastatic breast cancer," *Journal of the National Cancer Institute*, vol. 93, no. 15, pp. 1141–1146, 2001.

[20] D. J. Slamon, G. M. Clark, S. G. Wong, W. J. Levin, A. Ullrich, and W. L. McGuire, "Human breast cancer: correlation of relapse and survival with amplification of the HER-2/neu oncogene," *Science*, vol. 235, no. 4785, pp. 182–191, 1987.

[21] I. L. Andrulis, S. B. Bull, M. E. Blackstein et al., "Neu/erbB-2 amplification identifies a poor-prognosis group of women with node-negative breast cancer. Toronto breast cancer study group," *Journal of Clinical Oncology*, vol. 16, no. 4, pp. 1340–1349, 1998.

[22] R. E. Roses, E. C. Paulson, A. Sharma et al., "HER-2/neu overexpression as a predictor for the transition from in situ to invasive breast cancer," *Cancer Epidemiology Biomarkers & Prevention*, vol. 18, no. 5, pp. 1386–1389, 2009.

[23] S. Chia, B. Norris, C. Speers et al., "Human epidermal growth factor receptor 2 overexpression as a prognostic factor in a large tissue microarray series of node-negative breast cancers," *Journal of Clinical Oncology*, vol. 26, no. 35, pp. 5697–5704, 2008.

[24] F. Révillion, J. Bonneterre, and J. P. Peyrat, "ERBB2 oncogene in human breast cancer and its clinical significance," *European Journal of Cancer*, vol. 34, no. 6, pp. 791–808, 1998.

[25] R. Seshadri, F. A. Firgaira, D. J. Horsfall, K. McCaul, V. Setlur, and P. Kitchen, "Clinical significance of HER-2/neu oncogene amplification in primary breast cancer. the south australian breast cancer study group," *Journal of Clinical Oncology*, vol. 11, no. 10, pp. 1936–1942, 1993.

[26] H. Tsuda, S. Hirohashi, Y. Shimosato et al., "Correlation between histologic grade of malignancy and copy number of c-erbb-2 gene in breast carcinoma. a retrospective analysis of 176 cases," *Cancer*, vol. 65, no. 8, pp. 1794–1800, 1990.

[27] A. P. Dutra, N. V. M. Granja, F. C. Schmitt, and G. D. Cassali, "c-erbB-2 expression and nuclear pleomorphism in canine mammary tumors," *Brazilian Journal of Medical and Biological Research*, vol. 37, no. 11, pp. 1673–1681, 2004.

[28] A. Gama, A. Alves, and F. Schmitt, "Identification of molecular phenotypes in canine mammary carcinomas with clinical implications: application of the human classification," *Virchows Archiv*, vol. 453, no. 2, pp. 123–132, 2008.

[29] W.-L. Hsu, H.-M. Huang, J.-W. Liao, M.-L. Wong, and S.-C. Chang, "Increased survival in dogs with malignant mammary tumours overexpressing HER-2 protein and detection of a silent single nucleotide polymorphism in the canine HER-2 gene," *The Veterinary Journal*, vol. 180, no. 1, pp. 116–123, 2009.

[30] S. Mukaratirwa, "Prognostic and predictive markers in canine tumours: rationale and relevance. a review," *Veterinary Quarterly*, vol. 27, no. 2, pp. 52–64, 2005.

[31] T. Tanaka, T. Shimada, H. Akiyoshi et al., "Relationship between major histocompatibility complex class I expression and prognosis in canine mammary gland tumors," *Journal of Veterinary Medical Science*, vol. 75, no. 10, pp. 1393–1398, 2013.

[32] M. Furuya, M. Funasaki, H. Tani, and K. Sasai, "Identification of novel tumour-associated antigens in canine mammary gland tumour," *Veterinary and Comparative Oncology*, vol. 13, no. 3, pp. 194–202, 2015.

[33] M. F. Beal, R. J. Ferrante, K. J. Swartz, and N. W. Kowall, "Chronic quinolinic acid lesions in rats closely resemble Huntington's disease," *The Journal of Neuroscience*, vol. 11, no. 6, pp. 1649–1659, 1991.

[34] N. Braidy, R. Grant, S. Adams, B. J. Brew, and G. J. Guillemin, "Mechanism for quinolinic acid cytotoxicity in human astrocytes and neurons," *Neurotoxicity Research*, vol. 16, no. 1, pp. 77–86, 2009.

[35] P. Guidetti, G. P. Bates, R. K. Graham et al., "Elevated brain 3-hydroxykynurenine and quinolinate levels in Huntington disease mice," *Neurobiology of Disease*, vol. 23, no. 1, pp. 190–197, 2006.

[36] S. J. Pearson and G. P. Reynolds, "Increased brain concentrations of a neurotoxin, 3-hydroxykynurenine, in Huntington's disease," *Neuroscience Letters*, vol. 144, no. 1-2, pp. 199–201, 1992.

[37] M. A. Thevandavakkam, R. Schwarcz, P. J. Muchowski, and F. Giorgini, "Targeting kynurenine 3-monooxygenase (kmo): Implications for therapy in huntington's disease," *CNS and Neurological Disorders - Drug Targets*, vol. 9, no. 6, pp. 791–800, 2010.

[38] H. Jin, Y. Zhang, H. You et al., "Prognostic significance of kynurenine 3-monooxygenase and effects on proliferation,migration, and invasion of human hepatocellular carcinoma," *Scientific Reports*, vol. 5, Article ID 10466, pp. 1–12, 2015.

[39] P. Terness, T. M. Bauer, L. Röse et al., "Inhibition of allogeneic T cell proliferation by indoleamine 2,3-dioxygenase–expressing dendritic cells: mediation of suppression by tryptophan metabolites," *The Journal of Experimental Medicine*, vol. 196, no. 4, pp. 447–457, 2002.

[40] Y. Mándi and L. Vécsei, "The kynurenine system and immunoregulation," *Journal of Neural Transmission*, vol. 119, no. 2, pp. 197–209, 2012.

[41] L. N. Owen, *TNM Classification of Tumours in Domestic Animals*, World Health Organization, Geneva, Switzerland, 1st edition, 1980.

[42] B. Etschmann, B. Wilcken, K. Stoevesand, A. Von Der Schulenburg, and A. Sterner-Kock, "Selection of reference genes for quantitative real-time PCR analysis in canine mammary tumors using the GeNorm algorithm," *Veterinary Pathology*, vol. 43, no. 6, pp. 934–942, 2006.

[43] H.-C. Chiang, A. T.-C. Liao, T.-R. Jan et al., "Gene-expression profiling to identify genes related to spontaneous tumor regression in a canine cancer model," *Veterinary Immunology and Immunopathology*, vol. 151, no. 3-4, pp. 207–216, 2013.

[44] W. Remmele and H. E. Stegner, "Recommendation for uniform definition of an immunoreactive score (IRS) for immunohistochemical estrogen receptor detection (ER-ICA) in breast cancer tissue," *Der Pathologe*, vol. 8, no. 3, pp. 138–140, 1987.

[45] C.-C. Wu, R.-Y. Shyu, J.-M. Chou et al., "RARRES1 expression is significantly related to tumour differentiation and staging in colorectal adenocarcinoma," *European Journal of Cancer*, vol. 42, no. 4, pp. 557–565, 2006.

[46] J. R. Moffett and M. A. Namboodiri, "Tryptophan and the immune response," *Immunology & Cell Biology*, vol. 81, no. 4, pp. 247–265, 2003.

[47] S. A. Benjamin, A. C. Lee, and W. J. Saunders, "Classification and behavior of canine mammary epithelial neoplasms based on life-span observations in Beagles," *Veterinary Pathology*, vol. 36, no. 5, pp. 423–436, 1999.

[48] A. Egenvall, B. N. Bonnett, P. Öhagen, P. Olson, Å. Hedhammar, and H. Von Euler, "Incidence of and survival after mammary tumors in a population of over 80,000 insured female dogs in Sweden from 1995 to 2002," *Preventive Veterinary Medicine*, vol. 69, no. 1-2, pp. 109–127, 2005.

[49] E. G. MacEwen, "Spontaneous tumors in dogs and cats: models for the study of cancer biology and treatment," *Cancer and Metastasis Reviews*, vol. 9, no. 2, pp. 125–136, 1990.

[50] N. Stratmann, K. Failing, A. Richter, and A. Wehrend, "Mammary tumor recurrence in bitches after regional mastectomy," *Veterinary Surgery*, vol. 37, no. 1, pp. 82–86, 2008.

[51] S.-C. Chang, C.-C. Chang, T.-J. Chang, and M.-L. Wong, "Prognostic factors associated with survival two years after surgery in dogs with malignant mammary tumors: 79 cases (1998-2002)," *Journal of the American Veterinary Medical Association*, vol. 227, no. 10, pp. 1625–1629, 2005.

[52] D. A. P. C. Zuccari, A. E. Santana, P. M. Cury, and J. A. Cordeiro, "Immunocytochemical study of Ki-67 as a prognostic marker in canine mammary neoplasia," *Veterinary Clinical Pathology*, vol. 33, no. 1, pp. 23–28, 2004.

[53] K. K. Ting, B. Brew, and G. Guillemin, "The involvement of astrocytes and kynurenine pathway in Alzheimer's disease," *Neurotoxicity Research*, vol. 12, no. 4, pp. 247–262, 2007.

[54] K. R. Crozier-Reabe, R. S. Phillips, and G. R. Moran, "Kynurenine 3-monooxygenase from Pseudomonas fluorescens: substrate-like inhibitors both stimulate flavin reduction and stabilize the flavin-peroxo intermediate yet result in the production of hydrogen peroxide," *Biochemistry*, vol. 47, no. 47, pp. 12420–12433, 2008.

[55] S. Löb, A. Königsrainer, H.-G. Rammensee, G. Opelz, and P. Terness, "Inhibitors of indoleamine-2,3-dioxygenase for cancer therapy: can we see the wood for the trees?" *Nature Reviews Cancer*, vol. 9, no. 6, pp. 445–452, 2009.

[56] J. Urenjak and T. P. Obrenovitch, "Kynurenine 3-hydroxylase inhibition in rats: Effects on extracellular kynurenic acid concentration and N-methyl-D-aspartate-induced depolarisation in the striatum," *Journal of Neurochemistry*, vol. 75, no. 6, pp. 2427–2433, 2000.

[57] J. A. Kemp and R. M. McKernan, "NMDA receptor pathways as drug targets," *Nature Neuroscience*, vol. 5, pp. 1039–1042, 2002.

[58] W. G. North, G. Gao, V. A. Memoli, R. H. Pang, and L. Lynch, "Breast cancer expresses functional NMDA receptors," *Breast Cancer Research and Treatment*, vol. 122, no. 2, pp. 307–314, 2010.

[59] F. Fallarino, U. Grohmann, C. Vacca et al., "T cell apoptosis by tryptophan catabolism," *Cell Death & Differentiation*, vol. 9, no. 10, pp. 1069–1077, 2002.

[60] T. Hayashi, J.-H. Mo, X. Gong et al., "3-Hydroxyanthranilic acid inhibits PDK1 activation and suppresses experimental asthma by inducing T cell apoptosis," *Proceedings of the National Acadamy of Sciences of the United States of America*, vol. 104, no. 47, pp. 18619–18624, 2007.

Hindawi
Journal of Oncology
Volume 2019, Article ID 2316237, 13 pages
https://doi.org/10.1155/2019/2316237

Research Article

Human Mitotic Centromere-Associated Kinesin Is Targeted by MicroRNA 485-5p/181c and Prognosticates Poor Survivability of Breast Cancer

Huajun Lu,[1] Chaoqun Wang,[2] Lijun Xue,[3] Qi Zhang,[4] Frank Luh,[5] Jianghai Wang,[5] Tiffany G. Lin,[5] Yun Yen,[5,6] and Xiyong Liu [5,6]

[1]*Department of Oncological Radiotherapy, Affiliated Dongyang People's Hospital of Wenzhou Medical University, Dongyang, Zhejiang 322100, China*
[2]*Department of Pathology, Affiliated Dongyang People's Hospital of Wenzhou Medical University, Dongyang, Zhejiang 322100, China*
[3]*Department of Pathology, Loma Linda University Medical Center, Loma Linda, CA 92354, USA*
[4]*Department of Bioinformatics, Hangzhou Hepu Biotechnology Inc., Hangzhou, Zhejiang 310015, China*
[5]*Sino-American Cancer Foundation, Temple City, CA 91780, USA*
[6]*Department of Tumor Biomarker Development, California Cancer Institute, Temple City, CA 91780, USA*

Correspondence should be addressed to Xiyong Liu; xiyongliu@sacfamerica.org

Received 11 November 2018; Revised 23 February 2019; Accepted 7 March 2019; Published 3 April 2019

Guest Editor: Chia-Jung Li

Purpose. This study aims to evaluate the prognostic value of human Mitotic Centromere-Associated Kinesin (MCAK), a microtubule-dependent molecular motor, in breast cancers. The posttranscriptional regulation of MCAK by microRNAs will also be explored. *Methods*. The large-scale gene expression datasets of breast cancer (total n=4,677) were obtained from GEO, NKI, and TCGA database. Kaplan-Meier and Cox analyses were used for survival analysis. MicroRNAs targeting MCAK were predicted by bioinformatic analysis and validated by a dual-luciferase reporter assay. *Results*. The expression of MCAK was significantly associated with aggressive features of breast cancer, including tumor stage, Elston grade, and molecular subtypes, for global gene expression datasets of breast cancer ($p<0.05$). Overexpression of MCAK was significantly associated with poor outcome in a dose-dependent manner for either ER-positive or ER-negative breast cancer. Evidence from bioinformatic prediction, coexpression assays, and gene set enrichment analyses suggested that miR-485-5p and miR-181c might target MCAK and suppress its expression. A 3'UTR dual-luciferase target reporter assay demonstrated that miR-485-5p and miR-181c mimics specifically inhibited relative Firefly/Renilla luciferase activity by about 50% in corresponding reporter plasmids. Further survival analysis also revealed that miR-485-5p (HR=0.59, 95% CI 0.37-0.92) and miR-181c (HR=0.54, 95% CI 0.34-0.84) played opposite roles of MCAK (HR=2.80, 95% CI 1.77-4.57) and were significantly associated with better outcome in breast cancers. *Conclusion*. MCAK could serve as a prognostic biomarker for breast cancers. miR-485-5p and miR-181c could specifically target and suppress the MCAK gene expression in breast cancer cells.

1. Background

Microtubules (MTs) are essential biological polymers of fundamental importance for mitosis in eukaryotic cells. The human Mitotic Centromere-Associated Kinesin (MCAK) gene, also recognized as Kinesin Family Member 2C (KIF2C), encodes a kinesin-like protein that can depolymerize microtubules at the plus end, thereby promoting mitotic chromosome segregation during mitosis [1]. MCAK can interact with KIF18B to form an MCAK-KIF18B complex, which is negatively regulated by Aurora kinases through phosphorylation of MCAK [2]. Aurora kinases regulate MT plus-end stability through control of MCAK-KIF18B complex formation to constitute the major microtubule plus-end depolymerizing activity in mitotic cells. MCAK and KIF2B stimulate kinetochore-microtubule dynamics during distinct phases of mitosis to correct malorientations [3]. MCAK plays a role in chromosome congression and is required for the lateral

to the end-on conversion of the chromosome-microtubule attachment [4]. Both protein and mRNA levels of MCAK were upregulated in colorectal cancer, and expression levels correlated strongly with Ki-67 expression [5]. Overexpression of MCAK was also considered an independent predictor of overall survival and lymph node metastasis in colorectal cancer [6]. The MCAK gene expression was also found to be increased in glioma samples and associated with histopathological grades that impact poor survival of glioma [7].

Breast cancer is a common malignant disease among women in the world [8, 9]. Because of the heterogeneity of breast cancer cells, there is tremendous variation in clinical outcomes [10, 11]. Molecular-based classification of breast cancers has been widely used to predict outcomes and select the appropriate therapeutic regimen for patients. Currently, more therapeutic targets and corresponding inhibitors for breast cancers are being explored to improve treatment efficacy with fewer adverse side effects. Here, we hypothesize that MCAK could be a driver gene for tumorigenesis and could serve as prognostic biomarkers and/or therapeutic targets for breast cancer treatment.

In many cases, microRNAs play essential roles in gene regulation [12]. miR-485-5p has been reported to suppress mitochondrial respiration, cell migration, and invasion in breast cancer cell lines [13]. In oral tongue squamous cells, miR-485-5p antagonizes PAK1 to reverse epithelial to mesenchymal transition and promote cisplatin-induced cell death [14]. miR-485-5p also could serve as a prognostic biomarker and associate with better survival in gastric cancer [15–17]. Other microRNAs like miR-181c were reported to reduce the proliferation, migration, and invasion of neuroblastoma cells through targeting Smad7 [18]. However, another report demonstrated that miR-181c functioned as an oncogene and promoted proliferation through inhibiting PTEN protein expression by targeting 3'-UTR of PTEN mRNA in inflammatory breast cancer SUM149 cells [19]. The mature form of miR-181c could also translocate into mitochondria and suppress the mitochondrial function through targeting of the mt-Cox1 gene [20]. Moreover, miR-181c was also reported to be involved in chemoresistance and antagonized long non-coding RNA GAS5 in pancreatic cancers [21, 22]. It also contributed to the resistance of cisplatin in non-small cell lung cancer cells by targeting Wnt inhibition factor 1 [23]. Neither miR-485-5p nor miR-181c has been previously reported to target MCAK gene and reduce its expression level in cancers.

Here, we explored the clinical meaning and prognostic significance of MCAK by using 13 independent breast cancer datasets from Gene Expression Omnibus (GEO) and the Cancer Genome Atlas (TCGA). All eligible microRNAs that target MCAK were predicted by using bioinformatics and biostatistics analysis and validated by dual-luciferase 3'-UTR report assay. The clinical significance of MCAK and above two microRNAs were also observed.

2. Materials and Methods

2.1. Breast Cancer Cell Culture. MCF-7 (ER-positive) and MDA-MB-231 (ER-negative) cell lines were obtained from ATCC (American Type Culture Collection, Manassas, VA USA) in June 2011 and September 2013. Cells were incubated with 5% CO_2 at 37°C in a humidified incubator in Dulbecco's Modification of Eagle's Medium (DMEM) (Mediatech, Inc., Manassas, VA, USA) supplemented with 10% fetal bovine serum (FBS) (Omega Scientific, Inc., Tarzana, CA, USA) and penicillin and streptomycin (Thermo Fisher Scientific Inc.). Frozen aliquots were stored in liquid nitrogen vapor phase when we obtained cells from ATCC for long-term storage. Cells were cultured for no longer than six months after thawing. Cell lines were authenticated by ATCC before delivery and not reauthenticated in our laboratory.

2.2. pmirGLO Dual-Luciferase miRNA Target Reporter Assay. The pmirGLO dual-luciferase miRNA target expression vectors (Promega) were constructed as reporter plasmids. miR-485-5p and miR-181c, which target MCAK sense/antisense oligonucleotides, were annealed and then inserted into multiple cloning sites (MCS, PmeI, and XbaI) in the 3' untranslated region (UTR) of Firefly (luc2) gene in the pmirGLO vector.

About 5-10×10^5 MCF7 cells were seeded in each well of a 6-well plate and incubated at 37°C with 5% CO_2 overnight. The human miR-485-5p and miR-181c mimics were obtained from Vigene Biosciences (Rockville, MD). These pmirGLO reporter vectors and miRNA mimics were transfected in antibiotic-free Opti-MEM medium (Life Technologies, Carlsbad, CA, USA) with Lipofectamine 3000 reagent (Life Technologies) according to the manufacturer's instructions. Luciferase activity was performed 48 hours after transfection.

2.3. Dual-Luciferase Determination. Cells were plated into 24-well plates and transfected with pmirGLO-485-WT, pmirGLO-485-Mut, pmirGLO-181c-WT, or pmirGLO-181c-Mut, with corresponding miR-485-5p or miR-181c mimics. After transfection for 48 hours, luciferase activity of Firefly and Renilla was determined by a kit of the Dual-Luciferase Reporter Assay System (Promega). Relative luciferase activity of Firefly was measured by normalizing expression ratio to Renilla luciferase activity.

2.4. Worldwide Microarray Gene Expression Datasets. Eleven independent Gene Expression Omnibus (GEO) breast cancer microarray datasets (total n=2,248) and two breast cancer datasets (n=2,429) from the Cancer Genome Atlas (TCGA) [24] were collected for this study. All participants had clinical and follow-up annotations. The GEO datasets were GSE7390 [25], GSE2034 [26], GSE1456 [27], GSE4922 [28], GSE22226 [29], GSE24450 [30], GSE53031 [31], GSE25066 [32], GSE10885 [33], GSE58812 [34], and NKI [35]. Datasets without prognostic outcome information were excluded. Detailed information about these downloaded datasets is listed in Suppl. Table 1. To normalize the mRNA expression levels among all datasets, we restratified all MCAK scores and other related genes into four grades (Q1, Q2, Q3, and Q4) based on the percentile for each dataset. MCAK-low (Q1+Q2) and MCAK-high (Q3+Q4) are also divided by the median value of gene expression.

2.5. Gene Set Enrichment Analysis (GSEA). The GSEA software v3.0 was downloaded from www.broad.mit.edu/gsea and run on the JAVA 8.0 platform [36]. All dataset (.gct) and phenotype label (.cls) files were created and loaded into GSEA software, and gene sets were updated from the above website. The detailed protocol could see our previous publications [37]. Here, the permutations number was 1,000, and the phenotype label was MCAK-high versus MCAK-low.

2.6. Data Management and Statistical Methods. After datasets were downloaded from GEO and TCGA websites, the original datasets were converted, merged, and normalized using R 3.4.3 and Python 3.6.3. To make datasets compatible, we prenormalized all participants by Q1, Q2, Q3, and Q4 in each dataset and then merged for pooled analysis. The JMP and R software were used for group comparisons, $\chi 2$ analysis, Fisher's exact test, and the binomial test of proportions. Kaplan-Meier and Cox models were used to apply for analysis of overall survival (OS) and progression-free survival (PFS). Patients with distant metastasis were excluded in PFS analysis. Multivariate and stratification analyses were applied to reduce the potential confounding effect on the estimation of Hazard Ratio (HR). Missing data were coded and excluded from the analysis.

3. Results

3.1. MCAK Expression Is Associated with an Aggressive Form of Breast Cancer. The clinical relevance of MCAK mRNA expression levels was examined on GEO and TCGA datasets. Analysis results from GEO dataset suggest that MCAK expression significantly and positively associated with factors including younger than 50 years of age, tumor equal to or larger than 2 cm, ER-negative status, and higher Elston histology grade (Figure 1(a) and Suppl. Table 2). However, MCAK expression was not associated with lymph node involvement. These associations from GEO datasets were consistent with findings from the TCGA dataset (Figure 1(b) and Suppl. Table 2). We further analyzed the MCAK expression on breast cancer patients according to molecular subtypes. ANOVA analysis result confirmed that MCAK mRNA levels were relatively lower on normal-like and Luminal A patients and significantly higher in luminal B, HER2-positive, and basal-like breast cancer cases. This finding was seen in GEO datasets and TCGA datasets (Figures 1(c), and 1(d), and Suppl. Table 2).

The online search results from the STRING database (https://string-db.org/) [38] indicated that the top 10 proteins that interact with MCAK are the following: Aurora kinase B (AURKB), Baculoviral IAP repeat-containing 5 (BIRC5), Cyclin B1 (CCNB1), Budding uninhibited by benzimidazoles 1 homolog (BUB1), Budding uninhibited by benzimidazoles 1 homolog beta (BUB1B), Cell division cycle 20 (CDC20), Cell division cycle associated 8 (CDCA8), Centromere protein A (CENPA), Centromere protein F (CENPF), and Polo-like kinase 1 (PLK1) (Suppl. Figure 1). The above proteins are involved in the regulation of mitotic spindle assembly checkpoint, mitotic cell cycle, mitotic nuclear division, and the establishment of chromosome localization. GSEA results indicated that higher expression of MCAK was significantly associated with gene signatures, including Poola invasive breast cancer (up) (Normalized Enrichment Score, NES=1.65, p=0.001) and Riz erythroid differentiation (NES=2.11, p<0.001) (Suppl. Figures 2A and 2B). Meanwhile, MCAK also enriched other cancer invasion related gene sets, such as Mootha mitochondrial, Naderi breast cancer prognosis (up), Biudus metastasis (up), and Zhang breast cancer progenitors (up) (Suppl. Figure 2C)

Therefore, those above-mentioned large-scale population-based analyses validated that MCAK expression levels were significantly associated with factors related to the aggressiveness of breast cancers.

3.2. MCAK Prognosticates Poor Survivability of Breast Cancer. The above findings suggested that MCAK expression was associated with higher Elston grade and other aggressive phenotypes of breast cancer. Here, we hypothesized that the expression of MCAK might be associated with poor outcomes in breast cancer. To address this, we conducted Kaplan-Meier and Cox analysis to determine if MCAK impacted survival in breast cancer cases in GEO and TCGA microarray gene expression datasets. Here, we recategorized participants of each dataset into four subgroups (Q1, Q2, Q3, and Q4) according to the expression levels of MCAK. First, survival analysis was conducted for each dataset by using univariate and multiple Cox proportional hazard analysis (Table 1). The lowest expression subgroup (Q1) was the relative point of reference. The HR of MCAK OS and PFS increased as its expression levels increased in all datasets. In higher MCAK levels (Q4), the significance could be seen in almost all datasets. The adjusted HRs of higher MCAK (Q4) for OS were 2.27 (95% CI 1.30-4.11) and 2.22 (95% CI 1.65-3.01) in pooled GEO and TCGA datasets, respectively.

The prognostic performance of MCAK was illustrated in Figure 2. The mRNA level of MCAK was significantly associated with poor overall survival in breast cancer on GEO and TCGA datasets (Figures 2(a) and 2(b)). As MCAK levels increased, survival decreased in a dose-dependent manner. Generally, ER-negative breast cancers had a poorer prognosis [39]. We further stratified our Kaplan-Meier analysis and confirmed that MCAK mRNA levels were significantly associated with poor PFS in both ER-negative and ER-positive breast cancers (Figures 2(c) and 2(d)). This finding could also be observed on OS analysis from GEO and TCGA datasets. The prognostic significance of MCAK was also analyzed among molecular subtypes. In the pooled GEO set, MCAK significantly impacted survival in basal-like breast cancer (MCAK-high versus MCAK-low) (Figures 2(e) and 2(f)). Due to insufficient cases of basal-like breast cancers, this association could not be validated in the TCGA dataset. Nevertheless, MCAK prognosticated poor survivability of breast cancer regardless of ER status.

3.3. Reduction of MCAK Expression by miR-485-5p and miR-181c on Breast Cancer Cells. In general, microRNAs suppress gene expression level through posttranscriptional regulation. Here, all possible microRNAs that target MCAK were identified based on www.microrna.org website. Meanwhile,

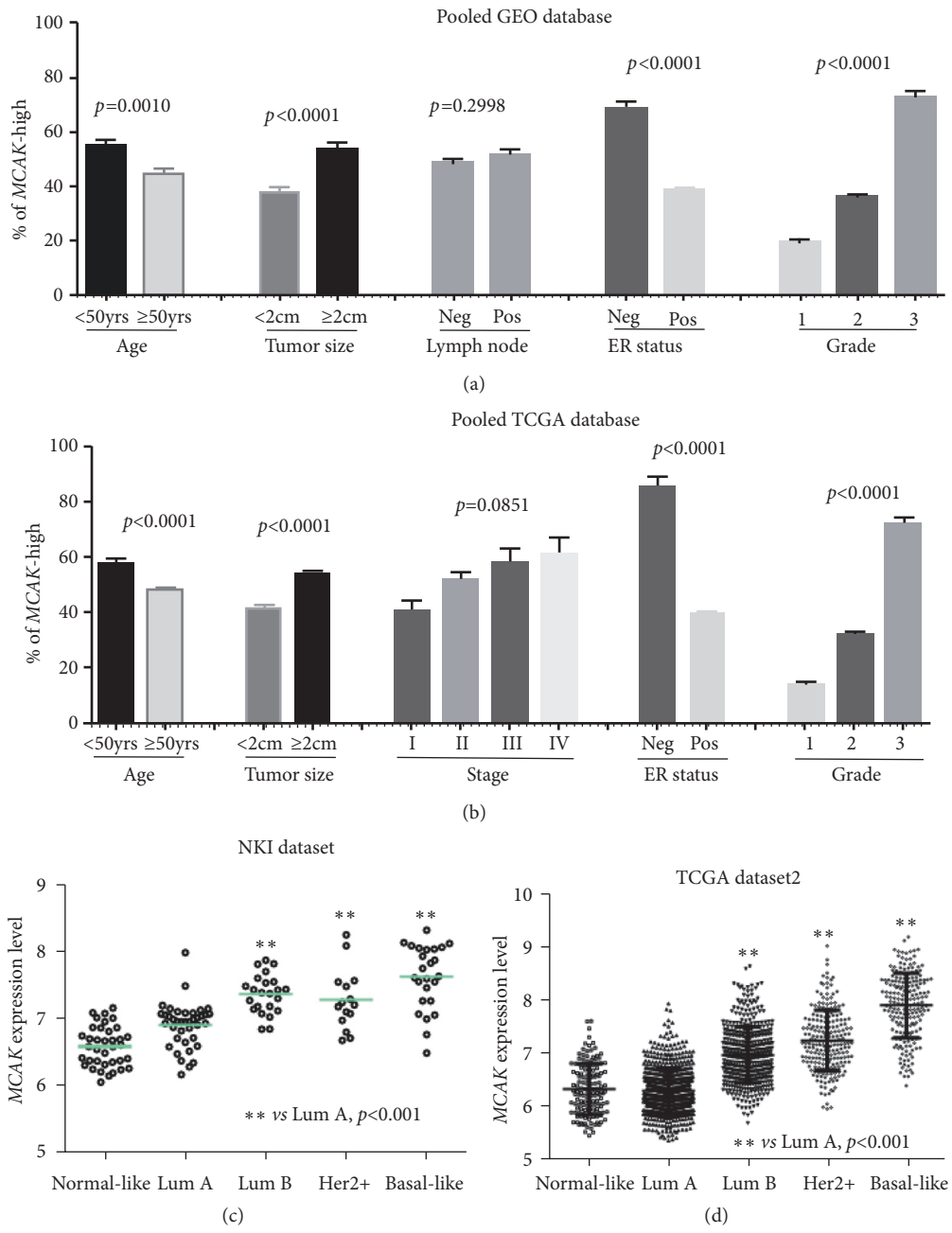

Figure 1: *Clinical relevance of MCAK in GEO and TCGA breast cancer datasets*. Here, MCAK-high was defined as MCAK mRNA level equal to or larger than median mRNA levels in each dataset. The mRNA levels of MCAK, tumor size, lymph node involvement, and Elston grade of breast cancer were analyzed in GEO (a) and TCGA (b) datasets. The mRNA levels of MCAK in different molecular subtypes of breast cancer were also examined in NKI dataset (c) and TCGA dataset (d).

the MCAK coexpressing microRNAs were listed from the GSE22220 dataset. GSEA also analyzed the targeting gene sets of microRNA enriched by MCAK. Only those predicted microRNAs, which were also negatively and significantly coexpressed with MCAK, were considered as eligible microRNAs targeting MCAK (Figure 3(a)). Here, two candidate microRNAs, miR-485-5p and miR-181c, were selected. The binding sites and gene map were outlined in Suppl. Figure 3. A 3'-UTR luciferase reporter assay was used to investigate inhibitory effects of these microRNAs through binding to the corresponding sequence on MCAK. The clinical significance of microRNAs was also evaluated for further validation.

It is based on predicted binding motifs of miR-485-5p and miR-181c that target MCAK mRNA; double-strand DNA fragments were synthesized and inserted into multiple cloning sites (MCS) of pmirGLO Dual-Luciferase miRNA Target Expression Vector (Figure 3(b)). The pmirGLO plasmid was transfected into MCF-7 cells and incubated for

Table 1: Uni- and multivariate analysis for *MCAK* and survival in microarray datasets.

Data set (cases)		Overall survival		Disease-free survival	
		HR (95% CI)	Adjusted HR (95% CI)∗	HR (95% CI)	Adjusted HR (95% CI)∗
GSE7390					
(n=198)	Q_1	Reference	Reference	Reference	Reference
	Q_2	2.93 (1.19-8.23)†	3.14 (1.27-8.84) †	2.30 (1.21-4.62) †	2.26 (1.18-4.55) †
	Q_3	4.84 (2.09-13.12) ‡	4.89 (1.96-13.94) ‡	3.41 (1.82-6.76) ‡	3.67 (1.85-7.62) ‡
	Q_4	2.32 (0.90-6.81)	1.72 (0.60-5.75)	1.65 (0.82-3.41)	1.85 (0.80-4.35)
GSE2034					
(n=286)	Q_1	N/A	N/A	Reference	Reference
	Q_2			1.56 (0.86-2.89)	1.55 (0.86-2.88)
	Q_3			2.13 (1.21-3.87) ‡	2.26 (1.27-4.13) ‡
	Q4			2.19 (1.24-4.00) ‡	2.47 (1.35-4.62) ‡
GSE1456					
(n=159)	Q_1	Reference	Reference	Reference	Reference
	Q_2	10.1 (1.90-187) ‡	1.6e+9 (4.06-2.7e+305) ‡	1.8e+9 (6.03-6.6e+179) ‡	1.5e+9 (4.55-9.0e+304) ‡
	Q_3	21.7 (4.46-392) ‡	3.1e+9 (7.91-3.6e+122) ‡	2.9e+9 (9.71-1.5e+254) ‡	2.2e+9 (6.58-1.8e+34) ‡
	Q_4	15.2 (3.03-276) ‡	1.9e+9 (4.59-6.9e+100) ‡	2.5e+9 (8.38-6.3e+55) ‡	1.4e+9 (3.81-1.2e+137) ‡
GSE4922					
(n-289)	Q_1	N/A	N/A	Reference	Reference
	Q_2			1.25 (0.65-2.41)	1.23 (0.63-2.43)
	Q_3			1.99 (1.08 -3.76)†	1.82 (0.95-3.56)
	Q_4			2.33 (1.28-4.36) ‡	1.65 (0.79-3.50)
GSE22226					
(n=129)	Q_1	Reference	Reference	Reference	Reference
	Q_2	0.71 (0.14-3.32)	0.92 (0.17-4.99)	0.83 (0.29-2.31)	0.68 (0.20-2.15)
	Q_3	2.24 (0.70-8.38)	1.73 (0.47-8.30)	1.27 (0.49-3.39)	1.10 (0.39-3.24)
	Q_4	3.94 (1.37-14.1) ‡	2.49 (0.71-11.7)	2.95 (1.30-9.27) ‡	2.18 (0.84-6.15)
GSE24450					
(n=183)	Q_1	Reference	N/A	Reference	N/A
	Q_2	0.60 (0.12-2.44)		0.50 (0.10-1.89)	
	Q_3	2.07 (0.74-6.66)		1.86 (0.69-5.47)	
	Q_4	4.29 (1.72-12.9) ‡		4.23 (1.80-11.6) ‡	
GSE53031					
(n=167)	Q_1	N/A	N/A	Reference	Reference
	Q_2			3.58 (1.30-12.6) †	2.87 (1.01-10.3) †
	Q_3			2.88 (1.00-10.3) †	1.99 (0.66-7.33)
	Q_4			2.91 (0.99-10.5)	1.30 (0.39-5.16)
GSE25066					
(n=198)	Q_1	N/A	N/A	Reference	Reference
	Q_2			2.13 (0.67-7.84)	1.62 (0.49-6.25)
	Q_3			5.03 (1.86-17.49) ‡	3.86 (1.33-14.2) †
	Q_4			4.54 (1.66-15.84) ‡	2.55 (0.80-10.1)
GSE10885					
(n=237)	Q_1	Reference	Reference	Reference	Reference
	Q_2	1.79 (0.70-4.89)	1.43 (0.49-4.50)	0.85 (0.35-2.02)	0.95 (0.36-2.44)
	Q_3	1.75 (0.65-4.91)	1.21 (0.40-3.79)	1.95 (0.94-4.22)	1.75 (0.77-4.17)
	Q_4	2.68 (1.18-6.85) †	2.01 (0.74-6.13)	1.97 (0.98-4.13)	1.77 (0.75-3.47)

Table 1: Continued.

Data set (cases)		Overall survival		Disease-free survival	
		HR (95% CI)	Adjusted HR (95% CI)∗	HR (95% CI)	Adjusted HR (95% CI)∗
GSE58812					
(n=107)	Q_1	Reference	Reference	Reference	Reference
	Q_2	0.73 (0.24-2.10)	0.83 (0.27-2.42)	1.39 (0.48-4.22)	1.54 (0.53-4.70)
	Q_3	1.13 (0.45-2.96)	1.39 (0.54-3.69)	1.84 (0.70-5.33)	2.22 (1.02-7.63)
	Q_4	0.55 (0.17-1.66)	0.67 (0.20-2.01)	0.91 (0.29-2.99)	1.10 (0.34-3.55)
NKI set					
(n=295)	Q_1	Reference	Reference	Reference	Reference
	Q_2	3.56 (1.28-12.57) †	2.64 (0.92-8.48)	1.87 (0.99-3.70)	1.60 (0.83-3.21)
	Q_3	9.12 (3.60-30.71) ‡	5.47 (2.07-18.9) ‡	3.89 (2.17-7.40) ‡	2.95 (1.59-5.80) ‡
	Q_4	11.16 (4.41-37.54)‡	4.39 (1.53-16.0) ‡	3.95 (2.19-7.55) ‡	2.37 (1.17-5.00) †
TCGA1					
(n=526)	Q_1	Reference	Reference	Reference	Reference
	Q_2	0.68 (0.36-1.27)	0.74 (0.39-1.38)	1.32 (0.63-2.84)	1.39 (0.66-3.07)
	Q_3	1.01 (0.55-1.84)	1.17 (0.63-2.16)	0.76 (0.30-1.84)	0.79 (0.30-1.96)
	Q_4	0.94 (0.52-1.70)	1.01 (0.50-2.02)	1.67 (0.83-3.51)	4.25 (0.78-4.25)
TCGA2					
(n=1903)	Q_1	Reference	Reference	NA	NA
	Q_2	1.99 (1.53-2.61) ‡	1.88 (1.43-2.50) ‡		
	Q_3	2.50 (1.94-3.26) ‡	2.08 (1.57-2.78)‡		
	Q_4	3.00 (2.33-3.89)‡	2.20 (1.63-2.99) ‡		
Pooled GEO					
(n=2248)	Q_1	Reference	Reference	Reference	Reference
	Q_2	1.83 (1.22-2.80) ‡	2.04 (1.20-3.60) ‡	1.64 (1.28-2.11)‡	1.54 (1.34-2.09) ‡
	Q_3	3.55 (2.45-5.27) ‡	3.13 (1.87-5.47) ‡	2.66 (2.11-3.38)‡	2.30 (1.71-3.14) ‡
	Q_4	3.77 (2.61-5.59)‡	2.27 (1.30-4.11) ‡	2.66 (2.11-3.38)‡	1.82 (1.31-2.54)‡
Pooled TCGA					
(n=2429)	Q_1	Reference	Reference	Reference	Reference
	Q_2	1.71 (1.35-2.19) ‡	1.85 (1.41-2.45) ‡	1.32 (0.63-2.84)	1.40 (0.66-3.07)
	Q_3	2.18 (1.73-2.77) ‡	2.08 (1.57-2.77) ‡	0.76 (0.30-1.84)	0.79 (0.30-1.96)
	Q_4	2.55 (2.03-3.22)‡	2.22 (1.65-3.01) ‡	1.67 (0.83-3.51)	1.79 (0.78-4.25)

Note: uni- and multivariate analyses were conducted to evaluate HR of *MCAK*.
∗For multivariate analysis, HR was adjusted by age, ER status, and Elston Grade in GSE7390, GSE4922, and GSE25066 and in pool analysis datasets. In the GSE2034 set, HR was adjusted by ER status and it was adjusted by age and ER status in GSE58812. The probe of *MCAK* was 209408_s_at.
HR was adjusted by age, ER status, and Elston Grade in GSE10885 and GSE22226 sets, in which the probe of *MCAK* was A_23_P34788.
The probe of *MCAK* was ILMN_1779153 in GSE24550.
HR was adjusted by age, ER status, and Elston Grade in the GSE53031 set, in which the probe of *MCAK* was 11745868_a_at.
∗† Statistical significance, $P<0.05$; ‡ Statistical significance, $P<0.01$.

48 hours. The breast cancer cell was harvested and tested by luminescence. The Firefly and Renilla luciferase activity was dramatically higher in pmirGLO-485-5p-WT and pmirGLO-181c-WT transfectants compared to blank control. In Figures 3(c) and 3(d), the analysis indicated that the Firefly and Renilla relative luciferase activities of pmirGLO-485-5p-WT and pmirGLO-181c-WT decreased by more than 50% when they were cotransfected with miR-485-5p and miR-181c expression vectors, respectively ($p<0.05$). However, the relative luciferase activity of pmirGLO-485-5p-WT was not reduced by the miR-181c mimic. The luciferase activity of pmirGLO-181c-WT was also not inhibited by the miR-485 mimic. On the other hand, miR-485-5p mimic could not quench the luciferase activity of pmirGLO-485-5p-Mut significantly. Similar results also could be seen on pmirGLO-181c-Mut/miR-181c cotransfection. Therefore, this investigation revealed that miR-485-5p and miR-181c would reduce the expression by specifically binding to corresponding motifs of MCAK mRNA.

3.4. miR-485-5p and miR-181c Might Suppress MCAK Expression and Associate with Better Outcome in Breast Cancer. The scatter plot displayed by the expression of MCAK was significantly and negatively correlated with miR-485-5p and miR-181c, respectively (Figure 4(a)) ($p<0.001$). Meanwhile, the mRNA expression of MCAK in miR-485-5p and miR-181c

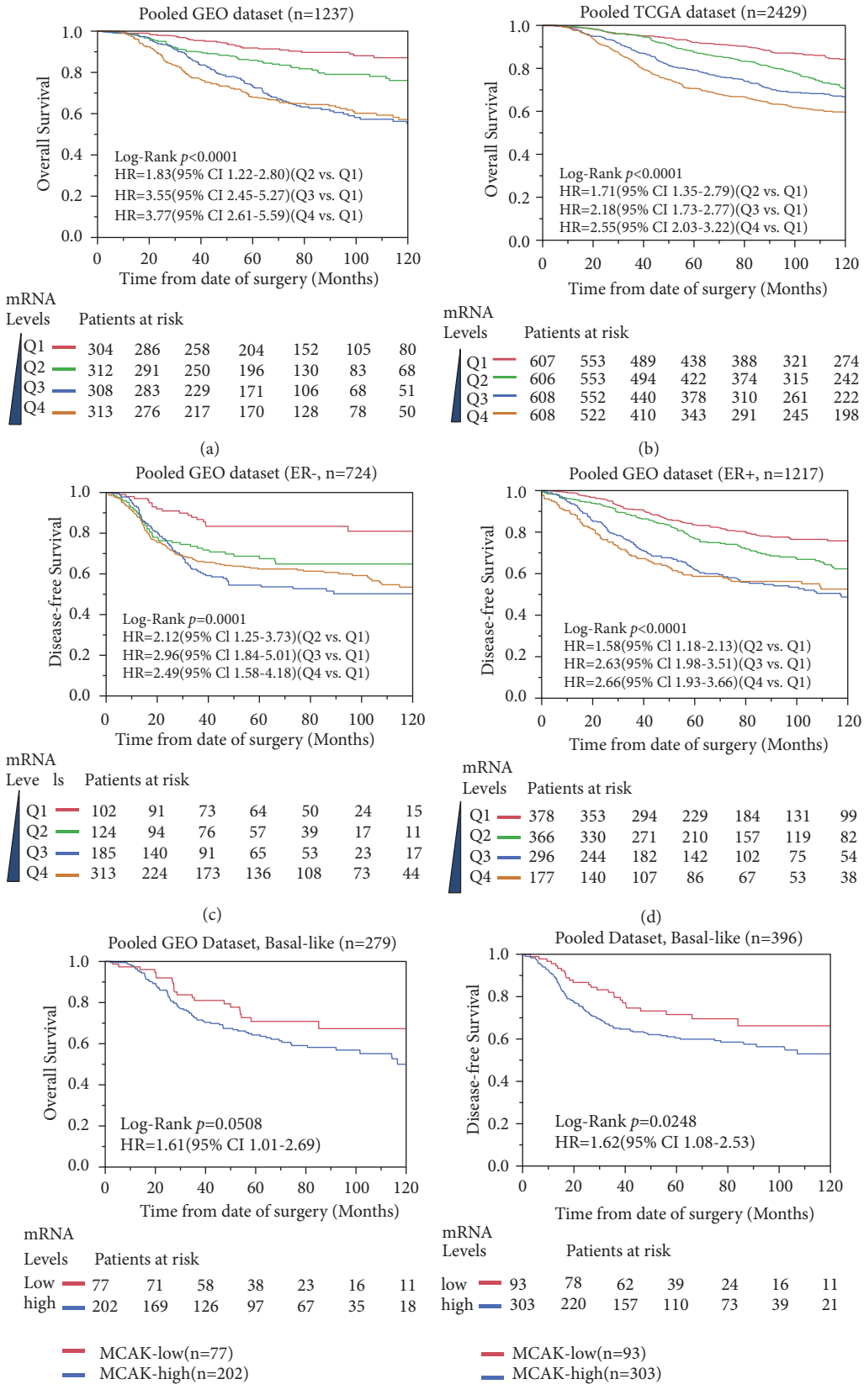

FIGURE 2: *Survival analysis of MCAK expression in GEO and TCGA breast cancer datasets*. The Kaplan-Meier curves were plotted to visualize MCAK expression levels and outcomes in breast cancer cases. The upper panel listed the overall analysis results of MCAK expression in pooled GEO dataset (a) and TCGA dataset (b). In the middle panel, MCAK was significantly associated with disease-free survival in ER-positive (c) and ER-negative (d) breast cancer patients in pooled GEO datasets. MCAK expression was significantly associated with poor disease-free (e) and overall survival (f) in basal-like breast cancer cases.

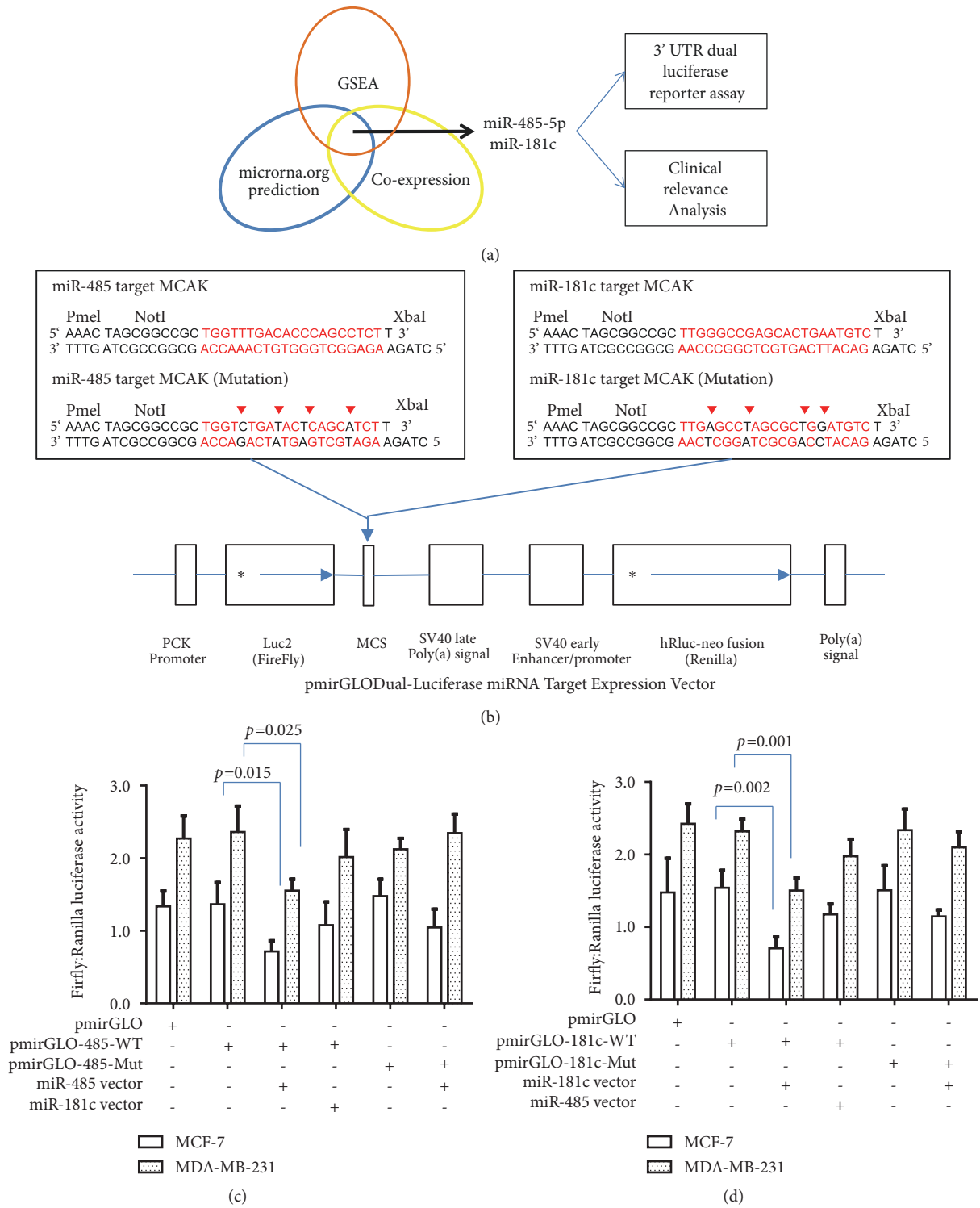

FIGURE 3: *Identification of microRNAs that modulate expression of MCAK in breast cancer cells*. The strategy to identify microRNA modulating MCAK expression was displayed on (a). First, the prediction of target microRNA for MCAK expression was researched on www.microrna.org. Second, the MCAK enriched microRNA gene signatures were also taken into consideration. Meanwhile, those eligible microRNAs were also significantly and negatively correlated with MCAK mRNA levels. Here, miR-485-5p and miR-181 were selected as eligible microRNAs that target MCAK in breast cancer. The double-strand DNA fragments of MCAK binding sites for miR-485-5p and miR-181c were synthesized (b). Mutation fragments were also synthesized for negative control. For each fragment, the PmeI and XhaI restrict enzyme sequence was inserted, and NotI enzyme sequence also inserted for internal control. These fragments were inserted into multiple cloning sites (MCS) of pmirGLO Dual-Luciferase miRNA Target Expression Vector, which was located on 3' untranslated region (3' UTR) of Firefly luciferase (*luc2)* gene. The pmirGLO-485-5pWT and pmirGLO-181cWT represent wild-type report plasmids of miR-485-5p and miR-181c targeting MCAK, respectively. The pmirGLO-485-5pMut and pmirGLO-181cMut were corresponding to mutants' report plasmids. These report plasmids were transfected into MCF-7 and MDA-MB-231 cells, and luminescence activity was tested after being incubated for 48 hours. The Firefly:Renilla luciferase activity was used to indicate the inhibition rate of reporter systems for miR-485-5p (c) and miR-181c (d), respectively.

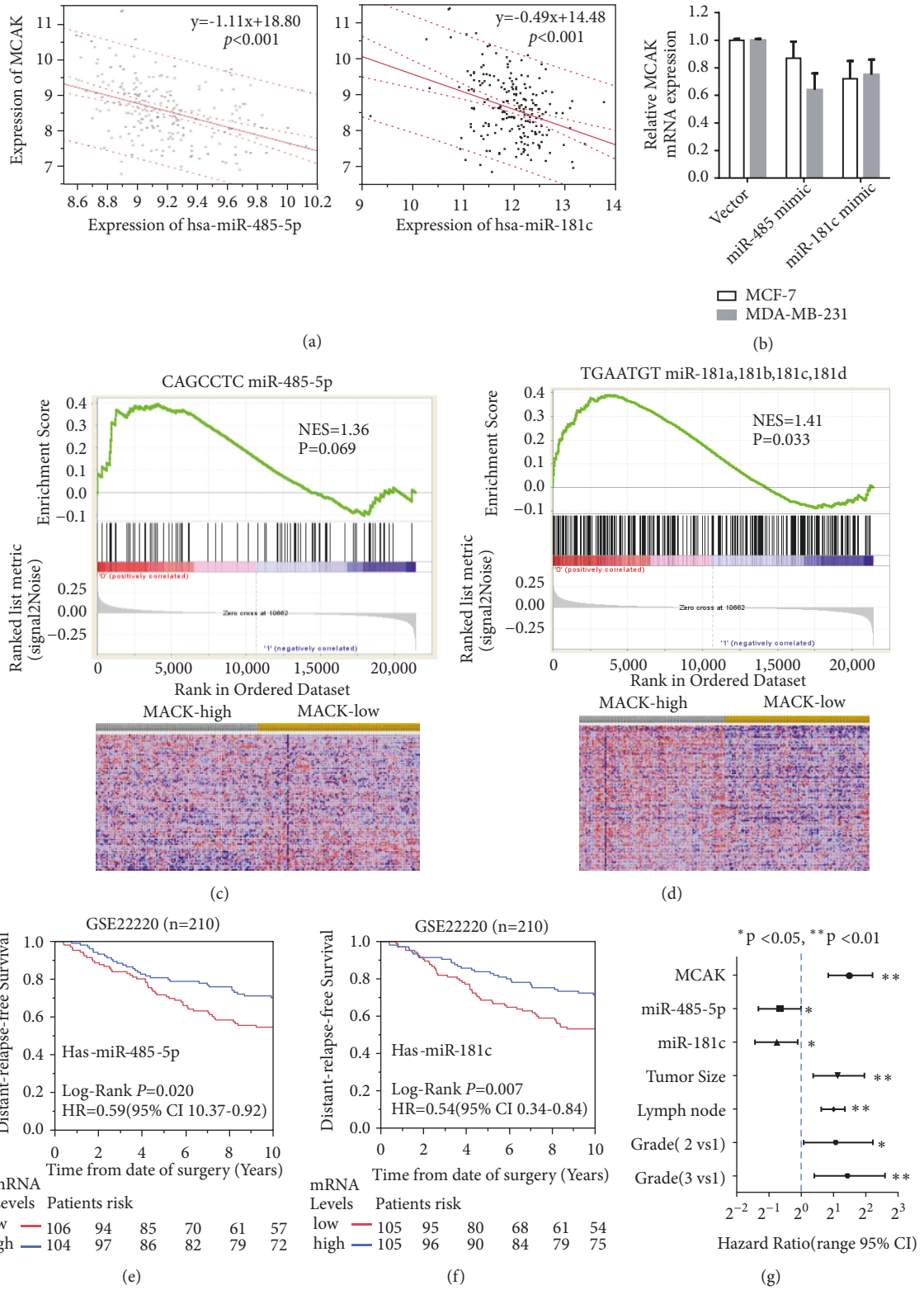

FIGURE 4: *miR-485-5p and miR-181c negatively correlated with MCAK expression and associated with better survival in breast cancer*. The scatter plots between MCAK and miR-485-5p and miR-181c were shown on (a). The mRNA expression of MCAK was reduced by mimics of miR-485-5p and miR-181c (b). A gene set enrichment analysis for MCAK and signatures of miR-485-5p/miR-181c were also displayed on (c) and (d). Cases were stratified into high and low subgroups based on expression levels of miR-485-5p and miR-181c. The Kaplan-Meier curves of these two microRNAs are shown in (e) and (f). Cox proportional hazard analysis for MCAK, miR-485-5p, miR-181c, tumor size, lymph node involvement, and Elston grade in GSE22220 dataset are shown on (g).

Table 2: Clinical relevance of miR-485 and miR-181c on GSE 22220 dataset.

	has-miR-485-5p			has-miR-181c		
	High (%*)	Low	p value†	High (%*)	Low	p value†
Age						
<50	41 (58.6)	29		26 (37.1)	44	
≧50	63 (45.0)	77	0.0632	79 (56.4)	61	0.0081
Grade						
1	27 (64.3)	15		26 (61.9)	16	
2	41 (50.0)	41		47 (57.3)	35	
3	40 (35.5)	73	0.0137	22 (35.5)	40	0.0092
Tumor size						
<2cm	38 (58.5)	27		36 (55.4)	29	
>=2cm	66 (45.5)	79	0.0823	69 (47.6)	76	0.2957
Lymph node						
0	59 (49.2)	61		65 (54.2)	55	
1-2	21 (47.7)	23		18 (40.9)	26	
>=3	24 (52.2)	22	0.9084	22 (47.8)	24	0.3036
ER status						
Negative	35 (42.7)	47		33 (40.2)	49	
Positive	69 (53.9)	59	0.1120	72 (56.3)	56	0.0233

Note: there are 1, 1, 1, 5, and 1 missing cases in age, tumor size, lymph node, grade, and ER status.
∗% represents positive rate of *has-miR-485-5p/has-miR-181c* is equal to $N_{High}/(N_{High}+N_{Low})\times 100\%$.
† *p* values were based on the Pearson Chi-square test.

mimic plasmid transfectants was reduced by 13% and 28%, respectively, in comparison to control vector in MCF-7 cell. Two microRNAs also could suppress MCAK by 36% and 25% in MDA-MB-231 cell (Figure 4(b)). It was reported that miR-485-5p targets PAK1 [14], and miR-181c targets Smad7 [18] and PTEN [19]. Here, the mRNA expressions of PAK1, Smad7, and PTEN were reduced 21%, 12%, and 22% by corresponding mimic plasmids In MCF-7 cell. However, it failed to show statistical significance. Similar results also could be seen in MDA-MB-231 cell. Further, GSEA also demonstrated that MCAK could enrich gene sets of miR-485-5p (CAGCCTC) and miR-181c (TGAATGT) (Figures 4(c) and 4(d)). The NES for miR-485-5p and miR-181c were 1.36 (p=0.069) and 1.41 (p=0.033), respectively.

The clinical relevance of miR-485-5p and miR-181c was analyzed on GSE22220 dataset (Table 2). Here, we stratified breast cancer patients as high and low subgroups based on the median scores of miR-485-5p and miR-181c, respectively. The expression of miR-485-5p and miR-181c was likely associated with age. Interestingly, miR-485-5p was higher in cases of breast patients younger than 50 years (p=0.0632), but miR-181c was significantly higher in 50-year-old or older patients (p=0.0081). Both miR-485-5p and miR-181c were significantly associated with lower Elston histology grade (p values were 0.014 and 0.009, resp.). Also, miR-181c, but not miR-485-5p, was significantly associated with ER-positive status (p=0.0233). Both miR-485-5p and miR-181c were not significantly related to tumor size and lymph node involvement. Because of insufficient clinical data, we could not analyze the clinical relevance of microRNAs on molecular subtypes of breast cancer. Nevertheless, these findings were compatible with previous MCAK clinical relevance data.

A further outcome study was conducted for miR-485-5p and miR-181c in breast cancer databases (Figures 4(e) and 4(f)). Here, Kaplan-Meier analysis visualized both microRNAs were significantly and positively associated with better survival of breast cancers. Further Cox proportional analyses were conducted to compare the prognostic performance of MCAK, miR-485-5p, miR-181c, tumor stage, lymph node stage, and Elston histology grade in breast cancer on GSE22220 dataset (Figure 4(g)). It was shown that MCAK, tumor and lymph node involvement, and histological grade were significantly associated with risk of breast cancer relapse. However, these two microRNAs significantly reduce the relative risk of recurrence (p<0.05). The HRs of miR-485-5p and miR-181c for PFS were 0.59 (95% CI 10.37-0.92) and 0.54 (95% CI 0.34-0.84), respectively. The HR of MCAK was 2.80 (95% CI 1.77-4.57). Therefore, miR-485-5p and miR-181c played opposing roles in MCAK outcome in breast cancer cases.

4. Discussion

In this study, analyses were conducted on GEO and TCGA datasets to identify prognostic biomarkers related to MCAK expression in breast cancer. Over 4,600 eligible breast cancer cases were included in this study. Patient profiles composed of multiple ethnicities and social-economic backgrounds (Suppl. Table 1). Because the gene expression data from each set stems from different platforms and research teams, a key challenge was to integrate all data without any bias systematically. The selection and publication biases were taken into consideration. Individual and pooled analyses were conducted to avoid biases in this study. Also, stratification

and multivariate analyses were used to reduce potential confounders. We believe that all findings yielded from this study are repeatable and reliable. Results from individual and pooled analysis consistently revealed that mRNA expression of MCAK was significantly associated with tumor size and Elston histological grade in breast cancer. MCAK expression was also significantly associated with poor outcome of breast cancer in a dose-dependent manner. The analysis results also show that MCAK predicts poor outcome in both ER-positive and ER-negative breast cancers, suggesting that MCAK might promote invasion of breast cancer regardless of ER status. Interestingly, MCAK significantly impacts poor survival in basal-like breast cancer. Even though the clinical relevance and prognostic significance of MCAK protein are not clear, we believe that MCAK might serve as a prognostic biomarker for breast cancer.

The biological mechanism of MCAK involving cancer invasiveness remains unclear. Recent research confirmed that MCAK plays essential roles in depolymerizing microtubules and transporting cargo along microtubules. Moreover, studies have focused on whether MCAK and KIF2A could be induced in mutant K-Ras-transformed cells [40, 41]. Recent studies have found that MCAK regulates lysosomal localization and lysosome organization in immortalized human bronchial epithelial cells (HBECs) [41]. In Ras-transformed cells, MCAK and KIF2A are required for Ras-dependent proliferation and migration to support the transformed phenotype. Depletion of either of these kinesins impairs the ability of cells transformed with mutant K-Ras to migrate and invade Matrigel [40]. However, it seems that depletion of these kinesins could not reverse epithelial to mesenchymal transition (EMT) caused by mutant K-Ras. The mRNA of MCAK dramatically increased in breast cancer tissue in comparison to adjacent normal samples. Inhibition of MCAK with small interfering RNA has inhibited the growth of the breast cancer cell lines T47D and HBC5 [42]. The above findings may explain how overexpression of MCAK plays a critical role in breast carcinogenesis. Nevertheless, further investigation is needed to explore the detailed mechanism of MCAK in cancer proliferation and invasion.

In addition to identifying the association between MCAK and breast cancer aggressiveness, we also demonstrate that microRNAs were related to MCAK. Here, several methodologies confirm that miR-485-5p and miR-181c target MCAK and negatively regulate regulatory steps in cancer development. First, bioinformatic analysis confirmed that miR-485-5p and miR-181c bind to CAGCCTC and TGAATGT motifs in MCAK, respectively (Figure 3(b) and Suppl. Figure 2). In our study, a dual-luciferase 3'-UTR reporter assay demonstrated that miR-485-5p and miR-181C specifically inhibited Firefly and Renilla relative luciferase actively by 50% by binding to these motifs (Figures 3(c) and 3(d)). Even the mimics of these two microRNAs only suppressed MCAK mRNA expression levels by 13-36% in breast cancer cells, but our population-based analysis also indicated that miR-485-5p and miR-181C are significantly and negatively coexpressed with MCAK in 214 breast cancer cases ($p<0.001$) (Figures 4(a) and 4(b)). Meanwhile, GSEA also validated that MCAK could enrich gene signatures of CAGCCTC miR-485-5p (NES=1.36, p=0.069) and TGAATGT miR-181a, 181b, 181c, and 181d (NES=1.41, p=0.033), respectively (Figures 4(c) and 4(d)). Previous studies demonstrated that miR-485-5p significantly reduces the invasive ability of breast cancer cells (MCF-7 and MDA-MB-231) [13] and gastric cancer cells (BGC-823 and SGC7901) [17]. Similarly, miR-181c has been included in prognostic signatures related to breast cancer [43, 44]. A study also showed that miR-181c inhibits the migratory and invasive behaviors of SK-N-SH and SH-SY5Y neuroblastoma cells [18]. However, another research team has reported that miR-181c could promote the proliferation and invasive ability in inflammatory breast cancer (SUM149 cells) which accounts for about 6% of breast cancers [19]. Some inconsistent findings might be due to different signaling pathways in cancer development. In our study, all participants included in the pooled analysis are early primary breast cancer patients [45]. Both miR-485-5p and miR-181c play opposing roles on MCAK expression but both are associated with better survival in breast cancer (Figures 4(e) and 4(f)). Overall, our study suggests that miR-485-5p and miR-181c suppress MCAK expression and invasiveness capability of breast cancers by targeting different sites.

5. Conclusions

This study demonstrated that mRNA expression of MCAK was significantly associated with poor outcome in breast cancer cases in a dose-dependent manner. Potentially, MCAK can serve as an independent prognostic biomarker for either ER-positive or ER-negative breast cancer. miR-485-5p and miR-181c expressions suppress MCAK gene expression and prognosticate better survival for breast cancer patients.

Abbreviations

MCAK:	Mitotic Centromere-Associated Kinesin, or Kinesin Family Member 2C (KIF2C)
MT:	Microtubule
GEO:	Gene Expression Omnibus
TCGA:	The Cancer Genome Atlas
ER:	Estrogen Receptor
PR:	Progesterone Receptor
MKI-67:	Marker of proliferation Ki-67
HER2:	Human Epidermal growth factor Receptor 2
GSEA:	Gene Set Enrichment Analysis
OS:	Overall survival
PFS:	Progression-free survival
HR:	Proportional Hazard Ratio
95% CI:	95% Confidence Interval.

Data Availability

The breast cancer datasets supporting this study are available at GEO (https://www.ncbi.nlm.nih.gov/geo/) and TCGA (https://cancergenome.nih.gov) datasets. And the datasets are cited at relevant places within the text as references [6, 8, 9, 15, 24–28, 31, 32, 35, 43, 45].

Conflicts of Interest

The authors declare no potential conflicts of interest concerning this manuscript.

Acknowledgments

This study was supported by the Clinical Research Funding Project (Grant no. 2017-YB002) of Dongyang Hospital and partially supported by Sino-American Cancer Foundation Grant.

Supplementary Materials

Supplementary Table 1: summary of worldwide breast cancer gene expression datasets. Supplementary Table 2: expression of MCAK/Kif2C and clinical features of breast cancer. Supplementary Figure 1: MCAK/KIF2C protein interaction network. Supplementary Figure 2: gene set enrichment analysis (GSEA) for MCAK enriched gene signatures. Supplementary Figure 3: the binding location and binding patterns of microRNAs on MCAK gene. *(Supplementary Materials)*

References

[1] A. R. Barr and F. Gergely, "MCAK-independent functions of ch-Tog/XMAP215 in microtubule plus-end dynamics," *Molecular and Cellular Biology*, vol. 28, no. 23, pp. 7199–7211, 2008.

[2] M. Tanenbaum, L. Macurek, B. van der Vaart, M. Galli, A. Akhmanova, and R. Medema, "A complex of Kif18b and MCAK promotes microtubule depolymerization and is negatively regulated by aurora kinases," *Current Biology*, vol. 21, no. 16, pp. 1356–1365, 2011.

[3] S. F. Bakhoum, S. L. Thompson, A. L. Manning, and D. A. Compton, "Genome stability is ensured by temporal control of kinetochore–microtubule dynamics," *Nature Cell Biology*, vol. 11, no. 1, pp. 27–35, 2009.

[4] R. Shrestha and V. Draviam, "Lateral to end-on conversion of chromosome-microtubule attachment requires kinesins CENP-E and MCAK," *Current Biology*, vol. 23, no. 16, pp. 1514–1526, 2013.

[5] S. Gnjatic, Y. Cao, U. Reichelt et al., "NY-CO-58/KIF2C is overexpressed in a variety of solid tumors and induces frequent T cell responses in patients with colorectal cancer," *International Journal of Cancer*, vol. 127, pp. 381–393, 2010.

[6] K. Ishikawa, Y. Kamohara, F. Tanaka et al., "Mitotic centromere-associated kinesin is a novel marker for prognosis and lymph node metastasis in colorectal cancer," *British Journal of Cancer*, vol. 98, no. 11, pp. 1824–1829, 2008.

[7] L. Bie, G. Zhao, Y. Wang, and B. Zhang, "Kinesin family member 2C (KIF2C/MCAK) is a novel marker for prognosis in human gliomas," *Clinical Neurology and Neurosurgery*, vol. 114, no. 4, pp. 356–360, 2012.

[8] K. McPherson, C. M. Steel, and J. M. Dixon, "ABC of breast diseases. Breast cancer-epidemiology, risk factors, and genetics," *BMJ*, vol. 321, pp. 624–628, 2000.

[9] D. M. Parkin, F. Bray, J. Ferlay, and P. Pisani, "Global cancer statistics, 2002," *CA: A Cancer Journal for Clinicians*, vol. 55, no. 2, pp. 74–108, 2005.

[10] T. FA and S. SJ, *Pathology of The Breast*, Elsevier, New York, NY, USA, 1992.

[11] J. K. Wiencke, "Impact of race/ethnicity on molecular pathways in human cancer," *Nature Reviews Cancer*, vol. 4, no. 1, pp. 79–84, 2004.

[12] V. Ambros, "microRNAs: tiny regulators with great potential," *Cell*, vol. 107, no. 7, pp. 823–826, 2001.

[13] C. Lou, M. Xiao, S. Cheng et al., "MiR-485-3p and miR-485-5p suppress breast cancer cell metastasis by inhibiting PGC-1α expression," *Cell death & disease*, vol. 7, p. e2159, 2016.

[14] X. Lin, C. He, T. Sun, X. Duan, Y. Sun, and S. Xiong, "hsa-miR-485-5p reverses epithelial to mesenchymal transition and promotes cisplatin-induced cell death by targeting PAK1 in oral tongue squamous cell carcinoma," *International Journal of Molecular Medicine*, vol. 40, no. 1, pp. 83–89, 2017.

[15] J. Duan, H. Zhang, S. Li et al., "The role of miR-485-5p/NUDT1 axis in gastric cancer," *Cancer Cell International*, vol. 17, no. 1, 2017.

[16] L.-L. Jing and X.-M. Mo, "Reduced miR-485-5p expression predicts poor prognosis in patients with gastric cancer," *European Review for Medical and Pharmacological Sciences*, vol. 20, no. 8, pp. 1516–1520, 2016.

[17] M. Kang, M.-P. Ren, L. Zhao, C.-P. Li, and M.-M. Deng, "MiR-485-5p acts as a negative regulator in gastric cancer progression by targeting flotillin-1," *American Journal of Translational Research*, vol. 7, no. 11, pp. 2212–2222, 2015.

[18] Y. Li, H. Wang, J. Li, and W. Yue, "MiR-181c modulates the proliferation, migration, and invasion of neuroblastoma cells by targeting Smad7," *Acta Biochimica et Biophysica Sinica*, vol. 46, no. 1, pp. 48–55, 2013.

[19] W. Zhang and J. Zhang, "miR-181c promotes proliferation via suppressing PTEN expression in inflammatory breast cancer," *International Journal of Oncology*, vol. 46, no. 5, pp. 2011–2020, 2015.

[20] S. Das, D. Bedja, N. Campbell et al., "miR-181c regulates the mitochondrial genome, bioenergetics, and propensity for heart failure in vivo," *PLoS ONE*, vol. 9, no. 5, article no. e96820, 2014.

[21] M. Chen, M. Wang, S. Xu, X. Guo, and J. Jiang, "Upregulation of miR-181c contributes to chemoresistance in pancreatic cancer by inactivating the Hippo signaling pathway," *Oncotarget* , vol. 6, no. 42, pp. 44466–44479, 2015.

[22] Z. Q. Gao, J. F. Wang, D. H. Chen et al., "Long non-coding RNA GAS5 antagonizes the chemoresistance of pancreatic cancer cells through down-regulation of miR-181c-5p," *Biomedicine & Pharmacotherapy*, vol. 97, pp. 809–817, 2017.

[23] H. Zhang, B. Hu, Z. Wang, F. Zhang, H. Wei, and L. Li, "miR-181c contributes to cisplatin resistance in non-small cell lung cancer cells by targeting Wnt inhibition factor 1," *Cancer Chemotherapy and Pharmacology*, vol. 80, no. 5, pp. 973–984, 2017.

[24] K. Zhang and H. Wang, "Cancer genome atlas pan-cancer analysis project," *Chinese Journal of Lung Cancer*, vol. 18, pp. 219–223, 2015.

[25] C. Desmedt, F. Piette, S. Loi et al., "Strong time dependence of the 76-gene prognostic signature for node-negative breast cancer patients in the TRANSBIG multicenter independent validation series," *Clinical Cancer Research*, vol. 13, no. 11, pp. 3207–3214, 2007.

[26] Y. Wang, J. G. M. Klijn, Y. Zhang et al., "Gene-expression profiles to predict distant metastasis of lymph-node-negative primary breast cancer," *The Lancet*, vol. 365, no. 9460, pp. 671–679, 2005.

[27] J. Smeds, L. D. Miller, J. Bjohle et al., "Gene profile and response to treatment," *Annals of Oncology*, vol. 16, supplement 2, pp. i195–i202, 2005.

[28] A. V. Ivshina, J. George, O. Senko et al., "Genetic reclassification of histologic grade delineates new clinical subtypes of breast cancer," *Cancer Research*, vol. 66, no. 21, pp. 10292–10301, 2006.

[29] L. J. Esserman, D. A. Berry, M. C. U. Cheang et al., "Chemotherapy response and recurrence-free survival in neoadjuvant breast cancer depends on biomarker profiles: results from the I-SPY 1 TRIAL (CALGB 150007/150012; ACRIN 6657)," *Breast Cancer Research and Treatment*, vol. 132, no. 3, pp. 1049–1062, 2012.

[30] T. A. Muranen, D. Greco, R. Fagerholm et al., "Breast tumors from CHEK2 1100delC-mutation carriers: genomic landscape and clinical implications," *Breast Cancer Research*, vol. 13, p. R90, 2011.

[31] H. A. Azim Jr., S. Brohée, F. A. Peccatori et al., "Biology of breast cancer during pregnancy using genomic profiling," *Endocrine-Related Cancer*, vol. 21, no. 4, pp. 545–554, 2014.

[32] C. Hatzis, L. Pusztai, V. Valero et al., "A genomic predictor of response and survival following taxane-anthracycline chemotherapy for invasive breast cancer," *Journal of the American Medical Association*, vol. 305, no. 18, pp. 1873–1881, 2011.

[33] B. T. Hennessy, A.-M. Gonzalez-Angulo, K. Stemke-Hale et al., "Characterization of a naturally occurring breast cancer subset enriched in epithelial-to-mesenchymal transition and stem cell characteristics," *Cancer Research*, vol. 69, no. 10, pp. 4116–4124, 2009.

[34] P. Jézéquel, D. Loussouarn, C. Guérin-Charbonnel et al., "Gene-expression molecular subtyping of triple-negative breast cancer tumours: Importance of immune response," *Breast Cancer Research*, vol. 17, no. 1, 2015.

[35] M. J. van de Vijver, Y. D. He, L. J. van 't Veer et al., "A gene-expression signature as a predictor of survival in breast cancer," *The New England Journal of Medicine*, vol. 347, no. 25, pp. 1999–2009, 2002.

[36] A. Subramanian, P. Tamayo, V. K. Mootha et al., "Gene set enrichment analysis: a knowledge-based approach for interpreting genome-wide expression profiles," *Proceedings of the National Acadamy of Sciences of the United States of America*, vol. 102, no. 43, pp. 15545–15550, 2005.

[37] J. Ding, M. Kuo, L. Su et al., "Human mitochondrial pyrroline-5-carboxylate reductase 1 promotes invasiveness and impacts survival in breast cancers," *Carcinogenesis*, vol. 38, no. 5, pp. 519–531, 2017.

[38] D. Szklarczyk, A. Franceschini, S. Wyder et al., "STRING v10: protein-protein interaction networks, integrated over the tree of life," *Nucleic Acids Research*, vol. 43, pp. D447–D452, 2015.

[39] L. A. Carey, C. M. Perou, C. A. Livasy et al., "Race, breast cancer subtypes, and survival in the Carolina Breast Cancer Study," *Journal of the American Medical Association*, vol. 295, no. 21, pp. 2492–2502, 2006.

[40] E. Zaganjor, J. K. Osborne, L. M. Weil et al., "Ras regulates kinesin 13 family members to control cell migration pathways in transformed human bronchial epithelial cells," *Oncogene*, vol. 33, no. 47, pp. 5457–5466, 2014.

[41] E. Zaganjor, L. M. Weil, J. X. Gonzales, J. D. Minna, and M. H. Cobb, "Ras transformation uncouples the kinesin-coordinated cellular nutrient response," *Proceedings of the National Acadamy of Sciences of the United States of America*, vol. 111, no. 29, pp. 10568–10573, 2014.

[42] A. Shimo, C. Tanikawa, T. Nishidate et al., "Involvement of kinesin family member 2C/mitotic centromere-associated kinesin overexpression in mammary carcinogenesis," *Cancer Science*, vol. 99, pp. 62–70, 2008.

[43] C. Gong, W. Tan, K. Chen et al., "Prognostic value of a BCSC-associated MicroRNA signature in hormone receptor-positive HER2-negative breast cancer," *EBioMedicine*, vol. 11, pp. 199–209, 2016.

[44] A. J. Lowery, N. Miller, A. Devaney et al., "MicroRNA signatures predict oestrogen receptor, progesterone receptor and HER2/neu receptor status in breast cancer," *Breast Cancer Research*, vol. 11, no. 3, 2009.

[45] F. M. Buffa, C. Camps, L. Winchester et al., "microRNA-associated progression pathways and potential therapeutic targets identified by integrated mRNA and microRNA expression profiling in breast cancer," *Cancer Research*, vol. 71, no. 17, pp. 5635–5645, 2011.